

# **Biotransformation of short chain fatty acids into sophorolipids for biomedical applications**

By

**Isha Hemant Abhyankar**  
**AcSIR Registration Number 10BB19J26011**

A thesis submitted to the  
Academy of Scientific & Innovative Research  
for the award of the degree of  
DOCTOR OF PHILOSOPHY  
in  
SCIENCE  
Under the supervision of

**Dr. Anuya Nisal**



CSIR-National Chemical Laboratory

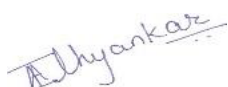


Academy of Scientific and Innovative Research  
AcSIR Headquarters, CSIR-HRDC campus  
Sector 19, Kamla Nehru Nagar,  
Ghaziabad, U.P. – 201 002, India

**July 2022**

# Certificate

This is to certify that the work incorporated in this Ph.D. thesis entitled, "Biotransformation of short chain fatty acids into sophorolipids for biomedical applications", submitted by Isha Hemant Abhyankar to the Academy of Scientific and Innovative Research (AcSIR) in fulfilment of the requirements for the award of the Degree of DOCTOR OF PHILOSOPHY in SCIENCE, embodies original research work carried-out by the student. We further certify that this work has not been submitted to any other University or Institution in part or full for the award of any degree or diploma. Research material(s) obtained from other source(s) and used in this research work has/have been duly acknowledged in the thesis. Image(s), illustration(s), figure(s), table(s) etc., used in the thesis from other source(s), have also been duly cited and acknowledged.



18<sup>th</sup> July 2022

Isha Abhyankar




18<sup>th</sup> July 2022

Dr. Anuya Nisal

## **STATEMENTS OF ACADEMIC INTEGRITY**

I Isha Hemant Abhyankar, a Ph.D. student of the Academy of Scientific and Innovative Research (AcSIR) with Registration No. 10BB19J26011 hereby undertake that, the thesis entitled “Biotransformation of short chain fatty acids into sophorolipids for biomedical applications” has been prepared by me and that the document reports original work carried out by me and is free of any plagiarism in compliance with the UGC Regulations on [“Promotion of Academic Integrity and Prevention of Plagiarism in Higher Educational Institutions \(2018\)”](#) and the CSIR Guidelines for *“Ethics in Research and in Governance (2020)”*.



**Signature of the Student**

Date :18<sup>th</sup> July 2022

Place :Pune

---

It is hereby certified that the work done by the student, under my supervision, is plagiarism-free in accordance with the UGC Regulations on [“Promotion of Academic Integrity and Prevention of Plagiarism in Higher Educational Institutions \(2018\)”](#) and the CSIR Guidelines for *“Ethics in Research and in Governance (2020)”*.



**Signature of the Supervisor**

Name :Dr. Anuya Nisal

Date :18<sup>th</sup> July 2022

Place :Pune

---

## Acknowledgements

This thesis is a culmination of work at CSIR- National Chemical Laboratory, Pune. Undertaking this PhD has truly been a life changing experience for me and it would have not been possible without the support and guidance that I received from many people. I would like to take this opportunity to acknowledge all those who have directly or indirectly helped me during my PhD tenure.

First and foremost, I would like to thank my guide Dr. Anuya Nisal for her constant support and motivation. Her immense knowledge, creative ideas and zeal for research was a constant motivation for me. Her calm and positive attitude made it easier to share and discuss ideas with her. She gave us the freedom to work and explore which helped me to grow as better researcher. She has an eye for details, be it in presentation or experiments; this was extremely beneficial for me to grow as a professional in my field. She patiently provided the vision and the necessary advice to explore different dimension to the work. The faith and the trust that she bestowed on me was a constant source of motivation and I am deeply thankful to Anuya ma'am for her support in professional and non-professional situations.

My research journey in NCL began under the guidance of Dr. Asmita Prabhune. I am extremely grateful to for her support and guidance. Asmita ma'am introduced me to research and ingrained the basics of research which molded me into a researcher. Her strong technical background and sheer knowledge set the bar of science very high for us. It was her efforts and determination that prepared me for the worst and the best. Her enthusiasm and passion for research always inspired me to do more. Moreover, her motherly nature and care have helped me tackle different situations in life. She encouraged me to explore different opportunities which ultimately led to the beginning of my Ph.D.

I have truly been blessed to have such profound scientists as my guide. Both of them (Dr. Anuya Nisal and Dr. Asmita Prabhune) are not only an excellent example of research guide but also successful women entrepreneurs and scientists at heart. My tenure in NCL was a pleasant journey only because of their mentorship and for this I will be truly grateful to them throughout my life.

---

Besides advisors, I would like to thank my Doctoral assessment committee (DAC) members, Dr J.Nithyanandhan, Dr.Kadhiravan and Dr.Mahesh Dharne for their timely suggestions and invaluable inputs. Their advice helped me to evaluate my work from several perspectives and led to successful completion of my PhD curriculum and research work.

Even though PhD was my work, this wouldn't have been possible without the strong technical support from NCL. I am thankful to Dr.Santhakumari and her student Mr.Ganesh for their technical assistance for HRMS studies. I am in debt to Santhakumari ma'am for sparing her time and answering my doubts and queries. I am thankful to Ganesh for his help in analyzing my samples and helping me with the analysis. I would also like to acknowledge Gholap sir, Chetan and Venkat for helping me with the SEM and TEM analysis. I am deeply thankful to Dr.Kalpana Trimukhe for her help with XRD and CMC data. I am thankful to Sangeetha ma'am for her assistance in TGA analysis. Likewise, I am thankful to Dr.G.V.N Rathna and Dr.Mahesh Dharne for permitting me to use the sonicator in their labs.

I wish to thank Dr.Ashish Lele, Director CSIR-NCL and HOD of both Biochemical Sciences Division (Dr.Narendra Kadoo) and PSE Division (Dr.Asha) for giving me the opportunity to work in this laboratory and for making the necessary facilities available for carrying out research. I am also thankful to all the scientist of Biochemical Sciences and PSE division, staff members of each department, Chairman- Students academic Office and all the members of SAC office for their cooperation. I acknowledge ICMR-SRF for providing the necessary funding and fellowship to pursue my research.

Besides having the best guides, I have been blessed with friendly and cheerful bunch of friends in and outside the lab. I cannot end this note without acknowledging my dear friends. I would like to thank my lab mates; Hensha, Alaka, Bijosh, Dr. Emmanuel, Swarali, Kartiki, Dr.Vinita and Nimisha ma'am for their moral support at personal and professional front throughout my PhD. It is because of all this people that Lab 948, feels like home now. Special word of appreciation for Nimisha ma'am for teaching me cell culture techniques and organizational skills. Her patient listening and helpful nature made my journey easier at NCL. I thoroughly enjoyed my days spent with them and I carry with me wonderful moments, trips and conversations. I thank them all from the bottom of my heart. Apart from this, I would like to thank my other lab mates: Dr. Priti, Dr. Amrita, Vikas for their support during my tenure. I am also grateful to my seniors: Dr Kasturi

---

Joshi, Dr Parul Dubey, Dr.Gayatri Gurjar, Dr.Animesh Deval and Dr.Venkat for their help and support.

I would like to acknowledge my first mentor in NCL, Late Dr. Pushpa Devi for encouraging me to pursue science and for helping me understand my strengths. I so wish she would have been here to witness this journey. I am also thankful to my batchmates; Pranav, Junaid, Smita, Rakesh, Sanjana, Rajni, Aishwarya, Amarnath and Anuja for their help and support whenever needed.

I would also like to acknowledge my loving friends; Isha, Sharayu, Mohi, Nikhita, Rajeshree, Pooja, Mayuri, Siddhi for their generous love and support throughout my Ph.D. Frequent conversations and meeting with these people helped me remain grounded and sail through this. I am also grateful to relatives and siblings for their care and understanding.

Finally, I acknowledge the people who mean the most to me, my parents, Aai and Baba. It was because of their rock-solid support that I could march on this journey. In spite of not understanding my research area, they supported me and boosted my morale whenever I was at my lowest. I dedicate my thesis to them. I would also like to acknowledge my loving sister, Poorva and my brother-in-law, Amey for their support and encouragement at every step of the way. Despite being away they have been my biggest strength. I can't express in words what I feel for all of them. I am eternally thankful to them for their unconditional love, care and support. I wish to make you proud. I am deeply thankful to my dear Aaji for her unfailing faith in my dreams and for celebrating my smallest achievement and to my Dada for his support and practical wisdom. I extend a heartfelt gratitude to my parents-in-law and sister-in-law, Sampada for their encouragement and support. Lastly, I would dedicate my accomplishment to my best friend and my dear husband Saransh for his unconditional love and support. His backing and motivation helped me to thrive. I really appreciate his patience and reassurance during tough situations. I am deeply grateful for his help throughout my PhD tenure.

Isha Abhyankar

---

## Synopsis

### Introduction

Surfactants are one of the most widely used bulk chemicals. Their amphiphilic nature decreases the interfacial tension between two phases like, liquid-liquid, liquid-air, solid-liquid. Surfactants are therefore used in various sectors: textile, paper, food, agriculture, pharmaceuticals and cosmetics. Nearly half of the produced volume is used in households and as laundry detergent. The tremendous usage of surfactant presents several environmental and health concerns regarding their production and use. Complete degradation of the surfactants from the surface is an unlikely event. The ecotoxicity, low biodegradability and bio accumulation of chemical surfactants have led to the advent of greener molecules or greener methods of synthesis.

Owing to this, there has been a significant advancement towards synthesis and characterization of biosurfactants. Biosurfactants from microbes are emerging as an exciting class of biomolecules with potential applicability in various sectors like detergents, biomedical, nanotechnology and pharmaceuticals. As they are biodegradable, non-toxic and cost-effective, they have emerged as promising substitutes for petroleum-derived conventional surfactants. Biosurfactants are divided into two categories: low molecular weight, consisting of glycolipids and lipopolysaccharides and high molecular weight biosurfactants, including polysaccharides, and proteins. Glycolipids are the most studied biosurfactants, synthesized from biological units. They are further divided into different categories, of which sophorolipids are of prime importance as they are synthesized by non-pathogenic yeast and have better production yields.

Sophorolipids (SL) are produced extracellularly by non-pathogenic yeast, *Starmerella bombicola* (ATCC2214). Structurally they are amphiphilic, possessing a hydrophilic head and a hydrophobic tail. Sophorolipids exists in 2 forms mainly acidic and lactonic. Both the components impart different properties to the molecule. Acidic sophorolipids are water soluble and aid in surfactant ability and solubility, whereas lactonic SL impart biological properties. Sophorolipids are known to possess various natural properties like anti-bacterial, anti-cancerous, anti-viral and anti-fungal agent. In addition to these, they are also finding application in the food industry, cosmetics and petroleum industry.

---

The preferred range of chain length of fatty acid for SL synthesis is C16-18. This limitation is attributed to (i) the substrate specificity of the enzymes cytochrome P450 monooxygenases (CYP52M1) and uridine diphosphate glucosyltransferase (UGTA1) and (ii) high preponderance of C18 in the *de novo* product. Therefore, SLs are commonly synthesized using fatty acids with 16–18 carbon atom chains. Nevertheless, SLs can also be produced using fatty acids with shorter chain lengths. The influence of fatty acid chain length on SL biosynthesis and product formation is only partially understood. Deeper understanding of the mechanism of short chain derived sophorolipids and their chemical, physical and biological properties will further increase the avenues where biosurfactants can bring a significant impact.

### **Statement of Problem**

Sophorolipids (SL) consists of a carbohydrate moiety linked to long fatty acid chain. The bioconversion is facilitated by different enzymes like cytochrome P450 monooxygenase, glucosyl transferase and acetyl esterase. These enzymes are inherent part of the yeast metabolism. On external supply of lipophilic sources, the enzymatic system of yeast converts fatty acids into a highly viscous product: sophorolipid which is secreted extracellularly. The crude product is then obtained by solvent extraction. By varying the fatty acid substrates, different sophorolipids could be synthesized. This property of sophorolipids, increases the applicability of the molecules in various sectors.

The use of pure medium/short-chain fatty acid as a sole lipophilic source for synthesizing SL is yet to be explored. As the structure of the synthesized SL substantially depends on the producing organism and the fermentation condition, appropriate process optimization is necessary.

Further, the synthesized SL is generally a mixture of molecules varying in the degree of acetylation, internal esterification between the carboxylic group of fatty acid and 4'' position of the sophorose molecule, hydroxylation of fatty acid, and chain length of fatty acid. For a deeper understanding of functional diversity, purification of the congeners is extremely essential.



---

Thus, the objective of this thesis is to synthesize sophorolipids using shorter chain fatty acids and study their physical, chemical and biological properties. Further, the different application of these short chain derived sophorolipids will be assessed.

## **Objectives**

### **Objective 1: Deciphering the effect of chain length of substrate on physical and biological properties of sophorolipid**

Objective 1 aims to synthesize sophorolipids using different chain length substrates like C14, C16, and C18. The synthesized sophorolipids were primarily characterized using High Performance Liquid Chromatography, Thin Layer Chromatography and oil displacement assay. Further, the structural characterization was done using High Resolution Mass Spectroscopy (LC-HRMS), Fourier transform infrared spectroscopy (FTIR). The physical properties of the SLs including critical micellar concentration were also studied. Moreover, the process parameters and the media components were also optimized by one factor method. Post characterization, the anti-bacterial activity of each synthesized sophorolipid was assessed against model gram positive, *S.aureus* and gram negative, *P.aeruginosa* bacterium by contact method at varied concentration and time intervals. Finally, the cytotoxicity was assessed against normal fibroblast cell line L929 by MTT (3-(4,5-dimethylthiazol-2-yl)-2,5-diphenyl tetrazolium bromide) assay.

### **Objective 2: Underlying mechanism of short chain substrates in sophorolipid production and its application**

To fully understand the mechanism involved in use of short chain fatty acids as substrate for sophorolipid synthesis, a set of fermentation experiments were performed. These experiments were conducted to evaluate the effect of new substrate on product yield and yeast cell growth. Further, the myristic acid derived sophorolipid was purified to obtain individual congeners. The purification was done by column chromatography. The individual fractions were assessed through HRMS. Finally, the individual fractions were analyzed for its anti-cancer activity. The anti-cancer activity of each purified congener was assessed against cervical cancer cell line by MTT assay and compared with crude sophorolipid.

---

### **Objective 3: Nanoparticle synthesis using myristic acid derived sophorolipid**

Myristic acid derived sophorolipid was used as capping agent to obtain calcium phosphate nanoparticles. The synthesized nanoparticles were characterized by SEM, TEM, XRD and FTIR. Further the presence of sophorolipids on nanoparticles was confirmed by TGA and lectin binding assay. Later, these nanoparticles were incorporated into silk solution for bone tissue applications. Different *in vitro* studies were performed on the obtained scaffolds.

### **Methodology:**

#### **Objective 1: Deciphering the effect of chain length of substrate on physical and biological properties of sophorolipid**

We have synthesized sophorolipids using different substrate (Myristic acid, palmitic acid, stearic acid). The fermentation process was as follows: briefly, the parent moieties, glucose and fatty acid are supplemented in the growth media along with 2 % cell loading and kept for 4-5 days at room temperature. The biotransformation was brought about by the yeast *S.bombicola*, resulting in brown viscous extracellular product. This product was then solvent extracted to obtain native / crude SL (Refer [Figure I](#)). As different unconventional substrates were used, the media parameters were optimized so as to obtain better yield (Refer [Figure II](#)).

The crude SL was then characterized using different techniques. The preliminary test includes, TLC and HPLC. These tests were performed to assess the acidic and lactonic ratios of the SL. Further, the surfactant ability of the product was tested by CMC and oil displacement assay. Structural characterization was done by HRMS (High resolution mass spectroscopy) to evaluate the glycosylation and acetylation pattern. Furthermore, the successful incorporation of parent molecules into SL was assessed by FTIR.

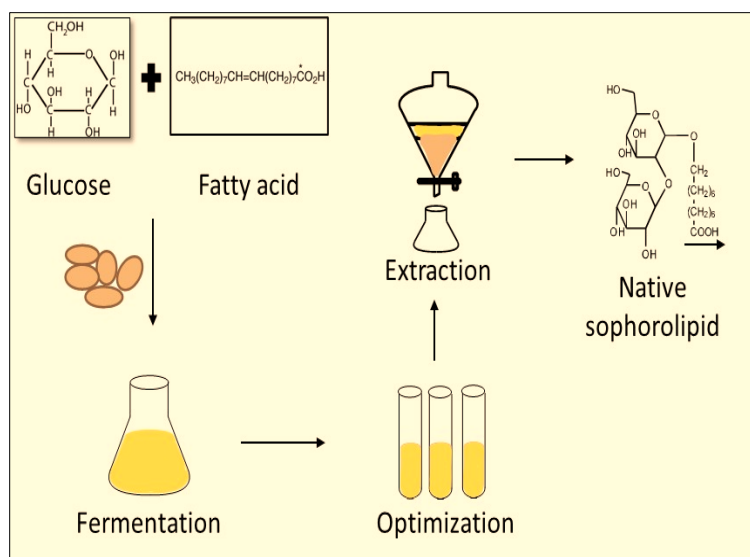


**Figure I: Fermentation process of sophorolipids**

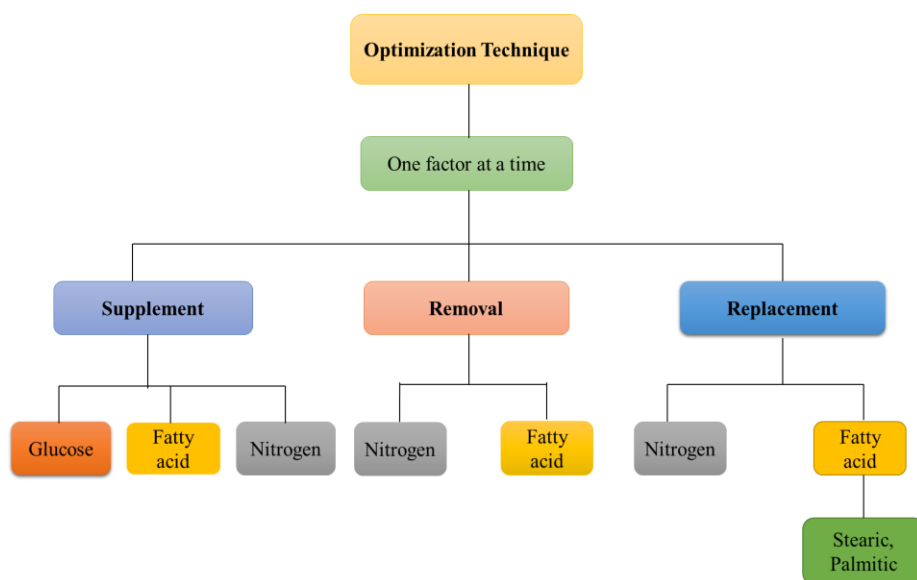


**Figure II: Optimization protocol for sophorolipid synthesis**

The anti-bacterial activity was assessed using contact method: briefly, the bacterial cell suspension was prepared and O.D was adjusted to 0.1, after which it was serially diluted and mixed with sophorolipid. After specific intervals, the suspension was plated onto agar plates and incubated at 37°C. After incubation the number of colonies were counted and graph was plotted (Refer [Figure III](#)). To further assess the cytotoxicity of synthesized sophorolipid, MTT assay against normal fibroblast cells L929 was performed.

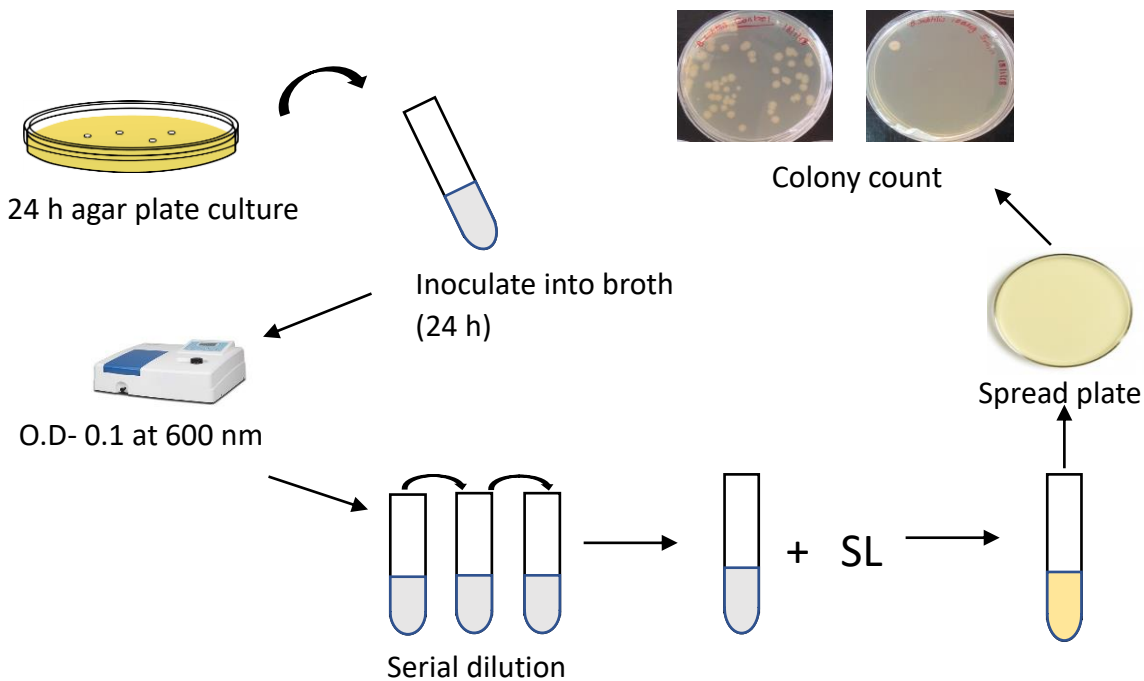


**Figure III: Antibacterial assay: Contact method**

**Objective 2: Underlying mechanism of short chain substrates in sophorolipid production and its application**

The effect of shorter chain substrates on cell growth was monitored using fermentation experiments. The product conversion was compared with oleic acid derived sophorolipid. Further, the individual congeners were separated using column chromatography and each fraction was analyzed by HRMS. The anti-cancer activity of each congener was assessed using MTT assay against cervical cancer cell line, MG 63. The activities of each congener were compared with crude sophorolipids.

**Objective 3: Nanoparticle synthesis using myristic acid derived sophorolipid**

Calcium phosphate nanoparticles were synthesized by bottom-up synthesis using short chain derived sophorolipid. The synthesized nanoparticles were characterized using XRD and FTIR to

---

analyze the composition of nanoparticles. Further, the structural orientation of nanoparticles was determined using SEM/ TEM. Furthermore, the presence of sophorolipid on nanoparticles was confirmed by TGA and lectin binding assay. Lastly, *in vitro* studies like proliferation assay and ALP assay of the nanoparticles were performed on bone cells MG 63. The experiment was performed for 14 days.

## Summary

The toxicity of short chain fatty acids combined with the C16–C18 chain length specificity of the yeast enzymes limits the avenues for producing SLs. In this work, we have demonstrated, the synthesis of a shorter chain SL derived from (C14) myristic acid, palmitic acid and stearic acid. All the obtained SL have been characterized structurally using spectroscopic techniques. The FTIR experiments confirmed substitution of sophorose moiety on to the fatty acid chains as well as acetylation on the glucose in the sophorose moiety. The characterization suggests that glycosylation occurs preferentially at the methyl end group of the fatty acid chain and leads to the formation of a mixture of acidic and lactonic SL containing monoacetylated and diacetylated forms for myristic acid derived sophorolipid; whereas the glycosylation happens at both ends for higher fatty acids, palmitic and stearic acid derived SL. Further, the HRMS analysis showed formation of different congeners i.e. acidic, lactonic forms of SLs and their mono or diacetylated variants. All the SLs showed excellent surface-active properties as determined by their critical micellar concentration. The results highlight the plausible correlation between the chain length of fatty acid substrate and their CMC. The lowest CMC was observed for myristic acid derived sophorolipid.

Moreover, the biological properties of SL are greatly dependent on the nature of lipophilic substrate used. Shorter chain derived SL exhibit excellent anti-bacterial activity against gram positive and gram-negative bacteria. Furthermore, the short chain derived SL are less lethal to the normal cells than longer chain substrates. These results are presented through schematic in [Figure IV](#).

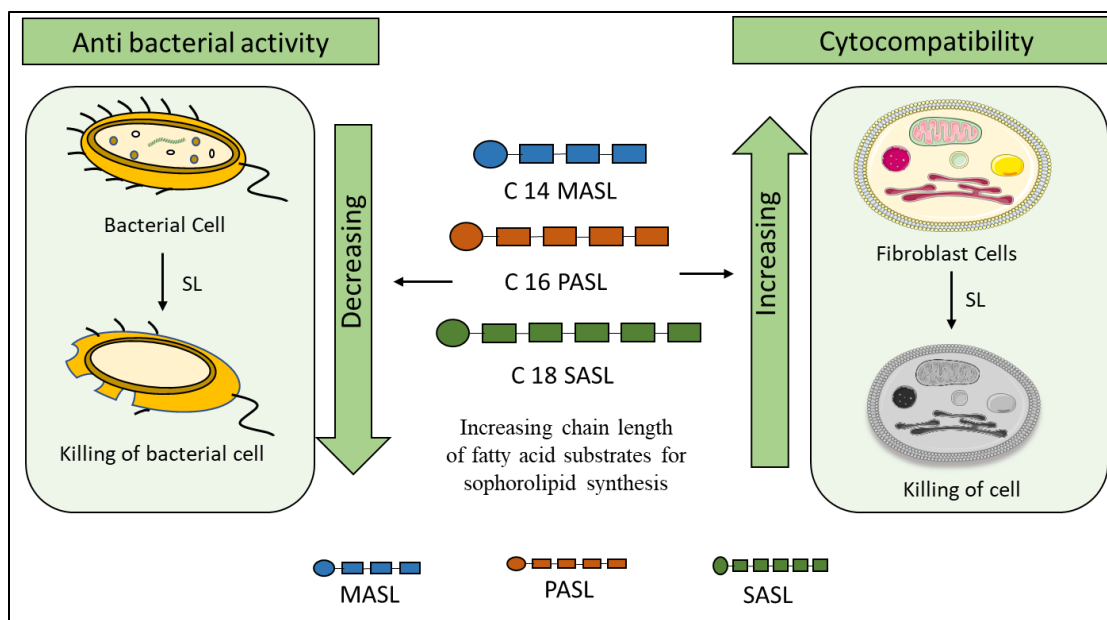


**Figure IV-** Schematic depicting the anti-bacterial and cytocompatibility of synthesized SL

Apart from anti-bacterial activity, MASL has good anti-cancer potential and are not lethal to the normal cells. It was observed that crude MASL exhibited better anti-cancer activity than individual congeners. The amalgamation of both acidic and lactonic components into the crude SL proves beneficial in enhancing the applicability of the molecule. Interestingly, the mechanism of action of SL on bacterial cell and mammalian cell is related to the chain length of substrate, depicted in [Figure V](#). For mammalian cells, the higher specificity of saturated fatty acids towards membrane receptors renders it lethal to the cells whereas, the low surface activity of such higher chain derived SL limits their anti-bacterial potential.

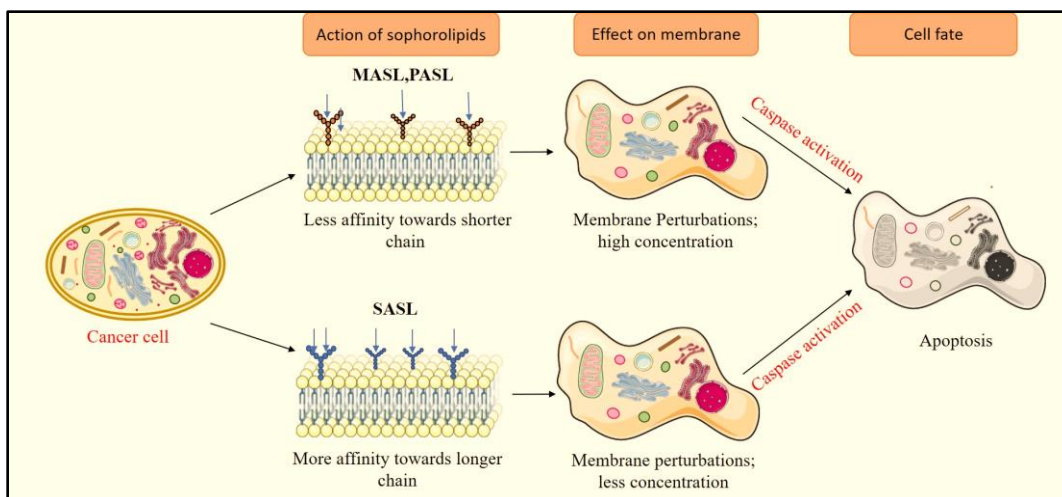


**Figure V-** Schematic describing the effect of fatty acids on cellular membranes

To further assess its potential, we have synthesized calcium phosphate nanoparticles using MASL. This happens to be the first report on synthesis of inorganic nanoparticles using short chain derived sophorolipid. These nanoparticles were obtained by using biological and physical method of synthesis. The resulting nanoparticles were characterized using different techniques.

Interestingly, by this method of synthesis composite nanoparticles consisting of brushite and TCP are formed. It was observed that amphiphilic nature of SL acts as catalyst in synthesizing the nanoparticles. Moreover, it was evident that presence of SL effectively changes the compositional and morphological properties of the nanoparticles as observed in [Figure VI](#).

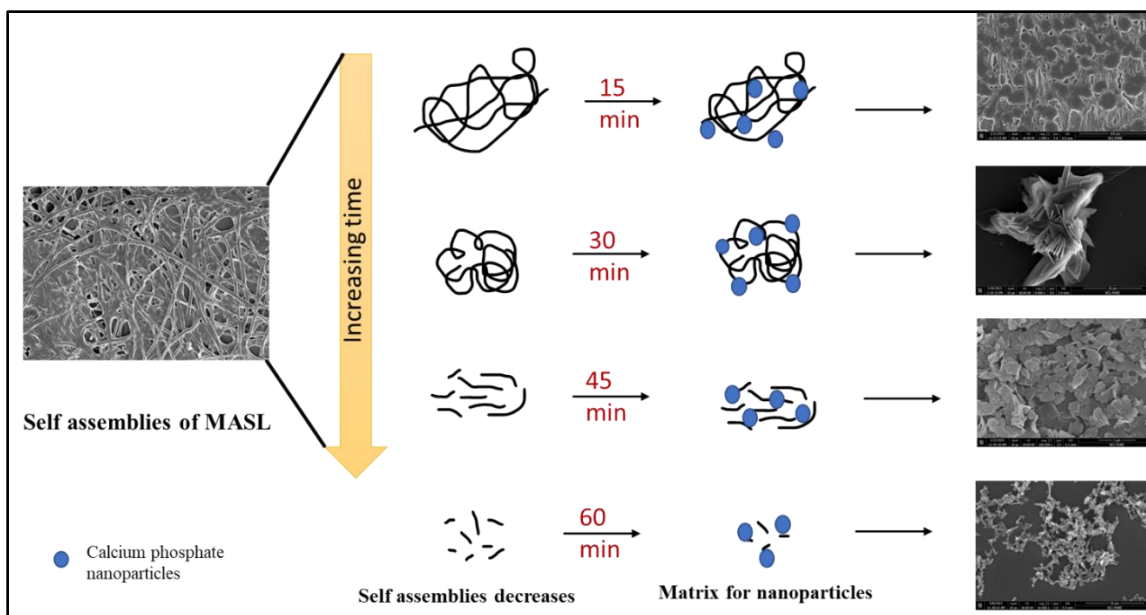


**Figure VI-** Schematic describing the mechanism involved in synthesis of nanoparticles using SL

To summarize, this work demonstrates the production of sophorolipids using various fatty acid substrates and highlights its superior biological properties like anti-bacterial, anti-cancer. Further, the work also demonstrates the ability of SL to synthesize inorganic nanoparticles, thereby establishing a promising future for this biosurfactant.

## 6. Future directions

- ❖ *In-vitro* studies to evaluate the mechanism of anti-cancer activity of sophorolipids along with its selective permeability.



---

## Publications

### International Journal Publications

1. **Isha Abhyankar**, Asmita Prabhune, Anuya Nisal, ' Myristic acid derived sophorolipid: efficient synthesis and enhanced anti-bacterial activity, ACS Omega, 2021 (DOI: 10.1021/acsomega.0c04683)
2. **Isha Abhyankar** #, S Hirlekar #, K Kane, K Trimukhe, A Prabhune, A Nisal, 'Green anti bacterial molecules: Sophorolipids with varying fatty acid chain. Trends in Biomaterials & Artificial Organs 35 (5) 2021 (# Contributed equally)
3. **Isha Abhyankar**, Asmita Prabhune, Anuya Nisal, Synthesis of SL-coated calcium nanoparticles for bone tissue application (Manuscript under preparation)
4. **Isha Abhyankar**, Asmita Prabhune, Anuya Nisal, Selective mechanism of short chain derived sophorolipids against cancer ((Manuscript under preparation)

### Book Chapter:

1. Philem Pushparani Devi, **Isha Abhyankar**, Pradeep Kumar Singh; Endophytes as Nanofactories, Nanotechnology in sustainable agriculture, CRC Press (2021)

### Provisional patent filing

1. "Composition of calcium phosphate nano-particles with sophorolipids and process of synthesis thereof. No- 202211035664.

---

## Table of contents

<b>1</b>	<b>Chapter I Introduction.....</b>	<b>29</b>
1.1	Introduction.....	29
1.2	Scope of the work: .....	30
1.3	Thesis Outline: .....	31
<b>2</b>	<b>Chapter II Literature Review.....</b>	<b>33</b>
2.1	Surfactants: .....	34
2.2	Biosurfactants: .....	34
2.2.1	Types of biosurfactants: .....	35
2.2.2	Glycolipids:.....	35
2.3	Sophorolipids: .....	41
2.3.1	Producer strain: .....	41
2.3.2	Physiological role of sophorolipid in nature: .....	41
2.3.3	Structure of sophorolipid: .....	42
2.3.4	Biosynthetic pathway:.....	43
2.3.5	Market scenario:.....	45
2.3.6	Substrates used for sophorolipid synthesis: .....	47
2.3.7	Hydrophilic substrate: .....	48
2.3.8	Lipophilic Substrates.....	51
2.3.9	Properties of SL: .....	54
2.3.10	Applications of SL in varied sectors: .....	58
<b>3</b>	<b>Chapter III Deciphering the effect of chain length of substrates on physical properties of sophorolipid .....</b>	<b>62</b>
3.1	Introduction.....	63
3.2	Materials and Methods.....	66
3.2.1	Chemicals and microorganisms used.....	66
3.2.2	Synthesis of sophorolipid.....	67
3.2.3	Extraction of sophorolipid .....	68
3.2.4	Characterization of sophorolipid.....	69
3.3	Results and discussions:.....	72
3.3.1	Synthesis and extraction of Sophorolipid: .....	72
3.3.2	Oil displacement assay:.....	72

3.3.3	High performance liquid chromatography:.....	73
3.3.4	Fourier transform infrared spectroscopy:.....	75
3.3.5	High Resolution Mass Spectroscopy: .....	78
3.3.6	Critical micellar concentration:.....	83
3.4	Conclusion: .....	85
<b>4</b>	<b>Chapter IV Deciphering the effect of chain length on sophorolipid production: Emphasizing biological properties .....</b>	<b>87</b>
4.1	Introduction:.....	88
4.2	Materials and method:.....	90
4.2.1	Microorganisms: .....	90
4.2.2	Anti-bacterial activity: .....	91
4.2.3	Cell culture.....	92
4.3	Results and discussions:.....	94
4.3.1	Anti-bacterial activity of SL: .....	94
4.3.2	Cytotoxicity against L929 cells: .....	101
4.3.3	Anti-cancer activity of SL against cervical cancer: .....	102
4.4	Conclusion: .....	106
<b>5</b>	<b>Chapter V Deducing the incorporation of short chain substrates into sophorolipid: production and its application .....</b>	<b>108</b>
5.1	Introduction.....	109
5.2	Materials and method:.....	111
5.2.1	Microorganisms and Maintenance .....	111
5.2.2	Media Optimization .....	111
5.2.3	Purification of MASL .....	112
5.2.4	Anti-cancer activity of SL:.....	113
5.2.5	Fluorescence activated cell sorting: .....	113
5.2.6	Chemicals for FACS: .....	114
5.2.7	FACS protocol: .....	114
5.3	Results and discussions:.....	115
5.3.1	Media optimization: .....	115
5.3.2	Purification of MASL: .....	119
5.3.3	High-Resolution Mass Spectrometry: .....	120
5.3.4	Anti-cancer activity of MASL: .....	125
5.3.5	Fluorescence assisted cell sorting: .....	128
5.4	Conclusion: .....	132

---

<b>6</b>	<b>Chapter VI Synthesis of calcium phosphate nanoparticles using short chain derived sophorolipid</b> .....	<b>134</b>
6.1	Introduction:.....	135
6.2	Materials and method:.....	138
6.2.1	Chemicals:.....	138
6.2.2	Biosynthesis of nanoparticles: .....	138
6.2.3	Optimization studies: .....	140
6.2.4	Characterization of nanoparticles:.....	140
6.2.5	Determination of sophorolipides on nanoparticles: .....	141
6.2.6	Silk fibroin: .....	142
6.2.7	<i>In vitro</i> studies of nanoparticles .....	144
6.3	Results and discussion: .....	145
6.3.1	Optimization studies: .....	145
6.3.2	Characterization of synthesized nanoparticles:.....	158
6.3.3	Determination of SL on nanoparticles: .....	161
6.3.4	Scaffold preparation:.....	164
6.3.5	<i>In vitro</i> studies of nanoparticles .....	165
6.4	Conclusion: .....	169
<b>7</b>	<b>Chapter VII Conclusions and future work</b> .....	<b>170</b>
7.1	Conclusions:.....	171
7.2	Future prospects .....	174
7.2.1	Upscaling of short chain derived sophorolipids.....	174
7.2.2	Self assembling abilities of short chain derived Sophorolipids .....	175
7.2.3	Effect of short chain sophorolipids on gelation of silk fibroin .....	176
<b>8</b>	<b>Appendix:</b> .....	<b>178</b>
<b>9</b>	<b>Bibliography</b> .....	<b>192</b>

---

## List of figures

<u>Figure</u> 2.2.1 Schematic describing the physiological role of sophorolipid in nature .....	42
<u>Figure</u> 2.2.2 Structural representation of different forms of SL; acidic and lactonic .....	43
<u>Figure</u> 2.2.3 : Step wise biosynthetic pathway of SL. Different enzymes involved are: 1.Cytochrome P450 monooxygenase, 2.Alcohol dehydrogenase, 3.Aldehyde dehydrogenase, 4.Lipase, 5.Cytochrome P450 monooxygenase, 6.Glucosyltransferase I, 7.Glucosyltransferase II, 8. Lactone esterases, 9. Acetyl transferase .....	45
<u>Figure</u> 2.2.4 Graph depicting the number of patents being filed each year up to 2015 on SL .....	47
<u>Figure</u> 2.2.5 Schematic representation of renewable substrates identified from different commercial sectors.....	48
<u>Figure</u> 3.1 Description of method used for optimization studies: one factor at a time.....	68
<u>Figure</u> 3.2 Schematic representation describing the biotransformation process involved in SL synthesis .....	69
<u>Figure</u> 3.3 Oil displacement assay for each synthesized SL. The clear halo in the test sample indicates surfactant ability of the SL .....	73
<u>Figure</u> 3.4 HPLC graph of MASL indicating the acidic and lactonic ratios.....	74
<u>Figure</u> 3.5 HPLC graph of PASL indicating the acidic and lactonic ratios.....	74
<u>Figure</u> 3.6 HPLC graph of SASL indicating the acidic and lactonic ratios.....	75
<u>Figure</u> 3.7 FTIR graph of MASL; presence of ether bond at 1030 confirms successful SL synthesis .....	76
<u>Figure</u> 3.8 FTIR graph of PASL; presence of ether bond at 1036 confirms successful SL synthesis .....	77
<u>Figure</u> 3.9 FTIR graph of SASL; presence of ether bond at 938 confirms successful SL synthesis .....	77
<u>Figure</u> 3.10 Graphical representation of surface tension reduction by MASL .....	84
<u>Figure</u> 3.11 Graphical representation of surface tension reduction by PASL .....	84
<u>Figure</u> 3.12 Graphical representation of surface tension reduction by SASL .....	85
<u>Figure</u> 4.1 Schematic representation describing the anti-bacterial assay protocol .....	<b>Error!</b>

**Bookmark not defined.**

---

<u>Figure 4.2</u> Antibacterial activity of MASL against different organisms- % Survival at different concentrations (50–450 µg/mL) of MASL and at different time points (5–60 min) plotted (A) Gram positive, <i>S. aureus</i> , (B) Gram negative, <i>P. aeruginosa</i> .....	95
<u>Figure 4.3</u> Antibacterial activity of PASL against different organisms- % Survival at different concentrations (50–450 µg/mL) of PASL and at different time points (5–60 min) plotted (A) Gram positive, <i>S. aureus</i> , (B) Gram negative, <i>P. aeruginosa</i> .....	96
<u>Figure 4.4</u> Antibacterial activity of SASL against different organisms- % Survival at different concentrations (50–450 µg/mL) of SASL and at different time points (5–60 min) plotted (A) Gram positive, <i>S. aureus</i> , (B) Gram negative, <i>P. aeruginosa</i> .....	97
<u>Figure 4.5</u> Summary of anti-bacterial activity of each synthesized sophorolipid.....	98
<u>Figure 4.6</u> Schematic describing mode of action of SL on bacterial cell .....	99
<u>Figure 4.7</u> Schematic describing induction of autolysis in bacteria .....	101
<u>Figure 4.8</u> Cytotoxicity of all synthesized SL against fibroblast cell line .....	102
<u>Figure 4.9</u> Anti-cancer activity of crude MASL against HeLa cell line.....	103
<u>Figure 4.10</u> Anti-cancer activity of crude PASL against HeLa cell line .....	104
<u>Figure 4.11</u> Anti-cancer activity of crude SASL against HeLa cell line .....	104
<u>Figure 4.12</u> Effect of chain length of substrate on biological properties of sophorolipid .....	106
<u>Figure 5.1</u> Schematic describing the protocol followed for purification of crude MASL.....	112
<u>Figure 5.2</u> Working principle of FACS .....	114
<u>Figure 5.3</u> Graph indicating the yield obtained on using different fermentation methods for synthesizing MASL .....	116
<u>Figure 5.4</u> Graph depicts the effect of short chain substrate on the growth of yeast cells post the fermentation process .....	117
<u>Figure 5.5</u> Schematic representing the importance of myristic acid for yeast metabolism and other cellular function.....	118
<u>Figure 5.6</u> Graph denotes the comparison of product conversion between oleic acid and myristic acid derived SL .....	119
<u>Figure 5.7</u> Extracted ion chromatogram and mass spectrum of fraction I.....	120
<u>Figure 5.8</u> Extracted ion chromatogram and mass spectrum of fraction II .....	121
<u>Figure 5.9</u> Extracted ion chromatogram and mass spectrum of fraction III .....	122
<u>Figure 5.10</u> Extracted ion chromatogram and mass spectrum of fraction IV .....	123

---

<u>Figure 5.11</u> Extracted ion chromatogram and mass spectrum of fraction V .....	124
<u>Figure 5.12</u> Graph describes the anti-cancer activity of lactonic congeners against cervical cancer .....	126
<u>Figure 5.13</u> Graph depicting the anti-cancer potential of acidic congeners against cervical cancer .....	127
<u>Figure 5.14</u> Diagrammatic representation of different pathways leading to death of cell.....	128
<u>Figure 5.15</u> Graph denoting the cell cycle curve of control sample .....	129
<u>Figure 5.16</u> Graph denoting the cell cycle curve after treatment with lower concentration of MASL .....	130
<u>Figure 5.17</u> Graph highlighting the subG1 phase of cell cycle.....	130
<u>Figure 5.18</u> Graph denoting the sub G1 population after treatment with higher concentration of MASL .....	131
<u>Figure 5.19</u> Schematic representation of mechanism of action of SL on cancerous cells.....	132
<u>Figure 6.1</u> Schematics describing the different methods used for synthesizing nanoparticle ....	136
<u>Figure 6.2</u> Diagrammatic representation of advantages and limitations of using SL for nano particle synthesis.....	137
<u>Figure 6.3</u> Protocol used for synthesizing calcium phosphate nanoparticles using biosurfactant .....	139
<u>Figure 6.4</u> Schematic describing the principle of lectin binding assay.....	142
<u>Figure 6.5</u> Protocol used for preparation of silk solution .....	143
<u>Figure 6.6</u> XRD pattern of nanoparticles synthesized with 15 minutes process time .....	146
<u>Figure 6.7</u> XRD pattern of nanoparticles synthesized with 30 minutes process time .....	147
<u>Figure 6.8</u> XRD pattern of nanoparticles synthesized with 45 minutes process time .....	147
<u>Figure 6.9</u> XRD pattern of nanoparticles synthesized with 60 minutes process time .....	148
<u>Figure 6.10</u> XRD pattern of nanoparticles synthesized using SL with 15 minutes process time	149
<u>Figure 6.11</u> XRD pattern of nanoparticles synthesized using SL with 30 minutes process time	149
<u>Figure 6.12</u> XRD pattern of nanoparticles synthesized using SL with 45 minutes process time	150
<u>Figure 6.13</u> XRD pattern of nanoparticles synthesized using SL with 60 minutes process time	150
<u>Figure 6.14</u> Changes in the values of TCP over different process times and in presence of SL	152
<u>Figure 6.15</u> Graph denoting the % TCP obtained at optimal condition for control and SL nanoparticles .....	153

<u>Figure 6.16</u> Graph denoting the % brushite obtained at optimal condition for control and SL nanoparticles .....	154
<u>Figure 6.17</u> Graph denoting the % TCP at increasing concentration of SL along with control .	157
<u>Figure 6.18</u> SEM images of nanoparticles synthesized with increasing concentration of MASL .....	158
<u>Figure 6.19</u> TEM images of nanoparticles synthesized with increasing concentration of MASL .....	159
<u>Figure 6.20</u> Underlying mechanism of calcium phosphate nano particle synthesis using SL....	160
<u>Figure 6.21</u> Schematics describing the process of nucleation in presence of biosurfactant .....	161
<u>Figure 6.22</u> TGA analysis of SL nanoparticles along with control nanoparticles and crude MASL .....	162
<u>Figure 6.23</u> Graph measures the turbidity obtained at different concentrations of nanoparticles on binding to lectin. ....	163
<u>Figure 6.24</u> SEM images of scaffolds synthesized using silk fibroin and nanoparticles.....	164
<u>Figure 6.25</u> Graph denotes the effect of synthesized nanoparticles with increasing loading on proliferation of cells up to 14 days .....	166
<u>Figure 6.26</u> Actin staining highlighting the proliferating cells upon treatment with SL.....	167
<u>Figure 6.27</u> Graph denotes the effect of synthesized nanoparticles with increasing loading on ALP activity of cells up to 14 days.....	168
<u>Figure 7.1</u> SEM images of pH dependent self assemblies of MASL .....	176
<u>Figure 7.2</u> Rheology experiments on MASL and OASL.....	177
<u>Figure 8.1</u> Mass spectra of native sophorolipid (MASL); A) acidic component; B)Lactonic component.....	178
<u>Figure 8.2</u> Mass spectra of monoacetylated sophorolipid (MASL); A) acidic component; B)Lactonic component.....	179
<u>Figure 8.3</u> Mass spectra of diacetylated sophorolipid (MASL); A) acidic component; B)Lactonic component.....	180
<u>Figure 8.4</u> Mass spectra of native sophorolipid (PASL); A) acidic component; B)Lactonic component.....	181
<u>Figure 8.5</u> Mass spectra of monoacetylated sophorolipid (PASL); A) acidic component; B)Lactonic component.....	182



---

<u>Figure</u> 8.6 Mass spectra of diacetylated sophorolipid (PASL); A) acidic component; B) Lactonic component.....	183
<u>Figure</u> 8.7 Mass spectra of native sophorolipid (PASL) with binding from COOH side A) acidic component.....	184
<u>Figure</u> 8.8 Mass spectra of monoacetylated sophorolipid (PASL) with binding from COOH side A) acidic component; B) Lactonic component .....	185
<u>Figure</u> 8.9 Mass spectra of diacetylated sophorolipid (PASL) with binding from COOH side A) acidic component .....	186
<u>Figure</u> 8.10 Mass spectra of native sophorolipid (SASL) A) acidic component; B) Lactonic component.....	187
<u>Figure</u> 8.11 Mass spectra of monoacetylated sophorolipid (SASL) A) acidic component; B) Lactonic component.....	188
<u>Figure</u> 8.12 Mass spectra of diacetylated sophorolipid (SASL) A) acidic component .....	189
<u>Figure</u> 8.13 Mass spectra of native sophorolipid (SASL) with binding from COOH side A) acidic component; B) Lactonic component.....	190
<u>Figure</u> 8.14 Mass spectra of monoacetylated sophorolipid (SASL) with binding from COOH side A) acidic component; B) Lactonic component .....	191

---

## **List of Tables**

<b><u>Table 1</u></b> Description of different classes of biosurfactants along with their proposed applications.....	40
<b><u>Table 2</u></b> Chemical composition of commonly used lipophilic substrates for sophorolipid synthesis .....	65
<b><u>Table 3</u></b> Chemical composition of coconut oil as lipophilic substrate ....	65
<b><u>Table 4</u></b> Media composition for sophorolipid synthesis.....	67
<b><u>Table 5</u></b> Summary of acidic: lactonic forms for each SL .....	74
<b><u>Table 6</u></b> Different structural modification obtained from MASL .....	79
<b><u>Table 7</u></b> Different structural modification obtained from PASL.....	81
<b><u>Table 8</u></b> Different structural modification obtained from SASL.....	82
<b><u>Table 9</u></b> Comparative SEM images of synthesized nanoparticles obtained at different time intervals .....	156

---

## List of acronyms

(3-(4,5-dimethylthiazol-2-yl)-2,5-diphenyl tetrazolium bromide) MTT, 87		G	growth medium (GM), 62
	A		H
Alkaline phosphatase (ALP), 140			High performance liquid chromatography (HPLC), 65
antibiotic resistance genes (ARGs), 83			High resolution mass spectrometry (LC-HRMS), 66
antimicrobial peptides (AMPs), 83			
	C		L
concanavalin A ConA, 137			lithium bromide LiBr, 138
control nano-particles CNP, 137			M
Critical micellar concentration (CMC), 65			Malt extract Glucose Yeast extract Peptone MGYP, 62
	D		Myristic acid (MA), 61
Deionized water DI, 137			Myristic acid derived MASL, 63
Dulbecco's modified eagle medium DMEM, 88			O
	F		Oleic acid derived sophorolipid OASL, 138
Fourier transform infrared spectroscopy (FTIR), 66			P
			Palmitic acid (PA), 61

---

Palmitic acid derived SL

PASL, 63

PCR, 97

Powder X-ray diffraction

PXRD, 136

production medium

(PM), 62

## R

Regenerated silk fibroin

RSF, 138

## S

sophorolipid nano-particles

SL-NP, 137

Sophorolipids

(SL), 34

Stearic acid

(SA), 61

Stearic acid derived SL

SASL, 63

## T

Thermogravimetric analysis

(TGA), 137

Transmission electron microscopy

(TEM), 137

Tri calcium phosphate

$\beta$  TCP, 147

## Chapter I

### Introduction

#### 1.1 Introduction

Sphorolipids (SLs) are extracellularly synthesized biosurfactants obtained from yeast *S.bombicola*. The fermentation process requires supplementation of hydrophilic and lipophilic substrates. The viscous product obtained at the end of fermentation cycle is a mixture of molecules. These include different modifications like; acidic and lactonic, mono acetylation and deacetylation based on the structural diversity. The structural variations are dependent on the nature of substrates and fermentation conditions.

SL are important biosurfactants exhibiting varied biological properties. These properties along with their amphiphilic nature renders these biomolecules worthy for commercial market. Despite their discovery decades ago, the commercial applicability is still restrictive. The main reason for this is the chain length of lipophilic substrate and production cost. The biotransformation process is catalyzed via enzymatic machinery of the yeast. Traditionally, SL are synthesized using oleic acid (unsaturated fatty acid- C18:1) as primary lipophilic source owing to its involvement in the fatty acid synthetase system of the yeast. However, this chain length specificity restricts the usage. Lowering the chain length of substrate might enhance the physical and biological properties of the biosurfactants.

With this view, the thesis focuses on synthesizing SL using unconventional substrates and thereby understanding the effect of short chain fatty acids on physical and biological attributes. This understanding will assist in exploring the substrate range for synthesis of SL along with their plausible use for commercial application.

### **1.2 Motivation and objective:**

SL are magic molecules which find application in all sectors due to its multifaceted properties. Such valuable properties prompted researcher to push the boundaries and synthesize numerous forms of SL with a view to expand its use. With combined efforts SL have been commercialized by various companies and used in detergent products. Despite the commercialization, the main hinderances like; production cost, downstream processing and product variability hinders its application. To bridge the cost gap, several novel renewable and sustainable substrate alternatives have been tried for synthesizing SL, but not yet commercialized. Moreover, efforts have been made to modify the yeast strain so as to obtain enhanced production, however, this process is highly cumbersome and expensive.

Apart from the process requirement, the physical properties of SL are equally important. Industrial application requires fulfilment of certain criteria's like; hydrophilic/ hydrophobic balance, viscosity, good solubility and low CMC. These properties are often overlooked while synthesizing SL. The research emphasizes more on the developing alternate substrates for SL synthesis. Ironically, majority of the substrates used fall in the range of C16-C18 fatty acid. This substrate specificity has been constant.

With this view, the aim of this work is to synthesize SL using shorter chain length substrate. The SL will be synthesized using glucose as hydrophilic source and C14 myristic acid as lipophilic source. The interaction of short chain substrate with yeast was studied in depth to unravel the mechanism of successful synthesis. Further, the short chain derived sophorolipid was structurally characterized and purified. Moreover, the effect of chain length of substrate on chemical, physical and biological properties of SL been assessed. We have also extensively explored the anti-bacterial and anti-cancer activity of short chain derived SL and its mechanism of action. These properties of the newly synthesized SL prove their potential for biomedical application.

SLs have been widely used for synthesizing different metallic nanoparticles. SL act as capping and reducing agent for the process. Owing to the exemplary properties of shorter chain SL, we for the first time evaluate the use of these for synthesizing calcium nanoparticles. The underlying mechanism of the use of sophorolipid in synthesis of nanoparticles were studied in depth. Also, the effect of different parameters driving the formation of nanoparticles was studied. Further, the potential of these synthesized nanoparticles for bone tissue engineering application were explored.

### **1.3 Thesis Outline:**

The thesis has been divided into following chapters:

#### **Chapter I: Introduction**

The thesis outline along with the scope of work is discussed in the introduction chapter.

#### **Chapter II: Literature review**

The chapter begins with introduction to the field of biosurfactant, its types and classification. SL, the main focus of the work has been discussed in detail with respect to synthesis, global scenario and applications. The need for alternate substrate for SL synthesis has been emphasized. Based on this, the scope and objective of the thesis have been outlined.

#### **Chapter III: Deciphering the effect of chain length of substrates on sophorolipid production through physio-chemical characterization**

The third chapter focuses on synthesizing SL using saturated fatty acids as substrates. The fatty acids C14 myristic acid, C16 Palmitic acid, C18 Stearic acid were chosen for the study. The work includes physical and detailed chemical characterization to optimize the production of SL and understand the acetylation pattern.

### **Chapter IV: Deciphering the effect of chain length on sophorolipid: Emphasizing biological properties**

The fourth chapter focuses on understanding the effect of substrate on different biological properties. Anti-bacterial and anti-cancer activity of synthesized SL were extensively studied. Further, the cytotoxicity of each synthesized SL was assessed against normal fibroblast cell line.

### **Chapter V: Myristic acid derived sophorolipid: production, purification and biomedical application**

The fifth chapter focuses on understanding the mechanism for successful incorporation of short chain substrate into SL. Further, the individual congeners were purified by column chromatography. The anti-cancer activity of each congener was analyzed and the mechanism of action was deduced.

### **Chapter VI: Synthesis of calcium phosphate nanoparticles using short chain derived sophorolipid**

The sixth chapter reports the synthesis of calcium phosphate nanoparticles using SLs. The nanoparticles are thoroughly characterized for the chemical and morphological properties. Further, the involvement of SL into nanoparticle synthesis has been deduced followed by the application of these nanoparticles for bone tissue engineering.

### **Chapter VII: Conclusion and future work**

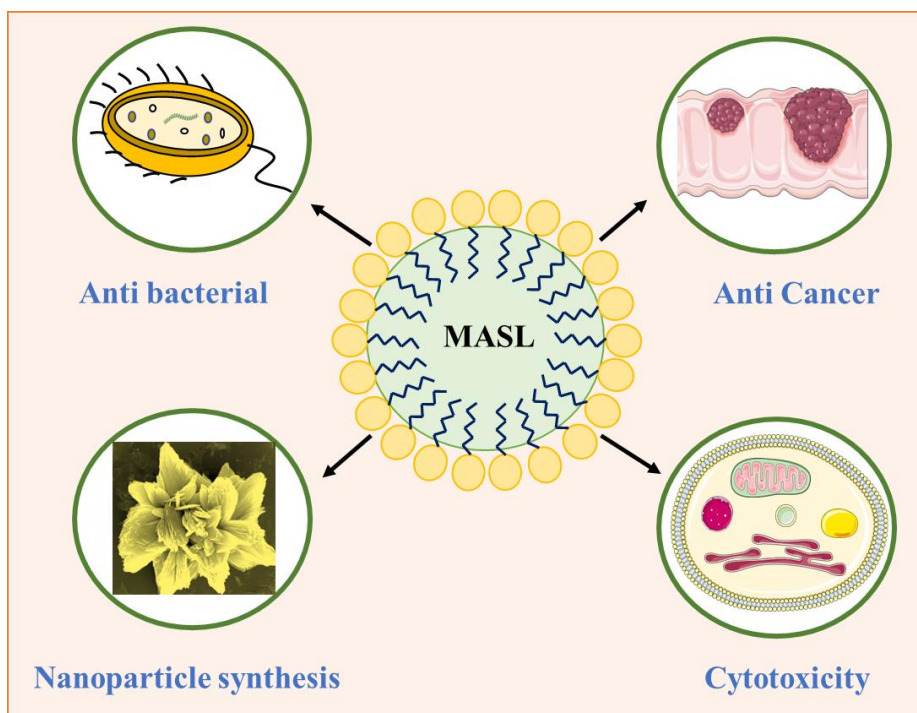
The last chapter summarizes the work of the thesis and emphasizes on the potential uses of the short chain SL especially for biomedical applications. Short chain SLs could be further explored for commercial market.



## Chapter II

### Literature Review

This thesis focuses on synthesizing glycolipid named sophorolipid using different unconventional substrates. This chapter focuses on understanding the biomolecules; sophorolipids, including its synthesis, importance in nature and application. The biosynthetic pathway along with the structural diversity of the molecules has been discussed. Moreover, the wide variety of substrates used, its advantages, disadvantages have been thoroughly discussed. Furthermore, the different unique properties of SL like anti-bacterial, anti-fungal, anti-viral and anti-inflammatory have been mentioned. Based on the structural and functional properties, the probable application of SL in different commercial domains have been explored.



### **2.1 Surfactants:**

Surfactants are one of the most widely used bulk chemicals. The annual global production amounts to more than 17 million tons<sup>1</sup>. Their amphiphilic nature decreases the interfacial tension between two phases like, liquid-liquid, liquid-air, solid-liquid. Due to these surfactants are used in various sectors: textile, paper, food, agriculture, pharmaceuticals and cosmetics. Nearly half of the produced volume is used in households and as laundry detergent<sup>2</sup>. The tremendous usage of surfactant presents several environmental and health concerns regarding their production and use<sup>3-5</sup>. Also, the major drawback associated with the use of synthetic surfactants is its degradation process. Under aerobic conditions, majority of the surfactants, form homologous monomers catalyzed by bacterial species. However, under anaerobic conditions, the degradation process is complicated and time-consuming. Complete degradation of the surfactants from the surface is an unlikely event<sup>6</sup>. The ecotoxicity, low biodegradability and bio accumulation of chemical surfactants propelled the development of greener molecules. Owing to this, there has been a significant advancement towards synthesis and characterization of biosurfactants which are eco-friendly, non-toxic and biodegradable molecules. These properties are highly desirable to overcome the current environmental issues of chemical surfactant.

### **2.2 Biosurfactants:**

Biosurfactants are surface active molecules naturally derived from bacteria, yeast and fungi. The intrinsic properties of biosurfactants; biodegradability, low toxicity and cost effectiveness render them beneficial for the commercial market. They are emerging as an exciting class of biomolecules with potential applicability in various sectors like detergents, biomedical, nanotechnology and pharmaceuticals<sup>7,8</sup>. The vast range of substrates and microbes available for synthesizing biosurfactants allows acquisition of varied molecules with distinct structural characteristics and properties. Owing to these properties, they have now emerged as promising substitutes for petroleum-derived conventional surfactants.

### 2.2.1 Types of biosurfactants:

Based on the ionic charge on the polar head, the chemical surfactants are classified as cationic, anionic and non-ionic. However, biosurfactants are classified into different types depending on the nature of hydrophilic head, chemical composition and microbial producer strain. Based on this the domain of biosurfactants is broadly divided into two categories: low molecular weight biosurfactants, consisting of glycolipids and lipopeptides and high molecular weight biosurfactants, including polysaccharides and neutral lipids<sup>9</sup>. Table 1 summarizes the classes and application of all biosurfactants.

### 2.2.2 Glycolipids:

Glycolipids are the most studied biosurfactants, synthesized from biological units. It consists of carbohydrate moiety (one or many) attached to fatty acid by glycosidic bond. Depending upon the type of carbohydrate attached, they are further divided into 5 types namely: Rhamnolipids, trehalose lipids, mannosylerythritol, cellobiose and SL<sup>10</sup>.

Rhamnolipids are glycolipids generally synthesized by bacteria, *Pseudomonas aeruginosa*. Structurally it consists of rhamnose sugar (s) linked to hydroxy fatty acid via glycosidic bond<sup>11</sup>. Quite recently efforts have been made to synthesize rhamnolipids by *Burkholderia* sp. Rhamnolipids possess good anti-bacterial, anti-biofilm activity and are also used for heavy metal removal. Even though rhamnolipids have been used commercially their usage in industries is restricted. This is mainly due to the use of opportunistic pathogen as the producer strain. It is regarded as group II pathogen and pose high risk of infection at higher production levels. This limits the applicability of the rhamnolipids into sectors involving human intervention (Biomedical, cosmetic). Apart from this, the cost of production of rhamnolipids is extremely high; thereby reducing the upscaling<sup>12</sup>.

Trehalose lipids or trehalolipids are surface active biomolecules synthesized by *Rhodococcus*, *Nocardia* sp. It consists of trehalose i.e non reducing disaccharide, linked by  $\alpha$ -1,1- glycosidic linkage, linked to lipid moiety at C6 position. The chain length of fatty acids attached is smaller as compared to other glycolipids<sup>13</sup>. Trehalolipids possess good lipophilicity and are therefore

efficient in decontamination, dispersion and removal of oil spills. They also have good anti-microbial activity against gram- positive and gram-negative bacteria. Trehalolipids are generally synthesized intracellularly (Bound to the cell envelope). This type of synthesis imparts a negative consequence on the product yield and on downstream processing<sup>14</sup>.

Cellobiose lipids are secondary metabolites synthesized by organisms of *Ustilaginaceae* family. They are extracellular produced as a mixture consisting of D-glucose linked to hydroxy fatty acids preferably C16 fatty acid. They are reported for their anti-bacterial, anti-fungal and gelling properties. While cellobiose exhibit good biological properties, fundamental studies pertaining to its synthesis pathway and gene cluster of organisms is yet to be fully understood<sup>15,16</sup>.

Mannosyl erythritol are amphiphilic molecules consisting of mannopyranose/erythritol as hydrophilic head group and fatty acid or acetyl group as hydrophobic moiety. Based on the position of acetyl group they are divided in 4 types. They have gained interest due to its emulsifying property and anti-microbial activity. However, the low product yield followed by tough downstream processing limits its application<sup>17,18</sup>.

Sophorolipids (SL) are produced extracellularly by non-pathogenic yeast. SL have gained tremendous interest as it is produced in large quantities by yeast, *Starmerella bombicola*. They are known to possess various natural properties like anti-bacterial, anti-cancerous, anti-viral and anti-fungal agent<sup>19,20,21,22</sup>. In addition to these, they are also finding application in the food, cosmetic and petroleum industry<sup>23</sup>. Nevertheless, high cost of production and substrate specificity limits the application of SL.

Apart from glycolipids, the other class of low molecular weight biosurfactants include lipopeptides. These are extracellular secondary metabolites secreted by bacteria *Bacillus*, *Pseudomonas* and *Arthrobacter* sp. Lipopeptides are composed of several amino acids bonded to fatty acid chain. Lipopeptides are used for cosmetic application as they have anti-wrinkle and anti-bacterial properties. Due to the low product yield, upscaling is difficult. Moreover, the bioavailability of lipopeptides is low as they are degraded due to the action of peptidases<sup>24-26</sup>.

Neutral lipids are synthesized by different organisms; *Corynebacterium*, *Thiobacillus* and *Nocardia* sp. Structurally it consists of a mixture of fatty acids linked to carbohydrate moieties. Owing to its low yield capabilities, they are not yet explored<sup>27</sup>.

Polymeric surfactants are high molecular weight compounds exhibiting good mechanical properties along with biological properties. Classic example of this is emulsan secreted by *Acinetobacter* sp. They find application in cosmetic and food industry<sup>28</sup>.

Category	Groups	Class	Organism	Yield (g/L)	CMC (mg/L)	Uses	Disadvantages	Ref
Low molecular weight	Glycolipids	Rhamnolipid	<i>Pseudomonas sp, Burkholderia sp</i>		60-110	Anti-microbial, Anti biofilm	Synthesized by Pathogenic strain, High cost of production	<sup>29, 30</sup>
		Trehalose lipid	<i>Rhodococcus sp, Nocardia sp, Arthrobacter sp, Gordonia sp</i>	40	0.14	Anti-microbial	Cost incurring down stream processing, Batch variation in product	<sup>31</sup>
		Cellobiose	<i>Ustilago sp, Cryptococcus sp</i>	Upto 30	-	Anti-microbial, Anti-fungal,	Tedious downstream processing	<sup>32</sup>

						Gelling property		
		Mannosyl erythritol	<i>Pseudozyma sp,</i> <i>Ustilago sp</i>	<60	33	Anti-bacterial, Anti-cancer	Tedious downstream processing	<sup>33, 18</sup>
		SL	<i>S.bombicola</i>	422	100	Anti-bacterial, Anti-fungal, Anti-cancer, Anti-viral	Cost of production	<sup>34, 35</sup>
	Lipopeptides	Surfactin, viscosin, Licheniformin	<i>Bacillus sp,</i> <i>Pseudomonas sp,</i> <i>Arthrobacter sp</i>	Upto 4	100	Chelation of heavy metals, Anti-microbial	Expensive downstream processing, Low yield	<sup>36,37</sup>

High Molecular weight	Neutral lipids	Phospholipid, fatty acids	<i>Corynebacterium sp, Nocardia sp, Thiobacillus sp</i>	2-3	-	Anti-bacterial	Low yield	<sup>27</sup>
	Polymeric	Emulsam	<i>Acinetobacter sp</i>	2-3	-	Anti-bacterial	Low yield	<sup>38</sup>

Table 1 Description of different classes of biosurfactants along with their proposed applications



Amongst the different classes of glycolipids, sophorolipids are widely studied due to its high yield and good physical properties. Sophorolipids (SL) display unique biological properties like anti-bacterial, anti-fungal, anti-viral, anti-cancer and cyto-compatible; thereby making them worthy for commercial market. Moreover, the robustness of yeast and their tailor-made synthesis allows incorporation of varied substrates into SL synthesis. To further explore their potential, the thesis work is focused on SL synthesis.

### **2.3 Sophorolipids:**

SL are produced extracellularly by nonpathogenic yeast. This section will discuss in detail about the production of SL's using various yeast strains, biosynthetic pathways for SL synthesis, physical, chemical and biological properties of SL's, different substrates used in SL synthesis and the current status of commercialization potential of SL's.

#### **2.3.1 Producer strain:**

SL were discovered in 1961 by Gorin *et al.* as extracellular biosurfactant synthesized by *Torulopsis magnolia*<sup>39</sup>. Later the strain name was declared as *Torulopsis*, *Torulopsis apicola* and *Torulopsis bombicola*. Further it was changed to *Candida bombicola* and now known as *Starmerella bombicola*. The other species of *Candida* producing SL are: *Candida floricola*, *Candida batistae*, *Candida rugosa*, *Candida kuoi*, *Candida tropicalis*<sup>40,41</sup>. Apart from *Starmerella*, the other organisms capable of producing SL are: *Wicherhamiella dimericqiae*, isolated from contaminated oil<sup>42</sup>, *Pichia anomala*, a thermo-tolerant yeast isolated from Thai food<sup>43</sup>, *Cyberlindnera samutprakarnensis* isolated from industrial wastes<sup>44</sup>.

#### **2.3.2 Physiological role of sophorolipid in nature:**

The yeast strain *S.bombicola* was inhabitant of foot pads of bumble bees. The honey bee wanders around and collect pollen from different flowering plants. The collected pollen is stored in the gut and transferred into the bee hive. The foot pads play active role in pollination process. As there is abundance of sugar content in the bee hive and foot pads, the strain developed inherent ability to utilize this and form SL. This process is known as the *de novo* synthesis i.e SL synthesis in absence of fatty acid/ lipophilic substrate.

As depicted in [Figure 2.2.1](#) the plausible reason for SL synthesis are:

a) Anti-bacterial agent - the collected pollen is stored in the form of pot pollen for feeding the bees. This is generally a mixture of nectar and fatty acids and proteins. SL have anti-bacterial activity, and hence help to preserve and maintain the pot pollen from contamination and thereby increase the shelf life of the pot pollen

b) Osmotic pressure reduction- Due to the high amount of sugar content, the osmotic pressure increases, SL being amphiphilic molecules assist in reducing the osmotic pressure<sup>45,46</sup>.

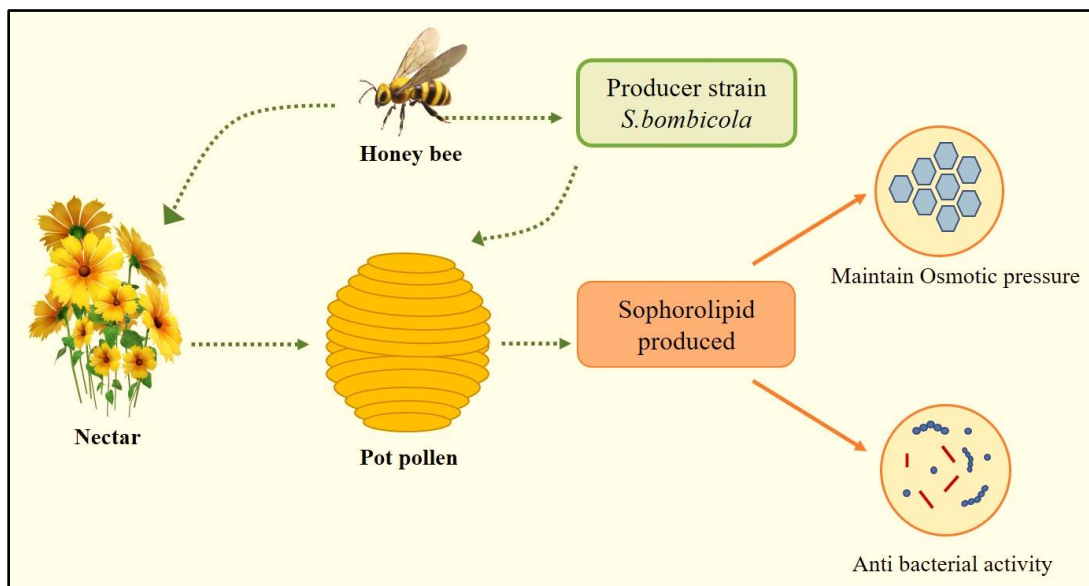


[Figure 2.2.1](#) Schematic describing the physiological role of sophorolipid in nature

### 2.3.3 Structure of sophorolipid:

The yeast strain *S.bombicola* produces copious amounts of secondary metabolites i.e sophorolipid. Sophorolipid synthesis occurs due to the enzymatic machinery of the yeast. With external supply of secondary carbon source, the product yield is significantly higher. Structurally it consists of hydrophilic polar disaccharide head group with  $\beta$  1-2 linkage, called sophorose, which is linked to hydrophobic tail chain length C16- C18. Hydroxylated fatty acid is linked to the moiety by ether linkage. The extracellular product obtained is a mixture of 2 components mainly: acidic and lactonic. Acidic sophorolipid have an open ring structure as the carboxylic end of fatty acid remains free, whereas the lactonic components are closed ring structure formed by internal esterification of carboxylic end of fatty acid to C4 of glucose molecule (Refer [Figure 2.2.2](#)). The ratio of acidic: lactonic depends on factors like: the fermentation conditions, substrate used and type of strain. Prolonged incubation often leads to higher lactonic percentage. The physical appearance of SL is dependent on the percentage of acidic : lactonic. Higher lactonic content yields crystalline product whereas high acidic produces viscous product. The other variation in SL involves acetylation of sugar at 6' &/or 6'' leading to mixture of different forms. The different structural types lead to variation in the physical properties of the molecule<sup>7</sup>.

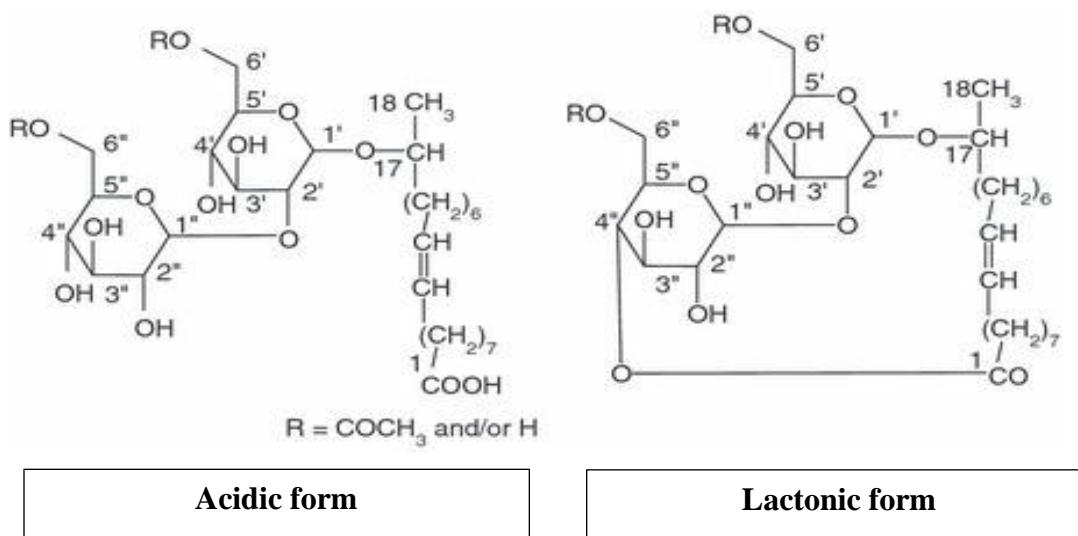


[Figure 2.2.2](#) Structural representation of different forms of SL; acidic and lactonic<sup>47</sup>

### 2.3.4 Biosynthetic pathway:

The yeast *S.bombicola* catalyzes the biotransformation of fatty acids into SL by inherent enzymatic machinery. The fermentation pathway adapted from Van Bogear *et al* is represented below (Figure 2.2.3). The primary components needed for sophorolipid formation are glucose and fatty acid. These are supplemented directly through media or indirectly by supplementing alkanes; which are then converted into fatty acids and then utilized for biosynthesis. First step of biosynthesis begins by activation (Hydroxylation) of the fatty acids. In yeast the hydroxylation (terminal[ $\omega$ ] or sub terminal [ $\omega-1$ ]) is carried by cytochrome P450 monooxygenase. This enzyme mediates hydroxylation of alkanes and/or fatty acids with the help of NADPH. The resulting fatty acids are utilized by the cell<sup>48</sup>. If no hydrophobic substrate is provided through the media, the yeast will synthesize its own fatty acids and then produce sophorolipid. This process is known as *de novo* synthesis. Upon conversion of fatty acids into hydroxy fatty acids, two UDP activated glucose molecules are added serially. Glucose molecule is glycosidically (C1 position) linked to  $\omega$  or  $\omega-1$  hydroxyl group of fatty acid by enzyme glycosyltransferase I. Similarly, second glucose molecule is glycosidically coupled to the C2 position of first glucose moiety by action of glycosyltransferase II. These transferases utilize nucleotide activated glucose (UDP- glucose) as glucosyl donor. The hydrophobic fatty acid tail binds to the sophorose moiety by ether bond thereby forming a rigid backbone structure of SL. After glucosylation, acidic non acetylated molecules are obtained. There are other certain modification or variations caused by acetylation and lactonization. Acetylation at 6 ' and /or 6'' is governed by acetyl coA dependent acetyl transferase. Lactonization happens between the carboxylic end group of fatty acid and C4 of glucose. This reaction is mediated by lactone esterase<sup>49</sup>.

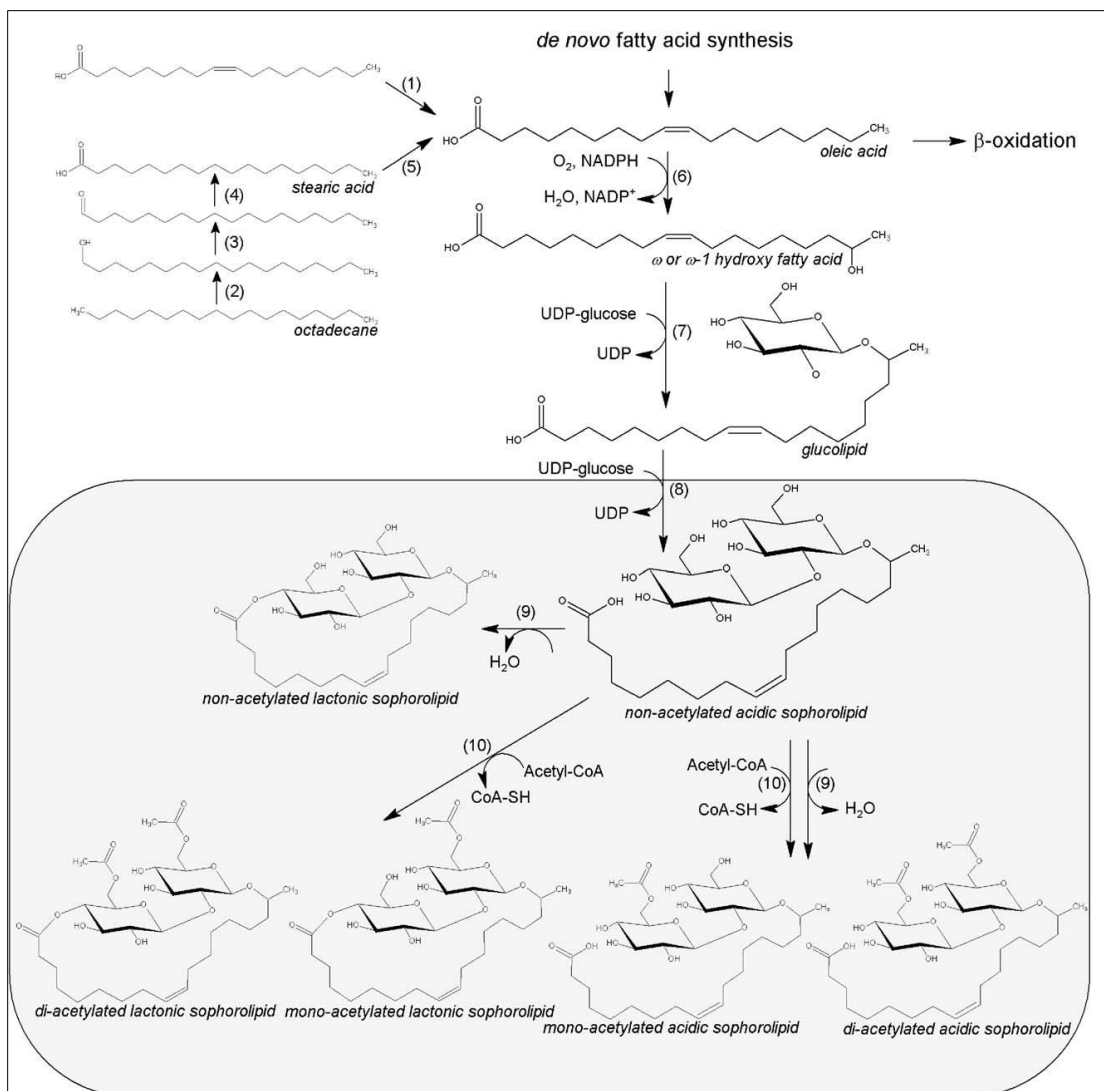


**Figure 2.2.3 :** Step wise biosynthetic pathway of SL. Different enzymes involved are: 1.Cytochrome P450 monooxygenase, 2.Alcohol dehydrogenase, 3.Aldehyde dehydrogenase, 4.Lipase, 5.Cytochrome P450 monooxygenase, 6.Glucosyltransferase I, 7.Glucosyltransferase II, 8. Lactone esterases, 9. Acetyl transferase

### 2.3.5 Market scenario:

The unprecedented and staggering impact of COVID -19 led to tremendous increase in the demand for surfactant. The annual demand for surfactants is now expected to reach more than 45 million tons by 2025. To meet the growing needs, the market for biosurfactants is highly rising. Amongst

the different biosurfactants produced SL contribute significantly to the global usage of biosurfactants. More than 100 patents have been filed and numerous papers are published on sophorolipid synthesis and fermentation<sup>50</sup>. Refer Figure 2.2.4. The potential of these products to be safe and biodegradable significantly triggered to capacity expansion, resulting into launch in commercial market. Not only in the academic sector, SL have now paved their way into the commercial market and are commercially produced by certain companies like Ecover (Belgium), Soliance (France), Kaneka (Japan) and Saraya (Japan) for applications in detergents and cosmetics<sup>51</sup>.

Although the commercial market for SL seems promising, certain drawbacks associated with it need to be addressed. The main disadvantage is the price of commercial sophorolipid. The price of common chemical surfactant (SDS) in bulk falls in the range of 100-140 Rs /kg whereas the cost of sophorolipid is in between 2000-2500 Rs/kg [<sup>34</sup>]. This major difference in the price isn't economically viable. Of the total cost, 60-70 % refer to raw material/ feedstock and rest 30-40% includes the fermentation process and downstream processing. Thus, research in this field aims is focused on reducing the production cost of SL by investigating renewable and low-cost substrates, optimizing the process and improving the strain for enhanced production.

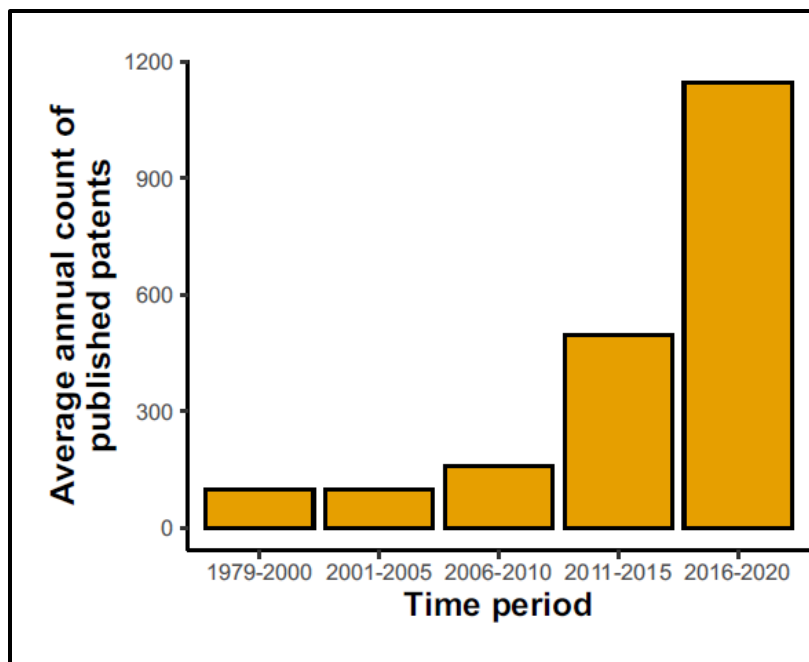
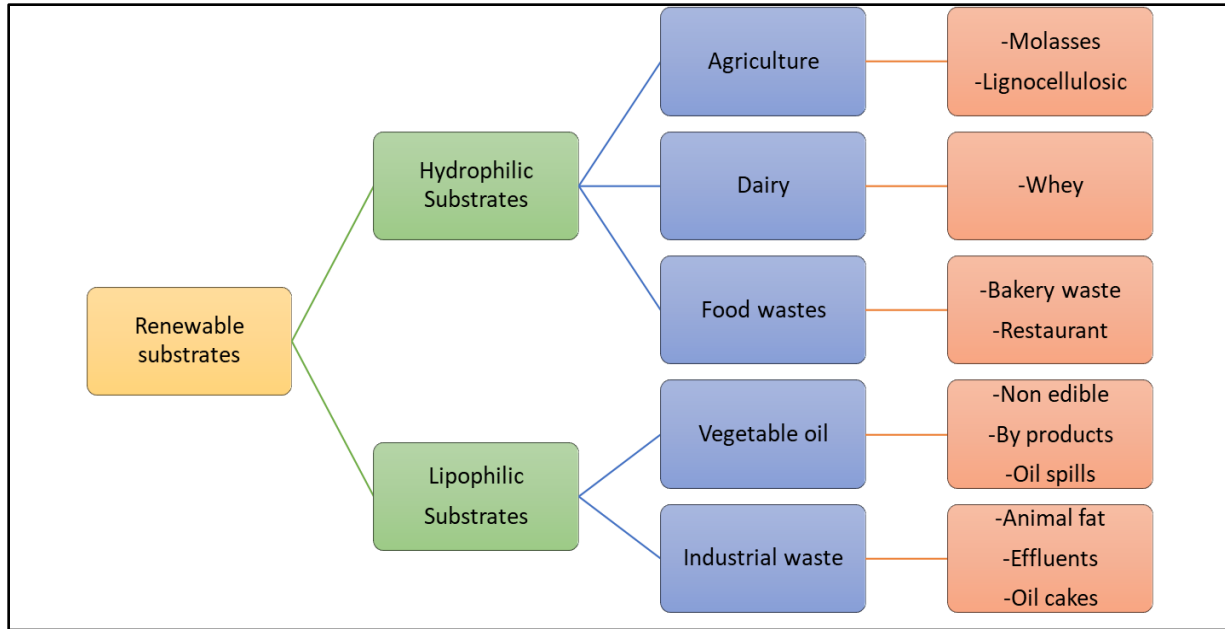


Figure 2.2.4 Graph depicting the number of patents being filed each year up to 2020 on SL<sup>46</sup>

### **2.3.6 Substrates used for sophorolipid synthesis:**

As mentioned earlier, the bioprocess for SL synthesis requires hydrophilic and lipophilic substrates. An interesting property of SL is the tailor-made synthesis i.e by varying the substrate, SLs with varied physiochemical properties can be synthesized. Changing either the lipophilic or hydrophilic substrate results in different sophorolipid.

Up till now various substrates from different sectors have been identified for synthesizing SL. Low-cost substrates from different sectors namely agriculture, dairy, vegetable oil, industrial and food have been discussed. Sectors like agricultural, dairy and food waste contribute for hydrophilic substrates and vegetable oil and industrial wastes contribute as lipophilic components for sophorolipid synthesis (Figure 2.2.5). Each sector has been individually discussed below:



**Figure 2.2.5** Schematic representation of renewable substrates identified from different commercial sectors

### 2.3.7 Hydrophilic substrate:

Mentioned below are the different sectors that generate significant wastes which could possibly be used as hydrophilic sources for sophorolipid production.

#### 2.3.7.1 Agricultural Sector:

Agricultural products like wheat bran, rice bran, molasses, bagasse, corn fiber, cassava and beet molasses are some of the relatively cheaper substrates available as carbon sources for the sophorolipid production. Such wastes are rich in carbohydrates and lipids and thus could be used for microbial growth and sophorolipid production <sup>52</sup>.

Molasses, byproducts of sugar production obtained from sugarcane, soy and beet. Molasses consists of water, sugar, lipids, non-sugar content and minerals. Sophorolipid production was carried out using sugarcane molasses and soybean oil in fermenter, the yield obtained was 63.7



gm/L after 60h of fermentation. The fermentation cycle was continued up to 120h but maximum yield was obtained at 60h<sup>53</sup>. Sophorolipid synthesis using sugarcane molasses and coconut oil was carried out by Houngh *et al*, the yield obtained was 12 gm/L. The low yield is attributed to the chemical composition of coconut oil<sup>54</sup>. Another study on molasses was performed by Takahashi *et al*, in this molasses was used as the only source of substrate. No external lipophilic substrate was added. The yield thus obtained was 23 gm/L. As molasses itself possesses lipid and sugar content, it was used as the only source. *C.bombicola* was able to utilize this substrate and convert it into sophorolipid successfully<sup>55</sup>.

Apart from sugarcane molasses, soy molasses has also been tried as substrates for sophorolipid synthesis. Soy molasses along with oleic acid as lipophilic source have been studied by Soliaman *et al*, the product yield obtained was 75 gm/L and 53 gm/L<sup>56,57</sup>. Soy molasses are byproducts of soybean processing. It contains 30% carbohydrates and small amount of lipid content. Similarly, rice bran and wheat bran have also been used as hydrophilic substrate along with jatropha oil<sup>58</sup>. The yield obtained was 122 gm/L after 9 days of fermentation. Despite higher yield, the lipophilic source used here (Jatropha oil) contains toxin like curcumin and phorbol esters (PE). These toxins were present in the final product and complete elimination is possible by subjecting the sophorolipid to alkaline hydrolysis which thereby increases the cost of production<sup>59</sup>.

Efforts are being made to synthesis sophorolipid using lignocellulosic waste like corn cob, sorghum bagasse, corn stover hydrolysate along with lipophilic substrate. Abundant lignocellulosic wastes are generated, which are renewable and rich source of cellulose, hemicellulose and lignin. The composition of hydrolysate is complex, consisting of sugar and non-sugar moieties. Sorghum bagasse hydrolysate contains sugars like glucose, xylose and arabinose and non-sugar components like acetic acid, luteic acid, and formic acid. These components might hinder with the fermentation process of SL. Interestingly, bioprocess performed using sweet sorghum bagasse and corn fibers as carbon sources and soybean oil as lipophilic sources resulted in a yield of 84 and 15 gm/L respectively. These results confirm that *S.bombicola* (formerly known as *C.bombicola*) is able to successfully convert mixed lignocellulosic waste supplemented with 5 and 6 C sugars into SL. Similarly, only corn cob hydrolysate along with glucose and olive oil

yielded 33 gm/L of SL<sup>41</sup>. Among the lignocellulosic waste, sorghum baggase provides better yield of sophorolipid. However, despite good yield of sophorolipid production, lignocellulosic wastes are not that preferred substrates as it requires pretreatments which are time consuming and cost incurring<sup>60,61</sup>.

### 2.3.7.2 Dairy wastes:

Dairy industries produce large quantities of whey that includes, curd whey, whey waste, cheese whey and lactic whey, all of these are readily available as raw substrates for metabolites production. Whey is composed of lactose, vitamins, proteins and organic acids. It is a waste product obtained from cheese production that represents a major pollution problem for countries depending on dairy economics and is otherwise used as an animal feed.

In order to utilize whey as substrate material, the chosen organism must be able to consume lactose and its breakdown products, glucose and galactose<sup>62</sup>. Interesting studies have been reported regarding use of whey as hydrophilic substrates for sophorolipid production. A study by Zhou *et al* reports that sophorolipid is synthesized successfully by using lactose and olive oil. The inbuilt lactose transport system and lactase enzyme present in the yeast, facilitates sophorolipid synthesis. Similarly, SL have been produced by a 2 step process using deproteinized whey as carbon source and rapeseed oil as the lipophilic source. In initial studies it was found that *C.bombicola* was ineffective in utilizing lactose component completely. The same research group then used another yeast, *C.curvatus*. The yeast was grown on whey substrate, wherein of lactose was consumed completely and biomass as well as intracellular triglycerides were produced. These cells were the harvested and disrupted. The crude contents were then used as feed for *C.bombicola* along with lipophilic substrate. This method yielded 422 gm/L of SL<sup>63,64,65</sup>. Similarly, deproteinized whey with oleic acid was also studied by Davarey *et al*, in 1 step process. The yield thus obtained was 33 gm/L<sup>66</sup>.

s

These reports confirm that SL can be synthesized using lactose and other sugars. The extracellular supply of sugars activates RAS/PKA pathway in yeast. This pathway allows incorporation of several sugars like glucose, sucrose, lactose, and fructose which thereby facilitate SL synthesis. Though the yield obtained is high, the pretreatment of whey and the fermentation processes are cumbersome.

### **2.3.7.3 Food waste:**

Another abundantly available hydrophilic feedstock are food wastes. This includes the left-over food and spoiled food which are generally biodegradable but amount in which they are generated is a matter of concern. Food waste accounts for 30-50 % of total solid waste globally. Food wastes are rich in nutrients which could be used for production of different metabolites and industrially important compounds. It contains bakery wastes, restaurant waste over and liquid based wastes.

As these wastes are complex in nature, enzymatic pretreatment is needed prior to fermentation process. The yield obtained by using hydrolyzed food waste with oleic acid is 115 gm/L. A comparative study conducted by Wang *et al*, concluded that bakery wastes (bread,pastry,cake) have higher potential to produce sophorolipid than restaurant waste (chicken, egg, noodles, rice) <sup>67,68</sup>.

## **2.3.8 Lipophilic Substrates**

### **2.3.8.1 Oils**

The yeast *S.bombicola* is robust enough to incorporate varied lipophilic substrates. SL produced by *de novo* synthesis comprises of oleic acid and therefore it is the most preferred substrates. However, refined fatty acids or oils are expensive. Upscaling of similar condition is practically not possible. To cut down the cost, low-cost lipophilic substrates could be used. Various vegetable oils and oil residues from industries and waste water represent as renewable substrates for production of microbial surface-active agents. Efforts have been made to synthesize SL using non edible and different vegetable oils like: Non edible castor oil was used as lipophilic substrate with glycerol as

hydrophilic substrate to yield 40 gm/L of sophorolipid. The castor oil gets hydroxylated at  $\omega$ - 1 position and result in SL production <sup>69</sup>. Similarly, coconut oil supplemented with molasses and glucose as carbon source resulted in 2-3 gm/L of SL<sup>70</sup>. Use of meadowfoam oil along with glucose yielded 16 gm/L of SL <sup>71</sup>. The low yield thus obtained are mainly due to the composition of oil, which proves to be toxic to the yeast cells thereby hampering the SL production.

Corn oil which is a byproduct of corn processing units contains mainly linoleic acid. The yield obtained by using corn oil and glucose is 3 gm/L<sup>72</sup>. Similarly, sunflower oil when utilized as the sole lipophilic source yield, 12 gm/L of SL, whereas when it is added along with soybean oil the yield increases to 49 gm/L. Supplementation of additional lipophilic components (Soybean oil) helps to increasing the biomass thereby the conversion is higher<sup>73,74</sup>. Safflower oil when utilized as the sole lipophilic source yield, 48 gm/L of SL<sup>75</sup>.

Oil spills a major problem on global level and these oils are difficult to dispose due to environmental concerns like persistence and resistance to biodegradation. Utilization of these oil spills into useful products is extremely beneficial. Various other crude oils like tapis, melita and ratawi which are associated with oil spills were used as lipophilic substrates with glucose for SL synthesis. The yield obtained from respective oils are 26, 21 and 19 gm/L <sup>76</sup>.

Amongst the different sole lipophilic sources used, highest production of SL is obtained by using rapeseed oil. Rapeseed oil used in automotive and chemical industries is rich in linoleic acid. The yield obtained on supplementation of glucose is 600 gm/L whereas with molasses as carbon source the yield obtained is 280 gm/L <sup>77</sup>.

### **2.3.8.2 Industrial wastes:**

Meat processing industries like food, leather produce significant quantity of animal fat. Compared to vegetable oil, the demand for animal fat is considerably less and much of it becomes a problem as it is difficult to dispose <sup>78</sup>. An alternate option for such product is utilization as raw material for commercial metabolites compounds. Animal fat has been reported to act as stimulator for

sophorolipid production. The yeast *S.bombicola* is able to grow on the mixture of glucose and animal fat and stimulate SL synthesis. The yield obtained by this is 120 gm/L<sup>79</sup>.

Waste water generated from dairy industries are rich in carbohydrates and oils which to some extents are difficult to degrade. Dairy waste water supplemented with soybean oil yielded 62 gm/L of sophorolipid<sup>80</sup>. The deciding factor for alternative sources is that the substrates should promote growth of the organism and product accumulation. Cassava waste water generated from cassava plantations contains sugar and mineral essential for growth of yeast. Cassava water supplemented with soybean oil yielded 200 gm/L of SL<sup>81</sup>.

Majority of the edible oils, vegetable oils, saturated and unsaturated fats are routinely used by food processing industries. Once the oils are processed for food production, the residues become harmful pollutants for the environment. Waste from food industries contain high amount of carbohydrates and fats which act as base material for fermentation process<sup>82</sup>. Restaurants utilize gallons of oil each week for various purposes. With this huge amount available, fermentation process can be carried out using this as substrates. Restaurant oil waste supplemented glucose was used to synthesize sophorolipid. The yield thus obtained was 34 gm/L<sup>83</sup>. Similarly, waste frying oil extracted from the grills and deep fryers were used as raw materials. The fermentation media was supplemented with glucose and yielded 49 and 55 gm/L SL<sup>84,85</sup>. Oil refinery waste along with glucose yielded 50 gm/L of SL<sup>86</sup>.

Similarly, oil cakes are semisolid gummy products produced from oil processes by chemical extraction. The oil cakes are rich sources of fats and oils. Oil cakes have no potential application apart from being used as raw materials. Various oil cakes are generated like: sunflower, soybean, corn oil, olive oil and rapeseed oil. Of these some of them are used for SL production. A byproduct of soybean oil processing is a black colored oil known as soybean dark oil (SDO) which is inedible in nature. In a study by Wadekar *et al*, SDO was evaluated for synthesizing SL by supplementation of glucose. The product synthesized by these substrates was 90 gm/L<sup>87</sup>. Similarly, sunflower oil along with glycerol as the hydrophilic substrate was used to obtain a yield of 7 gm/L. Also, beet molasses along with residual oil cake generated a yield of 8.5 gm/L<sup>88</sup>.

### 2.3.9 Properties of SL:

#### 2.3.9.1 Self-assemblies of SL:

Amphiphiles have the inherent ability to self-assemble into variety of structures including micelles, vesicles, nanotubes, nanofibers and lamella. These assemblies resemble with the biological systems of cells like the lipid membrane, protein coat etc. and hence are studied widely<sup>89</sup>. Self-assemblies of SL have been well reported. Self-assembly can be defined as the ability of surfactants to form specific arrangements driven by self-interactions between themselves beyond a certain concentration (Critical micellar concentration)<sup>48</sup>.

The asymmetric structure of acidic sophorolipid consisting of bulky carbohydrate head group linked to lipophilic tail group with pH responsive carboxylic acid renders this particular congener attractive for self-assemblies. Apart from this the acidic component possess higher solubility than lactonic form. Thus, there are few reports available on self assemblies of lactonic form.

In aqueous environment, acidic SL are capable of forming different shaped assemblies like ribbons, rods and spherical micelles. The shape of assemblies depends on various factors like pH, temperature, concentration, chain length of fatty acid and degree of unsaturation of fatty acid<sup>90</sup>. Zhou *et al* were the first to report the self-assemblies of SL with respect to pH and time<sup>91</sup>. Later, the effect of lipophilic substrate on assemblies was reported by Dhasiyan *et al*. As per the reports; at similar conditions, stearic acid resulted in flat sheet like structures while eladic acid formed twisted ribbon and oleic acid resulted in ribbon like structure. The molecular geometry of fatty acids ( $\pi$ - $\pi$  stacking and packing structures) influences their assemblies<sup>92</sup>. Later, the same group conducted reported the extensive studies on pH dependent self-assemblies of cis and trans form of C18; i.e stearic acid and eladic acid to deduce the helical structure of the assemblies<sup>93</sup>. Apart from this, self-assemblies of oleic acid derived SL are widely studied including stimuli responsive assemblies, assemblies at basic pH range, nature of assemblies on dip coated surfaces and as structure directed agents for nanostructured films.

### 2.3.9.2 Anti-microbial activity:

The interesting factor about SL promoting their wide application is the anti-microbial activity. Various studies over the last decade have validated this fact that SL possess good anti-microbial activity against bacteria, fungi, algae and viruses.

Various studies report that these glycolipids are capable of inhibiting both gram positive (*Staphalococcus aureus*, *Bacillus subtilis*, *Propionobacterium acne*) and gram negative bacteria (*Pseudomonas aeruginosa*, *Slamonella typhimurium*, *E.coli*)<sup>19</sup>. Extensive research over the years established that the activity is more pronounced against gram positive bacteria as compared to gram negative, owing to the difference in the structural orientation of the two organisms. Here the amphiphilic nature of SL affects the permeability of the bacterial cell membrane thereby leading to leakage of intracellular components. Due to the presence of rich peptidoglycan layer in the gram-positive bacteria, they are more susceptible to inhibition than gram- negative bacteria<sup>48</sup>. The methods for assessing the anti-bacterial activity are also well documented, these include: Well diffusion assay, disc diffusion assay, contact method, malate dehydrogenase assay and ethidium monoxide staining<sup>94,95</sup>.

Efforts are now being made to understand the relationship between the nature of substrate (lipophilic substrate, hydrophilic substrate) and their biological properties. Abhyankar *et al*, reported that altering the head or tail groups, affect the physical and biological properties of the synthesized SL. Along with nature of substrate, ratio of lactonic to acidic drives the anti-bacterial property<sup>96</sup>.

Apart from this, SL's synthesized by using essential oils as substrates possess ability to disrupt the biofilm formation by hampering the quorum sensing activity of bacteria indicating their potential use to tackle multidrug resistance in bacteria. Similar studies have been reported wherein the anti-biofilm activity, anti-adhesive property of SL have been assessed<sup>97</sup>.

Anti-fungal activity of SL's has also been studied. As reported by Hipolito, SL are effective in inhibiting different fungi like: *Aspergillus* sp, *Fusarium*, *Rhizopus* sp and *Botrytis* sp<sup>98</sup>. SL are also efficient in killing different phyto pathogens like: *Phytophthora* sp, *Pythium* sp, *Trichophyton* sp and *Fusarium* sp. The mechanism involved in inhibition of fungal cell wall is yet to fully understood<sup>99</sup>.

Moreover, effect of SL on algal bloom mitigation has been reported by Sun *et al*<sup>100</sup>. Anti-viral activity of SL has also been documented by Shah, 2005 wherein they evaluated anti-viral activities of different congener of SL. It concluded that, surfactant property of SL hampers the sorption of viruses on the surfaces, thereby inhibiting the viruses<sup>101</sup>. Similar reports by Mukherjee *et al*, highlights the effects of SL on viral protein coat<sup>21</sup>. Quite recently, Daverey *et al* proposed the use of SL against the novel corona virus. However, there are no concrete results to verify this fact<sup>102</sup>.

### **2.3.9.3 Anti-cancer activity:**

Anti-cancer activity of SL from varied substrates has been reported against different cancer cells. Fu *et al* demonstrated the anti-cancer activity of different derivatives of SL against pancreatic carcinoma. The study revealed dose and structure dependent anti-cancer property. Ethyl diacetate ester proves better than lactonic and acidic forms of SL<sup>103</sup>. Another study demonstrated the effect of degree of unsaturation of fatty acids and acetylation pattern on esophageal cancer by Shoan *et al* wherein, lactonic diacetylated congener was reported to be most cytotoxic<sup>104</sup>. Apart from this, the effects of diacetylated lactonic congeners obtained from different substrates (C16, C18, C18:0, C18:1) have been studied against cervical cancer. Chain length of substrates influences their cytotoxicity<sup>104</sup>. Similar studies were conducted by Rebeiro *et al*, to understand the effect of diacetylated congeners synthesized by substrates with varying degree of unsaturation on breast cancer cell line. These reports suggest that the lactonic congeners with (C18:1) substrate prove more lethal to the cancer cells<sup>105</sup>. Comparative studies involving two SL synthesized by different substrates against different cancer cells has been reported by Dubey *et al*. Herein, the cetyl derived SL proves better for breast cancer and Oleic acid derived sophorolipid was more potent on cervical



cancer<sup>106</sup>. These findings suggest that the specificity of SL towards cancer cells, largely depends on of nature of substrate used.

The underlying mechanism of anti-cancer activity of SL have been deduced by various studies. Study by Chen *et al* on-liver cancer cell line (H7402) revealed that SL induce apoptosis into the cancerous cells<sup>42</sup>. Rebeiro *et al* reported the apoptosis in cancer cells by other apoptotic markers like reduction in nitric oxide content and reduction in cell migration of MCF -7 (breast cancer) on treatment with SL<sup>105</sup>. Apart from inducing apoptosis, SL promote cell differentiation in glioma cells, as reported by Joshi *et al*. Cancer cells have uncontrolled cell division, therefore differentiation of these cells reverses the primary action. This unique property of sophorolipid has only been reported against brain tumor and by using oleic and linoleic acid derived SL<sup>20</sup>.

### **2.3.9.4 Anti-inflammatory activity:**

Apart from anti-cancer activity, SL also possess anti-inflammatory activity. SL synthesized by *S.bombicola*, has been employed to cure sepsis infection. Bluth *et al* demonstrated the ability of SL to modulate inflammatory responses. SL caused reduction in nitric oxide levels and down regulates the expression inflammatory cytokines IL-1 and IL-8<sup>107</sup>. The same (Hardin *et al*) group conducted comparative studies to analyze the effect of different SL (Lactonic, acidic and ethyl ester) on sepsis. Treatment with SL, resulted in increased survival rate by 28 % within 24h and down regulation of pro inflammatory ctyokines<sup>108</sup>. Subramaniam *et al* reported that SL down regulate the IgE coding gene thereby acting as an anti-inflammatory molecule<sup>109</sup>. Shah *et al* demonstrated the spermicidal and anti-viral property of diacetylated ethyl ester form of SL. Reduction in the levels of pro inflammatory cytokines was reported<sup>101</sup>.

Inflammation is the cumulative effect of signals from different cells of immune system. Onset of inflammation causes release of ctyokines and interferons. Rodriguez demonstrated the ability of SL to induce transition of macrophages, from M1 phase to M2 phase (Pro- inflammatory to anti-inflammatory)<sup>110</sup>. These properties render SL extremely beneficial for implant surgeries to minimize the chances of graft rejection.

### 2.3.9.5 Nanoparticle synthesis:

The amphiphilic nature of SL paved a way for them into nanotechnology. Apart from this, biodegradability, non-toxicity of SL gained interest over time. Non - dispersity of nanoparticles in aqueous solution limits their potential. Kasture *et al* reported synthesis of cobalt nanoparticles using sophorolipid as reducing and capping agent. SL synthesized nanoparticles exhibited better solubility than control nanoparticles as the free sugar moiety of SL remains available for solvent interaction, thereby enhancing the solubility of nanoparticles<sup>111</sup>. Another study from same group reported the effects of lipophilic substrate on physiochemical properties SL. As SL act as reducing agent, the structural orientation of SL hinders its binding to the metal ion thereby affecting the morphology of nanoparticles. Herein, higher degree of unsaturation resulted large sized nanoparticles. Moreover, the anti-bacterial property of SL enhances the applicability of synthesized nanoparticles as well<sup>112</sup>. Baccile *et al* reported the potential of acidic SL for synthesizing iron oxide nanoparticles. The open structure of acidic SL assists in stabilizing the nanoparticles. Resulting carbohydrate coated iron oxide nanoparticles are biocompatible with increased dispersity<sup>113</sup>. Other nanoparticles synthesized by acidic SL are zinc oxide nanoparticles with efficient anti-bacterial activity against *Salmonella enterica* and *Candida albicans*<sup>114</sup>.

Apart from metallic nanoparticles SL have been used to obtain solid/ liquid nanoparticles. These types of nanoparticles act as encapsulating cargos for hydrophobic drugs. Presence of SL increases the entrapment efficacy, solubility, slow-release kinetics and improved availability of entrapped drugs<sup>115</sup>.

### 2.3.10 Applications of SL in varied sectors:

Surfactants have been primarily used for cleaning. Their demand increased drastically during the world pandemic situation. The deleterious effects of chemical surfactants on the environment and health promotes use of biosurfactant for varied applications. Owing to their varied biological

properties, SL gained application in various sectors. The different sectors incorporating SL are listed below:

### **2.3.10.1 Use of SL as cleansing agent.**

Application of SL as an ingredient for laundry detergent was discovered by Hall *et al* and Furuta *et al*<sup>116,117</sup>. Individual forms, acidic and lactonic and mixtures were incorporated into the detergent formulations. Later, SL synthesized from Jatropha oil was explored for stain removal from material. SL not only removed the stain efficiently but also was skin friendly<sup>118</sup>.

SL have also been used commercially for cleansing purpose; Sidolin, a product of German based company Henkel has been employing sophorolipid for glass cleaning formulations. Sophoron, commercially available low foam dish washer detergent synthesized by Saraya company<sup>51</sup>. Sophab, an instant vegetable wash employing SL has been commercialized by Green pyramid, India

### **2.3.10.2 Use of SL for bioremediation:**

Hydrocarbon contaminated soil with poor biodegradability was flushed with SL. Interestingly, the biosurfactant increased the extraction of hydrophobic contents through micellar solubilization and mobilization, resulting in increased bioavailability of microbial consortia for biodegradation. Moreover, the flushing efficiency was higher than commercial surfactant<sup>119</sup>. Feng *et al* reported that with SL, the total petroleum hydrocarbon removal attained 45 % as compared to 12 % by other commercial methods. SL assist in enhancing the desorption of pollutants into the aqueous phase, leading to increased bioavailability for degradation<sup>120</sup>. Similar studies were conducted by Minucelli *et al* where SL were employed for hydrocarbon and diesel oil removal. Emulsification and solubilization property of SL increased the pollutant removal from the contaminated soils<sup>121</sup>. Qi *et al* incorporated acidic SL into heavy metal contaminated soil. Higher surfactant ability of acidic form resulted in removal for heavy metals from soil. Nearly 84 % Cadmium and 45 % Lead

were extracted out from the soil. The free end of acidic congener complexes with the Cadmium ion thereby leading to removal as confirmed by structural analysis<sup>122</sup>.

### **2.3.10.3 Use of SL in cosmetics:**

Emulsifying abilities microbial based surfactants are useful for cosmetic application. Cho *et al* highlighted the skin exfoliating and moisturizing abilities of SL. A dose dependent effect with increasing concentration of SL was reported<sup>123</sup>. Apart from these, other effects imposed by SL on skin surfaces are; promote dermal fibroblast metabolism, collagen neosynthesis, reduce the inhibitory effects of free radicals, fibrinolytic properties, depigmenting agent, desquamating agent, assist in reducing subcutaneous fat overload. Due to these attributable properties, SL have been employed in lip cream, lip rouge and eye shadow. Lip gloss from water-in-oil emulsion was formulated with sophorolipid as stabilizer. Addition of SL into toothpaste formulation depicted similar properties like foamability, cytotoxicity and anti-bacterial activity as commercial<sup>124,125</sup>.

SL have also been synthesized using hydrophobic substrates mimicking the normal skin. Maeng *et al* synthesized SL using horse oil. Horse oil essentially contains unsaturated fatty acids like linoleic and palmoleic which are compatible to skin. The synthesized sophorolipid exhibited excellent anti-bacterial, anti-wrinkle properties. Moreover, it promoted proliferation of dermal fibroblasts<sup>126</sup>.

### **2.3.10.4 Use of SL in food industry:**

The wide stability of SL; thermotolerant, halotolerant and alkalotolerant coupled with good emulsifying ability makes them potential candidate for food industry. Gaur *et al* reported the anti-bacterial activity of sophorolipid against different food borne pathogens<sup>127</sup>.

SL have been employed in food industry for various structural and textural attributes; to control the agglomeration of fat globules, facilitate aeration, improve texture of starchy products. Solubilization ability of SL help in managing consistency, anti-spattering and mixing of flavor in

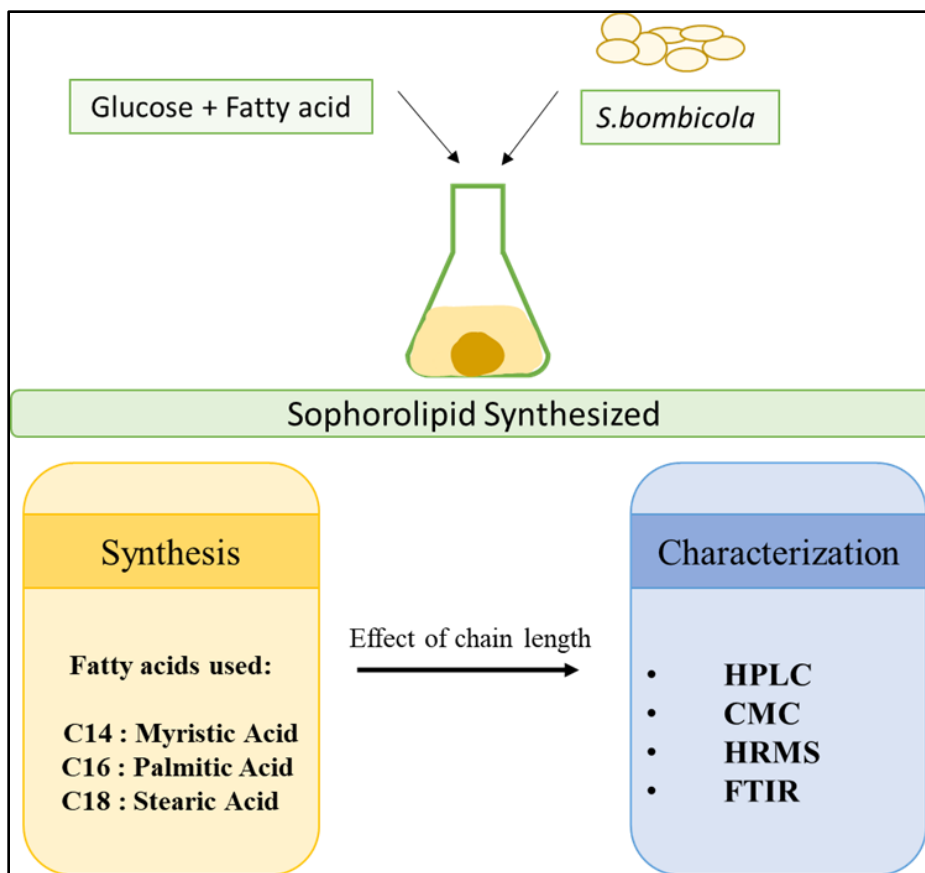
bakery and ice cream products. Moreover, the anti-bacterial activity of SL helps to improve the shelf life of vegetables, fruits and prevent staling of foods, thereby preserving the foods<sup>3</sup>.

Due to these properties SL have now been used for packaging applications. Hipolito casted films for food packaging using SL. These films were thermotolerant, flexible and anti-bacterial. These diverse properties provide newer opportunities to further explore the potential of SL<sup>128</sup>.

## Chapter III

### **Deciphering the effect of chain length of substrates on sophorolipid production through physio-chemical characterization**

SL are a class of biomolecules synthesized by non-pathogenic yeast *S.bombicola*. In this work we have synthesized SL using unconventional lipophilic substrates like myristic acid along with palmitic acid and stearic acid. The synthesized SL were thoroughly characterized by different spectroscopic and chromatographic techniques. The aim was to understand the effect of chain length of substrate on SL production. Further, the objective was also to study the chemical and physical properties of these SLs.



### 3.1 Introduction

SL belong to glycolipid class of biosurfactants and are synthesized extracellularly by non-pathogenic yeast *S.bombicola*. Similar to synthetic surfactants SL exhibit physiological properties such as detergency, lowering surface tension, emulsification, foaming and wetting ability. SLs have emerged as promising substitutes for petroleum-derived conventional surfactants as they are biodegradable, non-toxic, and cost-effective<sup>10,49</sup> These molecules have good surface biological properties such as antibacterial<sup>129</sup>, antifungal<sup>22</sup>, antiviral<sup>21</sup>, and anticancer properties<sup>106</sup>. Moreover, they also facilitate nanoparticle synthesis and possess self-assembling ability.

### Chapter III : Deciphering the effect of chain length of substrates on sophorolipid production through physio-chemical characterization

---

Despite their varied properties, the potential reasons for their restricted use in commercial market are high cost of production and diversity in physical properties of synthesized SL. To overcome this, efforts have been made to synthesize SL using different renewable hydrophilic or hydrophobic substrates. Glucose is commonly used as hydrophilic substrate; as it consumed easily by the yeast. However, the large quantities needed for synthesis, are cost incurring. Researcher have now explored the used of cheaper hydrophilic substrates for SL productions including lignocellulosic waste, whey, bagasse and molasses. Davarey *et al* reported a yield of 63 g/L using molasses as hydrophilic substrate and soybean oil as hydrophobic substrate<sup>79</sup>. Another study by Ma *et al* reported yield of 422 g/L using whey as hydrophilic substrate and rapeseed oil as hydrophobic substrate<sup>130</sup>. Although the yields seem promising, the pretreatment needed for lignocellulosic wastes to be used as hydrophilic substrates is cost incurring. Moreover, multiple cultures are required for obtaining the desired yield.

Similarly, alternative hydrophobic substrates have also been explored for SL synthesis including soybean oil, coconut oil, rapeseed oil and waste frying oil. Nooman *et al* reported yield of 48 g/L by using glucose as hydrophilic substrate and safflower oil as hydrophobic substrate<sup>75</sup>. Apart from this, SL have also been synthesized using different essential oils like Jatropa , Lemongrass, Peppermint, Cinnamon, Rosemary, Basil, Bergamot, Eucalyptus, Orange, Citronella, Tea tree, Ylang ylang, Frankincense<sup>96</sup>. However, the basic composition of primary lipophilic substrates dominantly consists of C16-C18 fatty acid chain (Table 2). This preferred range of chain length of fatty acid for SL synthesis is attributed to (i) the substrate specificity of the enzymes; cytochrome P450 monooxygenases (CYP52M1) and uridine diphosphate glucosyltransferase (UGTA1) and (ii) high preponderance of C18 in the *de novo* product<sup>48</sup>. Moreover, Van Bogeaert reported the ill effects of shorter chain fatty acid (C8–10) on the yeast cell growth and yield of SL. Therefore, SLs are commonly synthesized using fatty acids with 16–18 carbon atom chains<sup>71</sup>. The Table 2,3 describe the composition of different lipophilic substrates.



## Chapter III : Deciphering the effect of chain length of substrates on sophorolipid production through physio-chemical characterization

Oils	Composition of fatty acids (%)				
	Palmitic	Stearic	Oleic	Linoleic	Linolenic
Soybean	10	4	18	55	13
Mahua	18	14	46	18	-
Jatropha	15.4	6.2	45	33.4	-

**Table 2** Chemical composition of commonly used lipophilic substrates for sophorolipid synthesis

Oil	Composition of fatty acids (%)							
	Caprylic	Capric	Lauric	Myristic	Palmitic	Stearic	Oleic	Linoleic
Coconut	8	7	49	8	8	2	6	2

**Table 3** Chemical composition of coconut oil as lipophilic substrate

Majority of the studies on use of renewable substrates for SL synthesis have been focused on yield obtained rather than the nature of the SL synthesized. For upscaling purposes, the quality of the synthesized SL is paramount. Effect of different substrates on the physiochemical properties of SL remains unknown.

Short- and medium-chain length fatty acids have been successfully used for SL synthesis. This has been achieved by using different substrates such as secondary alcohol (C12–C14), coconut oil, and hydroxy fatty acids via chemical, biological, and biocatalytic methods. Refer [Table 3](#). These substrates were not explored further due to their lower yield. However, the influence of fatty acid chain length on SL biosynthesis and product formation is only partially understood<sup>70</sup>. Therefore, it is necessary to study the physical, chemical and biological properties of short chain SLs. The use of pure medium/short-chain fatty acid as a sole lipophilic source for synthesizing SL has not been explored.

Also, existing literature suggests tailormade biosynthesis of SLs by varying the fatty acid substrate. The pliable nature of yeast *S.bombicola*, allows successful incorporation of different substrates in

SL. This conversion is due to the robust enzymatic machinery of yeast, which converts varied substrates into SL. Over the years, the yeast has been genetically modified to obtain specific congeners. However, this process is time consuming and cost incurring. Moreover, the inherent nature of wild strain seems highly beneficial for fermentation processes<sup>23</sup>.

We hypothesize that changing the lipophilic substrate (lower chain length than the preferred chain length) might affect the physical and biological properties of the synthesized sophorolipid, thereby imparting wider applicability of molecule in various sectors. With this view, the current chapter focuses on synthesizing SL using 3 different substrates with increasing chain length: myristic acid C14, Palmitic acid C16, Stearic acid C18. The synthesized SL were then structurally characterized to access their structural orientation and modification. This chapter further includes physical attributes of the synthesized SL and the effects of chain length on these properties

### 3.2 Materials and Methods

#### 3.2.1 Chemicals and microorganisms used

Fatty acids i.e. Myristic acid (MA), Palmitic acid (PA) and Stearic acid (SA) were procured from Sigma chemicals. Various components of the culture medium used for sophorolipid synthesis and yeast culture namely glucose, Malt extract, Yeast extract, Mycological peptone were procured from Himedia, India. Luria Bertini medium, used to maintain bacterial cultures, was also obtained from Himedia, India. A non-pathogenic yeast *Starmerella bombicola* (ATCC 22214) was used for synthesis of different SL. The culture was maintained on MGYG agar slants (Malt extract-0.3g %, Glucose- 10g %, Yeast Extract-0.3g %, Mycological peptone-0.5g %); grown at 28 °C and stored at 4°C. For antibacterial assays, Gram positive (*Staphylococcus aureus* ATCC 9144) and Gram negative (*Pseudomonas aeruginosa* ATCC 9027) bacteria were used. They were maintained on LB agar slants at 37°C and stored at 4°C<sup>48</sup>.

### 3.2.2 Synthesis of sophorolipid

The biotransformation of fatty acids and glucose in presence of yeast enzymes results in sophorolipid production. The protocol for synthesizing C18 derived SL has been well established. However, this work emphasizes on using non-conventional substrates (mainly C 14 myristic acid) for sophorolipid production. Therefore, the preliminary studies involved optimizing the fermentation parameters so as to obtain better product yield. The fermentation parameters were finalized via optimization studies, varying one factor at a time method. Refer to [Figure 3.1](#) for optimization studies. This traditional method helps in understanding the effect of each individual media component on SL synthesis. All SLs was synthesized using the resting cell method. Briefly, *S. bombicola* was grown in 10 mL of MGYP broth for 24 h incubation (28 °C and 180 rpm); it was transferred to 90 mL of growth medium (GM) with mild shaking conditions of 180 rpm. After 48 h of growth, cells were harvested by centrifugation at 5000 rpm for 20 minutes. The pellet was then redispersed in the production medium (PM) supplemented with 1% (v/v) myristic acid and incubated at 28 °C at 180 rpm shaking for 8 days. Refer [Figure 3.2](#).

Types of media	Media components (g/L)					
	Glucose	Yeast extract	MgSO <sub>4</sub> ·7H <sub>2</sub> O	Na <sub>2</sub> HPO <sub>4</sub>	NaH <sub>2</sub> PO <sub>4</sub>	(NH <sub>4</sub> ) <sub>2</sub> SO <sub>4</sub>
Growth media	20	1	0.3	2	7	1
Production media	100	1	0.3	2	7	1

[Table 4](#) Media composition for sophorolipid synthesis

SLs (derived from: Palmitic acid and Stearic acid) were also synthesized by the resting cell method. Briefly, the *S. bombicola* cells were grown for 48h in MGYP medium, this was then used as a starter culture for the fermentation process. The cells were harvested by centrifugation and were inoculated in fermentation medium consisting of 10% glucose. The cells and fatty acid oil were

## Chapter III : Deciphering the effect of chain length of substrates on sophorolipid production through physio-chemical characterization

used at 2g% and 1g% loading in the final synthesis. Then the broth was incubated at 28oC for 7 days to allow synthesis of SL<sup>48</sup>. The following abbreviations will be used for the synthesized SL; MASL- Myristic acid derived SL, PASL- Palmitic acid derived SL and SASL- Stearic acid derived SL.

Optimization of the fermentation was done using the traditional one factor at a time method, wherein the individual components of the media were replaced or removed, so as to evaluate the product yield and to thereby, determine the effect of individual component of media on cell growth and fermentation. The [Figure 3.1](#) describes the optimization protocol used for synthesis.

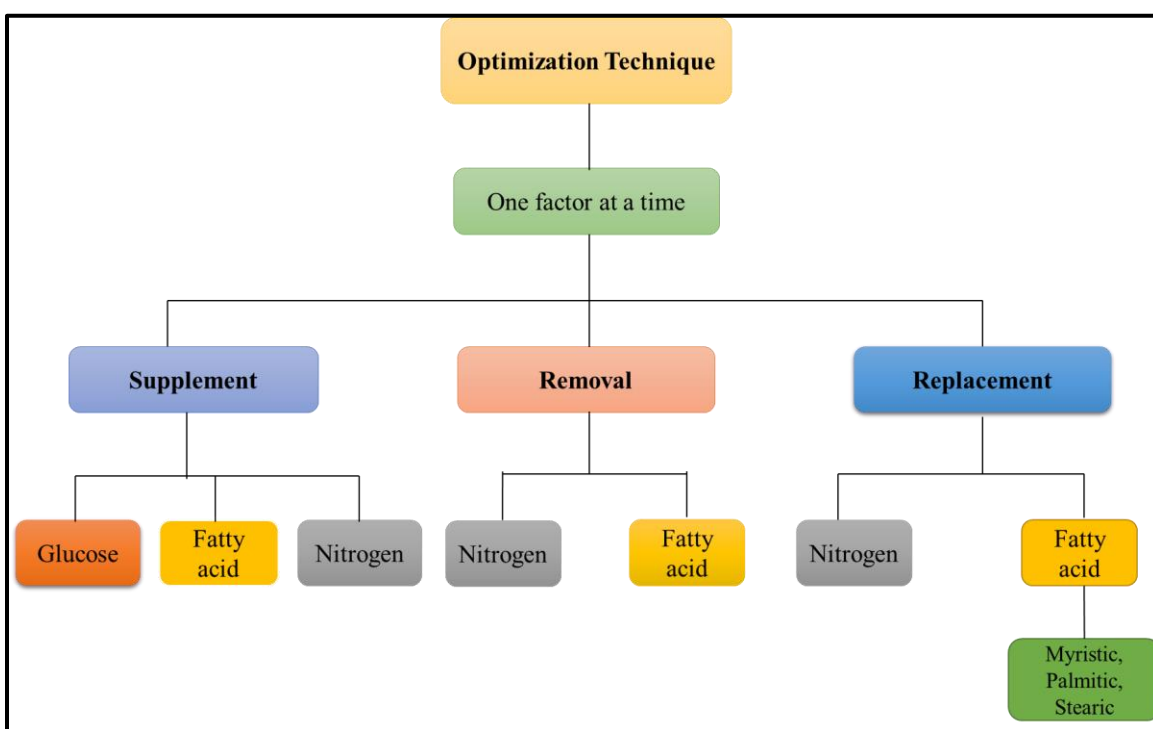


**Figure 3.1** Description of method used for optimization studies: one factor at a time

### 3.2.3 Extraction of sophorolipid

The formed SL were separated by solvent extraction methods using ethyl acetate as the organic solvent. The fermentation broth was mixed thoroughly with equal volumes of ethyl acetate. The water and organic phase were separated using a separating funnel. The SL products partitioned

## Chapter III : Deciphering the effect of chain length of substrates on sophorolipid production through physio-chemical characterization

into organic phase, which was collected separately. The solvent from the organic phase was evaporated by Rota-evaporation and the crude SLs were obtained. Refer [Figure 3.2](#).

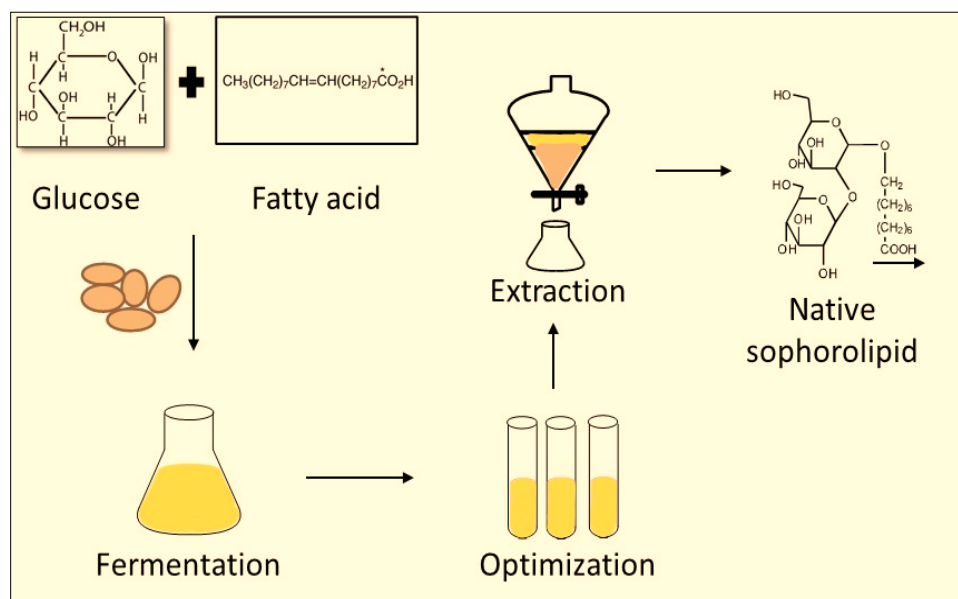


**Figure 3.2** Schematic representation describing the biotransformation process involved in SL synthesis

### 3.2.4 Characterization of sophorolipid

#### 3.2.4.1 Thin Layer Chromatography:

Preliminary characterization of different components was analyzed by performing thin layer chromatography on silica gel plates (Merck DC Keisegel 60 F254). The solvent system used was Chloroform/methanol/water in the ratio 65:15:2 v/v. Sample spots were loaded onto the plate by capillary and then immersed in solvent system. The solvent was allowed to run over the plate upto  $\frac{3}{4}$  distance. The sample spots were detected using anisaldehyde method. Briefly, the silica plate is immersed into the charring solution containing [absolute ethanol (135mL), conc. H<sub>2</sub>SO<sub>4</sub>(5mL), glacial acetic acid(1.5mL), p-anisaldehyde(3.7mL)] and then the plate is heated for visualization of the components<sup>131</sup>.

#### **3.2.4.2 Oil Displacement assay:**

The surfactant ability of synthesized SL (PASL and SASL) was assessed using oil displacement assay. Briefly, 20ml water was added to the petri dish (55mm). To this a thin film of oil was formed by using rapeseed oil. Further the crude SL were added gently onto the equilibrated film. On contact with oil, the film is disrupted creating a halo, hereby confirming the surfactant ability of the synthesized SL<sup>48</sup>.

#### **3.2.4.3 High performance liquid chromatography (HPLC):**

HPLC was performed to identify the acidic to lactonic ratio present in each synthesized SL. The analysis was done on Waters 515 system (C18 column) with a solvent system of Acetonitrile: Water (70:30). The injection volume was 50  $\mu$ L with retention time of 35 minutes and flow rate of 0.8 ml/minute.

#### **3.2.4.4 Critical micellar concentration (CMC)**

Surface tension was measured using Wilhelmy plate method, commonly known as the tensiometer. Here, a flat platinum plate is suspended onto the liquid surface, which on contact to the liquid, exerts a force on it. The generated force correlates to the surface tension of the liquid sample. This method was used for assessing the equilibrium surface tension of aqueous solutions of SL. The CMC of the SLs was determined by using Kruss K-11 Tensiometer. Initially, surface tension of pure water was measured. Later, multiple surface tension measurements were carried out with stepwise addition of SL (stepwise increasing concentration of SL in the solution). The addition of SL was carried out until the surface tension values of the solution became constant. The CMC of SL was calculated as the concentration as the concentration of SL needed to attain the lowest surface tension of the liquid<sup>48,96</sup>.

#### **3.2.4.5 Fourier transform infrared spectroscopy (FTIR)**

FTIR analysis was carried out for all SLs and their fatty acid precursors, to confirm substitution of glucose onto the fatty acid chain. The FTIR spectra were recorded on the Bruker Tensor II system in Platinum ATR mode. The measurements were done using 32 scans in the wavenumber range 500 - 4000 cm<sup>-1</sup> and air as background using 32 scans.

#### **3.2.4.6 High resolution mass spectrometry (LC-HRMS)**

Various congeners of SLs are formed during synthesis. LC-HRMS was performed to confirm the structures formed in the crude product. Hybrid Quadrupole Q-Exactive Orbitrap mass spectrometer from Thermo Scientific was used. The SL samples were prepared in acetonitrile. For LASL, a total run of 10 minutes was carried out by gradient solvent elution from 5% ACN in water to 100% ACN with a flow rate of 500 µl/minute. For other SLs, the solvent system Acetonitrile: water 70:30 was used. The samples were passed through Thermo Scientific Hypersil ODS C18 column length of 100 mm and 3 µm particle size using liquid chromatography pump (Accela 1250). A fixed volume of sample injected was 2 µL and scan was performed using positive polarity in the mass range 100-1500 m/z. The mass spectrometer was operated in positive electrospray ionization mode, with spray voltage 3600 V, capillary temperature 320°C, S-lens RF level 50, maximum injection time 120ms, and automatic gain control (AGC) 1×10<sup>6</sup>. Nitrogen was used as the sheath gas, spare gas and auxiliary gas, set at 35, 2, and 8 (arbitrary units) respectively. Thermo Scientific X Calibur software was used to analyze and scan the data for different proposed structures of SLs along with their hydrogen, sodium and ammonium adducts. Highest relative abundance peak were correlated to the molecular mass of different SL congeners. The mass to charge ratio enabled to identify specific congener of each synthesized SL<sup>131</sup>.

### **3.3 Results and discussions:**

#### **3.3.1 Synthesis and extraction of Sophorolipid:**

Around 10 g/L yield was obtained for myristic acid with resting cell method. This method allowed economic reuse of cells for consecutive 3 batches. Similar yield (85-90 % conversion) were obtained for palmitic and steric acid derived sophorolipid. Extracellularly synthesized viscous product was then subjected to solvent extraction to obtain sophorolipid. This crude form of SL was used for further characterization and application.

#### **3.3.2 Oil displacement assay:**

The surfactant ability of each synthesized SL was qualitatively assessed by oil displacement assay. As seen in the [Figure 3.3](#), the control samples (oil on water) formed a uniform layer on water surface. This layer was disrupted on addition of SL (test sample) thereby creating a halo. This clearly indicated that the synthesized compounds (SL) exhibited good surfactant ability.



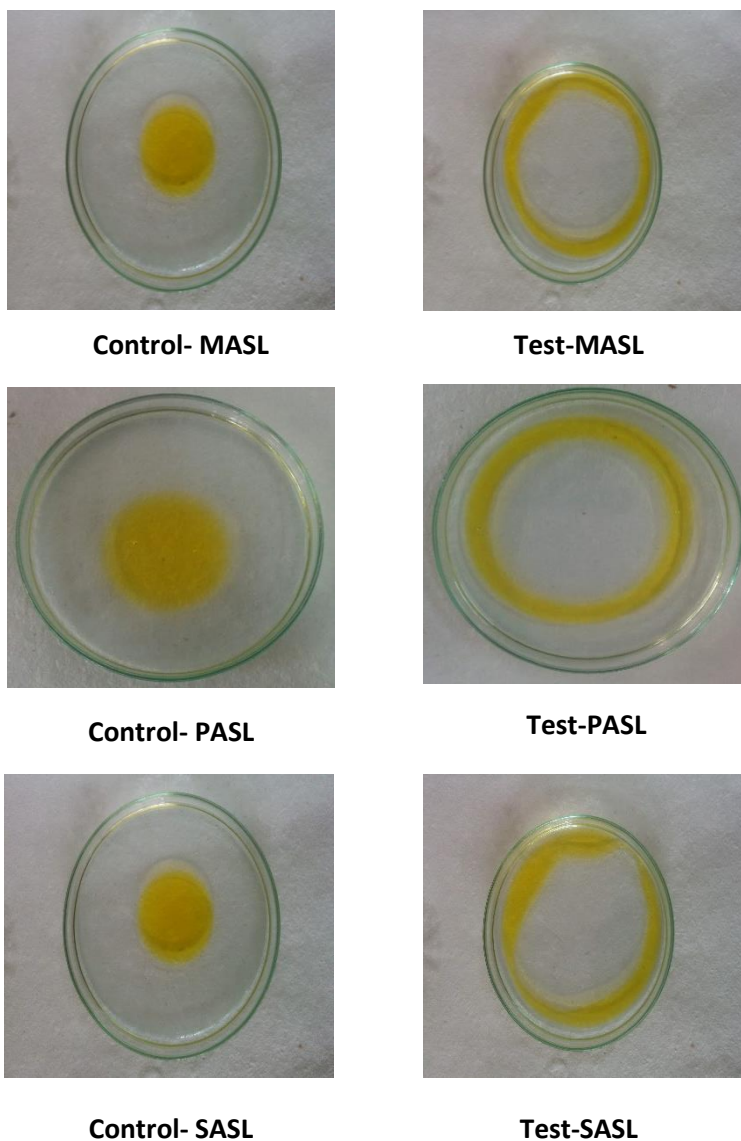


Figure 3.3 Oil displacement assay for each synthesized SL. The clear halo in the test sample indicates surfactant ability of the SL

### 3.3.3 High performance liquid chromatography:

HPLC was performed to quantitate the conversion of hydrophobic substrates (fatty acids) to less hydrophobic compounds, due to substitution of glucose molecule. The acidic forms are eluted first (retention time- upto 8 min) while lactonic forms are eluted later (Retention time beyond 8 min) due to their higher hydrophobicity. The [Table 5](#) summarizes the composition of acidic and lactonic

### Chapter III : Deciphering the effect of chain length of substrates on sophorolipid production through physio-chemical characterization

forms for each synthesized sophorolipid (MASL,PASL,SASL).Figure 3.4,3.5,3.6 depict the chromatogram for each synthesized SL.

SL synthesized	Acidic form (%)	Lactonic form (%)
MASL	80	20
PASL	95	5
SASL	80	20

**Table 5** Summary of acidic: lactonic forms for each SL

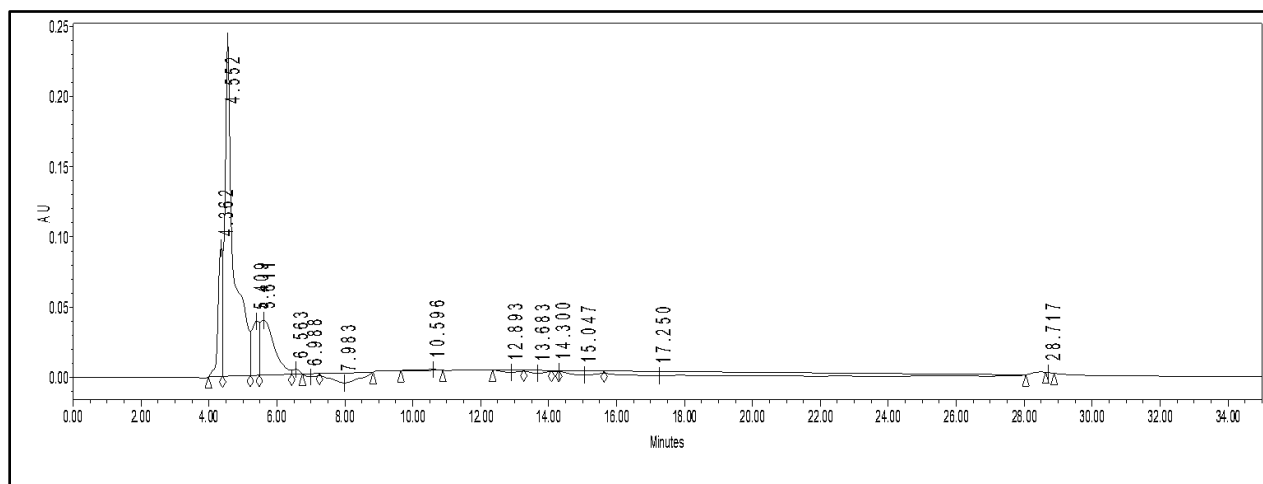


**Figure 3.4** HPLC graph of MASL indicating the acidic and lactonic ratios

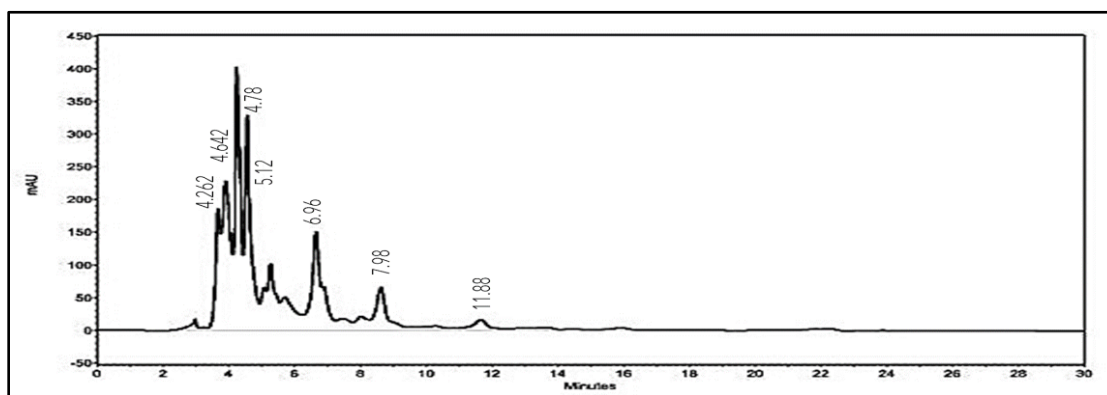


**Figure 3.5** HPLC graph of PASL indicating the acidic and lactonic ratios

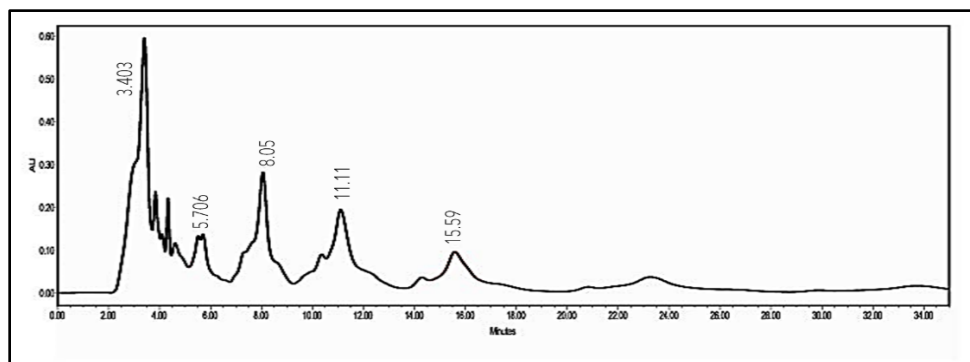


**Figure 3.6** HPLC graph of SASL indicating the acidic and lactonic ratios

### 3.3.4 Fourier transform infrared spectroscopy:

To confirm substitution of sophorose moiety on the fatty acid chain, FTIR measurements were carried out. The FTIR spectra of parent moieties i.e myristic acid (MA), glucose, and the crude-synthesized SL were noted (**Figure 3.7**). Myristic acid showed peaks at  $\sim 1400$ – $1500$ ,  $2918$ , and  $2854\text{ cm}^{-1}$ , which correspond to the  $-\text{CH}_2$  vibrations. The peak at  $1687\text{ cm}^{-1}$  corresponds to the carbonyl stretching. Characteristic peaks of glucose were seen at  $1030$  and  $984\text{ cm}^{-1}$ , which correspond to the C–O stretching vibration. The broad peak in the  $3200$  and  $3400\text{ cm}^{-1}$  corresponds to the  $-\text{OH}$  stretching. For MASL, the broad peak at  $\sim 3392\text{ cm}^{-1}$  corresponds to O–H stretching, which is present in the glucose molecule. Peaks at  $2918$  and  $2846\text{ cm}^{-1}$  represent symmetrical and asymmetrical stretching of the  $-\text{CH}_2$  group of fatty acid, respectively. A peak at  $1695\text{ cm}^{-1}$  corresponds to  $-\text{CH}_2$  bending. Stretching of C–O–C in the ether bond is represented at  $1084$  and  $1030\text{ cm}^{-1}$ .

The spectra of fatty acid precursors i.e. Palmitic acid (**Figure 3.8**) and Stearic acid (**Figure 3.9**) show a peak at  $1700$ . This peak corresponds to the carbonyl group in the carboxylic end. The peaks at  $2918$ ,  $2850$  and peaks between  $1400$ – $1500$  ( $\sim 1470$ ,  $1430$ ,  $1407$ ) correspond to  $-\text{CH}_2$  stretches from the long alkyl chain. Glucose spectra show characteristic peaks at  $\sim 3250\text{ cm}^{-1}$  which are typical peaks for hydroxyl ( $-\text{OH}$ ) groups. Other peaks between  $1016\text{ cm}^{-1}$  and  $998\text{ cm}^{-1}$  represent C–O stretches in glucose. In case of both SLs, several peaks from their fatty acid precursors can be

### Chapter III : Deciphering the effect of chain length of substrates on sophorolipid production through physio-chemical characterization

---

seen such as peak at vibrations of carbonyl group at  $1700\text{ cm}^{-1}$  and that of  $-\text{CH}_2$  stretches at  $2916$  and  $2850\text{ cm}^{-1}$ . Certain peaks from glucose moiety are also observed in the SL spectra such as at  $1080\text{ cm}^{-1}$  and  $938\text{ cm}^{-1}$  representative of CO groups in the sugar. The SL spectra also show a peak at  $1244\text{ cm}^{-1}$  for the ester bond i.e.  $\text{C}(\text{-O})\text{-O-C}$  that is formed between an acetyl group and 6'/6" carbon on glucose which forms the mono or diacetylated congeners of the sophorolipid. Thus, the FTIR spectra of all SL provide sufficient evidence that the synthesized compounds contains both precursor fatty acid and glucose moieties, and the ether peak validates of the presence of the SL molecule.

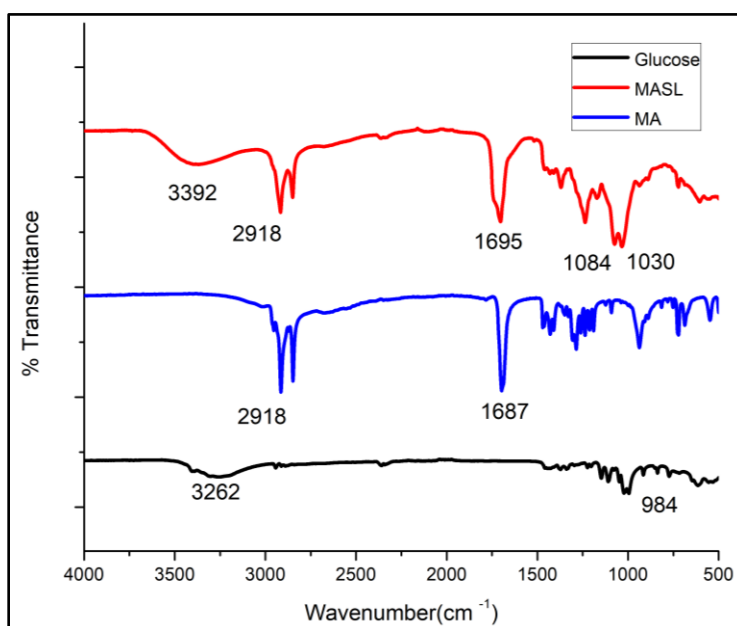


**Figure 3.7** FTIR graph of MASL; presence of ether bond at 1030 confirms successful SL synthesis

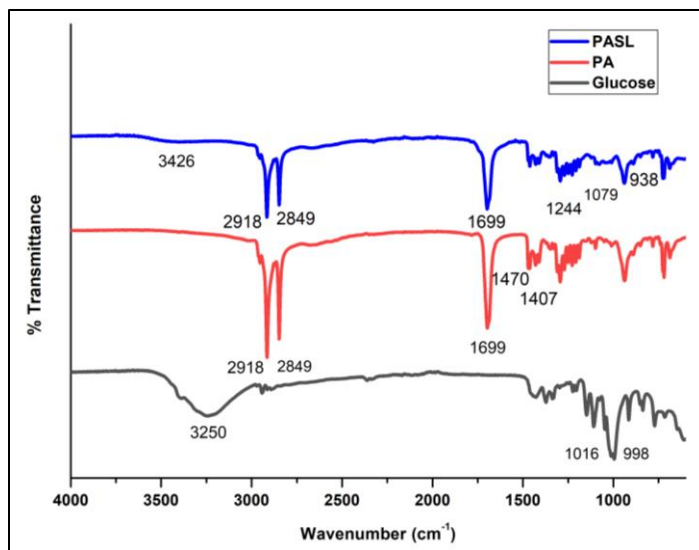


**Figure 3.8** FTIR graph of PASL; presence of ether bond at 1079 confirms successful SL synthesis

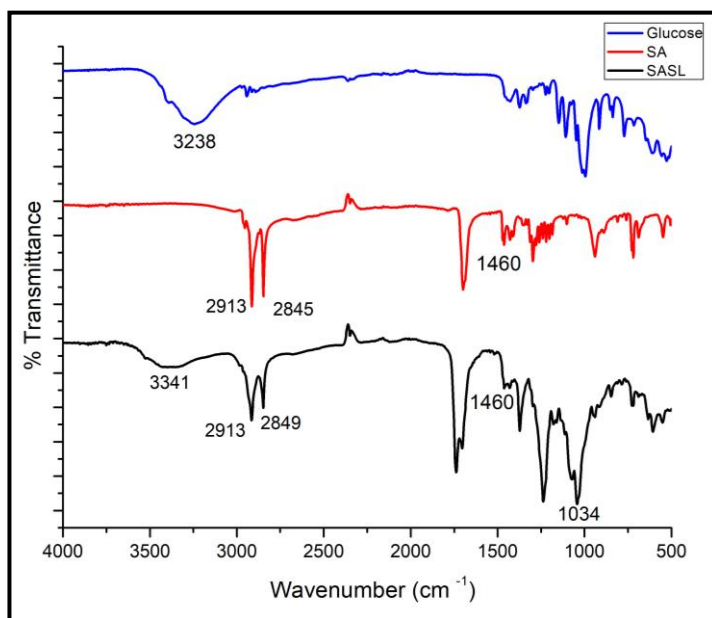


**Figure 3.9** FTIR graph of SASL; presence of ether bond at 1034 confirms successful SL synthesis

### 3.3.5 High Resolution Mass Spectroscopy:

SL synthesis occurs in the cytosolic environment of the cell. Biosynthesis begins by activation of fatty acid by hydroxylation, catalyzed by the microbial enzyme cytochrome P450 monooxygenase. Hydroxylation occurs at the terminal or subterminal region of the fatty acid. The second step involves attachment of the sophorose unit to the fatty acid molecule through an ether bond by glucosyltransferase I and II. Upon glycosylation, acidic non-acetylated SLs are obtained. Acidic SL is characterized by the free fatty acid chain, whereas the lactonic form results in the formation of a closed ring structure because of internal esterification at the carboxylic end of fatty acid with C4 of the sophorose moiety<sup>7</sup>. Further modifications include acetylation at the C6 position of the glucose moieties, resulting in the formation of monoacetylated and diacetylated SL molecules. These different modifications of synthesized SLs were analyzed by spectroscopy.

HRMS analysis revealed that MASL is a mixture of acidic and lactonic molecules with the preferred site for glycosylation through the methyl group. Mono- and diacetylated acidic and lactonic structures were also elucidated from the analysis. Refer to [Figures 8.1- 8.3](#) in the appendix for spectra of each modification. Glycosylation at the other end (carboxylic end) is not prevalent in the case of MASL. The different structures of have been summarized in [Table 6](#).

HR-MS analysis revealed that PASL contains both the mono and di-acetylated forms and that the glycosylation happens at both the ends. Similar results were obtained for stearic acid derived sophorolipid. The [Tables](#) below summarize the different modifications for both PASL and SASL. Chromatograms of each modification are included in the appendix section ([Figures 8.4- 8.14](#)). These results confirm that the SL can be synthesized using fatty acids having varying chain lengths.

Sr. No	Components - MASL	Molecular weight (Acidic)		Molecular weight (Lactonic)	
		Protonated	Na Adduct	Protonated	Na Adduct
1	No acetylation-CH <sub>3</sub>	569.31	591.22	551.63	573.28
2	Mono Acetylation-CH <sub>3</sub>	611.3	633.69	593.31	615.29
3	Di acetylation-CH <sub>3</sub>	653.72	675.72	635.71	657.31

Table 6 Different structural modification obtained from MASL

Chapter III : Deciphering the effect of chain length of substrates on sophorolipid production through physio-chemical characterization

Sr. No	Components - PASL	Molecular weight (Acidic)		Molecular weight (Lactonic)	
		Protonated	Na Adduct	Protonated	Na Adduct
1	No acetylation-CH <sub>3</sub>	596.34	619.34	578.69	601.69
2	Mono Acetylation-CH <sub>3</sub>	638.35	661.35	620.72	643.72
3	Di acetylation-CH <sub>3</sub>	680.36	703.36	662.72	685.76
4	No acetylation-COOH	580.35	603.36	562.69	585.69
5	Mono Acetylation-COOH	622.36	645.36	604.72	627.72



Chapter III : Deciphering the effect of chain length of substrates on sophorolipid production through physio-chemical characterization

---

6	Di Acetylation-COOH	664.37	687.37	626.6	649.6
---	---------------------	--------	--------	-------	-------

Table 7 Different structural modification obtained from PASL

Chapter III : Deciphering the effect of chain length of substrates on sophorolipid production through physio-chemical characterization

Sr. No	Components- SASL	Molecular weight (Acidic)		Molecular weight (Lactonic)	
		Protonated	Na Adduct	Protonated	Na Adduct
1	No acetylation- CH <sub>3</sub>	624.76	647.76	606.74	629.74
2	Mono Acetylation- CH <sub>3</sub>	666.79	689.76	648.76	671.78
3	Di acetylation- CH <sub>3</sub>	708.39	731.39	690.80	713.81
4	No acetylation- COOH	608.76	631.76	590.73	613.74
5	Mono Acetylation- COOH	650.79	673.79	632.76	655.78
6	Di Acetylation-COOH	692.83	715.83	674.81	697.81

Table 8 Different structural modification obtained from SASL

### 3.3.6 Critical micellar concentration:

In dilute solutions, surfactants behave as normal solute molecules, but as the concentration increases, abrupt changes in the physical properties are observed. This phenomenon is due to the formation of aggregates or micelles. The critical micellar concentration (CMC) value is measured using any micelle-influenced physical properties as a function of concentration. In the present work, the surface tensions of MASL, PASL and SASL were measured for different concentrations. The Figures 3.10- 3.12 represent the surface lowering abilities of each synthesized SL. As the concentration increased, the surface tension was found to continuously decrease. This reduction in surface tension is a further confirmation of successful synthesis of the SL molecule. After specific concentration, no further decrease in the surface tension was observed. The CMC value for each sophorolipid was calculated from the graph of concentration of SL (mg/mL) versus surface tension (mN/m).

The CMC values varied for all the different SLs where MASL and SASL were in the range of 15-40 mg/L. In contrast, CMC for PASL was found to be higher i.e. 110 mg/L. The surfactant ability is dependent on the various factors like: chain length, degree of unsaturation, charge and branching of molecules. For SL, two parameters contribute majorly towards the lower CMC: firstly, the acidic to lactonic ratio of synthesized SL. Higher lactonic content leads to lower CMC. In this study, the CMC of MASL and SASL are lower. This is due to the acidic lactonic ratio which is 80:20 in both and the ratio is 95: 5 for palmitic, explaining the higher CMC. Secondly, the micellization process is governed by the hydrophobic moiety of the surfactant. Bulky molecules require more time to form micelles, thereby increasing the CMC of the molecule i.e longer the hydrophobic chain, more time needed for micelle formation. The micellar assembly formed from SL is cylindrical micelles as inferred from its self-assembly pattern. Short chain SL i.e: MASL, form micelles at lower concentrations due to short fatty acid chains. However, longer fatty acid chain SL like PASL and SASL, are limited by their ability to diffuse and assemble into a cylindrical micelle.

### Chapter III : Deciphering the effect of chain length of substrates on sophorolipid production through physio-chemical characterization

---

The reported CMC value of SLs derived from oleic acid lies in the range 130–140 mg/L. For oleic acids and linolenic acids, being unsaturated fatty acids with double and triple bonds, the CMC value is eccentrically increased. Similarly, for stearic acid, being a saturated molecule, the CMC value is low. This is in agreement with our observations<sup>57,78</sup>. This implies that the acidic to lactonic ratio has a higher influence on CMC as compared to fatty acid chain length. The CMC value of MASL is distinctly low as compared to other SLs and thus makes MASL a promising candidate for various commercial surfactant applications.

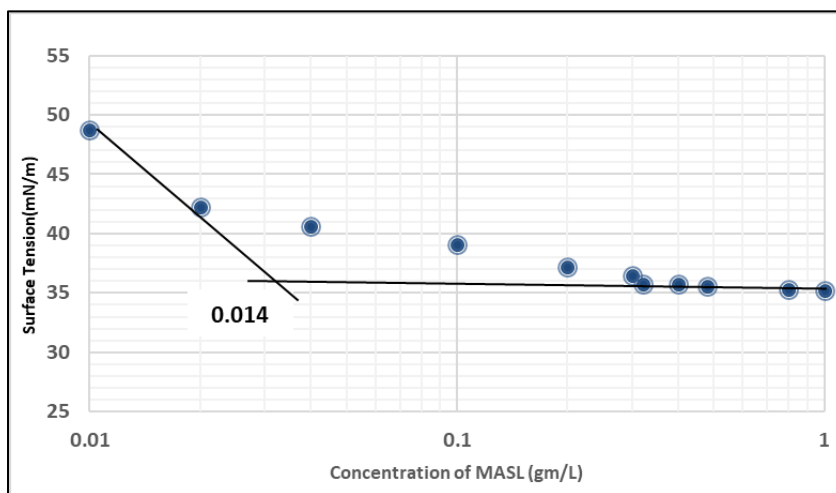


**Figure 3.10** Graphical representation of surface tension reduction by MASL

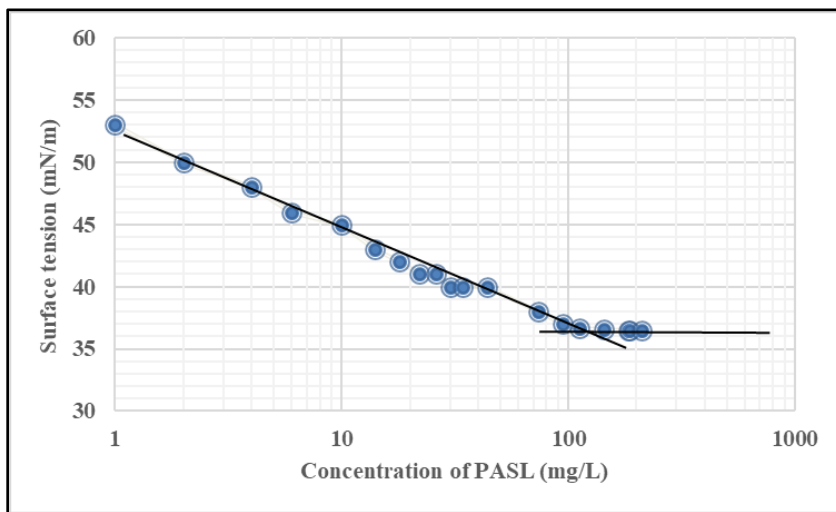


**Figure 3.11** Graphical representation of surface tension reduction by PASL

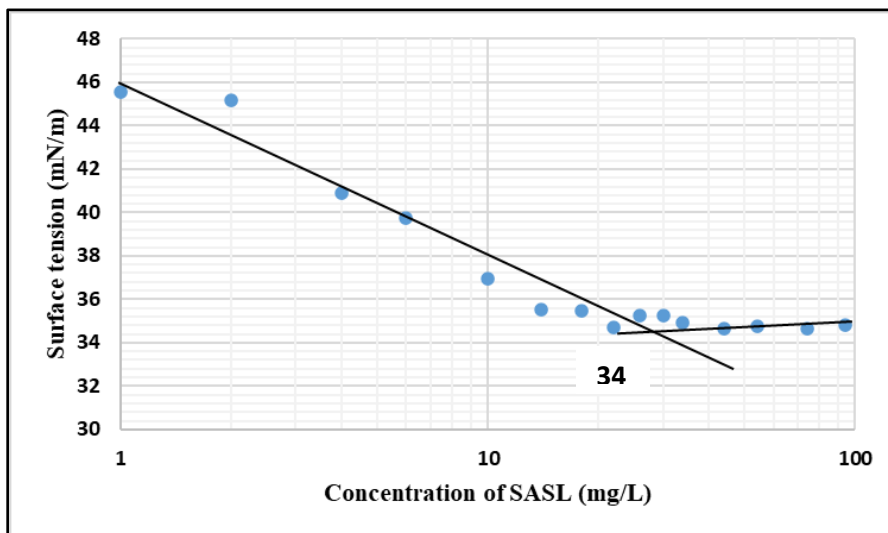


**Figure 3.12** Graphical representation of surface tension reduction by SASL

### 3.4 Conclusion:

SLs are an interesting class of biosurfactants as they exhibit several useful properties that add value in various application domains. In this study, we have described the synthesis of three different SL namely MASL, PASL and SASL. These SL have varying fatty acid chains and the length of the fatty acid chain increases from 14 carbon atoms in case of myristic acid SL to 18 carbon atoms for stearic acid derived SL. The toxicity of fatty acids with a short carbon chain combine with the C16–C18 chain length specificity of the yeast enzymes limits the avenues for producing SLs. In this work, we have demonstrated, using the resting cell method, the synthesis of a shorter (C14) chain SL derived from a novel source: myristic acid.

All the obtained SL have been characterized structurally using spectroscopic techniques. The FTIR experiments confirmed substitution of sophorose moiety on to the fatty acid chains as well as acetylation on the glucose in the sophorose moiety. The characterization suggests that glycosylation occurs preferentially at the methyl end group of the fatty acid chain and leads to the formation of a mixture of acidic and lactonic SL containing monoacetylated and diacetylated forms

### Chapter III : Deciphering the effect of chain length of substrates on sophorolipid production through physio-chemical characterization

---

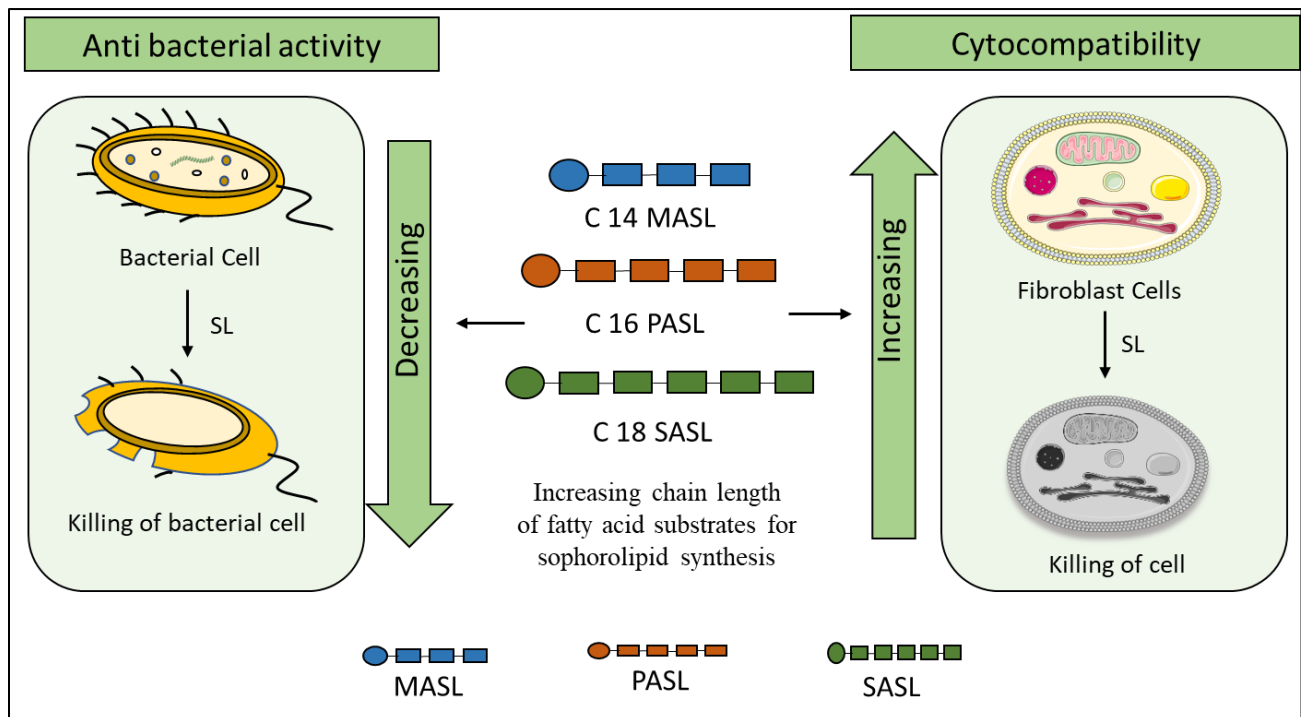
for myristic acid derived sophorolipid; whereas the glycosylation happens at both ends for higher fatty acids, palmitic and stearic acid derived SL. Further, the HRMS analysis showed formation of different congeners i.e. acidic, lactonic forms of SLs and their mono or diacetylated variants. All the SLs showed excellent surface-active properties as determined by their critical micellar concentration. The results highlight the plausible correlation between the chain length of fatty acid substrate and their CMC. The lowest CMC was observed for myristic acid derived sophorolipid.

To summarize, the physiochemical properties of SL are greatly dependent on chain length of fatty acids. Shorter chain derived SL have better physical properties than long chain derived SL, thereby expanding their avenues for various commercial applications. The next chapter discusses the biological properties of SL's as a function of their fatty acid chain length.

## Chapter IV

### Deciphering the effect of chain length on sophorolipid: Emphasizing biological properties

Chapter III revealed that SL production is dependent on the chain length of substrates. The nature of substrate affects the physical properties of the synthesized sophorolipid. Shorter chain derived SL possess better properties in terms of CMC and glycosylation pattern. For holistic understanding, we have assessed the effect of chain length on biological properties. This chapter primarily focusses on the anti-bacterial properties of SL's as a function of chain length of fatty acid substrate. Further, the cytotoxicity of various SL's has also been studied using fibroblast cell lines.



## 4.1 Introduction:

The deleterious effects of chemical surfactants on health and environment have led to advancement in the field of biosurfactants. The demand for greener products/ alternatives is gradually increasing. The amphiphilic nature of SL renders it extremely useful for diverse applications like drug delivery, enhanced bioavailability, nanoparticles synthesis and bioremediation. This chapter focuses on different biological properties namely; cytotoxicity, anti-bacterial and anti-cancer activity of SL. These activities were assessed for all the synthesized SL

Despite the advent of antibiotics a few decades ago, the rate of bacterial infections and mortality associated with it are increasing at an alarming rate. Overuse of antibiotics has led to development of mutated strains with antibiotic resistance genes (ARGs) and higher virulence. These ARGs are transferred horizontally (within a population of bacterial cells in a niche environment like biofilm) and vertically (from parent cells to offspring cells). Antibiotics and their metabolites are released in the environment through household and hospital feed, pharmaceutical waste and this further contributes to resistance<sup>132</sup>. Such organisms are unresponsive to the currently available drugs and thereby result in chronic infections affecting various organs. Classic example of this is a gram-positive bacterium: *S. aureus*, which has become a leading cause of bacteremia and infective endocarditis. It is now associated with hospital acquired infections, prosthetic device infections and skin and soft tissue infections<sup>133</sup>. Similarly, the gram-negative associated infections like cystic fibrosis in implants, severe lung infections caused by *P.aeruginosa*, are difficult to treat<sup>134</sup>.

Owing to this, there has been an increase in development of greener or natural antibiotic options to combat these infections. Several strategies have been explored for tackling the increasing antimicrobial resistance. Multiple studies have leveraged the antimicrobial potential of metal ions such as iron, copper, silver, gold, zinc, titanium as well as ions like fluorine. These ions are used in the form of nanoparticles or are doped in with other materials<sup>135</sup>. Certain functional biomolecules also have been shown to have potent antibacterial activity like functional DNA molecules, antimicrobial peptides (AMPs). AMPs have been shown to interact and disrupt the cell membrane of the bacteria disturbing the ion channels and integrity of the cell membrane<sup>136</sup>.



## Chapter IV: Deciphering the effect of chain length on sophorolipid production: Emphasizing biological properties

---

Cationic biomaterials such as chitosan, act on the bacterial cell wall and membrane<sup>137</sup>. Various plant extracts containing phytochemicals such as alkoids, phenolic compounds, terpenes, coumarins have also shown efficient antibacterial activity<sup>138</sup>.

SL, belonging to the glycolipid class of biosurfactants, are green molecules that have recently been evaluated for their antibacterial activity. They are synthesized extracellularly by nonpathogenic yeast *Starmerella bombicola*<sup>72</sup>. Structurally, they contain a hydrophilic head and a lipophilic tail. Their amphiphilic nature coupled with varied biological properties makes SL superior to synthetic surfactants. Natural SL exist in two forms; acidic and lactonic. Both the components impart different properties to the molecule i.e. acidic increases the solubility whereas lactonic imparts bioactive properties to the molecules<sup>139</sup>. Generally, majority of the literature on SL is focused on synthesizing SL using C16-18 fatty acids, this is primarily due to the presence of these substrates in *de novo* products. Shifting this paradigm, we aim to synthesize SL from lower chain fatty acids myristic acid. Changing the lipophilic substrate drastically affects the physical properties of the SL like lower CMC.

SLs have several advantages over the current antibacterial strategies. The synthesis of SL can be carried out in a short duration at ambient temperature with a high yield unlike nanoparticles, which would require higher temperatures or catalyst for the reaction. Synthesis of AMPs also can be a time-consuming process and requires multiple precursors and enzymes. The crude product of SL can be characterized and purified to identify various congeners or forms of SL molecules, whereas plant or natural extracts would have an indefinite composition and may have non-reproducible results. Apart from the antibacterial properties, the tailor-made synthesis of sophorolipid is equally interesting. The tailor-made synthesis allows incorporation of different fatty acids and / or sugars into the SL<sup>48</sup>.

Similar to anti-bacterial agents, the need for different anti-cancer drugs has been growing. Cervical cancer is the fourth most frequently diagnosed cancer globally. Although WHO issued worldwide elimination of cervical cancer, the disease is still prevalent. This is due to the varied etiological agents like; persistent HPV infections, socio economic status, lack of disease awareness and smoking. Newer treatment options like immunotherapy, precision medicine, personalized

therapies and genetic approaches have been used. Despite considerable advancement in treatment options, the debilitating side effects of treatment and economic burden on the patient is very worrisome. Moreover, resistance of tumor to chemotherapy and rapid progression to metastatic stages has also drastically increased<sup>140</sup>.

To combat this, several newer strategies have been discovered. Interestingly, SL exhibit anti-cancer activity against various cancer cells: cervical, breast, glioma, liver and pancreas. Joshi *et al* reported the ability of SL to induce differentiation of cells in glioma. However, the effect of chain length of substrate on biological attributes and on normal cells remains unexplored. An effective cancer drug inhibits the cancer cells without affecting the normal cells of the tissue. Therefore, the effect of different substrates on normal cell (L929) was also studied.

With this view, the current study focuses on understanding the effect of chain length of fatty acid on biological properties. Interestingly it was found that the biological properties of these SL viz anti-bacterial, cytotoxicity and also anti-cancer had a strong correlation to the fatty acid substrate used. Our results show that SL have huge potential in the biomedical applications.

## **4.2 Materials and method:**

### **4.2.1 Microorganisms:**

*Starmerella bombicola* (ATCC 22214) was used for the production of SL and was maintained on agar slants containing malt extract (0.3 g %), glucose (2 g %), yeast extract (0.3 g %), and peptone (0.5 g %) (MGYP media) and incubated at 28 °C for 48 h with subculturing every 4 weeks.

The test organisms *Staphylococcus aureus* (ATCC 9144) and *Pseudomonas aeruginosa* (ATCC 9027) were obtained from the National Collection of Industrial Microorganisms (NCIM), CSIR-NCL, Pune, and maintained on nutrient agar slants.

All the SL (MASL, PASL, SASL) were synthesized and characterized using the protocols mentioned in the Chapter III (Section3.2.2). Crude form of SL was used for all the biological application.

#### 4.2.2 Anti-bacterial activity:

The antibacterial activity was assayed using the contact method as per the protocol described in [Figure 4.1](#). Briefly, the test organisms *S. aureus* and *P. aeruginosa* were grown in Luria Bertani broth and incubated for 24 h at 28°C and 37 °C, respectively. The cell pellet was harvested by, centrifugation at 5000 rpm for 15 minutes and washed with saline. The supernatant was discarded, and the pellet was resuspended in saline and recentrifuged at 5000 rpm for 15 minutes. Serial dilutions were prepared up to 10<sup>-5</sup>. The cell count was quantified by adjusting the OD to 0.1 at 600 nm. MASL was diluted to 50, 150, 250, 350, and 450 µg/mL concentration for all organisms. Bacterial culture was mixed with each dilution of MASL and incubated up to 1 h. Aliquots of 0.1 mL were withdrawn at intervals of 15 minutes and plated on LB agar. Two controls were used: only bacterial cells and only lipophilic substrate. In addition, OASL was used as a positive control. For each experiment, myristic acid (450 µg/mL) was used as a control. The plates were then incubated at 37 °C/28 °C for 24 h. All experiments were performed in triplicates. After incubation, the number of colonies was counted, and % survival was calculated using the formula

$$\% \text{ cell survival} = 100 \times (NT/NC)$$

NT: number of bacterial colonies on plates.

NC: number of colonies observed on the control plate.

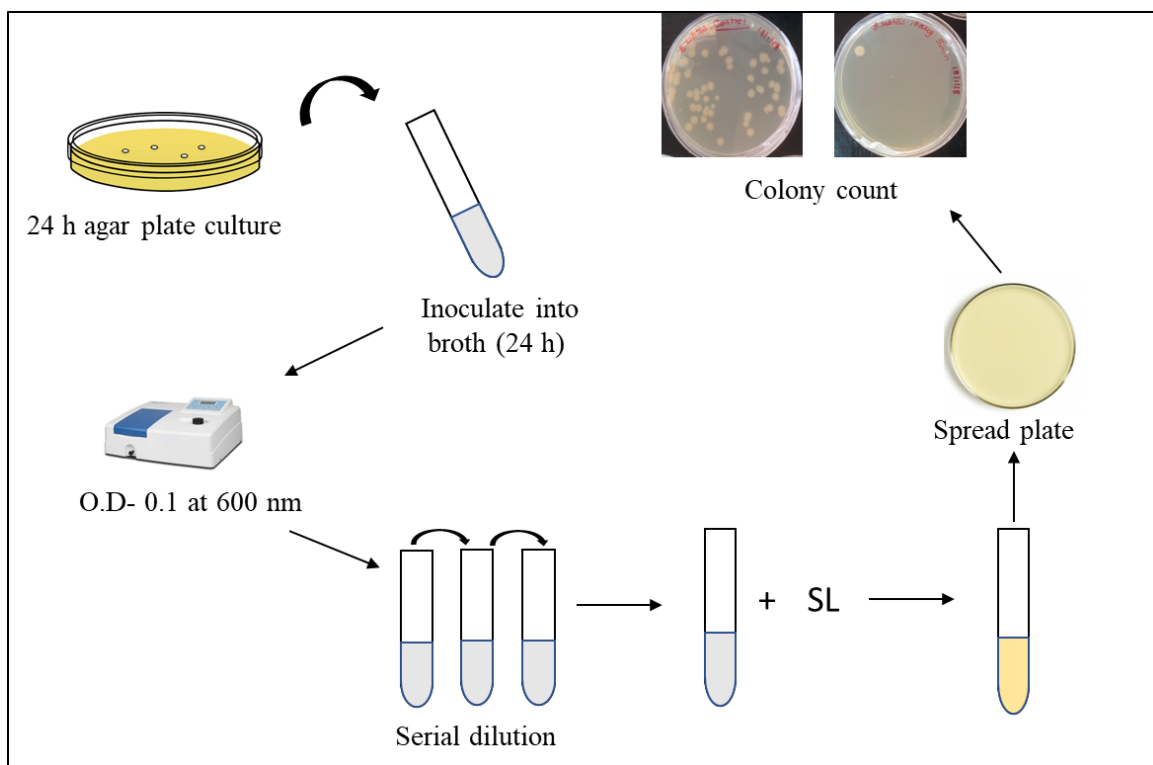


Figure 4.1 Schematic representation describing the anti-bacterial assay protocol

### 4.2.3 Cell culture

HeLa (Cervical cancer cell line) and L929 (Mouse fibroblast) cell line were purchased from National Centre for Cell Science (NCCS), Pune, Maharashtra, India. Cells were maintained in DMEM (Gibco) media with 10% FBS (Gibco) at 37°C with 5% CO<sub>2</sub>.

#### 4.2.3.1 Cytotoxicity assay:

Cytotoxicity of samples was determined with the help of MTT Assay. MTT, (3-(4,5-dimethylthiazol-2-yl)-2,5-diphenyl tetrazolium bromide) is a pale-yellow substrate that is cleaved by living cells to yield a dark blue formazan product. L929 cells were seeded in a flat-bottomed, adherent 96-well plate at a density of 10000 cells per well in 100 µL of complete growth media. The plate was incubated at 37°C with 5% CO<sub>2</sub> for 24h.

The SL sample was dissolved in DMEM media and was UV sterilized for half an hour. DMEM+10% FBS media was added to SL samples in order to obtain a definite concentration and

volume. Different concentrations of SL samples were prepared starting from 2µg/mL to 1mg/mL. Spent media was removed from the wells followed by sample addition. Plate was incubated at 37°C with 5% CO<sub>2</sub> for 24h. After 24h the SL sample was replaced with 10% working MTT reagent and plate was incubated for 4h at 37°C with 5%CO<sub>2</sub>. After incubation, MTT reagent was replaced with 100µl of DMSO in all sample and control wells. DMSO dissolves the formazan to give a homogenous purple-colored solution. Absorbance of the reduced solution was taken at 550 nm with the help of ELISA plate reader (Multiskan EX, Thermo Scientific). Absorbance was taken in triplicates and the normalized factor was reported as cell growth<sup>141</sup>.

#### **4.2.3.2 Anti-cancer activity of SL:**

Anti-cancer activity was determined by MTT assay, as per the protocol; Briefly, HeLa cells were seeded in a flat-bottomed, adherent 96-well plate at a density of 10000 cells per well in 100 µL of complete growth media. The plate was incubated at 37°C with 5% CO<sub>2</sub> for 24h. The SL sample was dissolved in DMEM media and was UV sterilized for half an hour. DMEM+10% FBS media was added to SL samples in order to obtain a definite concentration and volume. Different concentrations of SL samples were prepared starting from 2µg/mL to 1mg/mL. Spent media was removed from the wells followed by sample addition. Plate was incubated at 37°C with 5% CO<sub>2</sub> for 24h. After 24h the SL sample was replaced with 10% working MTT reagent and plate was incubated for 4h at 37°C with 5%CO<sub>2</sub>. After incubation, MTT reagent was replaced with 100µl of DMSO in all sample and control wells. DMSO dissolves the formazan to give a homogenous purple-colored solution. Absorbance of the reduced solution was taken at 550 nm with the help of ELISA plate reader (Multiskan EX, Thermo Scientific). Graph of concentration vs % survival was plotted. Inhibition concentration was determined by calculating the IC 50 value<sup>142</sup>.

### 4.3 Results and discussions:

#### 4.3.1 Anti-bacterial activity of SL:

The antibacterial activity of synthesized SLs was assessed against gram positive and gram negative bacteria: *S.aureus* and *P.aeruginosa*. These bacteria were selected for this study as these are the most common causes of hospital acquired infections and are also associated with graft rejection. The assay was performed at different concentrations and at different time intervals using contact method. As SL are partly soluble in water, their diffusion through disc or well into the agar is not uniform and it may be retained in the well leading to inaccurate results. Hence contact method was preferred over well/ disc diffusion method, in which two different parameters of antibacterial activity can be tested simultaneously.

In Figure 4.2, effective inhibition of both bacteria by MASL was observed, the % survival dropped to 20% at 150 µg/mL within 15 minutes of exposure to *S.aureus*. For *P.aeruginosa*, 18% survival was observed when 350 µg/mL MASL was employed with an exposure time of 1h.

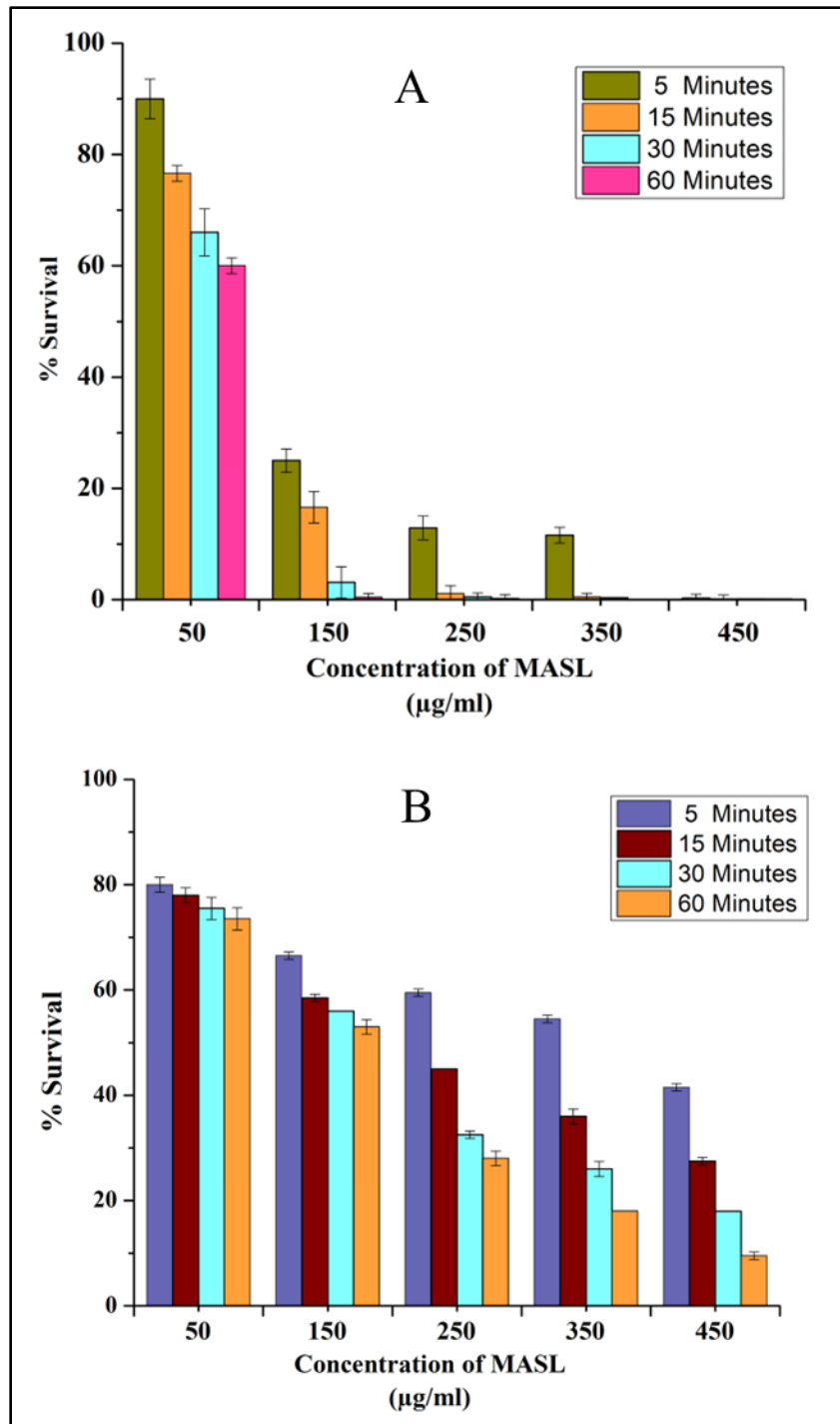


Figure 4.2 Antibacterial activity of MASL against different organisms- % Survival at different concentrations (50–450 µg/mL) of MASL and at different time points (5–60 min) plotted (A) Gram positive, *S. aureus*, (B) Gram negative, *P. aeruginosa*

## Chapter IV: Deciphering the effect of chain length on sophorolipid production: Emphasizing biological properties

For PASL, the % survival of *S. aureus* dropped to ~10 with a concentration of 150  $\mu\text{g/mL}$  within 2 h. Above 250  $\mu\text{g/mL}$  complete inhibition was obtained after 2h. Similarly, for gram negative organisms, *P. aeruginosa*, the % survival dropped to 12% with concentration of 250  $\mu\text{g/mL}$  within 3h. Complete inhibition was observed at 450  $\mu\text{g/mL}$  after 3h. Refer to [Figure 4.3](#).

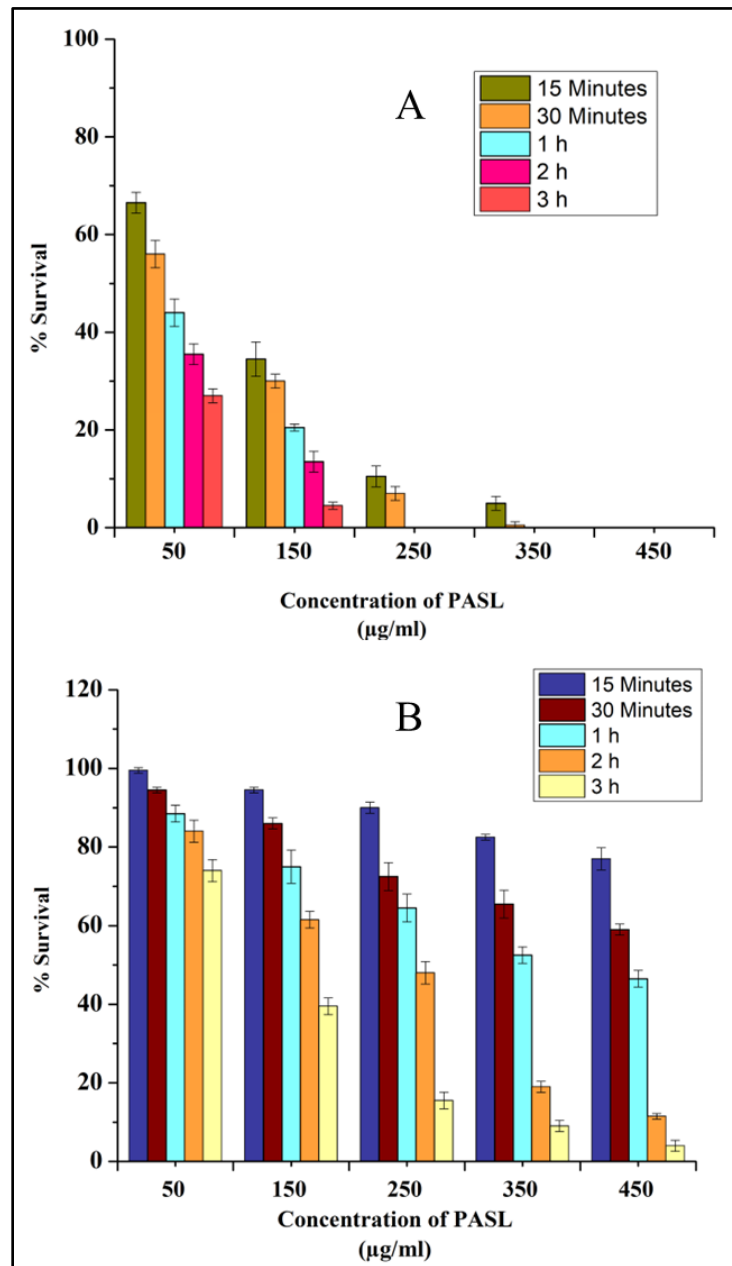


Figure 4.3 Antibacterial activity of PASL against different organisms- % Survival at different concentrations (50–450  $\mu\text{g/mL}$ ) of PASL and at different time points (5–60 min) plotted (A) Gram positive, *S. aureus*, (B) Gram negative, *P. aeruginosa*



## Chapter IV: Deciphering the effect of chain length on sophorolipid production: Emphasizing biological properties

Similar trend was observed for SASL, [Figure 4.4](#). The % survival dropped to 5% at 150  $\mu\text{g/mL}$  concentration within 2h. For *P. aeruginosa*, less than 20 % survival was observed at 350  $\mu\text{g/mL}$  concentration within 3h.

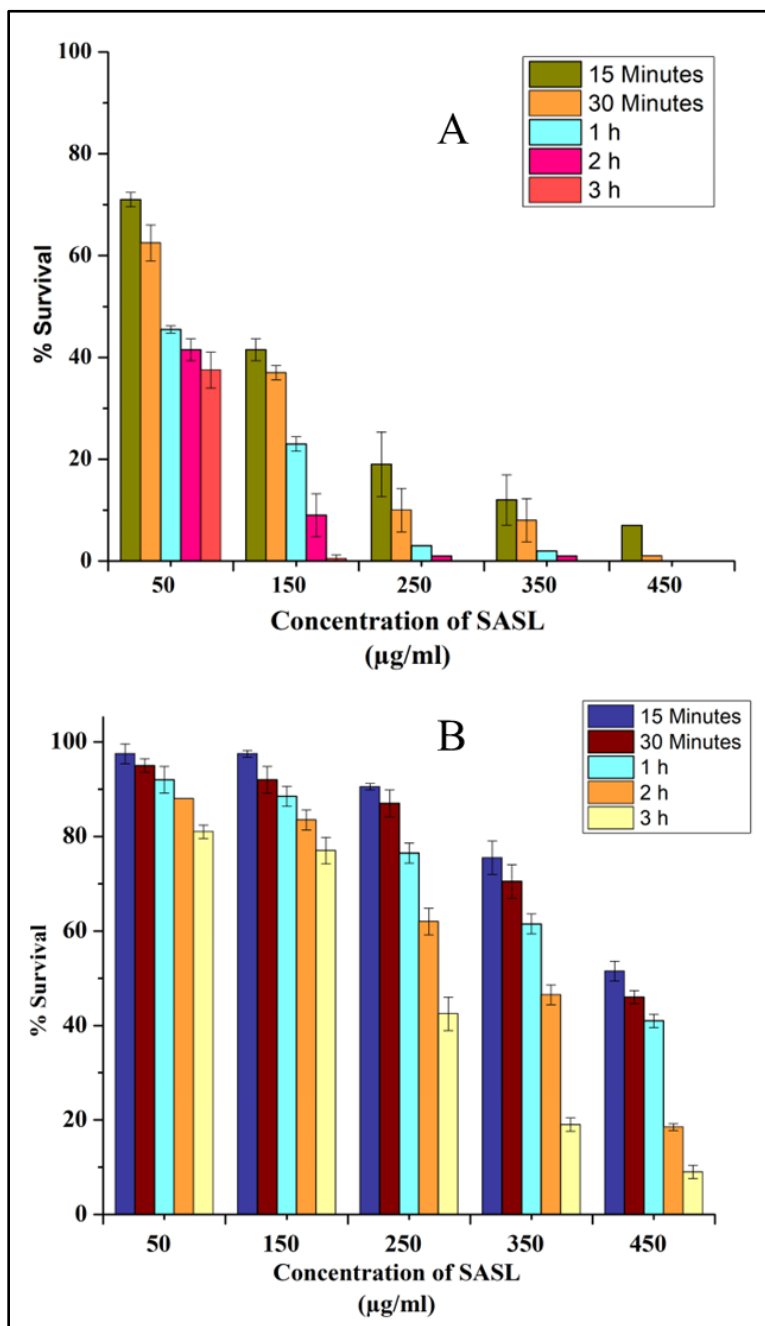


Figure 4.4 Antibacterial activity of SASL against different organisms- % Survival at different concentrations (50–450  $\mu\text{g/mL}$ ) of SASL and at different time points (5–60 min) plotted (A) Gram positive, *S. aureus*, (B) Gram negative, *P. aeruginosa*

## Chapter IV: Deciphering the effect of chain length on sophorolipid production: Emphasizing biological properties

---

From the results obtained it can be concluded that the anti-bacterial activity of SL is dependent on the chain length of the substrate. For short chain SLs i.e. MASL the 80% inhibition of bacterial cells is obtained at comparatively lower concentration as well as at much lower time of contact. As the chain length increases i.e. PASL and SASL with a C16 and C18 fatty acid chain, the concentration required for 80% inhibition of bacterial cells increases and the time of contact also increases. This is seen in case of both gram positive as well as gram negative bacteria. [Figure 4.5](#) highlights the effective concentration of each sophorolipids against both the model organisms.

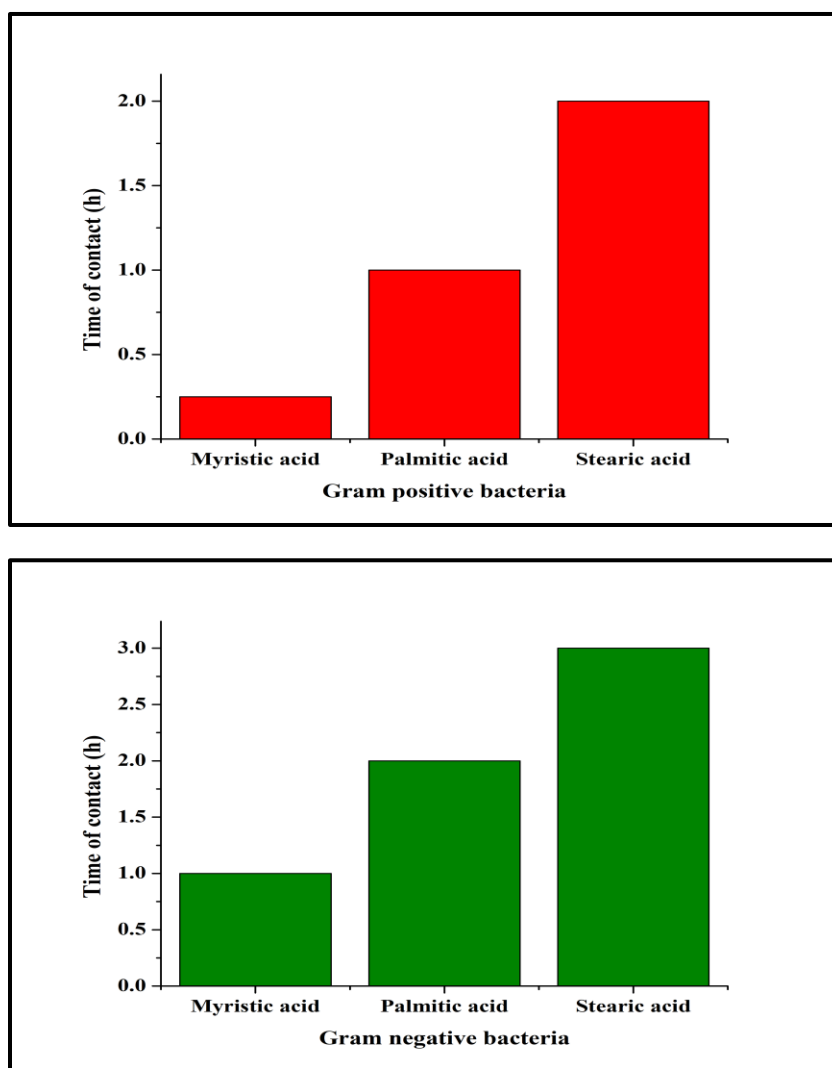
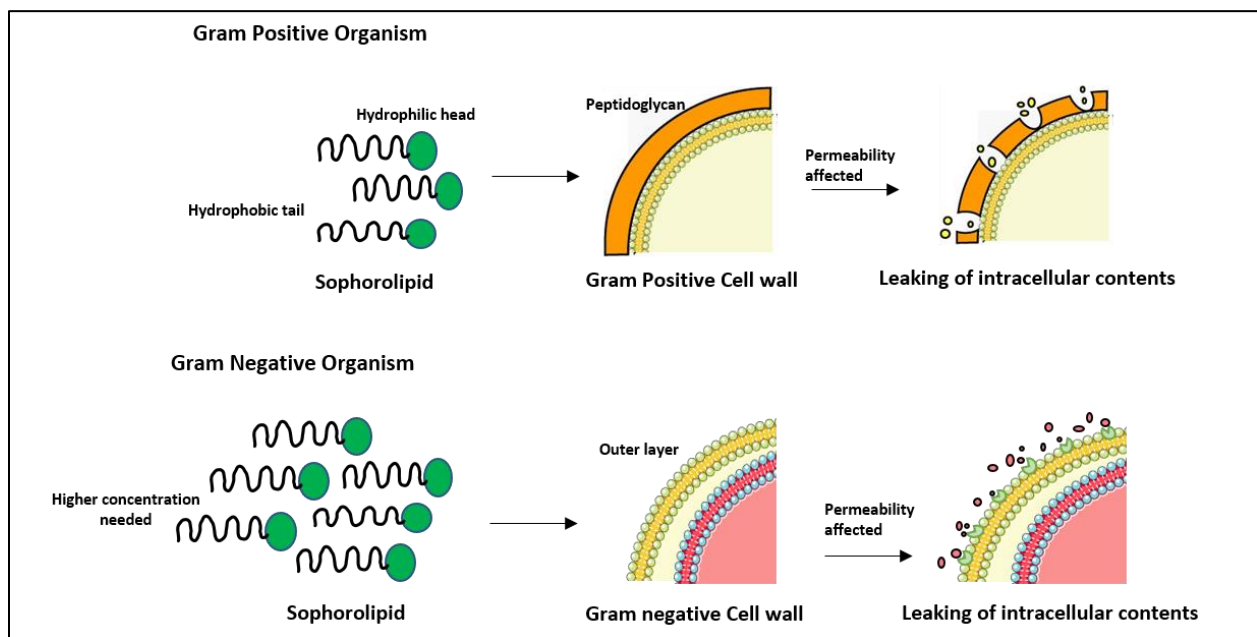


Figure 4.5 Summary of anti-bacterial activity of each synthesized sophorolipid

## Chapter IV: Deciphering the effect of chain length on sophorolipid production: Emphasizing biological properties

An interesting observation in this experiment was that the concentrations of SL required for inhibition of gram-negative bacterium are higher than that of gram positive. This could be primarily due to the structural variations between two bacteria. The cell wall of gram-positive bacteria consists majorly of peptidoglycan whereas that of gram-negative bacteria consist of a thinner layer of peptidoglycan. Also, gram negative bacterium has an extra outer membrane made of mainly lipopolysaccharides, thereby making a much thicker cell wall. Penetration of SL in the gram negative bacterial cell membrane from their hydrophobic tail is difficult owing to the outer membrane<sup>96</sup>. Therefore, higher concentration of SL is needed to inhibit gram negative bacteria as compared to gram positive bacteria and the SLs are more potent against gram positive bacteria. Refer to [Figure 4.6](#).



[Figure 4.6](#) Schematic describing mode of action of SL on bacterial cell

The mechanism by which SLs act on bacterial cells is by rupturing the cellular membrane. This induces leakage of cellular contents and consequent release of certain intracellular enzymes like malate dehydrogenase thereby confirming the direct interaction of SL with cellular membrane<sup>131</sup>.

Zhang *et al.* reported the anti-bacterial activity of SL by using stain ethidium monoxide along with PCR. On treatment with SL, there was considerable decrease in PCR amplification indicating the interaction of SL with cellular contents, as EMA specifically penetrates cells having compromised membrane or outpouring of cellular contents<sup>143,144</sup>. In another study by Dengle-Pulate *et al.*, the effect of SL on the cell membrane of various gram positive and negative bacteria was studied. The SEM studies showed rupture of cell membrane and leakage of cell contents<sup>22</sup>.

The effect of SL on bacterial membrane decreases as the chain length of substrate increases. Short chain derived SL; MASL are potent in killing the bacterial cells than stearic acid derives sophorolipid. As mentioned earlier, SL induce autolysis; which causes disintegration of cell membrane leading to leakage of intracellular contents. The trigger for autolysis is the autolysins (endogenous lytic enzymes) embedded into the cell membrane. The surfactant ability of SL causes solubilization of these autolysins leading to activation of autolysis within cells. As MASL exhibits lowest CMC, its activity is more pronounced on the bacterial membrane. Moreover, the binding of SL onto bacterial cell is dependent on the hydrophobicity of the molecules and therefore, higher chain length of substrate; more time needed to inhibit the bacteria<sup>145</sup>. The process has been schematically described in [Figure 4.7](#).

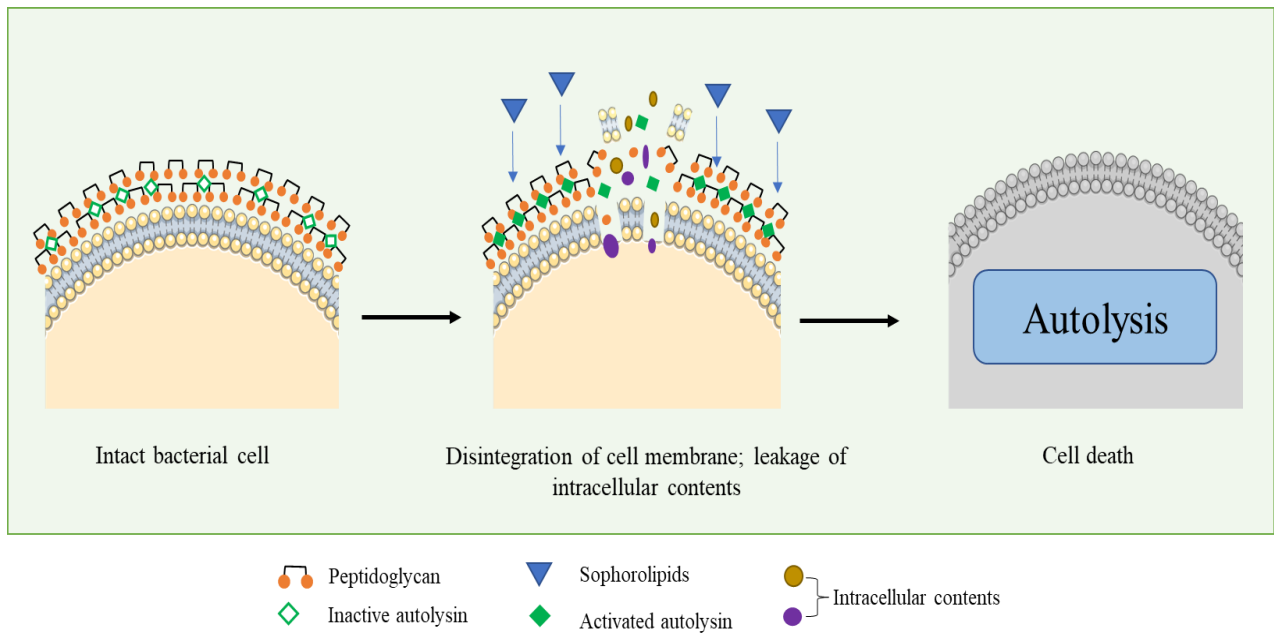


**Figure 4.7** Schematic describing induction of autolysis in bacteria

### 4.3.2 Cytotoxicity against L929 cells:

This section focusses on the cytotoxicity of SL synthesized using various fatty acid substrates. Interestingly, this observed trend is exactly reversed when compared to antibacterial activity. i.e. with increasing fatty acid chain length, the cytotoxicity of SLs increased. Refer to [Figure 4.8](#). For MASL the cytotoxic concentration accounting to 50 % killing of normal cells is 300 µg/ml, whereas, the cytotoxic concentration of PASL is 200 µg/ml and for SASL it is 80 µg/ml. The difference in the mechanism of interaction of SL with bacterial and mammalian cells has not been yet explored and is a part of an ongoing study.

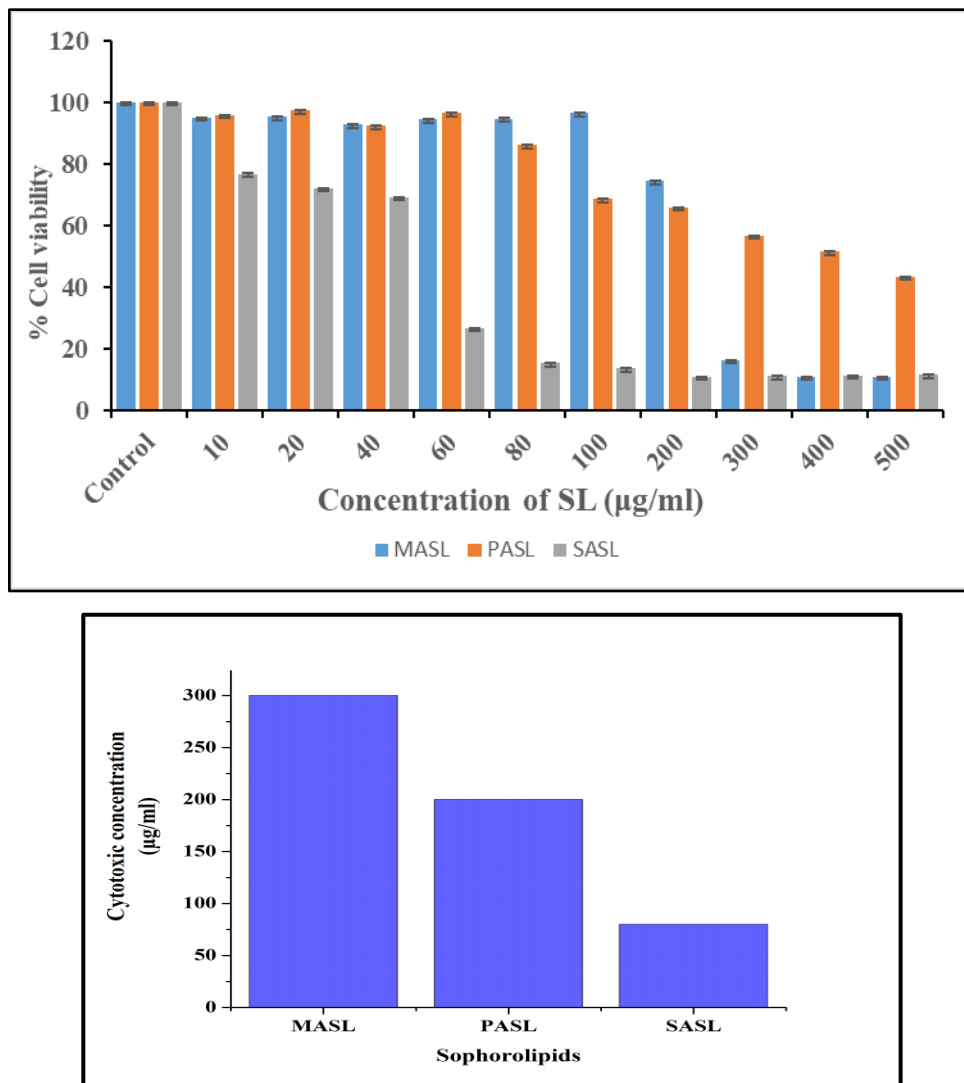


Figure 4.8 Cytotoxicity of all synthesized SL against fibroblast cell line

### 4.3.3 Anti-cancer activity of SL against cervical cancer:

Anti-bacterial activity of SL depicted a chain length dependent activity therefore to further explore the potential and to understand the trend of biological activity, we explored the anti-cancer potential of SL against cervical cancer cell lines. The activity was assessed for synthesized SLs.

Figure 4.9 depicts the anti-cancer activity of crude MASL. The anti-cancer activity revealed that 50 % inhibition observed with concentration of 200  $\mu\text{g/ml}$ . Whereas, concentration of 150  $\mu\text{g/ml}$  is sufficient in killing 80 % of bacterial cells.

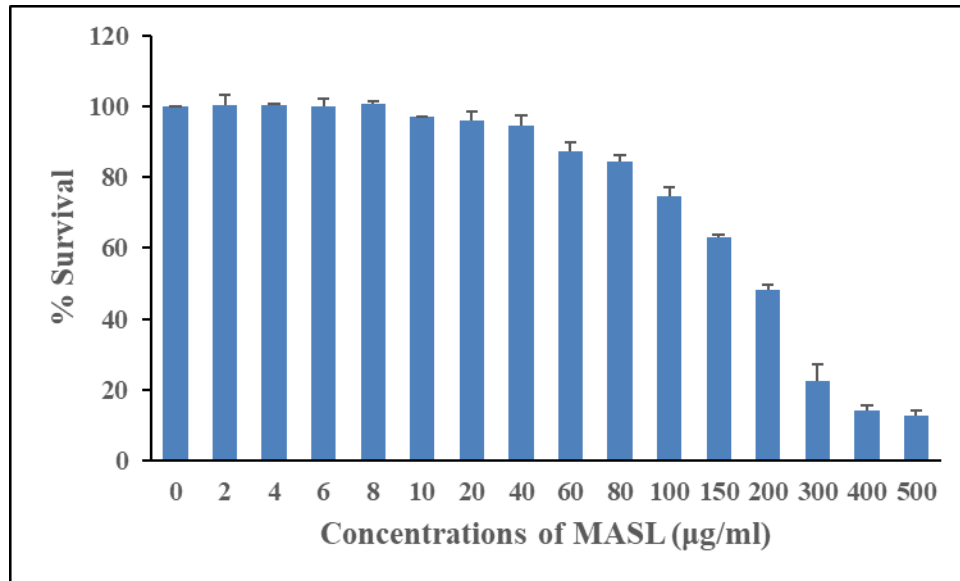
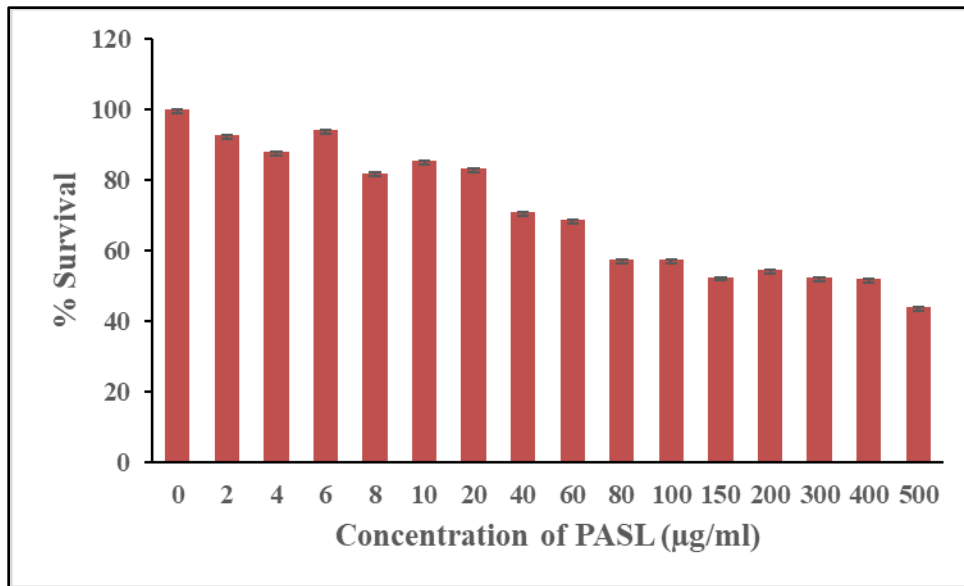


Figure 4.9 Anti-cancer activity of crude MASL against HeLa cell line

Similarly, for PASL, 50 % inhibition as observed at concentration of 500  $\mu\text{g/ml}$ . For PASL higher concentration is needed to achieve the inhibition. Moreover, the inhibition happens gradually as the concentration increases. Refer to Figure 4.10.



**Figure 4.10** Anti-cancer activity of crude PASL against HeLa cell line

Similarly, for SASL in [Figure 4.11](#), 50 % inhibition observed at concentration of 40 µg/ml. For SASL as the concentration increases, the % inhibition also increases.

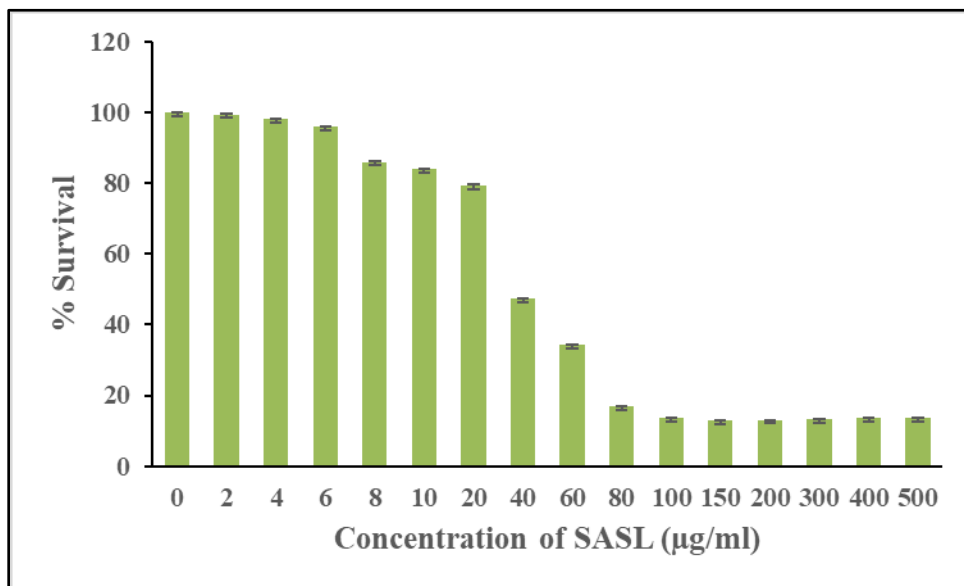


**Figure 4.11** Anti-cancer activity of crude SASL against HeLa cell line



## Chapter IV: Deciphering the effect of chain length on sophorolipid production: Emphasizing biological properties

---

From the results it is evident that SASL is more potent in killing the cancerous cells (at low concentration), however, the same concentrations of SASL proves to be lethal to the normal cells. Similar trend is observed for PASL, where 200 µg/ml concentration causes inhibition of both normal and cancerous cells. However, the trend is different for short chain derived SL. Concentration of 200 µg/ml inhibits 50 % of cancerous cells, without affecting the normal cells. This indeed validates that as the chain length of substrate increases, it affects the biological properties of SL.

From the results, it is observed that the mechanism of action of SL on normal and cancer cell is same. Moreover, it is also evident that as the chain length increases, the concentration needed to inhibit the cells decreases<sup>146</sup>, Figure 4.12. This is mainly because of the inherent need of C18 saturated fatty acids by the cell. Fatty acids alone play an important role in cellular signaling and metabolic pathways. C18 fatty acid have more affinity towards the membrane receptors than the lower chain fatty acid<sup>147,148</sup>. The interaction of fatty acid with receptors or its external supplementation results in membrane perturbation thereby affecting the cellular integrity and mechanism. As SASL contain saturated C18 fatty acid as parent moiety its affection towards membrane receptors is more and therefore, lesser concentration is needed to exhibit the activity<sup>149</sup>. However, in case of MASL and PASL, higher concentration is needed to exhibit the same effects as the affinity towards membrane receptors is less for these fatty acids.

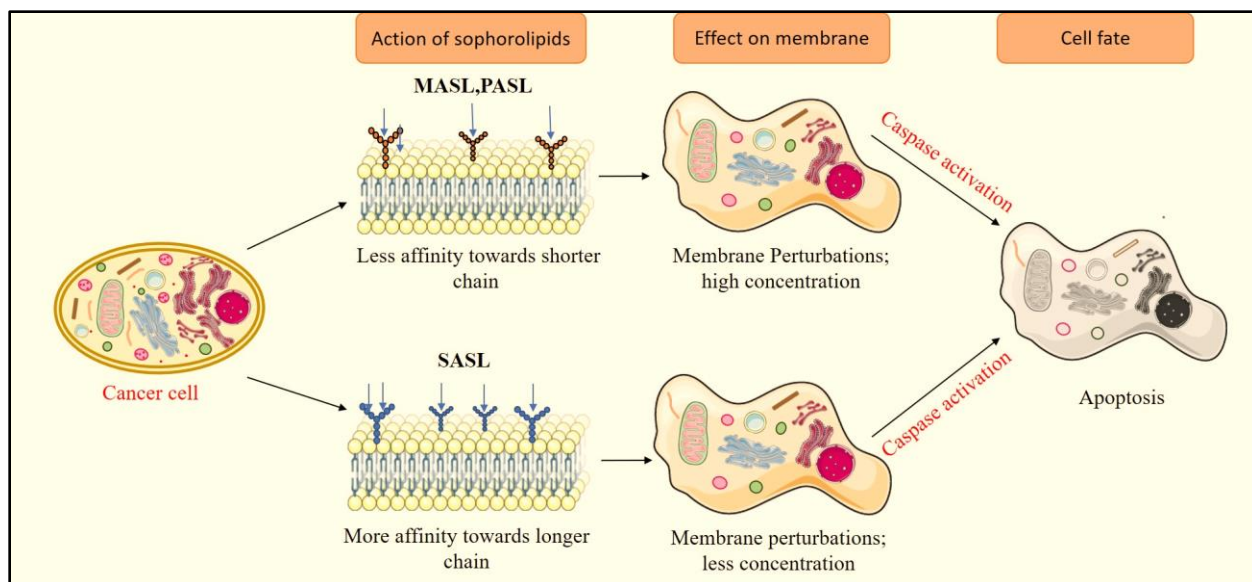


Figure 4.12 Effect of chain length of substrate on biological properties of sophorolipid

#### 4.4 Conclusion:

To summarize, the biological properties of SL are greatly dependent on the nature of lipophilic substrate used. Shorter chain derived SL exhibit excellent anti-bacterial activity against gram positive and gram-negative bacteria. This SL has good anti-cancer potential and are not lethal to the normal cells. These findings along with the results from earlier chapter, validate the fact that decreasing the chain length enhances the physiological and biological properties of the SL.

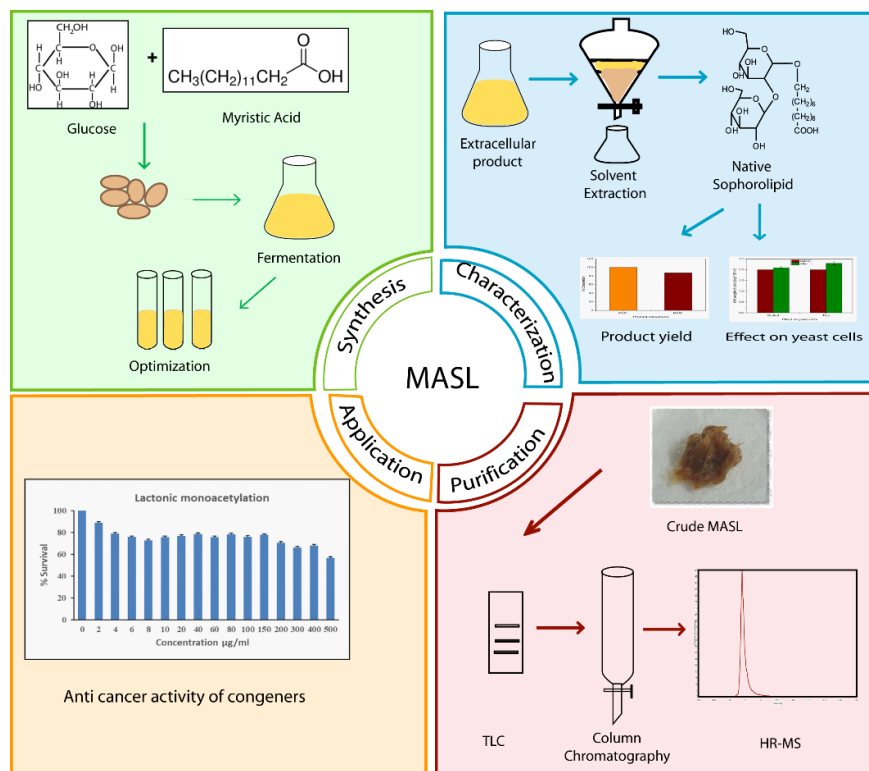
Interestingly, the mechanism of action of SL on bacterial cell and mammalian cell is related to the chain length of substrate. For mammalian cells, the higher specificity of saturated fatty acids towards membrane receptors renders it lethal to the cells whereas, the low surface activity of such higher chain derived SL limits their anti-bacterial potential.

To conclude, myristic acid derived SL exhibited better physical and biological properties as compared to longer chain substrate, thereby indicating the importance of lipophilic substrate on SL production.

## Chapter V

### **Myristic acid derived sophorolipid: production, purification and biomedical application**

Microbial glycolipids are one of the most interesting alternatives to chemical-based surfactants as they exhibit improved biodegradability and less toxicity. However, their potential has been limited because of specificity of the yeast toward fatty acids having a carbon 16 or carbon 18 chain. This study focuses on SL production by the yeast *Starmerella bombicola* using myristic acid, a medium-chain carbon-14 fatty acid that has not been used as a substrate for SL production. The production was optimized for inoculum size and lipophilic substrate concentration. Furthermore, we also studied the effect of medium-chain fatty acid on yeast cell growth and optimized the process for excellent yield. Individual congeners of the crude mixture were separated using dry column chromatography and then structurally characterized by mass spectrometry. Further the anti-cancer potential of each individual congener of MASL has been studied.



## 5.1 Introduction

The extracellularly synthesized SL constitute a mixture of mono acetylated or di acetylated acidic and lactonic forms of SL. These structural variations depend on the position of hydroxyl fatty acid, degree of saturation and fatty acid chain length<sup>150</sup>. Overall heterogeneity of SL is hampered due to the limited specificity of substrate length. Use of shorter chain length substrate would broaden the application range as this will result in shift of hydrophilic/hydrophobic balance of the molecule leading to better water solubility and improved surface lowering abilities. The substrate specificity of yeast *S.bombicola* towards, C16-18 fatty acid chains is governed by the enzyme cytochrome P450 monooxygenase. This specificity could be circumvented by using hydroxylated short chain substrates or by modifying the substrate thereby resembling to stearic acid or by modifying the fermentation process<sup>151</sup>. Hydroxylation of fatty acids marks the beginning of SL pathway; this includes etherification of fatty acids at its hydroxyl end to glucose molecule resulting in formation of glucolipid. Omitting this step by using hydroxylated fatty acids allows incorporation of different short chain substrates like secondary alcohols(C12-C16), ketone 2-,3-,4- dodecanones, 1,12-

dodecanediol and 12 hydroxydodecanoic acid. Furthermore, unconventional substrates could be incorporated by using substrates with internal ester bond and resemblance to stearic acid. These include: dodecyl glutarate, tetradecyl malonate and dodecyl pentanoate. The SL synthesized by these substrates are later subjected to alkaline hydrolysis so as to obtain short chain derived SL. Although, these modifications seem promising, their execution and upscaling could be cost incurring and time consuming<sup>152</sup>. Therefore, a promising alternative to this would be circumventing the fermentation process to synthesize short chain SL. At optimal temperature and pH condition, the wild strain yeast successfully converts a wide range of lipophilic substrate into SL production. Even in absence of lipophilic substrate, the yeast synthesizes SL by using its inherent enzymatic system. Using this property, we aim to optimize the fermentation process for synthesizing MASL by wild stain of *S.bombicola*.

Myristic acid being a novel substrate for SL synthesis, the influence of MASL on yeast cell growth and product yield were analyzed. The crude MASL was then purified and the individual congeners were separated by column chromatography and analyzed by LC-HRMS for elucidating the structural diversity of new synthesized SL. As described in Chapters III and IV, MASL exhibited better physical and biological properties than conventional substrates. Therefore, MASL was selected for further studies. Building on the data from Chapter IV, the biological potential of MASL was further assessed by studying the anti-cancer activity of individual congeners and deducing the mode of action of SL on cancerous cell.

This chapter focuses on understanding the mechanism involved in successful incorporation of myristic acid as substrate for SL synthesis and determining its effect on the yeast cell growth and yield. Moreover, as myristic acid was a novel substrate, the influence of each congener on the biological attributes of synthesized SL were studied along with the mode of action.

## 5.2 Materials and method:

### 5.2.1 Microorganisms and Maintenance

*S. bombicola* (ATCC 22214) was used for the production of SL and was maintained on agar MGYP media, composition as described in earlier chapter II.

SL synthesis and characterization was carried out as described in chapter III (Section 3.2.2). The synthesized product was referred as MASL and subjected to purification as mentioned below:

### 5.2.2 Media Optimization

Optimization studies were performed in triplicates. Different media compositions (growth associated, resting cell, induction, and nitrogen depletion) were used for media optimization. The bioprocess of SL consists of two phases: the growth phase and production phase. In the resting cell method, the cells were grown in MGYP media along with the lipophilic substrate (0.1%) and later transferred to production media (PM). For the induction experiment, myristic acid (0.1%) was added to the media during the growth phase, and then, fermentation was continued in the same media (with top-up of glucose and the lipophilic substrate). For growth-associated, the MGYP media was used for both the growth and production phases (with top-up of glucose and the lipophilic substrate). Nitrogen depletion was achieved by eliminating the nitrogenous sources from the media.

Another experiment was designed to analyze the effect of shorter chain fatty acids on yeast cell growth. For this, the test sample contained myristic acid (1%) as a lipophilic substrate for fermentation, while the control was devoid of any external lipophilic substrate, *de novo* fermentation. Biomass was calculated at the end of fermentation and compared.

### 5.2.3 Purification of MASL

Purification of synthesized MASL was carried out using dry column chromatography. Silica gel (UV–visible GF 254 nm) with a mesh size of 100–200 was used as the packing material, and dialysis tubing was used as a dry column. Before packing the column, silica gel was activated by heating at 110 °C for 4 h. Precisely, 100 g of activated silica gel was mixed thoroughly with 10 mL of distilled water. Distilled water was added to maintain the moisture level and for the reproducibility of the Rf value. Dialysis tubing of measurement 4 × 40 cm was sealed at one end. Crude MASL (2 g) dissolved in ethyl acetate was mixed with an equal amount of dry activated silica gel, and then, the resultant slurry was packed into the column. The solvent system (100 mL) consisting of chloroform/methanol/water (65:15:2, v/v/v) was loaded onto the column and allowed to migrate for 2 h until it reached the end of the column. The column was examined under UV–visible illumination at 254 nm. Five distinct bands with respective Rf were observed which were cut out with a surgical knife. The individual gel slices were added to ethyl acetate and stirred to form a slurry. The resulting supernatant was collected and rotary-evaporated. Each fraction was further analyzed by HR-MS<sup>153</sup>. Refer [Figure 5.1](#).

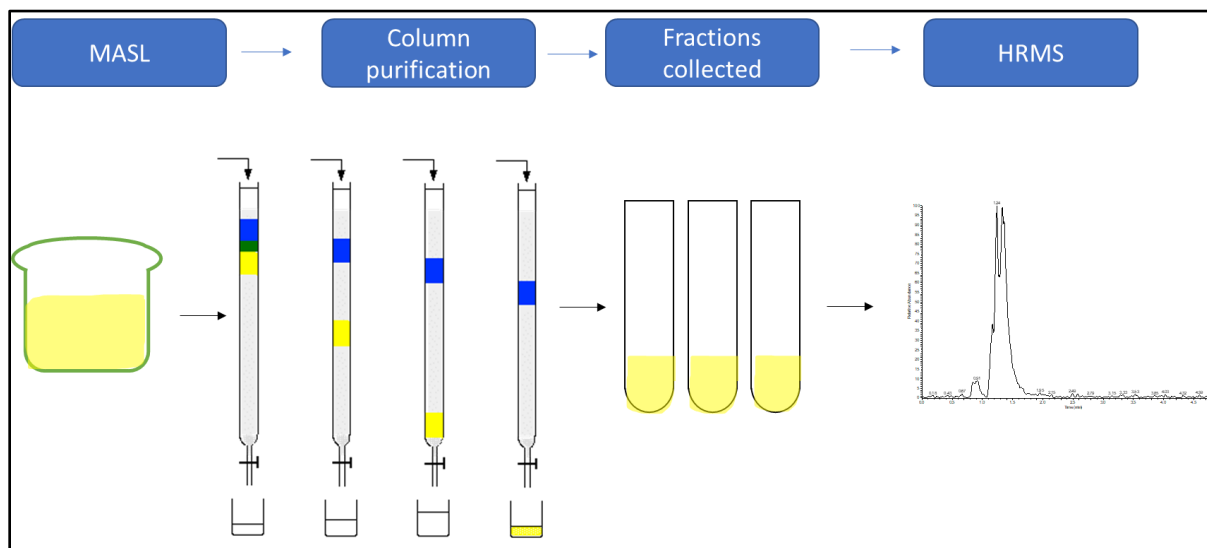


**Figure 5.1** Schematic describing the protocol followed for purification of crude MASL



#### **5.2.4 Anti-cancer activity of SL:**

The anti-cancer activity of each congener was studied by performing MTT assay. The protocol used for this assay is same as described in Chapter IV, section 4.3.3.

#### **5.2.5 Fluorescence activated cell sorting:**

Flow cytometry is a popular quantitative tool used to study cells cycle and DNA content. Through flow cytometry cells with defined genetic and biochemical properties could be identified. It helps in identification of cell death pathways viz; apoptosis or necrosis. [Figure 5.2](#) explains the working of flow cytometry which consists of 2 forms: non sorting and sorting. Sorting type possesses the ability to separate fluorescent labelled cells from a mixed population. The cytometer consists of cell sorter, optics and detector. The sample runs through the cell sorter and is transported to the light source. The excitation optics focuses on the cells and the collection optics gathers the light transmitted by the cells and pass it to the detector. Fluorescent compounds with specific wavelength are used depending on the nature of the sample. For protein samples the fluorochromes used are FITC, phycoerythrin, allophycocyanin. Fluorochromes used for nucleic acids, ethidium bromide and propidium iodide<sup>154</sup>.

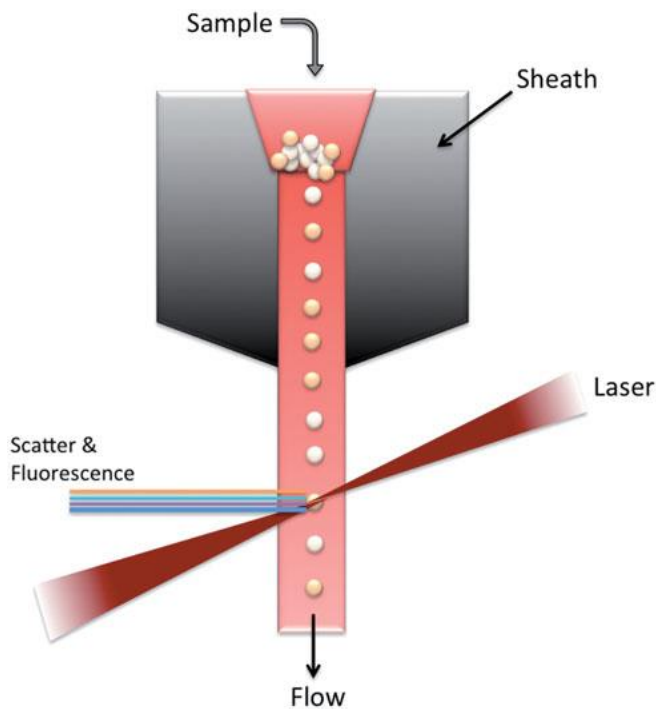


Figure 5.2 Working principle of FACS

### 5.2.6 Chemicals for FACS:

Triton X and propidium iodide were procured from Sigma Aldrich. RNaseA was obtained from Thermo Fischer. All the chemicals were stored as per the manufacturer guidelines until use.

### 5.2.7 FACS protocol:

The protocol used to access the anti-cancer activity of SL is described below:

HeLa cells with density  $2 \times 10^5$  were seeded in 6 well flat bottom plate. After 24h, the spent media was replaced with different concentration of SL ( $\mu\text{g/ml}$ ). The concentrations were decided based on the results obtained in Chapter III. The treated cells were detached by trypsinization and cells were harvested by centrifugation at 1000 rpm for 5 minutes.

The harvested cells were then fixed by 70 % cold ethanol at 4 ° C for 18h. Later, the cell pellet was re-suspended in 0.5 ml PBS containing 0.25 % Triton X 100 and incubated for 15 minutes at RT. The cell pellet was obtained by spinning down the cells by centrifugation at 1000 rpm for 4 minutes. Supernatant was discarded and cell pellet was re-suspended in PBS containing 10 µg/ml RNase A and 20 µg/ml propidium iodide and incubate for 30 minutes in dark conditions<sup>155</sup>.

### 5.3 Results and discussions:

#### 5.3.1 Media optimization:

Fatty acids of length C16–C18 such as oleic acid are most preferred substrates of enzymes involved in SL biosynthesis by *Starmerella bombicola*. Therefore, the first objective of this study was to optimize the synthesis of myristic acid SL (C14) with respect to yeast cell growth and yields. Preliminary optimization studies were performed using different media compositions (resting cell, growth-associated, induction, and nitrogen depletion). The results revealed that the maximum yield (12 g/L) of MASL was obtained with the resting cell method. Refer [Figure 5.3](#). In the resting cell method, the cells are harvested after the growth phase and subjected to new media during fermentation. Thus, the cells have fresh supply of components for production of SLs. Also, introduction of myristic acid during the growth phase leads to acclimatization of the cells to the unconventional substrate, resulting in good yield. It can thus be concluded that the resting cell method along with induction works best for synthesis of the short chain derived SL–MASL. The use of myristic acid as the substrates also has few advantages: its usage is FDA approved and is also declared GRAS clear by FEMA.

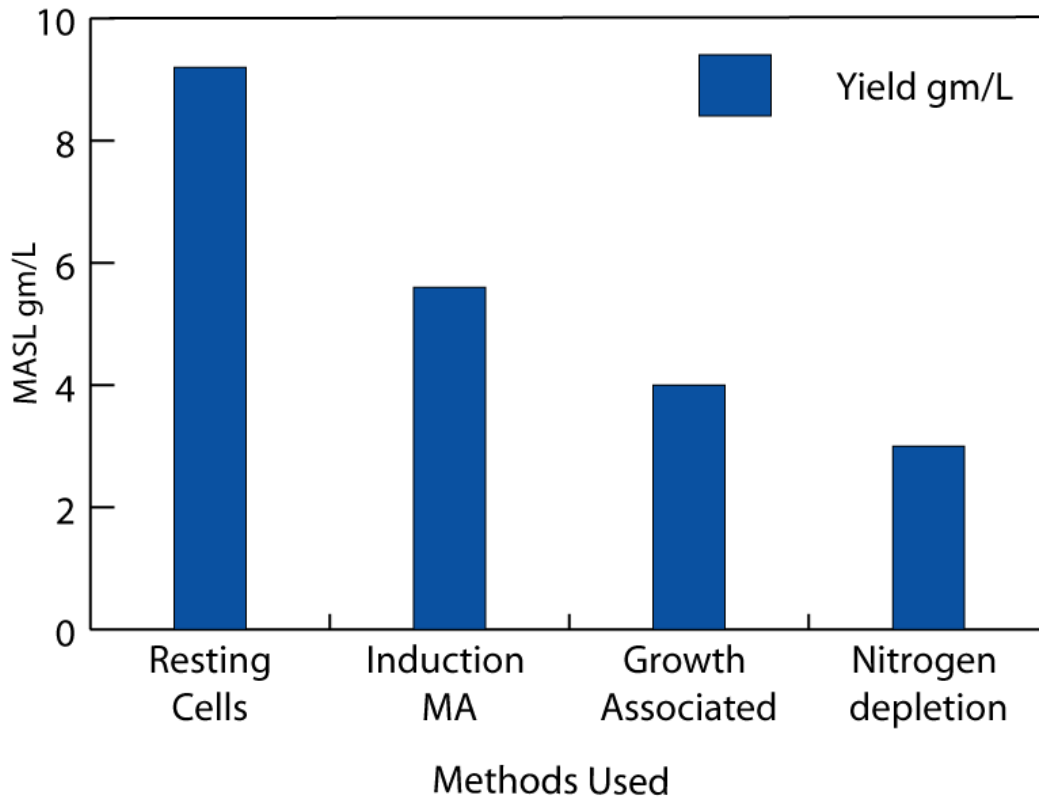


**Figure 5.3** Graph indicating the yield obtained on using different fermentation methods for synthesizing MASL

Our studies also showed that the optimized method of MASL production had no adverse effect on the cell mass ([Figure 5.4](#)). The probable reason for successful synthesis of this SL is its role in myristoylation: a lipid modification involving the addition of myristic acid to the N terminal of glycine. This lipidation reaction plays an essential role in protein–protein interaction and signal transduction pathways. Therefore, exogenous supply of myristic acid through the fermentation media activates the N-myristoyl transferase enzymes, which are involved in myristoylation. Moreover, myristic acid acts as a hydrophobic anchor in the lipid bilayer of the cell, thereby facilitating the association of G protein with the plasma membrane ([Figure 5.5](#)). Therefore, myristic acid is not considered foreign by the cell and is easily incorporated into the enzymatic machinery, further leading to SL synthesis<sup>156,157</sup>.

Moreover, *S. bombicola* possesses the inherent ability to synthesize the SL for its metabolism, and as a defense mechanism, this is known as the *de novo* product. This is carried out by the fatty acid synthase system (FAS) of the cell<sup>158</sup>. Nguyen *et al* studied the correlation between the FAS system and fatty acid profile of the cell using a wide range of fatty acids (C14–C20) and concluded that the exogenous supply of myristic acid is indeed beneficial for the growth of the yeast cells<sup>159</sup>. These studies agree with our results from the optimization studies and thereby verify that myristic acid, as the sole lipophilic substrate, is not harmful to the yeast cells.

Furthermore, the product conversion of MASL was compared with the conventional OASL and it was revealed that MASL yielded more than 85% conversion of lipophilic substrates. Refer to [Figure 5.6](#). This indicates that not all short chain substrates are lethal to cell and lead to low yield.

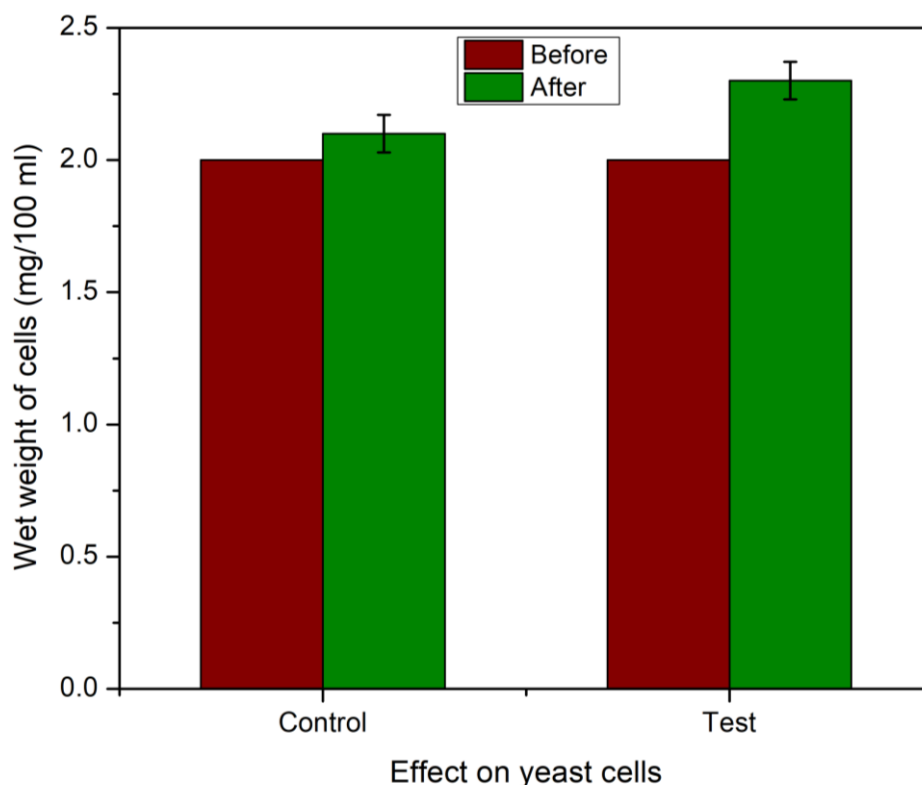


[Figure 5.4](#) Graph depicts the effect of short chain substrate on the growth of yeast cells post the fermentation process

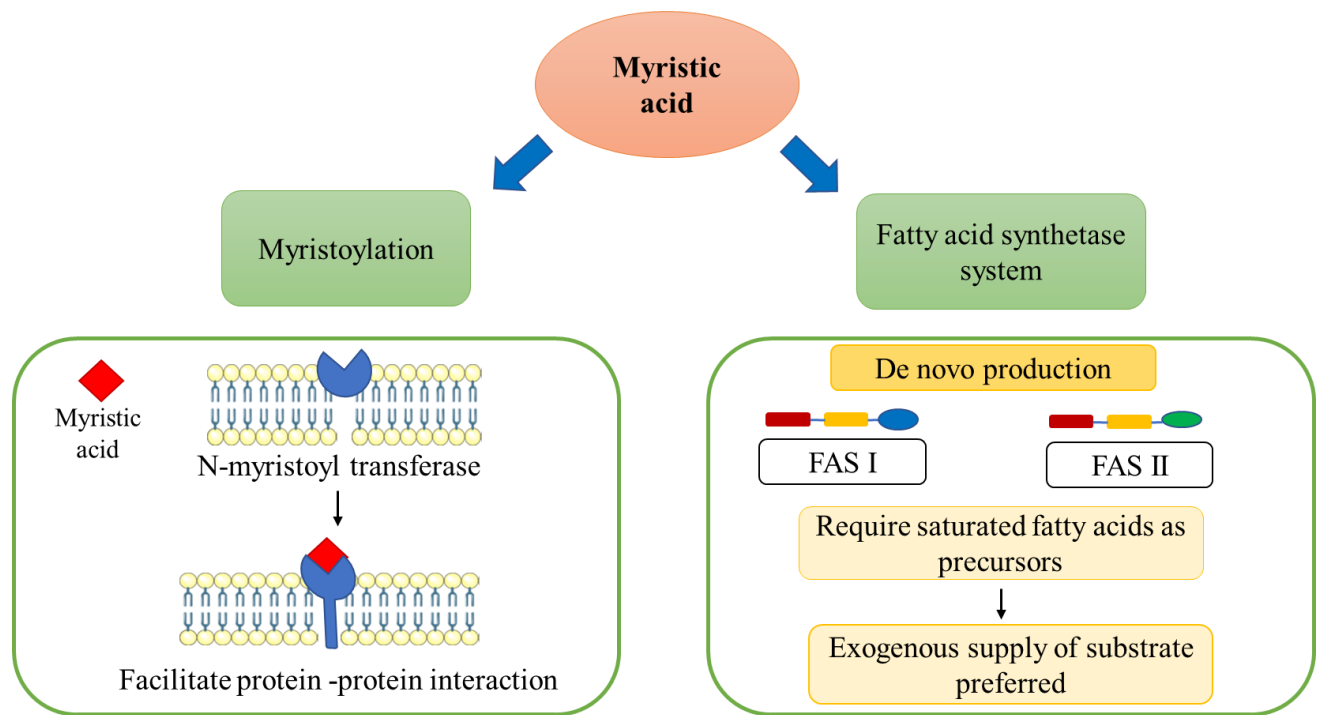


**Figure 5.5** Schematic representing the importance of myristic acid for yeast metabolism and other cellular function

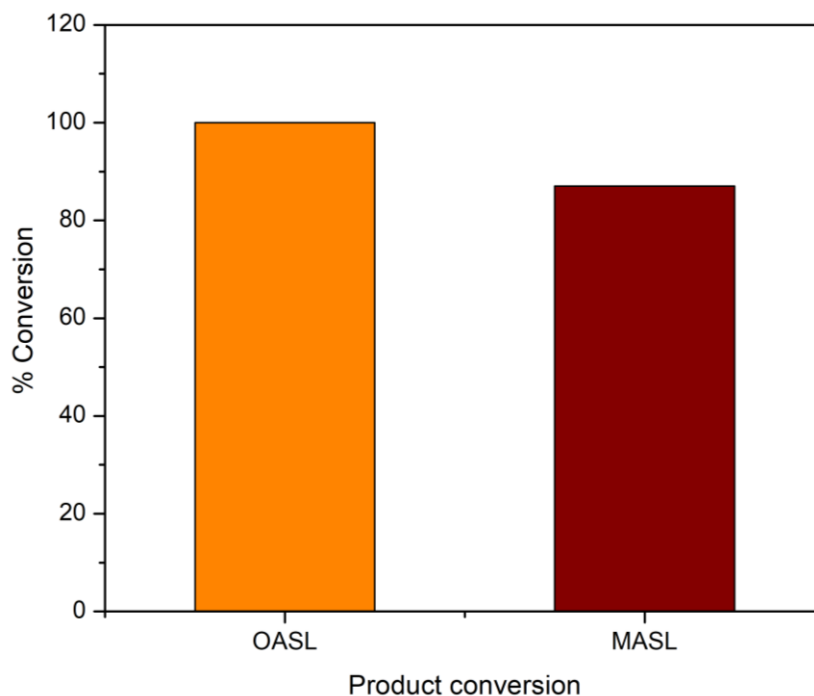


**Figure 5.6** Graph denotes the comparison of product conversion between oleic acid and myristic acid derived SL

### 5.3.2 Purification of MASL:

As described in Chapter III, section 3.3.5, the crude SL is a mixture of acidic and lactonic types of SLs with acetylation, diacetylation, or monoacetylation. The purification of this crude SL was performed in dialysis tubing, which resulted in separation of the mixture into well-defined bands. The yield of all the bands was 80% of the initial crude SL loaded onto the column. These separated SLs were then run-on TLC, and each fraction depicted a single band, thereby confirming their purity.

The individual fractions from purification were further analyzed using LC-HRMS to identify the molecular weight of individual components. The molecular weights of each congener were similar to that obtained in the crude mixture. The different modifications obtained from the congeners were: acidic SL, monoacetylated acidic SL, monoacetylated lactonic, diacetylated acidic form, and diacetylated lactonic SL.

### 5.3.3 High-Resolution Mass Spectrometry:

The below graphs depict the chromatogram and corresponding mass spectrum of individual congeners post purification (Fractions collected from dry column chromatography).

**Figure 5.7**, depicts fraction I, a peak obtained at 1.23 RT corresponds to acidic SL protonated ion, with molecular formula  $C_{26}H_{49}O_{13}$  and  $m/z$  569.3163.

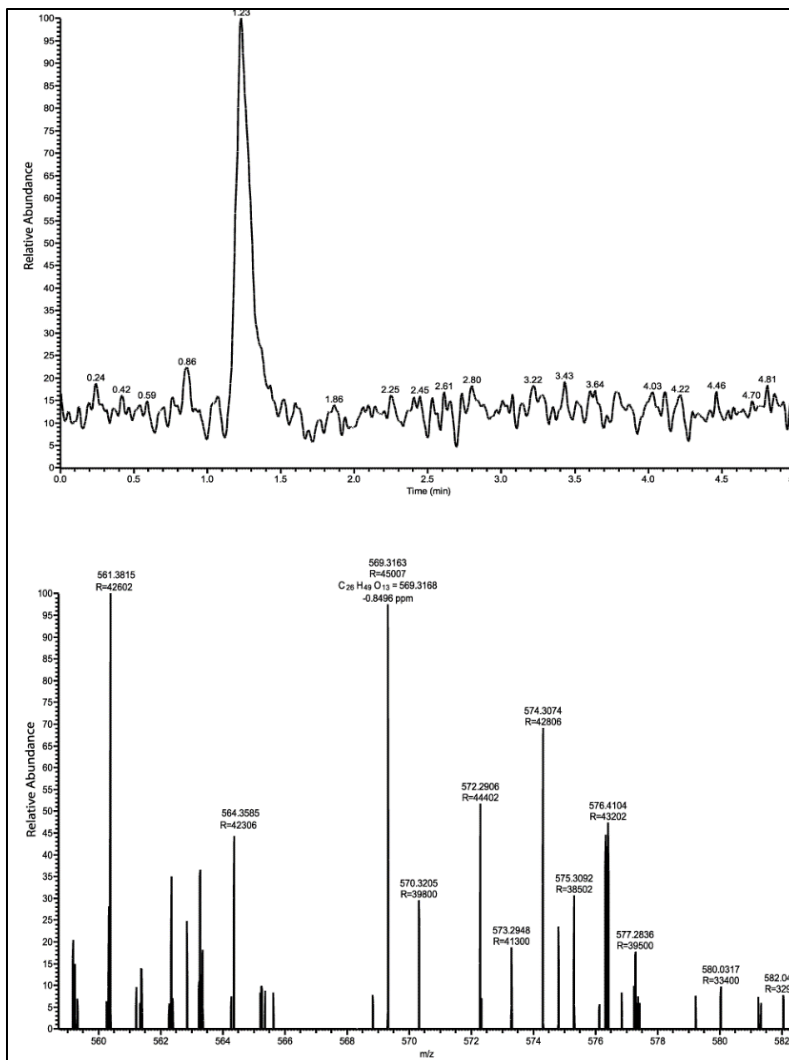


**Figure 5.7** Extracted ion chromatogram and mass spectrum of fraction I



## Chapter V: Myristic acid derived sophorolipid: production, purification and biomedical application

For fraction II a peak was obtained at 1.24 RT which corresponds to lactonic monoacetylated SL sodium adduct ion, with molecular formula  $C_{28}H_{48}O_{13}$  and  $m/z$  615.2985. Refer [Figure 5.8](#). The small peak at 0.91 is attributed to the solvent system used.

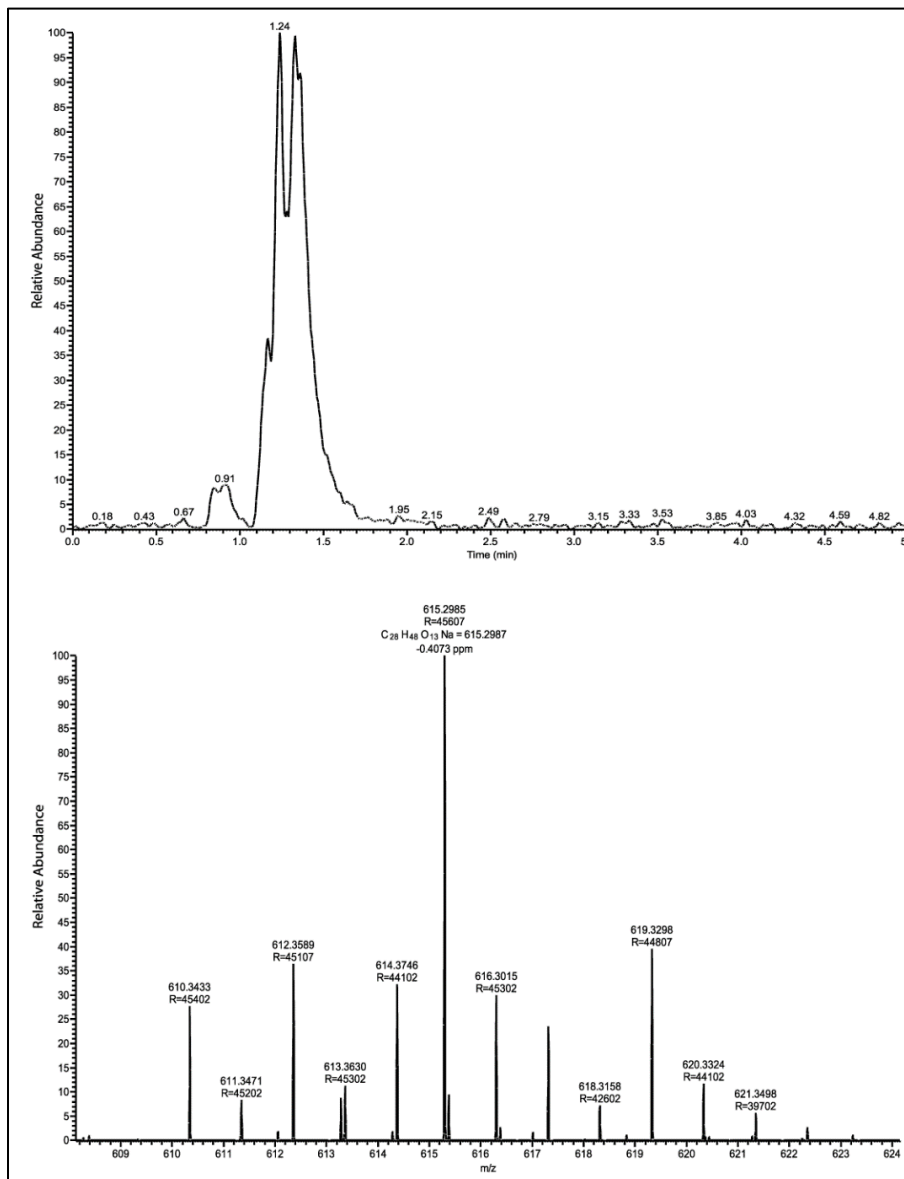


**Figure 5.8** Extracted ion chromatogram and mass spectrum of fraction II

Figure 5.9 depicts fraction III with peak obtained at 1.39 R.T, which corresponds to acidic monoacetylated sophorolipid sodium adduct ion, with molecular formula  $C_{28}H_{50}O_{14}Na$  and  $m/z$  633.3107.

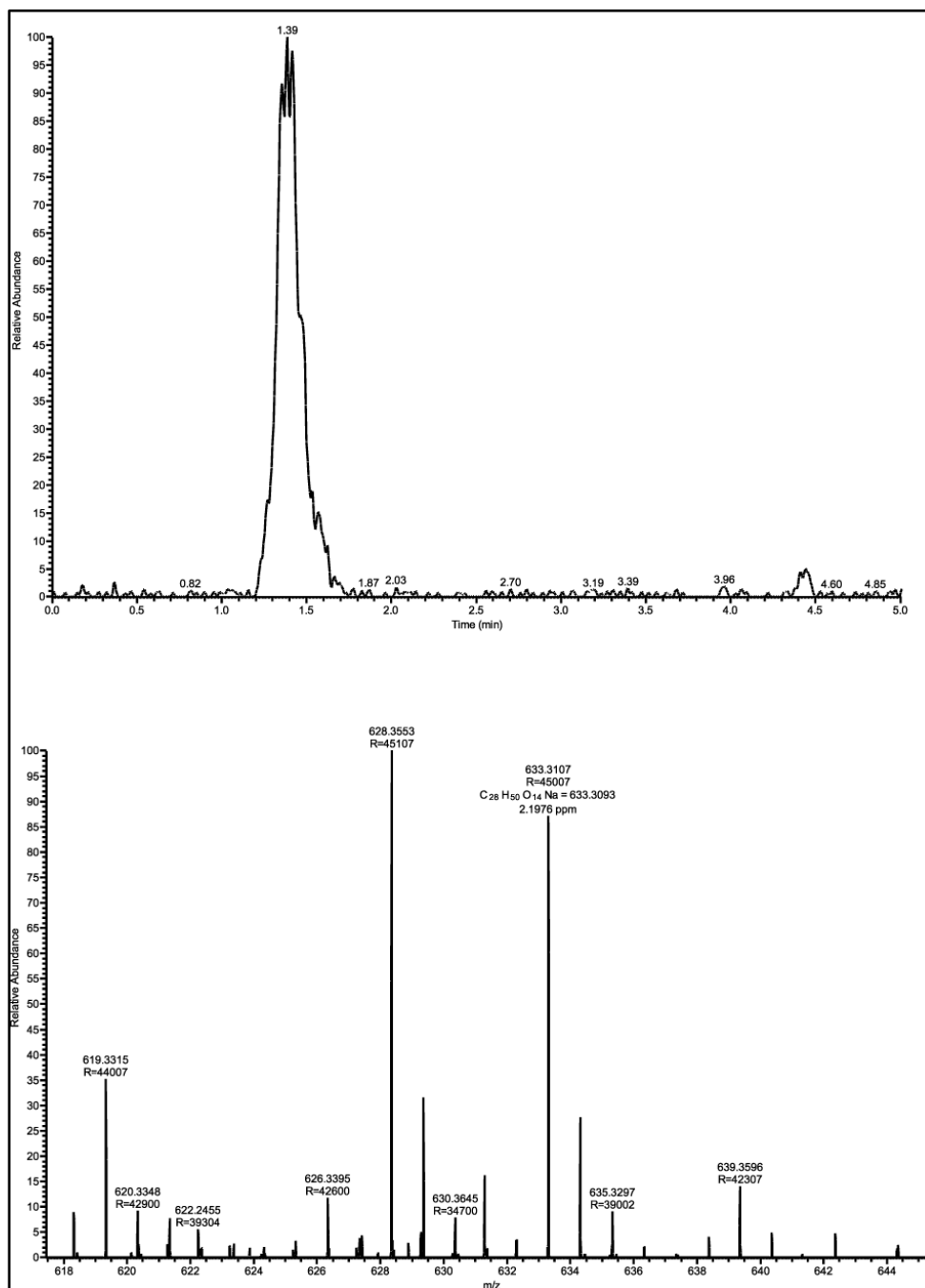
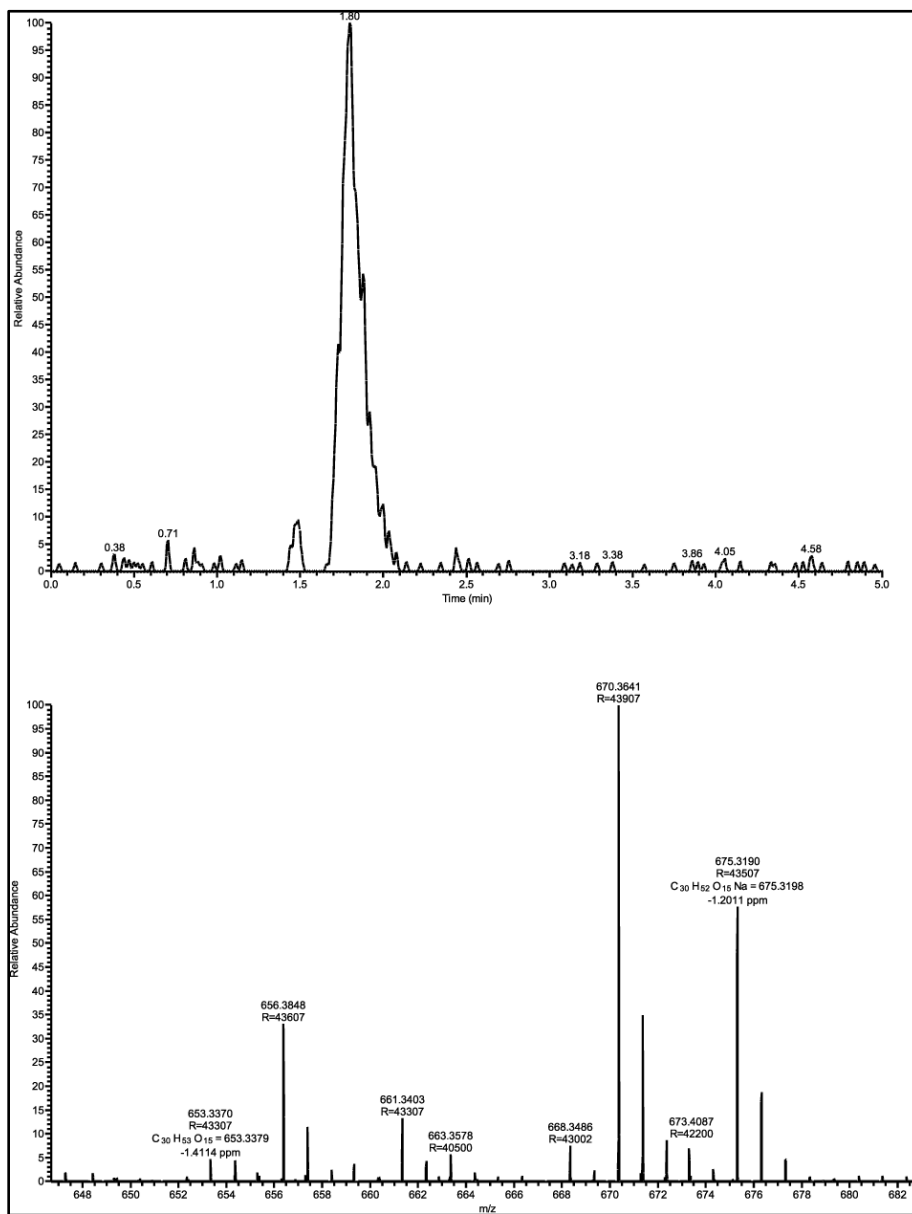


Figure 5.9 Extracted ion chromatogram and mass spectrum of fraction III

A sharp peak was obtained at 1.80 R.T for fraction IV which corresponds to acidic di acetylated SL sodium adduct at  $m/z$  675.3190, with molecular formula  $C_{30}H_{52}O_{15}Na$ . Refer [Figure 5.10](#).



**Figure 5.10** Extracted ion chromatogram and mass spectrum of fraction IV

## Chapter V: Myristic acid derived sophorolipid: production, purification and biomedical application

For fraction V a sharp peak was obtained at 1.39 RT, which corresponds to lactonic di acetylated SL protonated ion with molecular formula  $C_{30}H_{50}O_{14}$  and  $m/z$  657.3086. Refer [Figure 5.11](#).

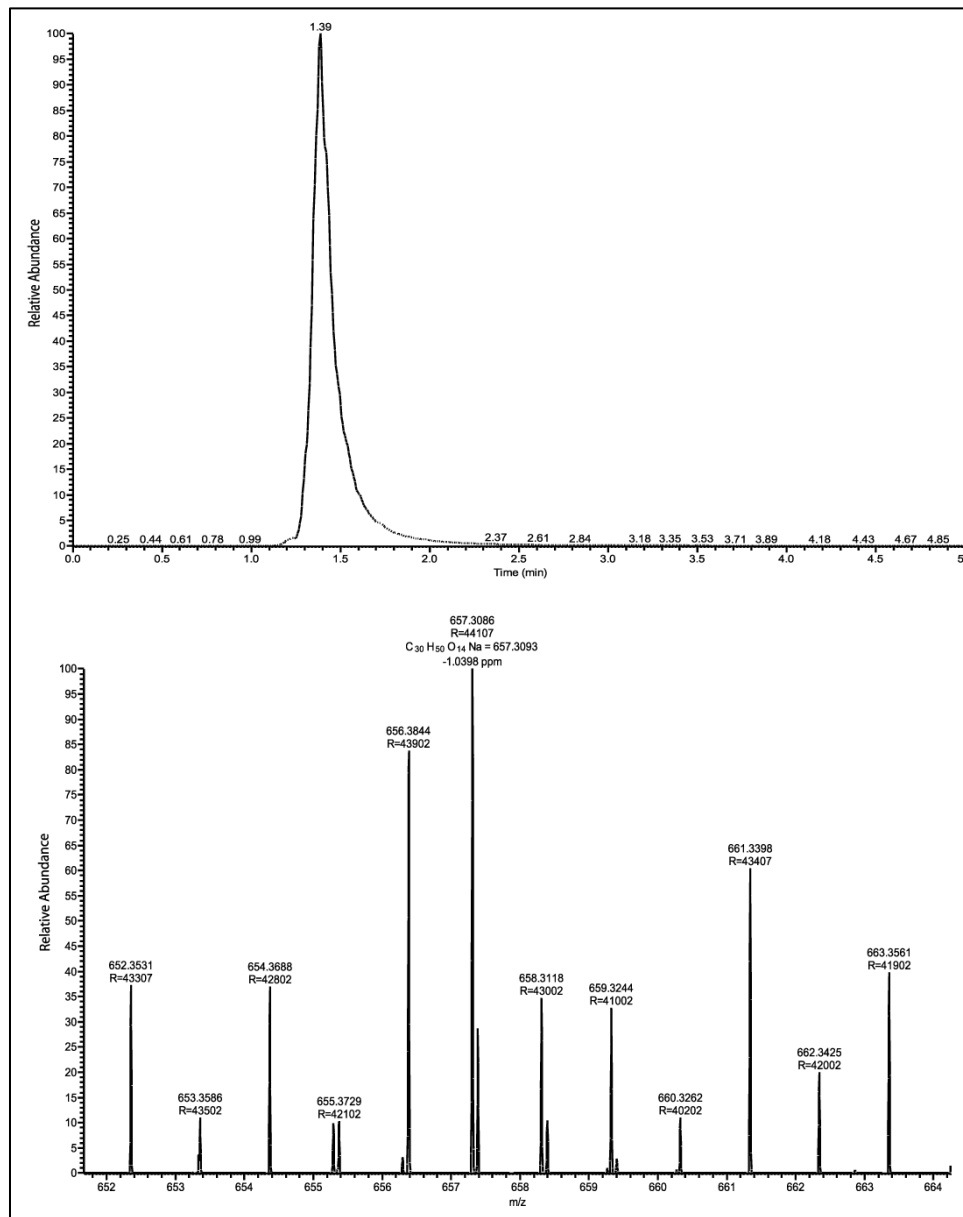


**Figure 5.11** Extracted ion chromatogram and mass spectrum of fraction V

It is also observed that MASL has preferential glycosylation at  $CH_3$  end. The [Table 6](#) in Chapter III depicts the different modifications present in MASL.

From column chromatography 5 different congeners were obtained which are in accordance with the modification mentioned in [Table 6](#). These include both forms of acidic and lactonic congeners i.e monoacetylation and deacetylation and native form of SL. For exploring the individual potential of each congener, anti-cancer activity mono and di acetylated acidic and lactonic congeners was assessed.

### 5.3.4 Anti-cancer activity of MASL:

The individual congeners were successfully separated and further assessed for their anti-cancer potential. In this, two types of both acidic and lactonic forms namely; monoacetylated and di acetylated were selected. From the [Figure 5.12](#) it is clear that of the two forms of lactonic congeners the diacetylated congener exhibited better anti-cancer activity. Concentration of 200  $\mu\text{g/ml}$  and above were able to inhibit 40-50 % of the cancer cells. Whereas, the same activity was achieved with higher concentration (500  $\mu\text{g/ml}$ ) for the mono acetylated congener. The difference in the anti-cancer activity of two congeners of same form are attributed by their structural variation thereby affecting their amphiphilic nature<sup>160</sup>.

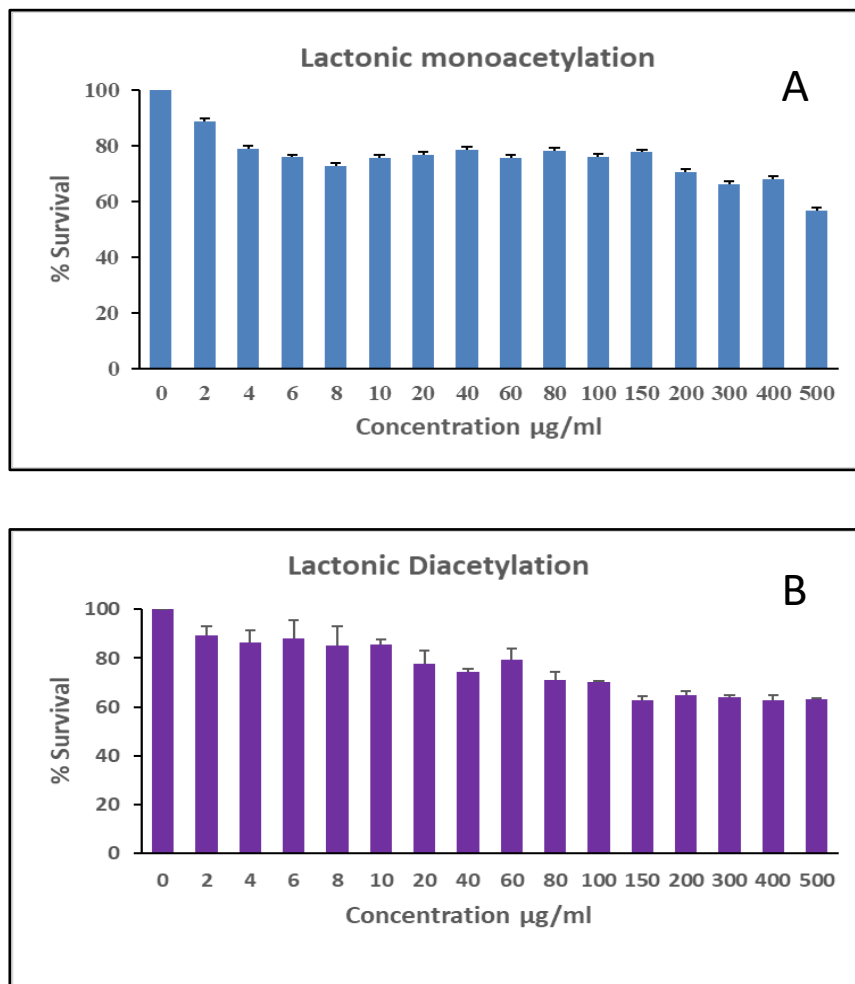


Figure 5.12 Graph describes the anti-cancer activity of lactonic congeners against cervical cancer

From the graphs (Figure 5.13) it is observed that the acidic congeners (mono and di) lack the anti-cancer activity. Even at highest concentration 10-20 % killing of cancer cells was observed. Acidic components contribute to the surfactant ability of SL and therefore, their biological potential is low. However, the lactonic components exhibit good biological properties but their solubility remains an issue. The anti-cancer potential of crude has been described in Chapter IV, section 4.3.3, it is evident that crude SL possesses better activity than the individual congeners. Each part i.e acidic and lactonic impart different properties to the molecules. A mixture of both results in combined properties for the SL. Thus, the crude SL possesses good anti-cancer property and is

also soluble in aqueous solutions owing to its acidic content. Therefore, for commercial application, the use of crude SL would prove beneficial.

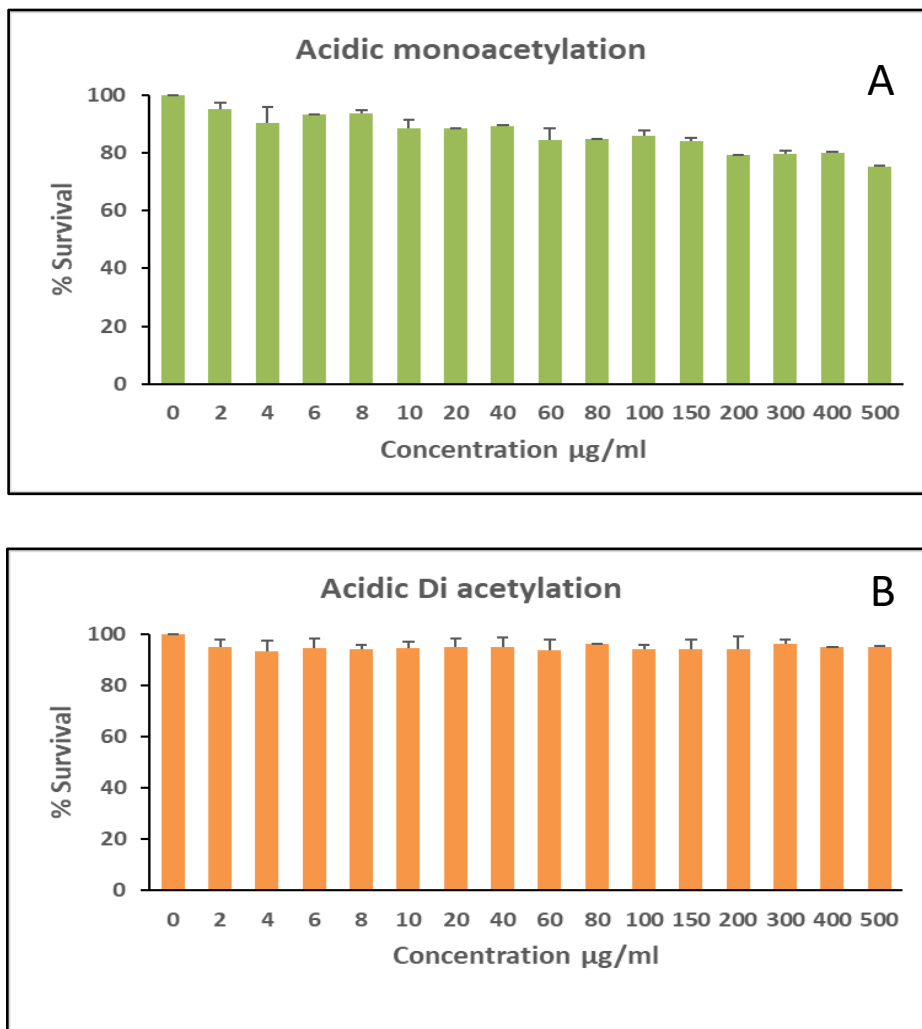
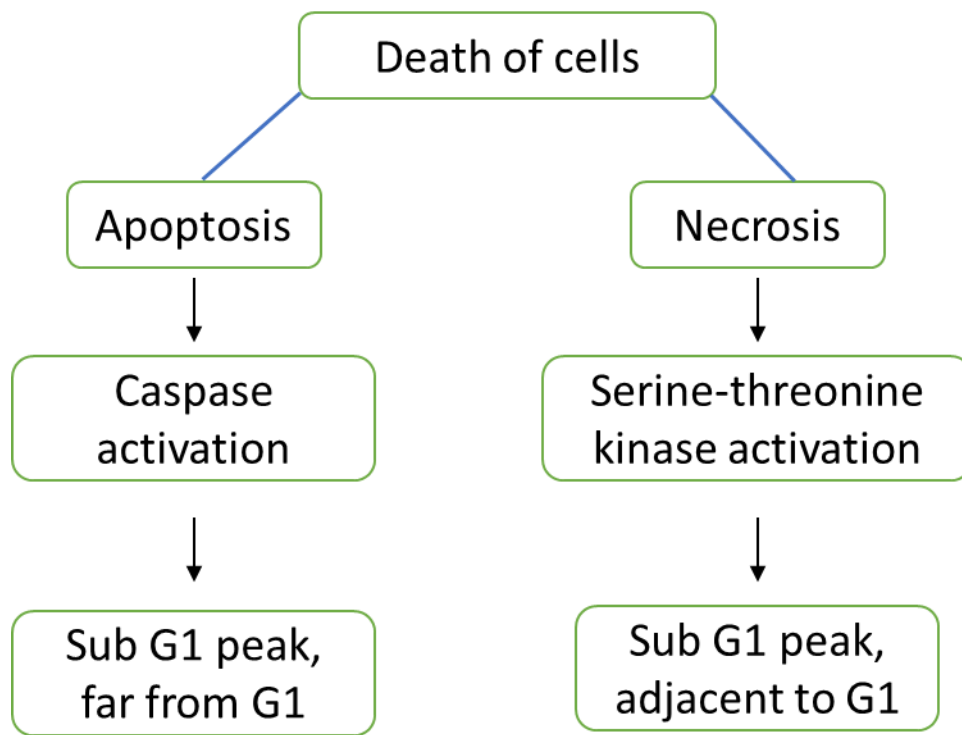


Figure 5.13 Graph depicting the anti-cancer potential of acidic congeners against cervical cancer

### 5.3.5 Fluorescence assisted cell sorting:

Earlier Chapter IV proved that MASL inhibits the cervical cancer cells efficiently. To further investigate the mechanism of action flow cytometry was used. The reasons for cell death are either apoptosis or necrosis (Figure 5.14). Apoptosis results in characteristic cellular changes like cell shrinkage, nuclear and chromosomal fragmentation and activation of caspases. Whereas, necrosis involves serine- threonine activation for inhibition. Through flow cytometry these changes could be identified<sup>161</sup>. Oleic acid derived SL have been known to induce apoptosis in human liver cell and breast cancer<sup>142</sup>.



**Figure 5.14** Diagrammatic representation of different pathways leading to death of cell

Cell cycle distribution was measured through FACS upon 24h treatment with different concentrations of MASL. The proper cell cycle graph was observed for control samples consisting of all 3 stages mainly; G0/G1, S and G2/M. G1 phase resembles growth, S for DNA synthesis and G2/M phase for meiosis and mitosis. Of the total population of cells, 42.5 % were G0/G1 phase,



18 % cell population for S phase and G2/M phase accounting for 30 %. The sub G1 phase was negligible (0.5 %) in control samples<sup>162</sup>. Refer [Figure 5.15](#).

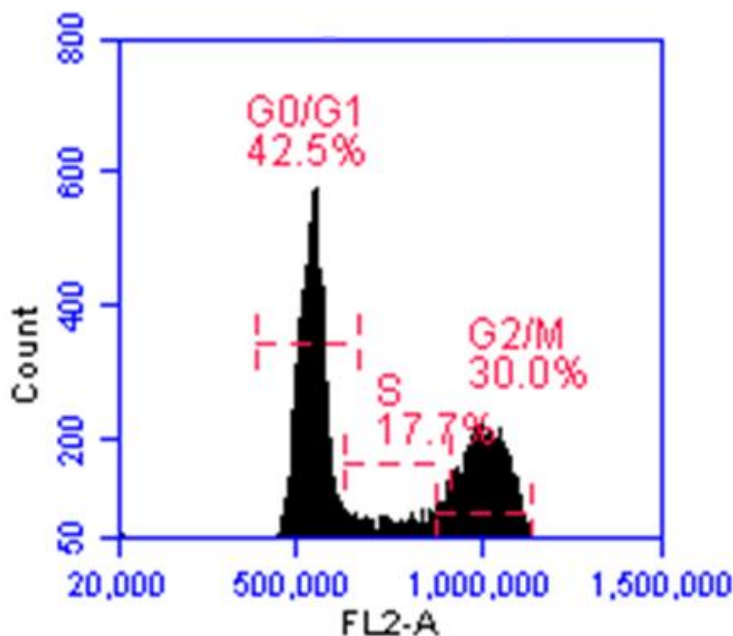


Figure 5.15 Graph denoting the cell cycle curve of control sample

For MASL treated samples, tremendous increase in the sub G1 population was observed ([Figure 5.17](#)). The appearance of sub G1 peak is a characteristic of apoptosis. For MASL sample with concentration of 200  $\mu\text{g/ml}$  the sub G1 phase was around 7 %, while the other phases were as follows: G0/G1- 40 %, S phase- 20 % and G2/M phase- 26 %.

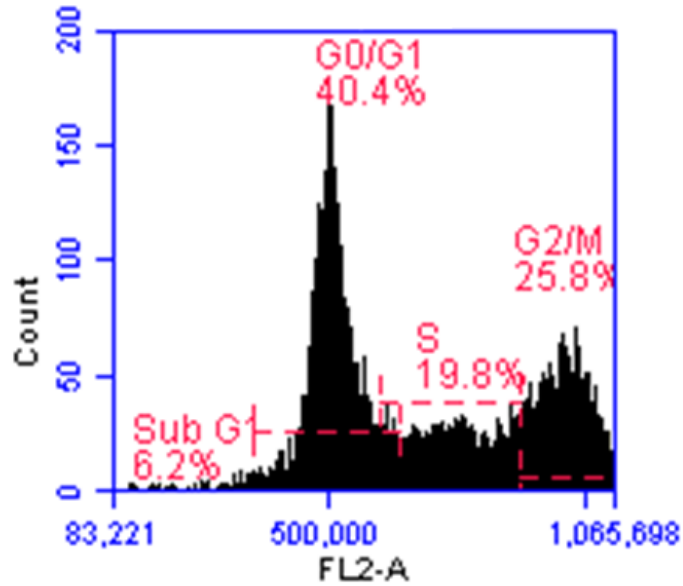


Figure 5.16 Graph denoting the cell cycle curve after treatment with lower concentration of MASL

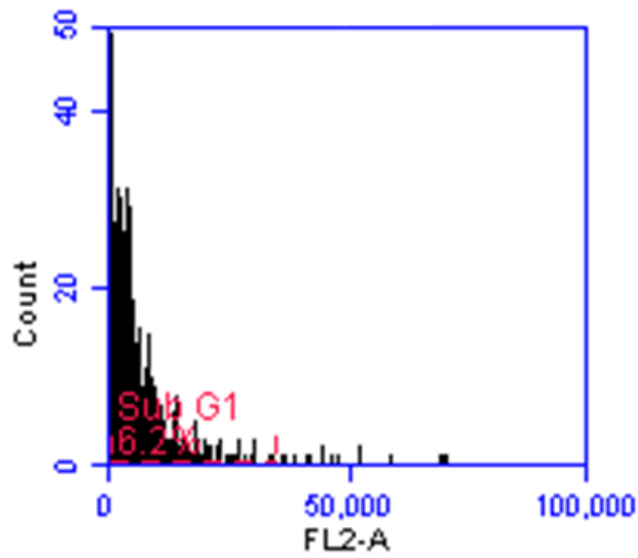


Figure 5.17 Graph highlighting the subG1 phase of cell cycle

On further increasing the MASL concentration (300  $\mu\text{g/ml}$ ), increase in sub G1 peak was observed. The Sub G1 accounted for nearly 42 % (Figure 5.18). This indirectly validates the concentration of MASL needed to inhibit 50 % of the cancerous cells (described in Chapter III). For higher concentration sub G1 peak was most prominent, the other peaks were very negligible.

These experiments confirms that MASL inhibits the cancerous cells by inducing apoptosis. Moreover, as the concentration of MASL increases, the anti-cancer activity of MASL also increases.

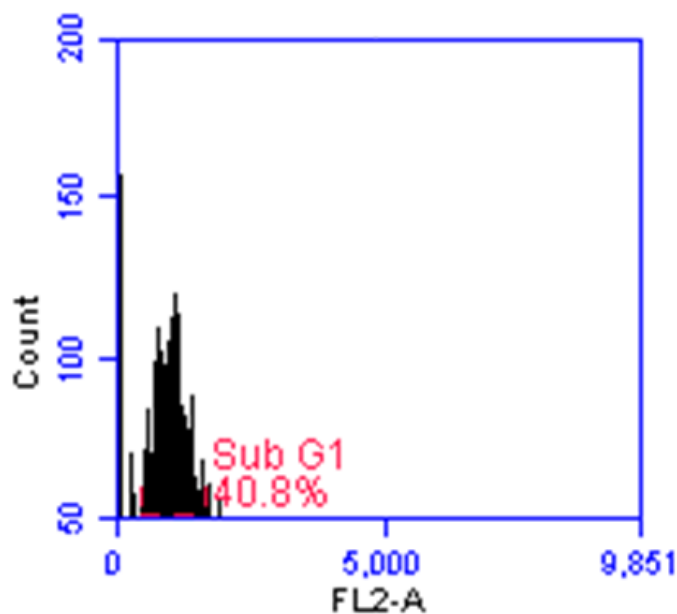


Figure 5.18 Graph denoting the sub G1 population after treatment with higher concentration of MASL

Apoptosis can be induced in different ways like: by death receptors, by mitochondria and by endoplasmic reticulum. Endoplasmic reticulum is an important organelle for protein biosynthesis and maintaining the intracellular calcium homeostasis. Interaction of SL with cancer cells induces perturbations in the membrane. This causes stress to the endoplasmic reticulum resulting in accumulation of  $\text{Ca}^{2+}$  ions in the cytoplasm as reported by Dubey *et al.* The higher calcium content

in the cytoplasm leads to endoplasmic reticulum stress. Onset of stress, activates the caspase pathway thereby resulting in apoptosis of the cells<sup>106,163</sup>. This mechanism indirectly supports the earlier FACS data thereby verifying the induction of apoptosis by MASL as described in [Figure 5.19](#).

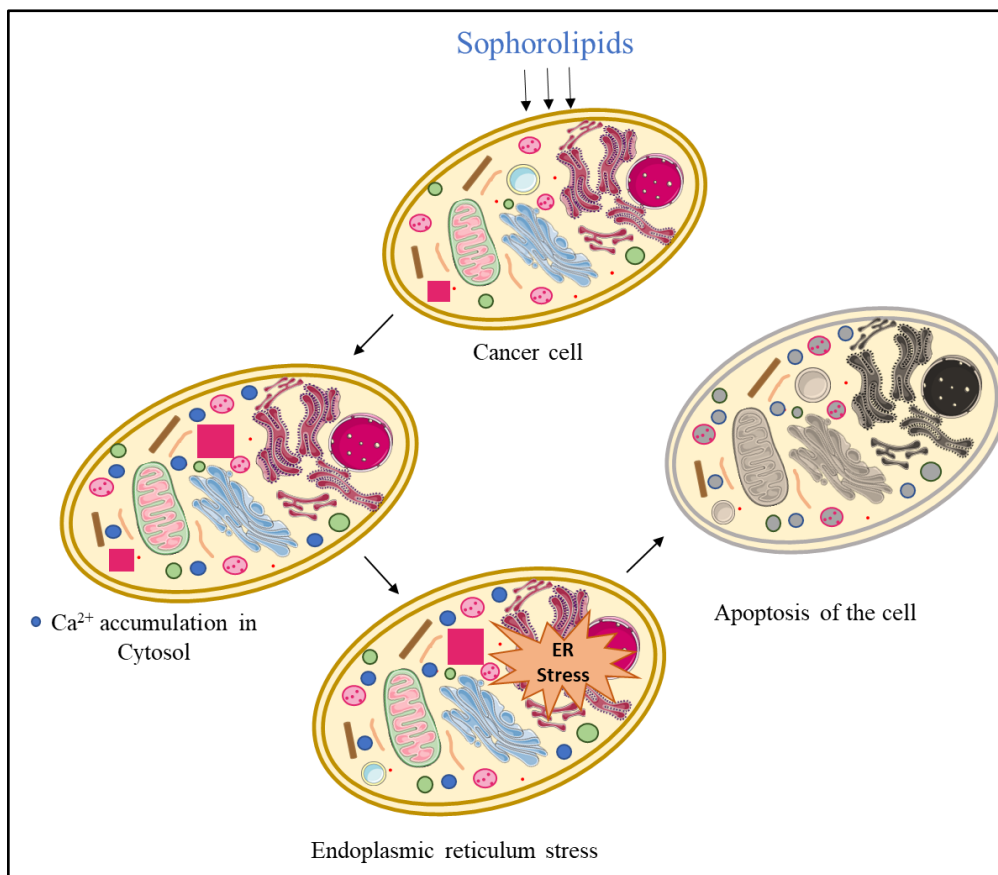


Figure 5.19 Schematic representation of mechanism of action of SL on cancerous cells

## 5.4 Conclusion:

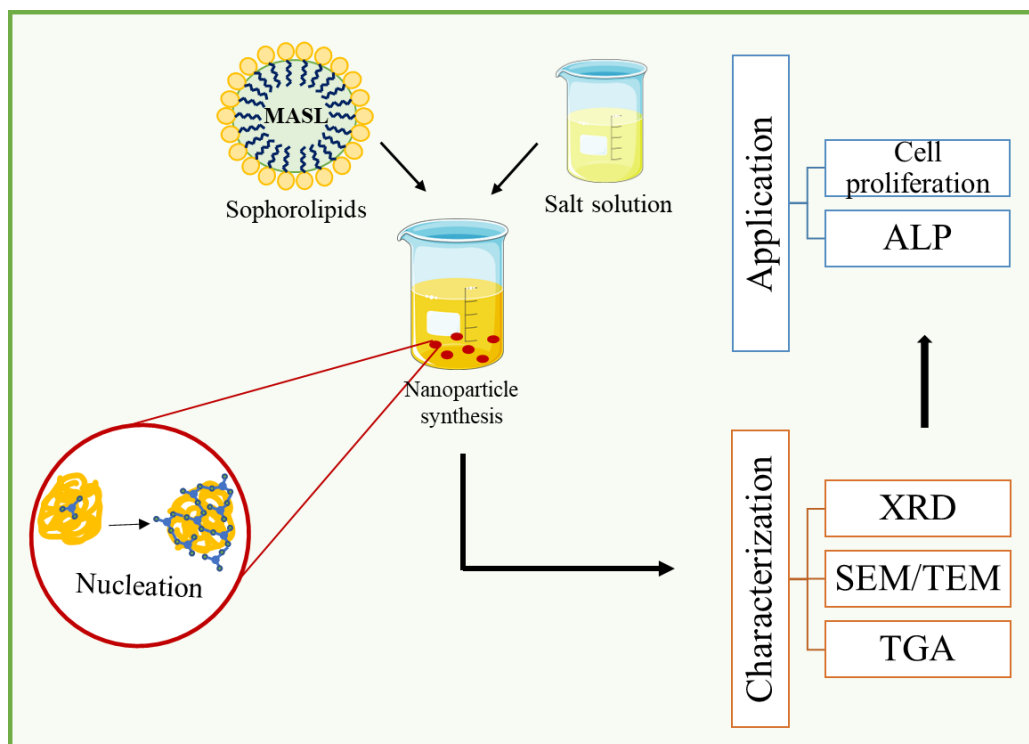
In conclusion, this study indicates that myristic acid as substrate is successfully incorporated into SL without hampering the cell growth or product yield. MASL was purified to identify each congener. It was observed that crude MASL exhibited better anti-cancer activity than individual

congeners. The amalgamation of both acidic and lactic components into the crude SL proves beneficial in enhancing the applicability of the molecule. Moreover, MASL inhibits the cancerous cells by arresting the cells in sub G1 phase. This inhibition effect was concentration dependent. The underlying mechanism involves stimulation of the activation of caspases leading to apoptosis of cancer cells. The caspase activation is linked to the distress caused to the endoplasmic reticulum. Thus, myristic acid proves to be a promising substrate for SL synthesis, exhibiting better physical and biological properties than the conventional substrates. Use of short chain fatty acids as substrates for SL synthesis could improve the applicability of these SL.

## Chapter VI

### Synthesis of calcium phosphate nanoparticles using short chain derived sophorolipid

SLs have been used for synthesizing metallic nanoparticles. However, use of SLs as capping/reducing agents for synthesis of inorganic/ceramic nanoparticles has not been explored. This chapter focuses on synthesizing calcium phosphate nanoparticles using short chain derived SL for bone tissue engineering application. The synthesized nanoparticles are characterized for their structural and morphological properties using different techniques. Furthermore, the mechanism of action of SL in nano particle has been deduced and presence of SL on the nanoparticles has been confirmed. Lastly, the nanoparticles have been used for *in vitro* studies and these studies demonstrate that the particles have promising applications in bone tissue engineering



## 6.1 Introduction:

Nanotechnology refers to small size i.e things in the size range of  $10^{-9}$  m. Size of particles is directly proportional to their properties. Nanoparticles have gained interest over the last decade due to unique properties and application in varied industrial sectors<sup>164</sup>. Nanomaterials are plausible solutions to various environmental and technological challenges like packaging, cosmetics, medicine, pharmaceuticals and biotechnology. Nanoparticles are generally synthesized by physical and chemical processes involving high temperature, pressure and toxic compounds. The most common way to synthesize nanoparticles are by converting metal salts into metal ions by different reducing agents like hydrazine, hydrides, citrate and ethylene glycol. These agents pose environmental and health hazards. Moreover, the mechanical methods adopt top-down approach wherein bulk materials are gradually broken down. This approach is destructive in nature and requires prolong synthesis<sup>165</sup>.

These concerns associated with the chemical method of synthesis led to advancement in the field of biosynthesis or green synthesis of nanoparticles<sup>166</sup>. Nanobiotechnology has emerged as an interesting branch involving integration of both nanotechnology and microbial biotechnology. Nanobiotechnology includes use of microbial systems and their products for synthesizing nanomaterials/ compounds. In biosynthesis, the microorganism, plant extracts, enzymes or secondary metabolites produced by microbes act as reducing agent for the conversion. The advantages of using biological systems for nanoparticle synthesis are: easy processes, economical, environmentally safe and non-toxic. Also, the biological methods follow nondestructive bottom-up approach, where the molecules are assembled into defined structures<sup>167</sup>. The Figure 6.1 describes the different methods of nanoparticle synthesis.

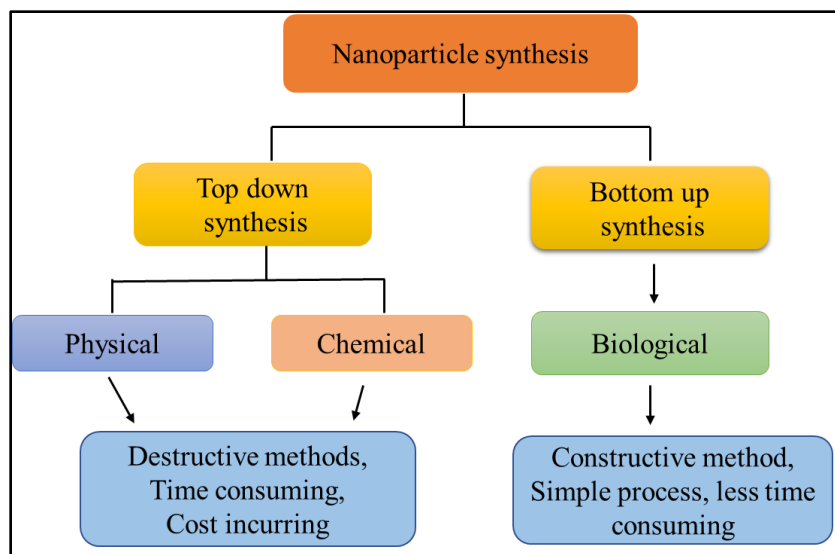


**Figure 6.1** Schematics describing the different methods used for synthesizing nanoparticle

Synthesis of metallic nanoparticles using different parts of plant have been reported earlier. Chandran *et al* reported synthesis of gold and silver nanoparticles using leaves of aloe vera. These nanoparticles were used for optical coatings<sup>168</sup>. Similarly, neem leaves have been used to synthesize zinc oxide nanoparticles<sup>169</sup>. Apart from plant extracts, different microorganisms have also been studied for nanoparticle synthesis. Spherical shaped silver nanoparticles have been synthesized by *L.casei*<sup>170</sup>. Gold nanoparticles have been obtained from *E.coli* and *B.subtilis*<sup>171,172</sup>. Certain fungi like *Aspergillus*, *Fusarium* and *Trichoderma* have been used to synthesize lead, platinum and silver nanoparticles<sup>173-175</sup>. Algal species like *Chlorella* and *Phaeodactylum* have been reported to produce gold and titanium nanoparticles for anti-bacterial and anti-cancer applications<sup>176,177</sup>. One of the most common enzymes involved in biosynthesis of metal nanoparticles is nitrate reductase. Most bacteria are known to secrete this NADH dependent enzyme<sup>167</sup>.

Apart from plants and microbes, nanoparticles could be synthesized by using biosurfactants<sup>113,178</sup>. Amphiphilic nature of biosurfactants allows biosynthesis of metallic nanoparticles. Kasture *et al* reported the use of SL for synthesizing cobalt and nanoparticles<sup>179</sup>. SL act as capping and reducing agent for synthesizing nanoparticles. Upon capping the nanoparticles, the sugar moiety if free and



exposed to solvent environment, thereby increasing the solubility and dispersibility of the nanoparticles. Another advantage associated with SL being, the process is extracellular i.e nanoparticles are extracellularly synthesized thereby minimizing the steps. Figure 6.2 summarizes the benefits and disadvantages of using SL for nanoparticle synthesis. Up till now only oleic acid derived sophorolipid (OASL) have been used for synthesizing metallic nanoparticles (Au,Ag, ZnO, Cu and Co)<sup>180,112</sup>. Use of SL for synthesizing inorganic nanoparticles is yet to be explored.

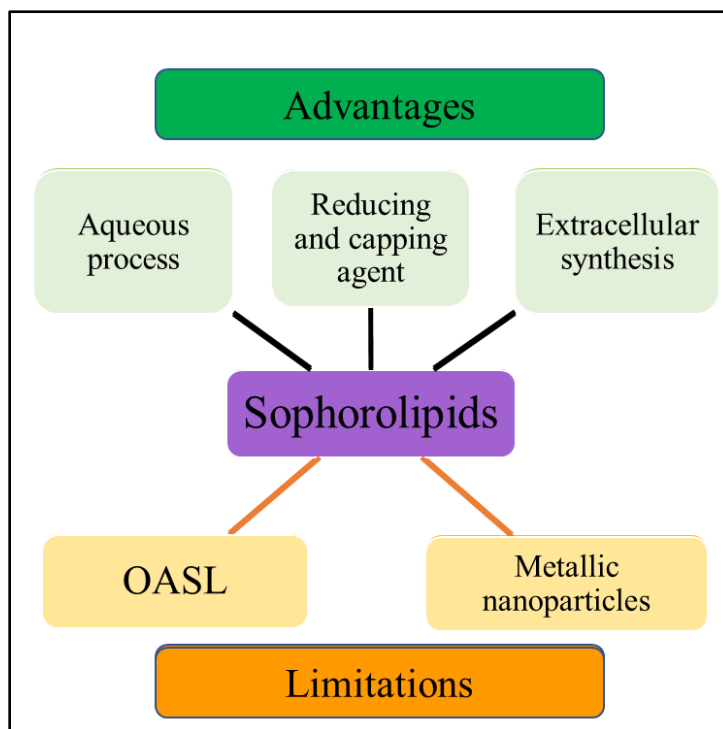


Figure 6.2 Diagrammatic representation of advantages and limitations of using SL for nano particle synthesis

Calcium phosphate nanoparticles are an efficient class of nanomaterials that are used for biomedical applications. They have gained increasing interest in medicine because of their high biocompatibility and good biodegradability. Recent studies are focused on synthesizing biodegradable and bioresorbable nanomaterials as it is more compatible with natural bone. These

nanoparticles are mostly synthesized by physical or chemical methods, which are time consuming and cost incurring<sup>181</sup>. Biological synthesis of calcium phosphate nanoparticles needs to be studied.

To summarize, this chapter is focused on synthesizing calcium phosphate nanoparticles using short chain derived SL. Use of SL in synthesizing these nanoparticles will further enhance the properties of nano-particles. The chapter elaborates the optimization studies followed by characterization of synthesized nanoparticles. Furthermore, the biological potential of the nanoparticles for biomedical application was assessed.

### **6.2 Materials and method:**

#### **6.2.1 Chemicals:**

The chemicals calcium chloride and sodium phosphate dibasic were procured from Sigma Aldrich.

#### **6.2.2 Biosynthesis of nanoparticles:**

The calcium phosphate nanoparticles were biosynthesized using physical and biological methods described in [Figure 6.3](#). Briefly, MASL was dissolved in 10 ml (0.1 M) Na<sub>2</sub>HPO<sub>4</sub>. This solution was sonicated for 10 minutes at 50-60 Hz for 10 sec/ 3 sec interval at room temperature. To this 10 ml of (0.1 M) CaCl<sub>2</sub> was added dropwise with sonication for 20 minutes at 50-60 Hz for 10 sec/ 3 sec interval. The precipitated nano-particles were centrifuged at 8000 rpm for 15 minutes and washed twice with water. The nano-particles were dried in the oven at 60 °C for 10h.

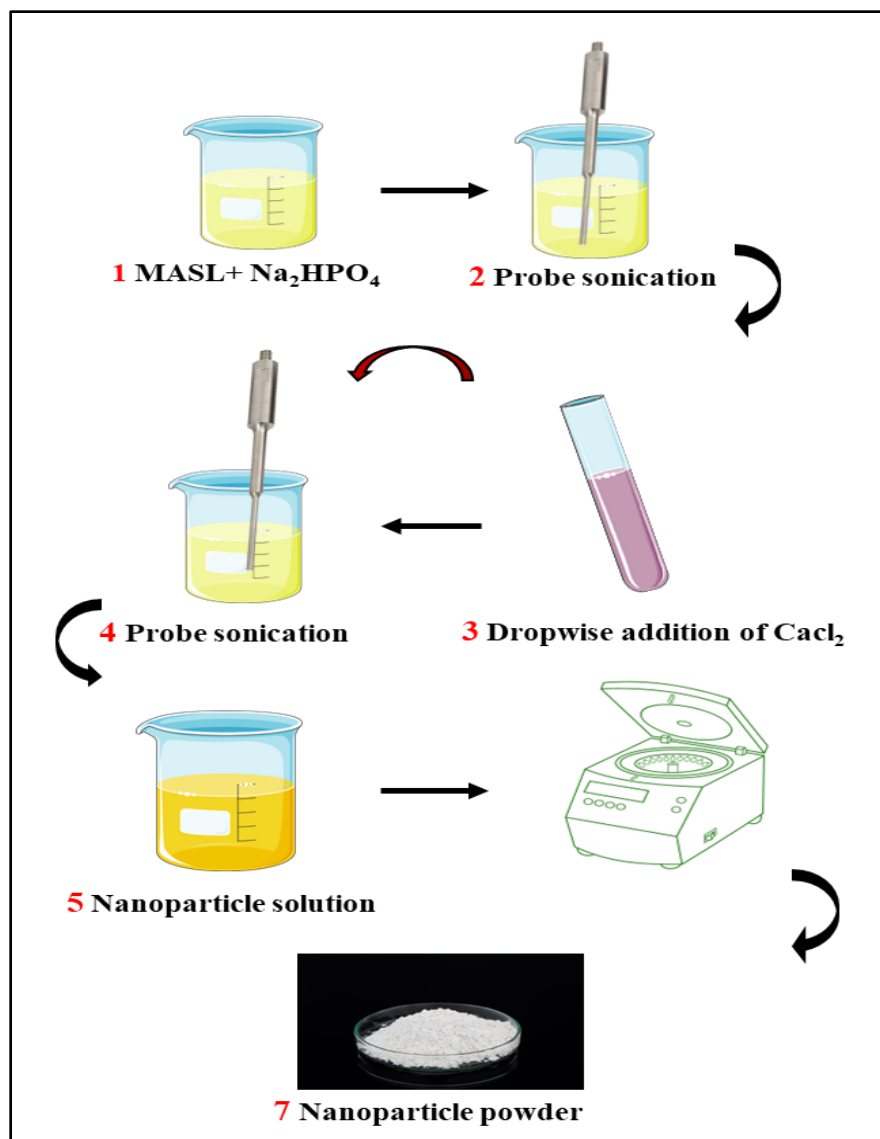


Figure 6.3 Protocol used for synthesizing calcium phosphate nanoparticles using biosurfactant

### **6.2.3 Optimization studies:**

This work reports synthesis of calcium phosphate nanoparticles using short chain SL. Optimization of process parameters was done to obtain optimum yield and characteristics of nanoparticles were studied. Optimization of time parameter and concentration of SL was assessed. The different time points selected were 15 minutes, 30 minutes, 45 minutes and 60 minutes. Three different concentration (0.5, 2.5 and 5 mg/ml) of SL were used.

For all the experiments crude MASL was used. Nanoparticles were also synthesized in absence of MASL. These nanoparticles were named as control nanoparticles, these are abbreviated as C-NP throughout the study. Also, MASL synthesized nanoparticles are abbreviated as SL-NP

### **6.2.4 Characterization of nanoparticles:**

All the synthesized nanoparticles (control and SL) were structurally characterized by XRD and FTIR, whereas morphological changes were studied by SEM and TEM.

#### **6.2.4.1 X- Ray Diffraction:**

X ray diffraction is a fast, easy and reliable tool for qualitative and quantitative structural analysis of compounds. The non-destructive technique proves useful for different biological samples.

The diffractometer consists of a cathode ray tube, sample holder and detector. The cathode ray produces X rays which bombard the sample at given angles. It moves and scans the sample over a range of  $2\theta$ , ensuring that all bands of diffraction are observed. Atoms from the samples diffract the incident beam resulting in constructive and destructive interference of X ray beams. These diffracted rays are collected by the detector which then reciprocate into peaks resembling different phases<sup>182</sup>.

Powder X-ray diffraction (PXRD) patterns were recorded on a Rigaku Micromax-007HF equipment with a high-intensity Microfocus rotating anode X-ray generator. All the samples were coated (10 mg/ per sample) on an aluminum holder, and the data was collected using a Rigaku R axis IV ++ detector. Data was collected from  $10^{\circ}$  -  $70^{\circ}$  (2 Theta). The composition of the synthesized nano-particles was evaluated through Powder X-ray diffraction (PXRD) patterns<sup>183</sup>.

### **6.2.4.2 Scanning electron microscopy:**

Morphological examination of synthesized nanoparticles was done using scanning electron microscopy. In this, 0.2 mg/ml of nano-particles were added in DI (Deionized water) water and bath sonicated for 2 minutes. 10 uL sample was loaded onto silicon wafer. The sample was dried completely and analyzed using Quanta (200 3D, FEI) scanning electron microscope (SEM). Prior to imaging, all samples were sputter coated with 5 nm gold coating using a polaron SC6420 sputter coater. Representative SEM images of CNP (control nano-particles) and SEM images of SL-NP (sophorolipid nano-particles) were recorded at suitable magnification<sup>184</sup>.

### **6.2.4.3 Transmission electron microscopy (TEM):**

Transmission electron microscopy measurements were recorded on FEI Technai F20 instrument at 100 KV. Samples were mounted on precoated copper grid and air dried. Dried sample were used for imaging.

### **6.2.5 Determination of sophorolipides on nanoparticles:**

#### **6.2.5.1 Thermogravimetric analysis (TGA):**

Capping of SL on nanoparticles was confirmed by TGA. Machine Q500 of TA was employed for performing thermogravimetric analysis on MASL and nanoparticles powder samples. The analysis was done in air atmosphere with rate of  $10^{\circ}$  C/ minute. The graph of weight loss vs temperature was plotted<sup>113</sup>.

### 6.2.5.2 Lectin binding assay:

Concanavalin A (Con A) is a lectin with specific affinity towards sugar moieties. To detect the presence of SL on synthesized nanoparticles, lectin binding assay was performed. Binding of concanavalin A to glucose molecules causes turbidity changes which can be measured spectrophotometrically.

In this, Con A (0.5mg/ml) was dissolved in 100 mM PBS buffer containing 0.1mM MnCl<sub>2</sub>, 0.1 mM CaCl<sub>2</sub> and 0.1 mM NaCl. Nanoparticles with varied concentrations (2,4,6,8,10,12,14 mg/ml) were gradually added into 500  $\mu$ l PBS. Upon addition, the solution was thoroughly mixed and transferred into cuvette. The turbidity measurements were recorded at 490 nm on Shimadzu UV-1601PC UV- vis spectrophotometer at room temperature<sup>185</sup>. Refer to [Figure 6.4](#).

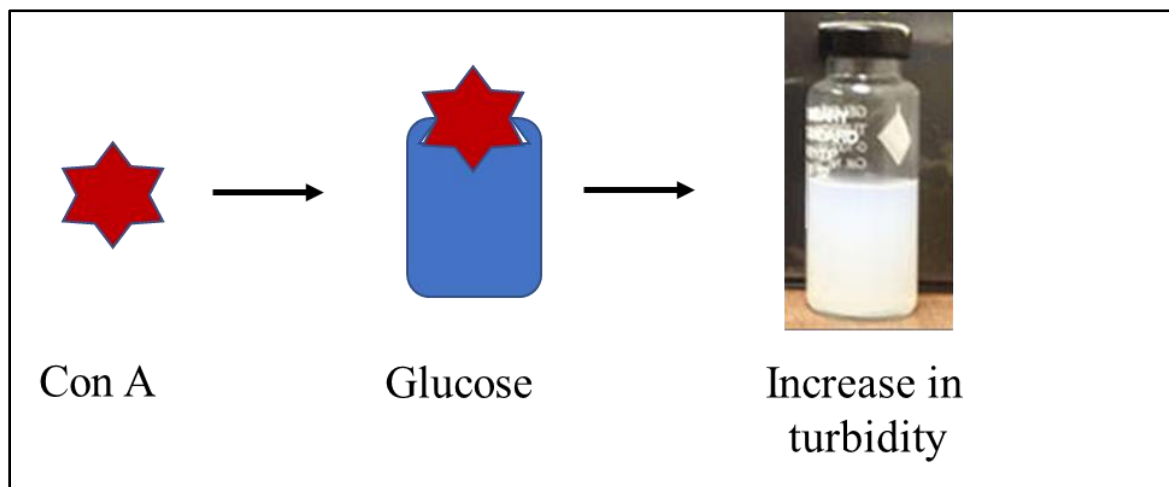


[Figure 6.4](#) Schematic describing the principle of lectin binding assay

### 6.2.6 Silk fibroin:

Even dispersion of nanoparticles was ensured by mixing the nanoparticle powder in silk fibroin solution. Due to its excellent biological properties, silk fibroin was used for this application. The silk solution was prepared as follows ([Figure 6.5](#)): *Bombyx mori* cocoons (**Procured from CSRTI- Central Sericultural research & Training Institute, Mysore**) were boiled in 0.5 w/v%

## Chapter VI: Synthesis of calcium phosphate nanoparticles using short chain derived sophorolipid

of  $\text{NaHCO}_3$  solution twice for 30 minutes each for sericin removal. Collected fibroin was vacuum dried at  $60^\circ\text{C}$  followed by dissolution in 9.3 M lithium bromide (LiBr) at  $60^\circ\text{C}$  for 4h. This solution was dialyzed extensively against water and the resultant solution (Regenerated silk fibroin -RSF) was used for further experiments<sup>186</sup>.

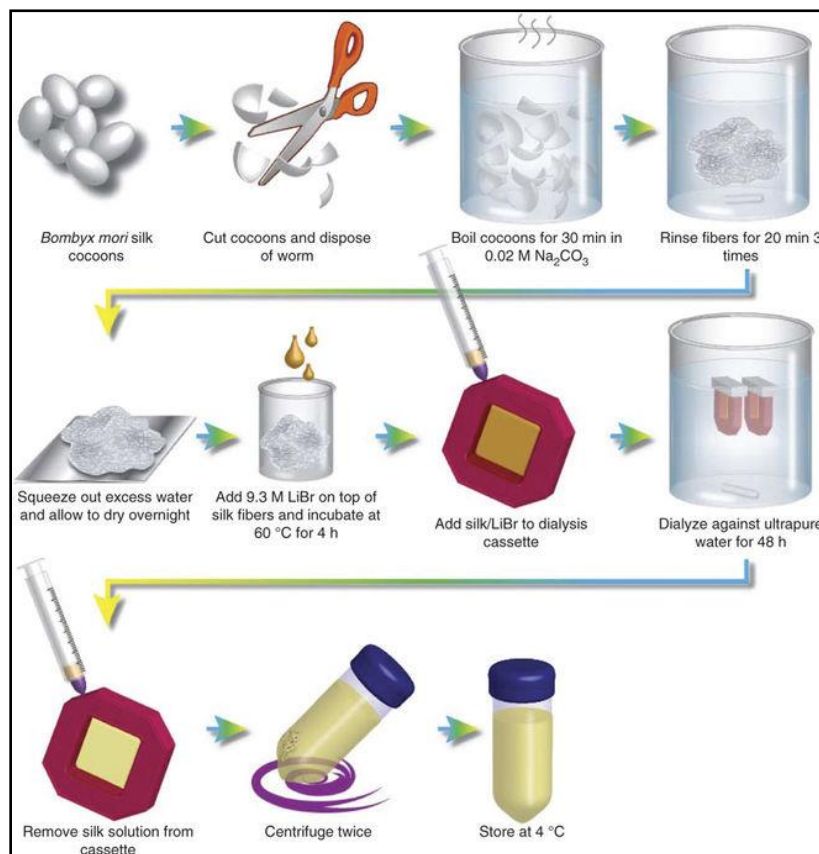


**Figure 6.5** Protocol used for preparation of silk solution

### 6.2.6.1 Scaffolds preparation:

The nano-particles were dispersed into distilled water and sonicated for 2 minutes. 3% RSF + NP solution was mixed and probe sonicated (30sec/40 amp/3 sec pulse). The final concentration of nanoparticles per scaffolds was 10 % and 20 %. The resultant solution was added into 96 well plate, keep at  $37^\circ\text{C}$ . After gelation, the plate was lyophilized and the scaffolds were removed<sup>187,188</sup>.

### **6.2.7 *In vitro* studies of nanoparticles**

#### **6.2.7.1 Cell proliferation assay:**

Cell proliferation was determined by Alamar blue assay. Before seeding the cells, scaffolds were incubated in complete media at 37°C with 5% CO<sub>2</sub> for 12h. MG 63 cells were seeded onto the scaffolds at a density of  $5 \times 10^3$  cells per scaffold in 20  $\mu$ L of complete media. The plate was incubated at 37°C with 5% CO<sub>2</sub> for 24h. During incubation, on the, 4<sup>th</sup>, 7<sup>th</sup>, 11<sup>th</sup> and 14<sup>th</sup> day, the media was replaced with 10 % Alamar blue prepared in DMEM (Dulbecco's Modified Eagle medium) and further incubated for 6 h at 37 °C with 5% CO<sub>2</sub>. Post incubation, the media was removed and transferred into another plate and fresh DMEM media was added to scaffolds and incubated. The reading of the collected media at 570 and 600 nm was noted. Assay was performed in triplicates<sup>189</sup>.

#### **6.2.7.2 Actin staining:**

Cellular structure of cells was determined using actin staining. Briefly, MG 63 cells were seeding onto nanoparticle loaded scaffolds with density of  $5 * 10^{-4}$  in 96 well plate containing DMEM media with 10 % FBS. Plate was incubated at 37 C for 14 days. Post incubation, the scaffolds were washed with PBS followed by fixation using 4 % paraformaldehyde at R.T for 15 minutes. The scaffolds were then washed 2 times with 0.1 % Triton X -100 for 5 minutes. The scaffolds were then washed with PBS twice and incubated with 5 % BSA for 20 minutes at R.T. Alexafluor was prepared in PBS (1:100 dilution) and added to the scaffolds and incubated in dark conditions for 30 minutes. The nucleus was stained with DAPI at 300 nM concentration for 4 minutes at R.T and then washed with PBS. Images were captured on epi-fluorescence Axio Observer Z1 Carl Zeiss microscope<sup>142</sup>.

#### **6.2.7.3 Alkaline phosphatase assay:**



Alkaline phosphatase (ALP) activity was assayed using colorimetric ALP kit (Abcam, U.K.). Briefly, MG 63 cells were seeded on scaffolds at a density of  $5 \times 10^4$  cells per scaffold in 50  $\mu\text{L}$  of complete media. The cells were allowed to be settled for 5–7 minutes at 37 °C with 5%  $\text{CO}_2$ . The additional 90  $\mu\text{L}$  media for cells was then added and the cell culture plate was then incubated at 37 °C with 5%  $\text{CO}_2$  for 7 days

On the second day of the experiment, seeding media was replaced with osteogenic differentiation media (Invitrogen). During incubation, on the 4<sup>th</sup>, 7<sup>th</sup>, 11<sup>th</sup> and 14<sup>th</sup> day, spent media from cell seeded scaffolds was collected and stored. Post incubation, 20  $\mu\text{L}$  of the spent media and 60  $\mu\text{L}$  of assay buffer was incubated with 50  $\mu\text{L}$  of p-nitrophenyl phosphate (5 mM) solution at room temperature for 1 h in the dark. At the end of the incubation, enzyme activity was stopped by ADDING 20  $\mu\text{L}$  of stop solution. Simultaneously, standard curve was plotted as per manufacturer's instruction. The amount of p-nitro-phenol produced was measured by measuring absorbance at 405 nm<sup>189</sup>.

### **6.3 Results and discussion:**

Calcium phosphate nanoparticles were synthesized using physical and biological method. Sonication was used as a physical component whereas the biological agent; SL stimulated the reduction process. The nanoparticles thus synthesized were fine, greyish white colored powder.

#### **6.3.1 Optimization studies:**

##### **6.3.1.1 Effect of time parameter on synthesis of nanoparticles:**

Optimization of the certain process parameters was performed. The time interval of synthesis was varied starting with 15 minutes to 1h. Each synthesized nanoparticles were further structurally characterized.

The XRD data was used for in depth details regarding the crystal structure and composition of synthesized compound. The XRD spectra of nanoparticles includes three prominent peaks with  $2\theta$  values of 11.67, 20.9 and 29.7 corresponding to with crystal lattice planes (020), (021) and (041)

of brushite and tri calcium phosphate respectively. The diffraction data is in compliance with the JCPDS data id (00-009-0077 for brushite and 00-009-0348, 00-032-0176 for tri calcium phosphate). The diffraction pattern reveals that the CNP possess a composition of both brushite and tri calcium phosphate. For further confirmation the area under the peak was deduced from the XRD graph and the % area corresponding to each peak was identified<sup>190,191</sup>.

The Figures below (6.6-6.9) depict the XRD pattern of control nanoparticles obtained with different process time.

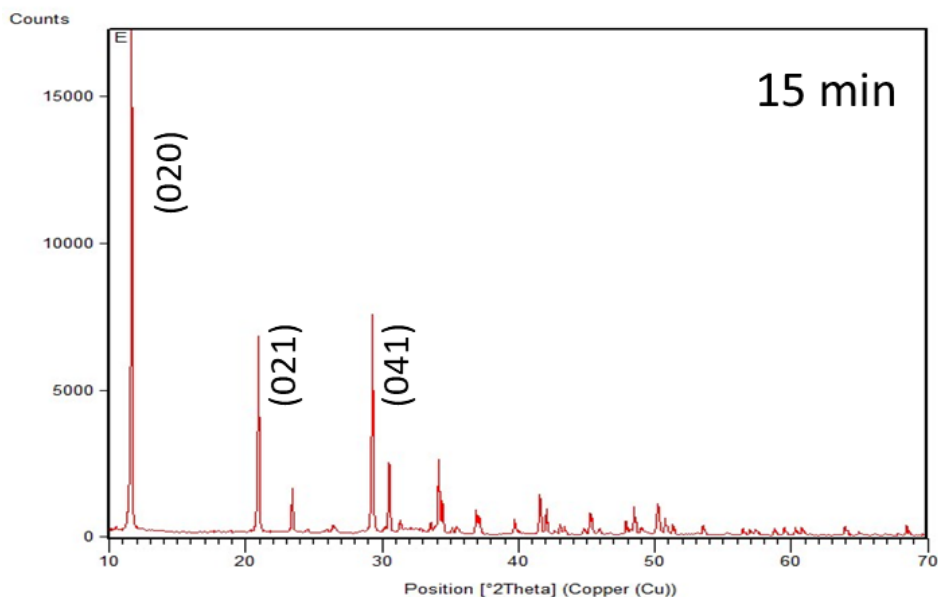


Figure 6.6 XRD pattern of nanoparticles synthesized with 15 minutes process time

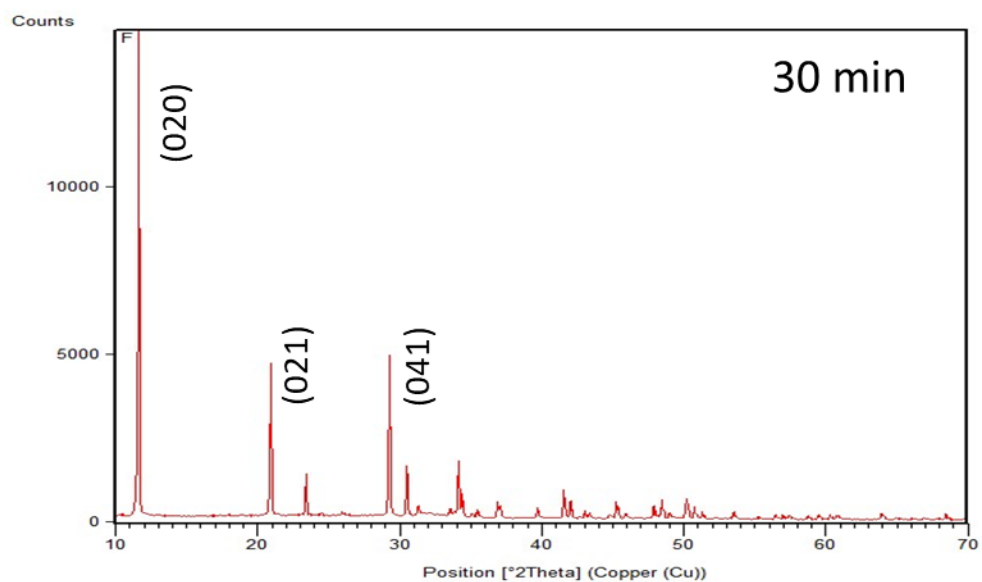


Figure 6.7 XRD pattern of nanoparticles synthesized with 30 minutes process time

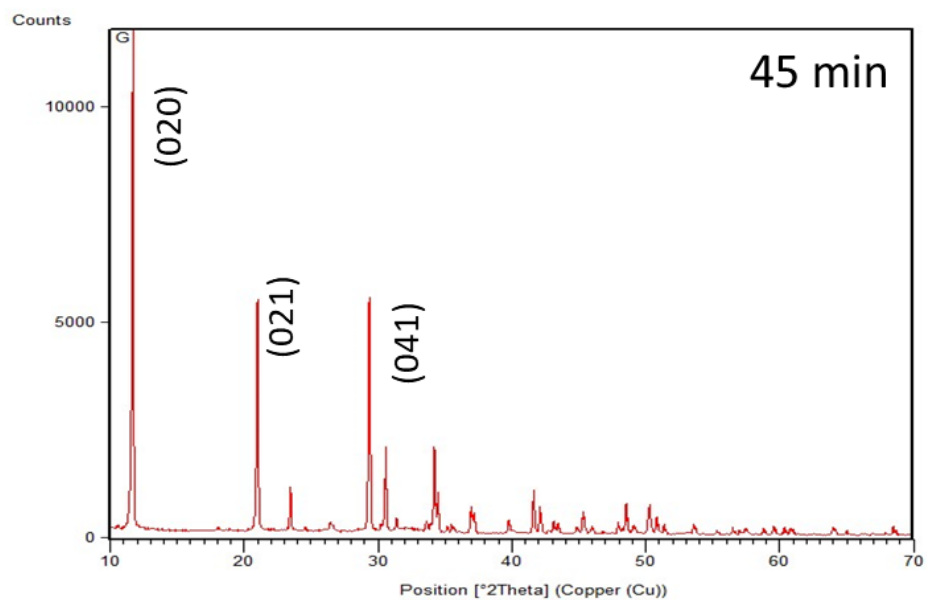
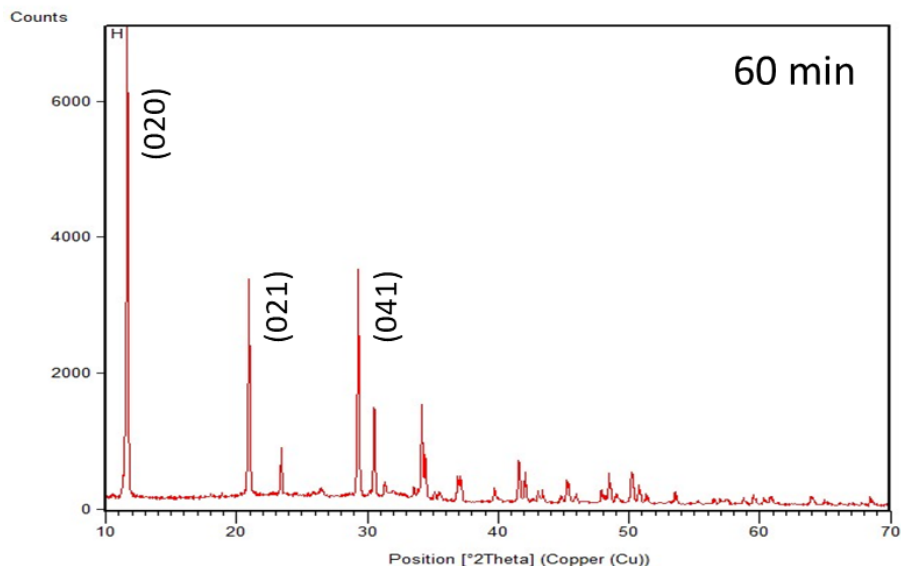
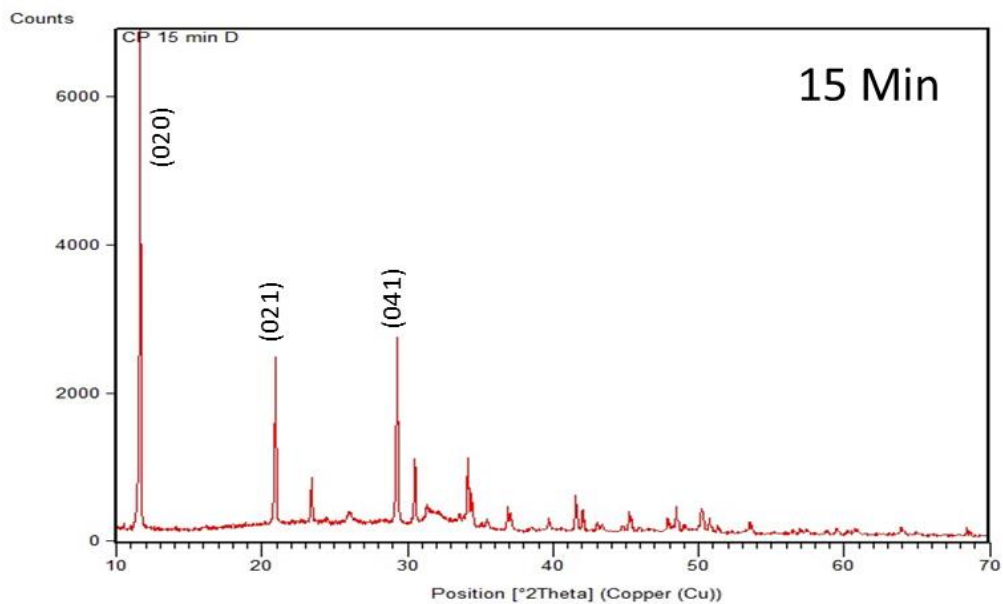


Figure 6.8 XRD pattern of nanoparticles synthesized with 45 minutes process time



**Figure 6.9** XRD pattern of nanoparticles synthesized with 60 minutes process time

The XRD spectra of SL nanoparticles also had three prominent peaks with  $2\theta$  values of 11.67, 20.9 and 29.7 corresponding to with crystal lattice planes (020), (021) and (041) of brushite and  $2\theta$  values of 30.5 and 34.1 correspond to lattice plane (110) and (170) of tri calcium phosphate. The diffraction data is in accordance with the JCPDS id data (00-009-0077 for brushite, 00-009-0348, 00-032-0176 for tri calcium phosphate). The diffraction pattern reveals that the SL incorporated nanoparticles possess different composition, consisting of brushite with high concentration of tri calcium phosphate. It was observed that the composition of nanoparticles was enhanced by presence of SL. For further confirmation the area under the peak was deduced from the XRD graph and the % area corresponding to each peak was identified. The **Figures** (6.10- 6.13) depict the XRD pattern of SL loaded nanoparticles at different time intervals.



**Figure 6.10** XRD pattern of nanoparticles synthesized using SL with 15 minutes process time

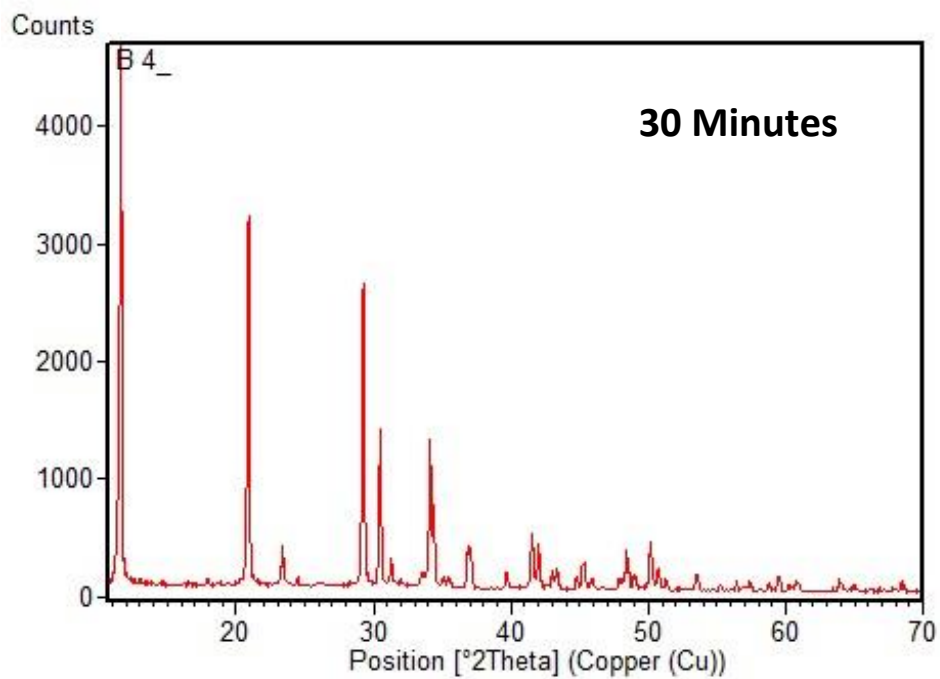


**Figure 6.11** XRD pattern of nanoparticles synthesized using SL with 30 minutes process time

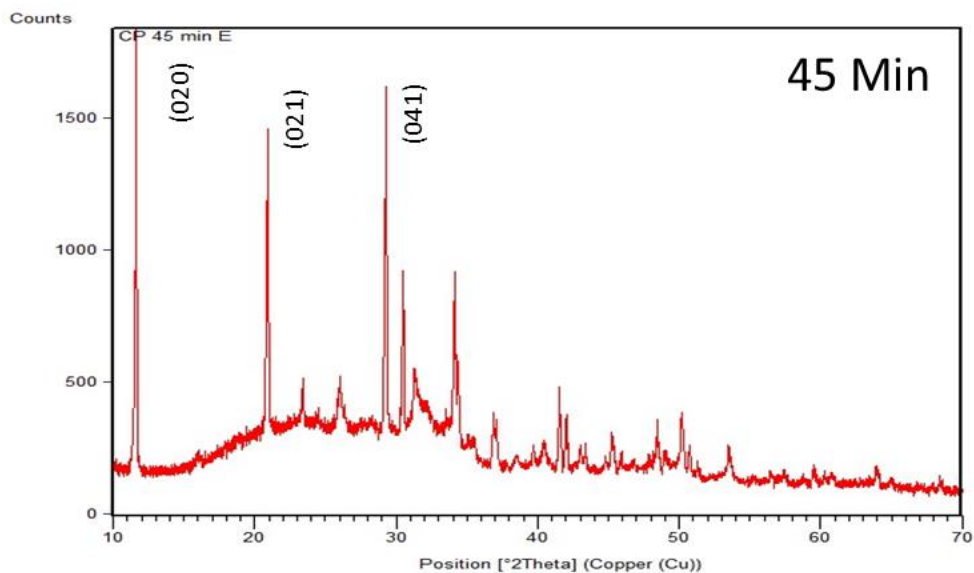


**Figure 6.12** XRD pattern of nanoparticles synthesized using SL with 45 minutes process time

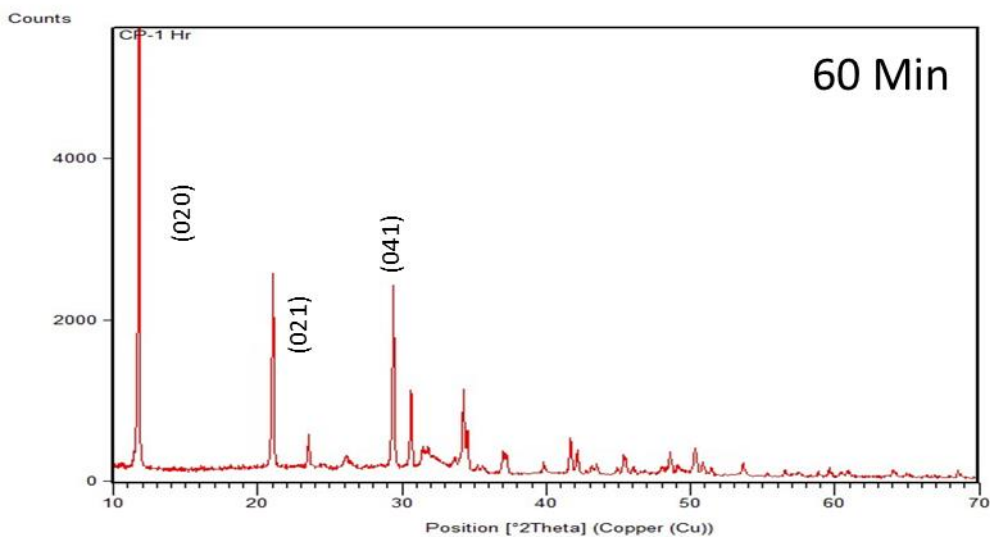


**Figure 6.13** XRD pattern of nanoparticles synthesized using SL with 60 minutes process time

XRD data revealed that the composition of nanoparticles consists majorly of brushite (di calcium phosphate dihydrate) and tri calcium phosphate ( $\beta$  TCP). There are different types of calcium phosphate cements available namely; mono calcium phosphate, di calcium phosphate, tri calcium phosphates, octa calcium phosphates and hydroxyapatite. Hydroxyapatite resembles the inorganic component of the natural bone and thus was extensively studied; however, its low biodegradability and resorption led to research on different cements<sup>166</sup>.

Primary criteria for bone cement are malleability and its ability to easily resorb into the body. Brushite and tri calcium phosphates have gained considerable interest in the last decade, because they are biocompatible, osteoconductive and osteoinductive. Brushite also known as di calcium phosphates possesses good properties like biocompatibility, non- immunogenic, less expensive and non- toxic<sup>192</sup>. Similarly,  $\beta$  TCP (form of tri calcium phosphate) is resorbable, readily replaced by new bone, osteoconductive and non-toxic<sup>193</sup>. Owing to these advantages, efforts have been made to synthesize nanoparticles with specific composition of brushite and  $\beta$  TCP. However, these composite nanoparticles are synthesized by mixing individual cements<sup>194</sup>. Interestingly, with our process of synthesis, a mixture of brushite and  $\beta$  TCP is formed naturally. This ideal composition is achieved due to the process condition and in presence of SL.

From the XRD graph the area under the peaks was calculated and the composition of each nanoparticles was deduced. It was observed that the  $\beta$  TCP content increases in presence of SL. A time dependent analysis revealed the effect of SL on composition of nanoparticles. Control samples CNP possess high amount of brushite along with TCP, whereas, presence of SL, results in higher TCP content and lower brushite content. XRD data reveals identical peaks for both samples (CNP, SL-NP). However, the quantitative composition enhances in presence of SL. From the graph, it was also evident that a process cycle of 30 minutes resulted in optimum concentration of brushite and TCP and therefore, this time point was further used. At optimal conditions control nanoparticles exhibit a composition of brushite: 60 % and  $\beta$  TCP: 8 % whereas, SL incorporated nanoparticles exhibit brushite: 50 % and  $\beta$  TCP: 16%. Refer [Figure 6.14 - 6.16](#).

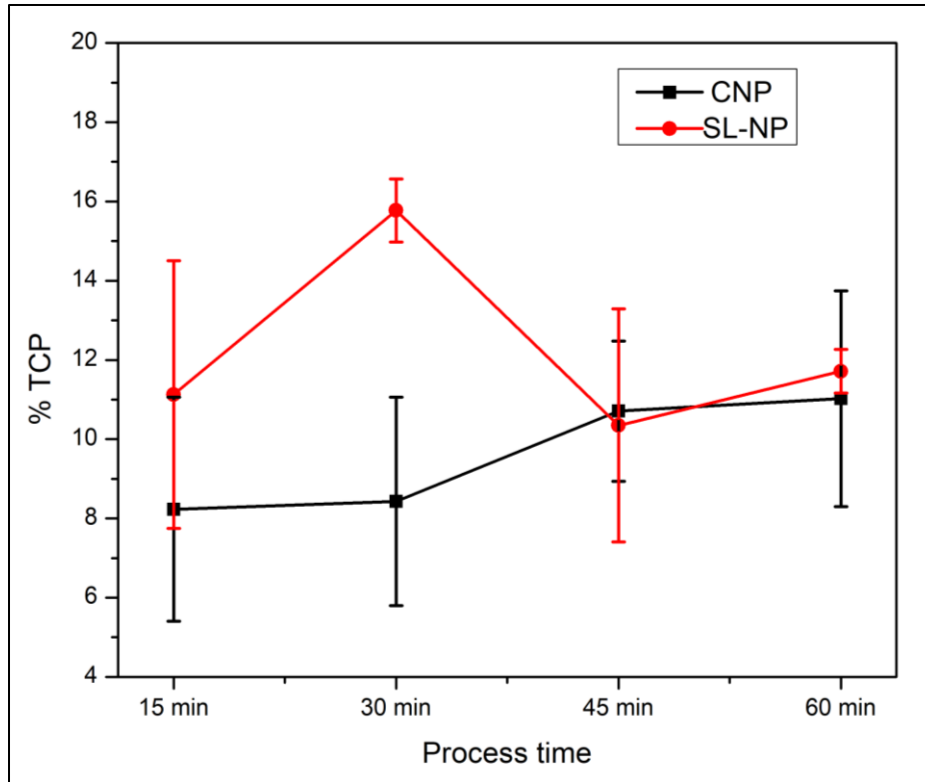
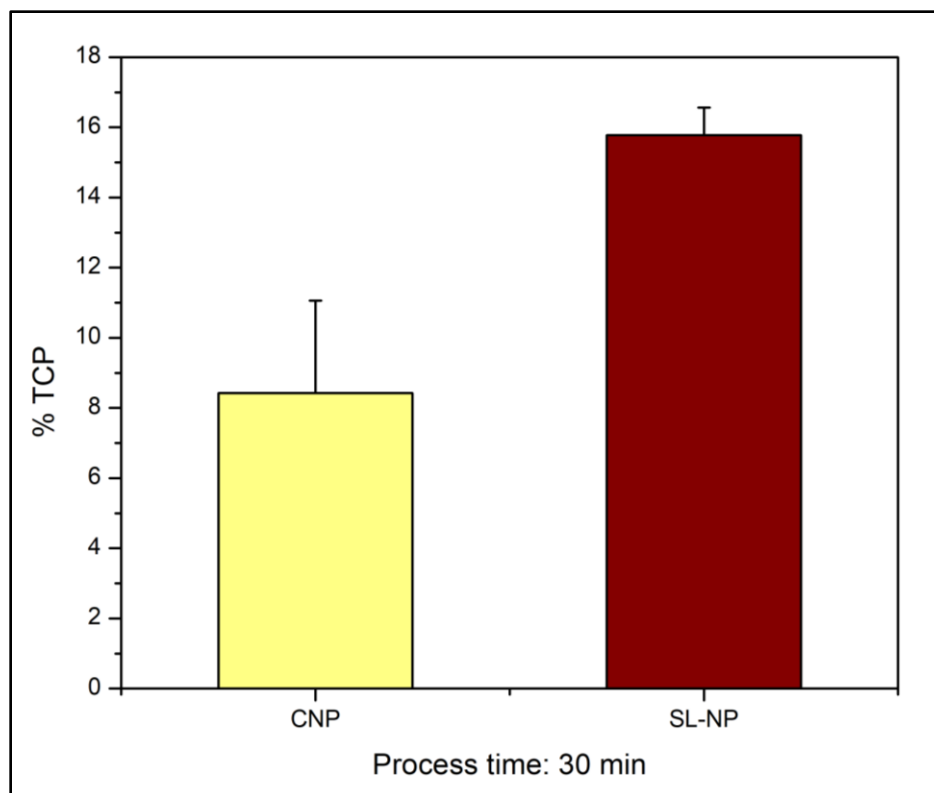
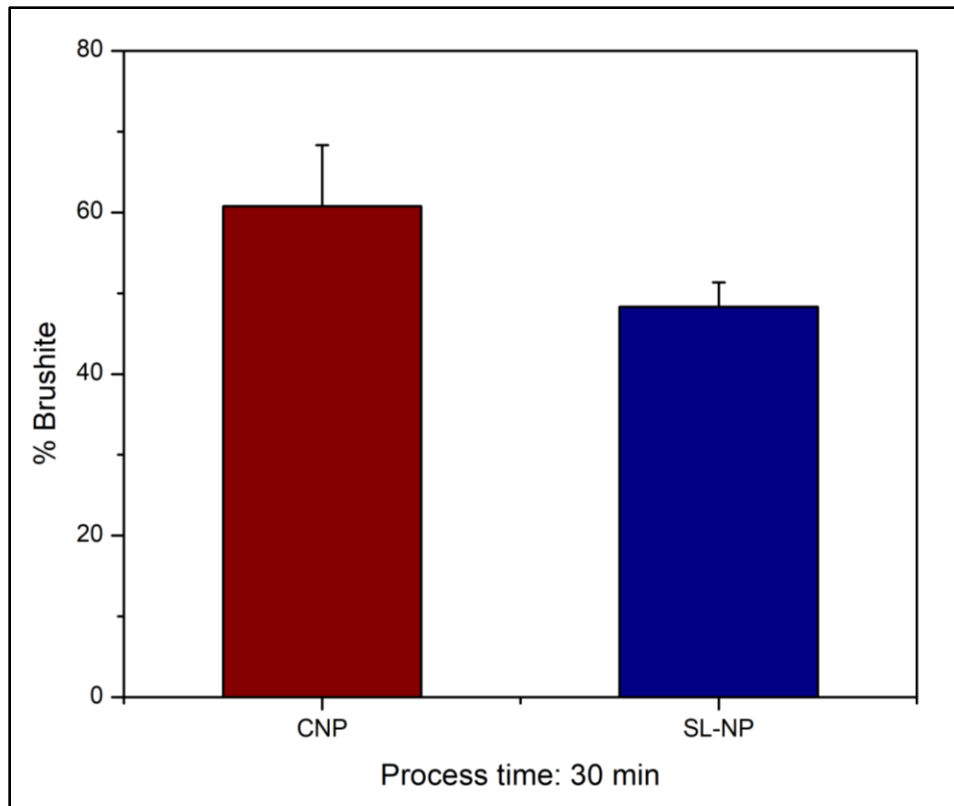


Figure 6.14 Changes in the values of TCP over different process times and in presence of SL





**Figure 6.15** Graph denoting the % TCP obtained at optimal condition for control and SL nanoparticles



**Figure 6.16** Graph denoting the % brushite obtained at optimal condition for control and SL nanoparticles

Earlier results revealed that the incorporation of SL into the process of synthesis results in nanoparticles with higher % of TCP. This indirectly proves the pivotal role of SL on the composition of nanoparticles.

To further analyze this effect of SL on the structure of nanoparticles, morphological images were observed. A clear trend in morphology was observed i.e with increasing time parameter from 15 minutes to 1h, decrease in the size and orientation of the nanoparticles was observed. Similarly, clear distinction within the morphology of nanoparticles was observed in presence of SL. In control nanoparticles at 15 minutes no defined morphology was observed. However, with further increase in process time the aggregates were observed. These aggregates lacked defined morphology throughout the process time. In SL incorporated nanoparticles at 15 minutes budding pattern was observed, at 30 minutes well defined sharp flower like nanoparticles were observed.

## Chapter VI: Synthesis of calcium phosphate nanoparticles using short chain derived sophorolipid

Further increase in time resulted in smaller flowers like structure and at 60 minutes, minute flower aggregates were observed. It was thus observed that incorporation of SL into nanoparticle synthesis enhances the compositional and morphological structure of synthesized nanoparticles. Moreover, process time of 30 minutes resulted in well-defined architecture of nanoparticles and thus it was preferred for further synthesis and experimentation. The SEM images of synthesized nanoparticles in presence and absence of SL have been summarized in the Table 9.

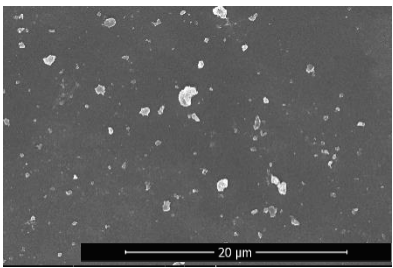
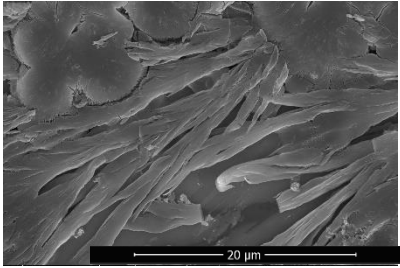
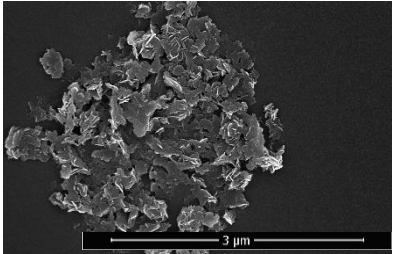
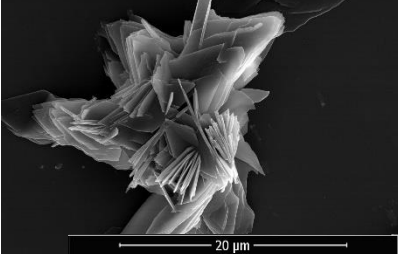
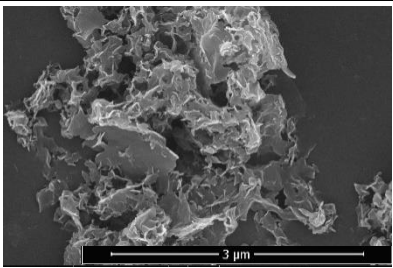
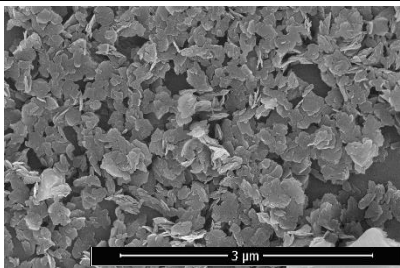
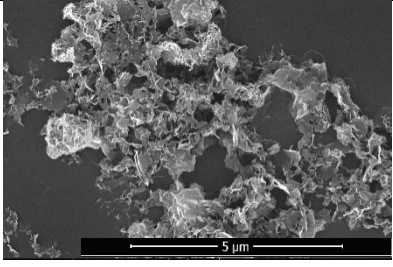
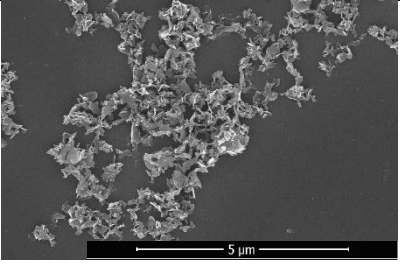
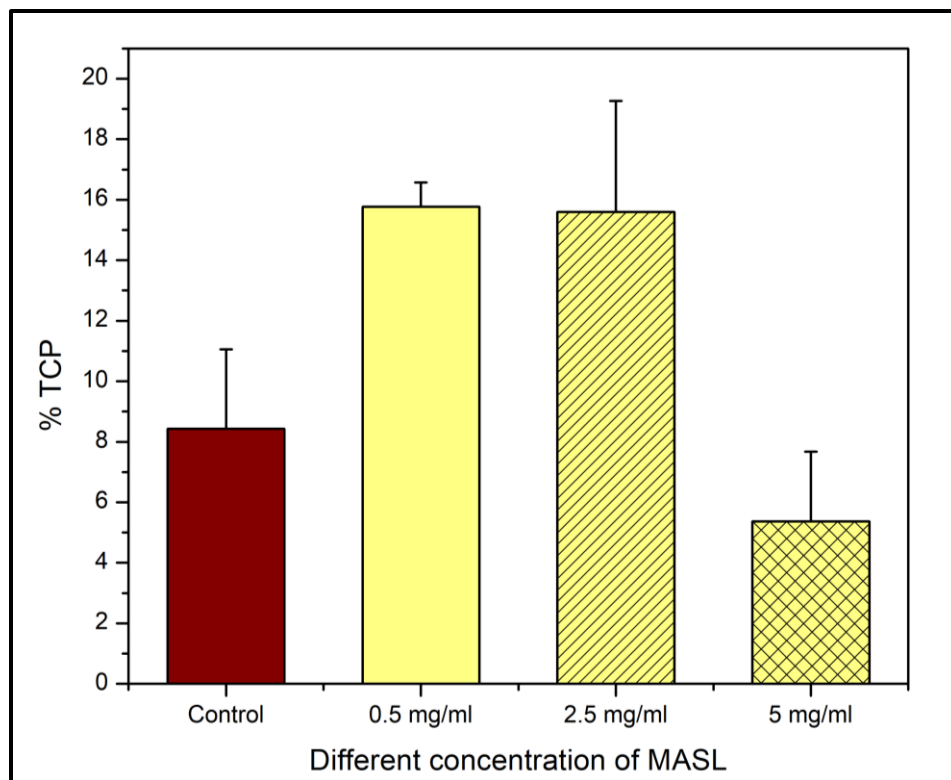
Process time	SL-NP	CNP
15 minutes		
30 minutes		
45 minutes		
60 minutes		

Table 9 Comparative SEM images of synthesized nanoparticles obtained at different time intervals

### **6.3.1.2 Effect of concentration of sophorolipid on synthesis of nanoparticles:**

Different concentrations of MASL (0.5, 2.5 and 5 mg/ml) were used for synthesizing nanoparticles. Earlier studies validated the composition of nanoparticles, consisting of higher TCP content, therefore increase in TCP was monitored with increase in MASL concentration. It was observed that at lower concentration considerable increase in TCP content was observed as compared to control samples. With increase in concentration the TCP content remained same and further increase in concentration led to decrease in TCP %. This highlights the fact that up to 5 mg/ml concentration of MASL, the TCP % remains unchanged i.e. with increasing concentration of MASL, the same composition of nanoparticles was observed ([Figure 6.17](#)).

Furthermore, the morphological changes with respect to concentration of MASL were also studied. No evident changes in the morphological orientation were observed with respect to increase in concentrations observed in [Figure 6.18](#). At higher concentration of MASL, flower shaped morphology was observed. To summarize, the structure and composition of nanoparticles remains consistent with increasing concentration of MASL. Therefore, the concentration of 0.5 mg/ml was preferred for further studies.



**Figure 6.17** Graph denoting the % TCP at increasing concentration of SL along with control

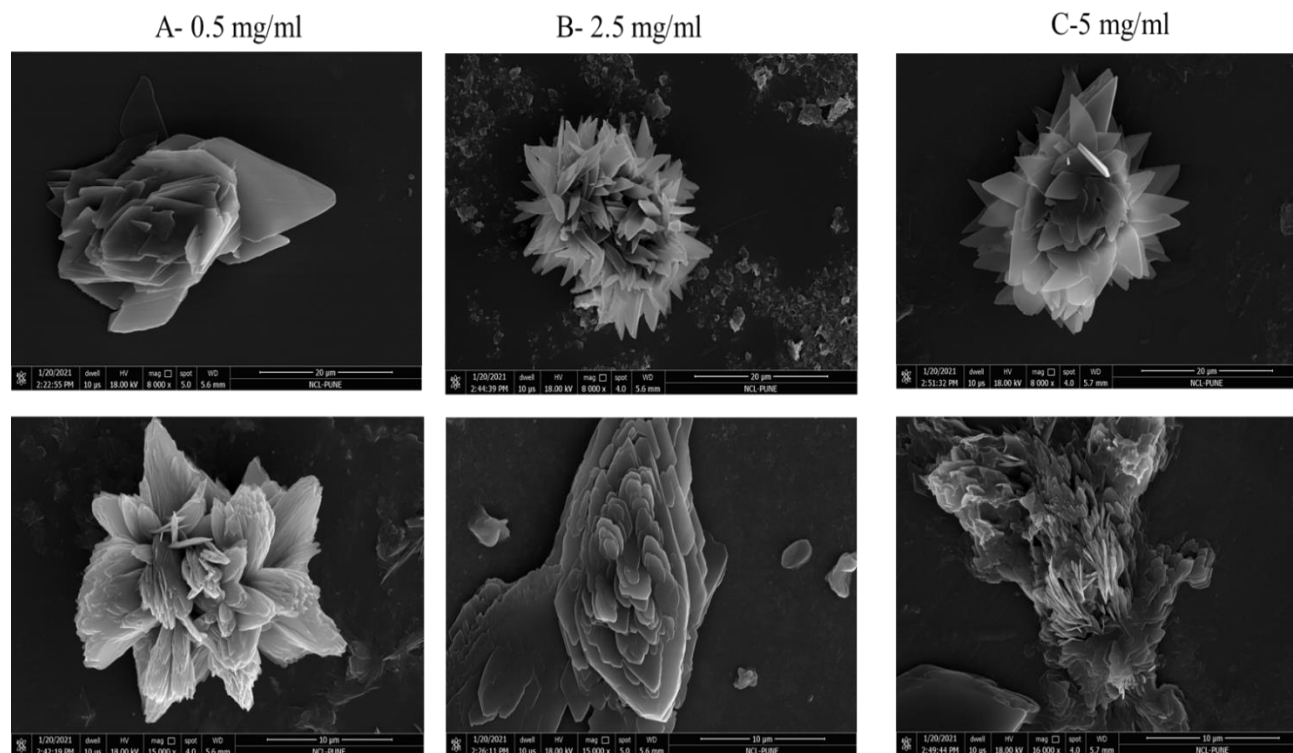


**Figure 6.18** SEM images of nanoparticles synthesized with increasing concentration of MASL

### 6.3.2 Characterization of synthesized nanoparticles:

As observed in the above images, SL assisted nanoparticles exhibited flower shaped morphology. These flower shaped nanoparticles are aggregates of smaller particles. In order to determine the size of these particles, TEM was performed (Refer [Figure 6.19](#)). The TEM images reveal clusters of nanoparticles with size ranging from 60-80 nm. The size of nanoparticles was similar throughout the different concentrations of MASL. The individual shape of nanoparticles resembles a rod or flake like pattern. The composition of natural bone ranges in the nanoscale dimensions and therefore, mimicking this architecture could lead to improved properties of the nanoparticles<sup>181</sup>. These results validate that incorporation of SL, results in formation of nano scale calcium phosphate particles useful for biomedical application.

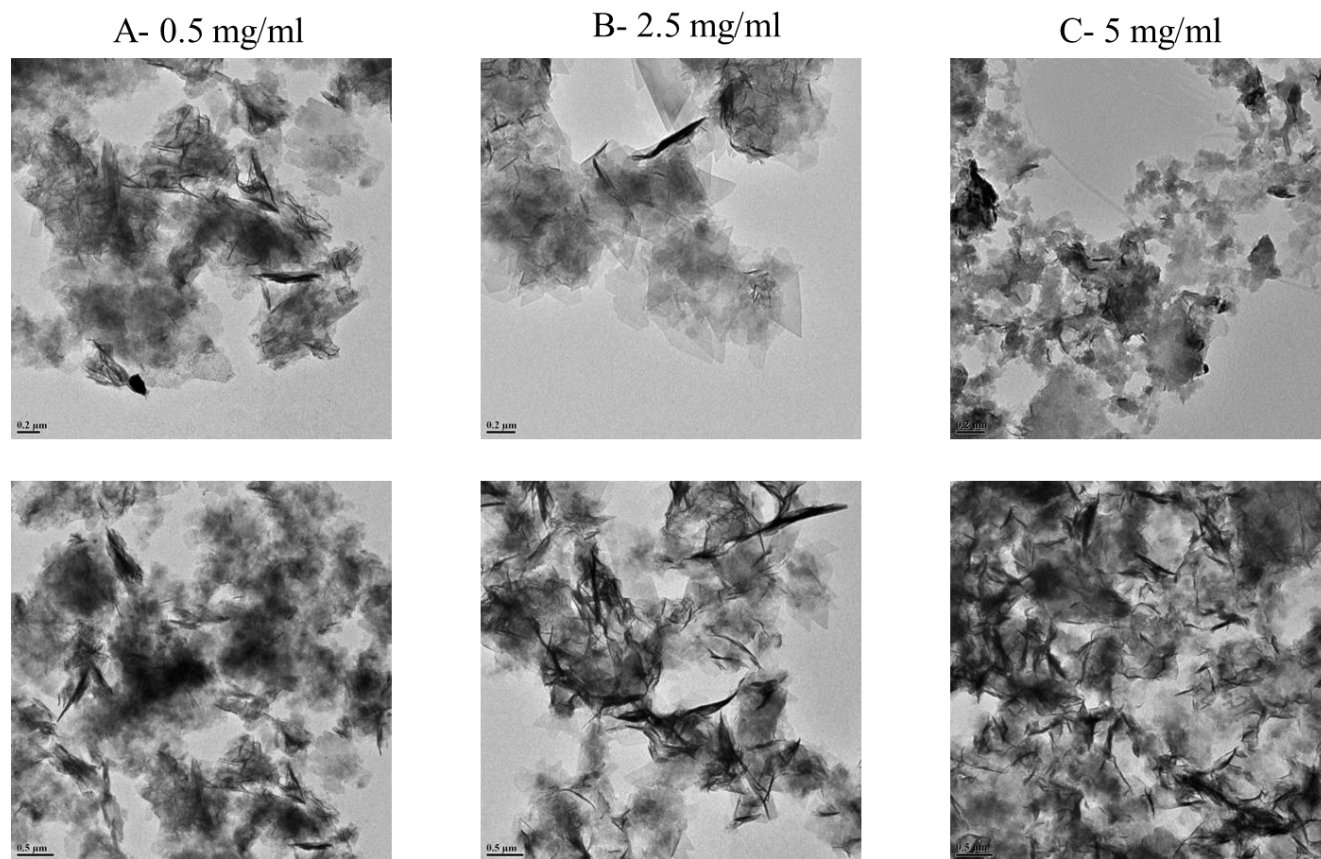


**Figure 6.19** TEM images of nanoparticles synthesized with increasing concentration of MASL

Calcium phosphate nanoparticles could be fabricated by various chemical and physical methods<sup>195</sup>. In the current study, SL have been used as reducing agents for nanoparticle synthesis. Previous studies have employed the use of chemical surfactants for nanoparticles synthesis. However, use of biosurfactant for inorganic nanoparticle synthesis is yet to be explored.

Nano particle synthesis involves two steps: nucleation and growth. Nucleation may be defined as process involving free atoms or ions in solution which assemble together to produce a thermodynamically stable cluster. The size of nucleus depends on the material of synthesis and its dispersity. Action of reducing agents stimulates changes into nanocrystal structure leading to growth of crystal phases. The rate of crystal growth depends on the concentration and time process<sup>196,197</sup>. The underlying mechanism for synthesis of calcium phosphate nanoparticles relies

## Chapter VI: Synthesis of calcium phosphate nanoparticles using short chain derived sophorolipid

on the amphiphilic nature of SL (Figure 6.20 & 6.21). SL stimulates formation of self-assemblies in aqueous solutions<sup>198</sup>. At acidic pH MASL forms dense mesh like network of flat rods. pH dependent assemblies of MASL have been reported earlier (Refer to section 7.2.2 for the images)<sup>48</sup>. These assemblies provide soft template for initiation of the nucleation process. The deposition of calcium ions onto the soft template activates the growth phase. Growth of the crystals happens in the micro confinements of the soft template<sup>199</sup>. At minimum disturbance (low process time), dense network of assemblies is formed, which results in huge flower shaped nanoparticles. However, at longer process time, the self-assemblies are disrupted due to the sonication resulting in smaller flower shaped nanoparticles.

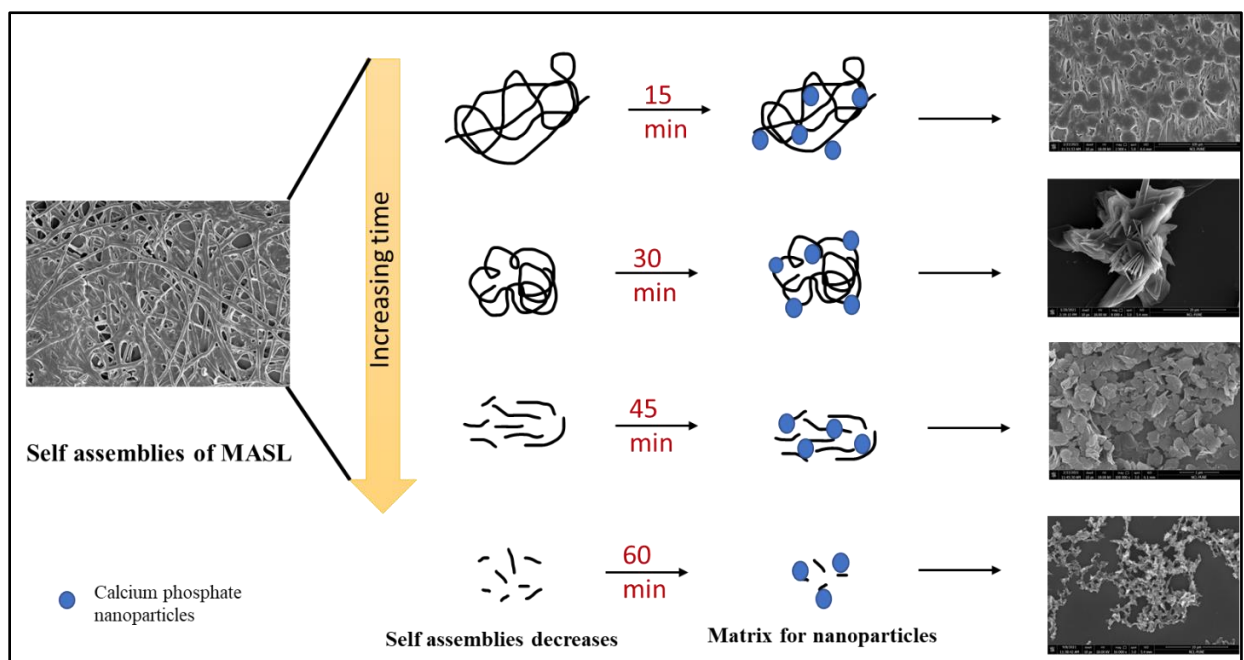


**Figure 6.20** Underlying mechanism of calcium phosphate nano particle synthesis using SL



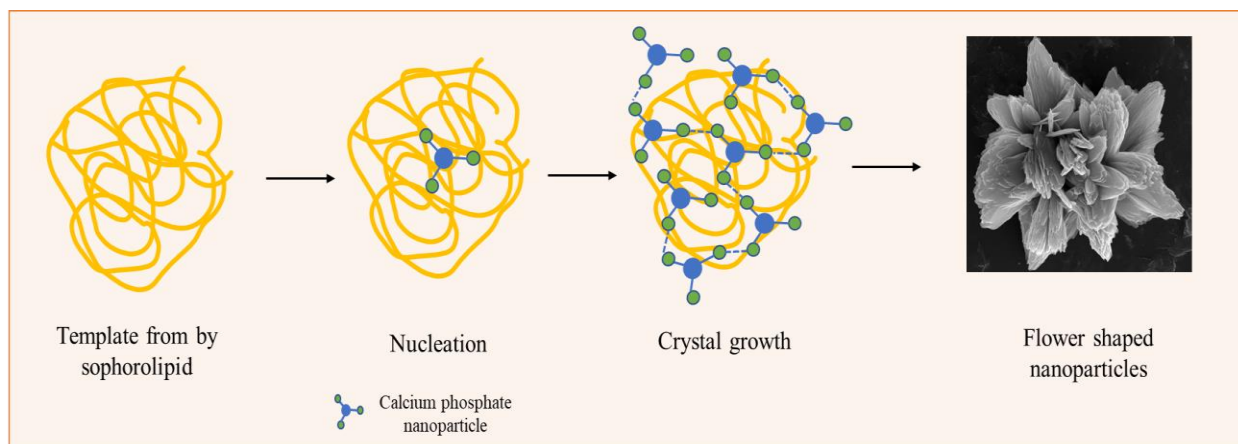


**Figure** 6.21 Schematics describing the process of nucleation in presence of biosurfactant

### 6.3.3 Determination of SL on nanoparticles:

As described earlier, the calcium phosphate nanoparticles are synthesized by SL (MASL). To detect the presence of SL on these nanoparticles different assays have been performed.

#### 6.3.3.1 Thermogravimetric analysis:

Earlier results confirm the successful formation of calcium phosphate nanoparticles and the effect of sophorolipids on its morphology. However, it is necessary to experimentally detect the presence of sophorolipids on these nanoparticles. For this, thermogravimetric analysis was performed. It measures the mass of sample over time under different temperatures. If the nanoparticles have coating of SL, then the corresponding weight loss will be observed at high temperature, thereby validating its presence onto the nanoparticles. For TGA analysis, crude MASL was used as control and nanoparticles with increasing concentration of SL and control nanoparticles were studied. From the graph- [figure 6.22](#), a two-stage degradation is observed for MASL at 409 and 622 °C. For control samples, mass loss at 200 °C was observed which corresponds to the water of hydration in the nanoparticles. For SL nanoparticles two stage degradation was observed, first at 200 °C and then at 400°C. Moreover, a clear trend in weight loss was observed as the concentration of SL increases. The organic content of the samples is directly proportional to the weight loss i.e higher

organic content results in increased weight loss<sup>180</sup>. TGA, thus confirms the presence of SL on the synthesized calcium phosphate nanoparticles.

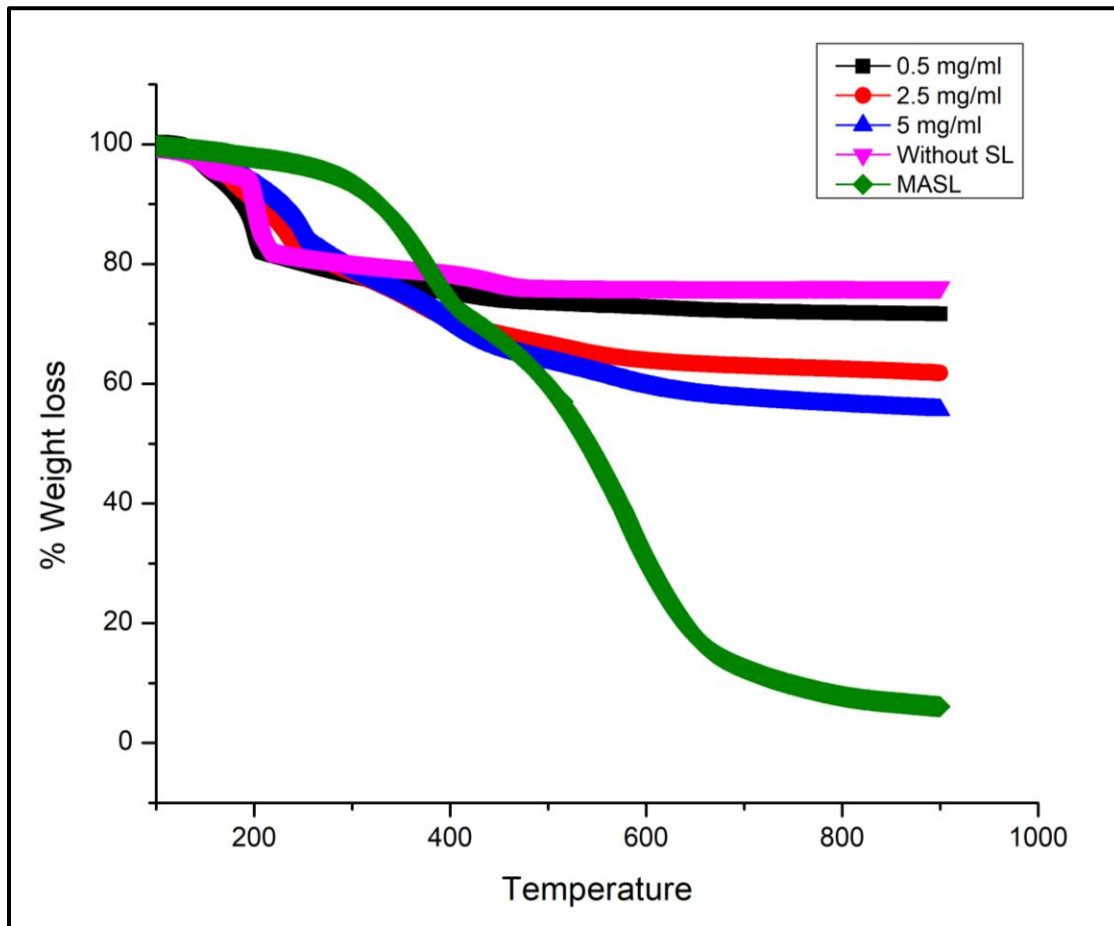
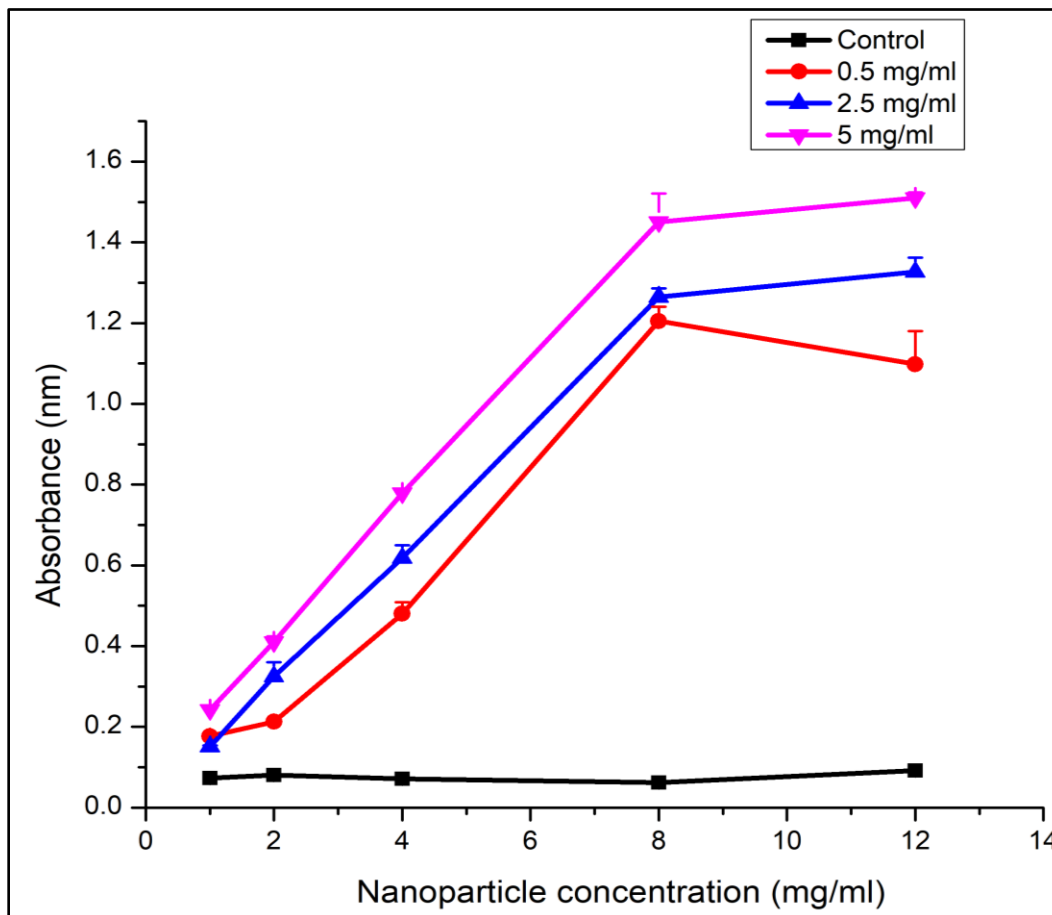


Figure 6.22 TGA analysis of SL nanoparticles along with control nanoparticles and crude MASL

### 6.3.3.2 Lectin binding assay:

Concanavalin A, is a plant-based lectin with affinity towards sugar molecules. To confirm the capping of SL unto the nanoparticles; lectin binding assay was performed. Structurally SL consists of a sugar moiety linked to the hydroxy fatty acid chain. For the assay, control nanoparticles along with SL- nanoparticles were used. Assay was performed over a range of concentration. The graph

depicts the absorbance vs nanoparticle concentration. The control nanoparticles lacked the turbidity changes due to absence of SL. Whereas for SL nanoparticles, a clear trend in turbidity was observed; as the concentration of nanoparticles increase, the turbidity of the samples also increased. Moreover, nanoparticles with highest content of SL exhibited highest turbidity. This confirms the capping of SL on the synthesized calcium phosphate nanoparticles. Refer [Figure 6.23](#).



[Figure 6.23](#) Graph measures the turbidity obtained at different concentrations of nanoparticles on binding to lectin.

#### 6.3.4 Scaffold preparation:

The optimization and characterization studies revealed the effects of SL on the composition and morphology of nanoparticles. Furthermore, the presence of SL on the nanoparticles was also confirmed. To further determine the biological potential, these nanoparticles were dispersed into silk fibroin solution. Silk fibroin has been widely used for biomedical applications because of its inherent biological and mechanical properties. Silk fibroin has been used for various applications like bone regeneration, skin regeneration and eye regeneration<sup>200,201</sup>. Scaffolds of silk fibroin and nanoparticles were obtained by lyophilization. The structural architecture of the scaffolds was determined by SEM. The images ([Figure 6.24](#)) reveal a good porous network of the scaffolds at different concentration of nanoparticles. Such porous networks are beneficial for biomedical applications.

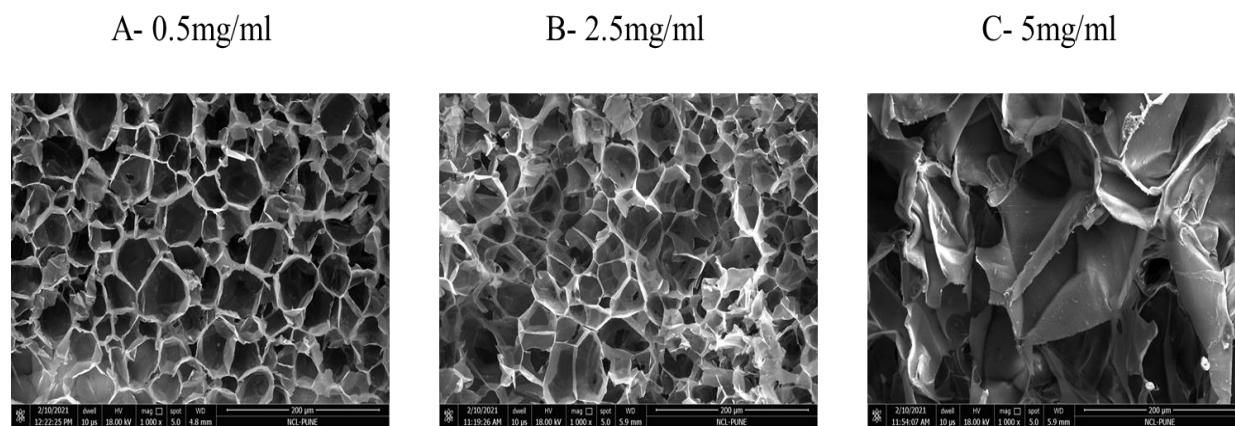


**Figure 6.24** SEM images of scaffolds synthesized using silk fibroin and nanoparticles

### 6.3.5 *In vitro* studies of nanoparticles

#### 6.3.5.1 Cell proliferation assay:

The control and SL- nanoparticles were evaluated using *in vitro* cell studies. MG63 cell line was used for this study due to its high proliferation rate. *In vitro* studies were performed for 14 days as it provides sufficient time period to assess the performance of material for bone tissue applications. To access the cell viability of MG63 on the scaffolds, alamar blue assay was performed. The graph denotes the proliferation of cells on 7 and 14 day on different scaffolds. Here, only cells and silk fibroin alone were used as control. Both the test (SL nanoparticles-SL-10 and SL-20) and the control samples (CP 10 and CP 20) contained two different concentration of nanoparticle loading: 10 % and 20 %.

It is observed that as the time progresses, proliferation of cells increases. No significant difference in the proliferation of control samples was observed. Whereas, significant difference in the proliferation of SL coated nanoparticles was observed. SL incorporated nanoparticles exhibited excellent cell proliferation on 14 days. The rate of proliferation increases with increase in nanoparticle loading as observed in [Figure 6.25](#). However, for control samples, proliferation remained consistent with the increased loading of nanoparticles.

Cellular morphology was evaluated by F-actin staining with Alexafluor 488 phalloidin. From the images, significant cell growth with clear morphology were observed. Elongated cells with increased viability were observed for SL nanoparticles. These images are in accordance with the proliferation assay. Refer [Figure 6.26](#).

The striking difference between the control and SL samples is attributed by capping of SL on the nanoparticles. Inherent biological properties of SL enhance the biological potential of the synthesized nanoparticles.

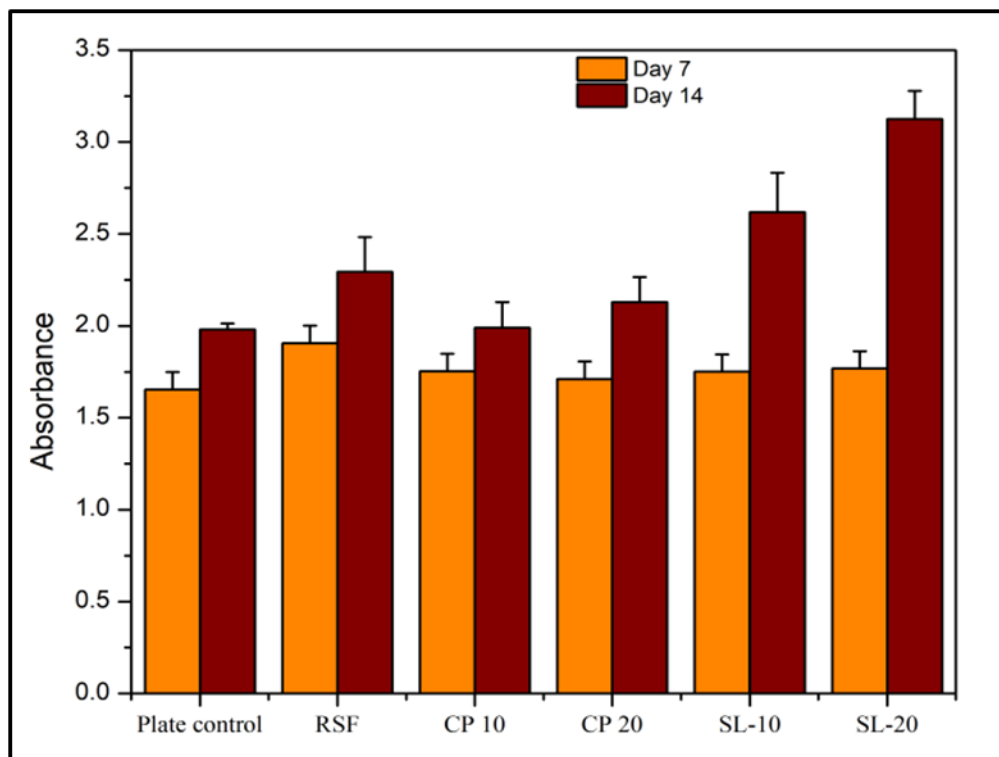


**Figure 6.25** Graph denotes the effect of synthesized nanoparticles with increasing loading on proliferation of cells up to 14 days

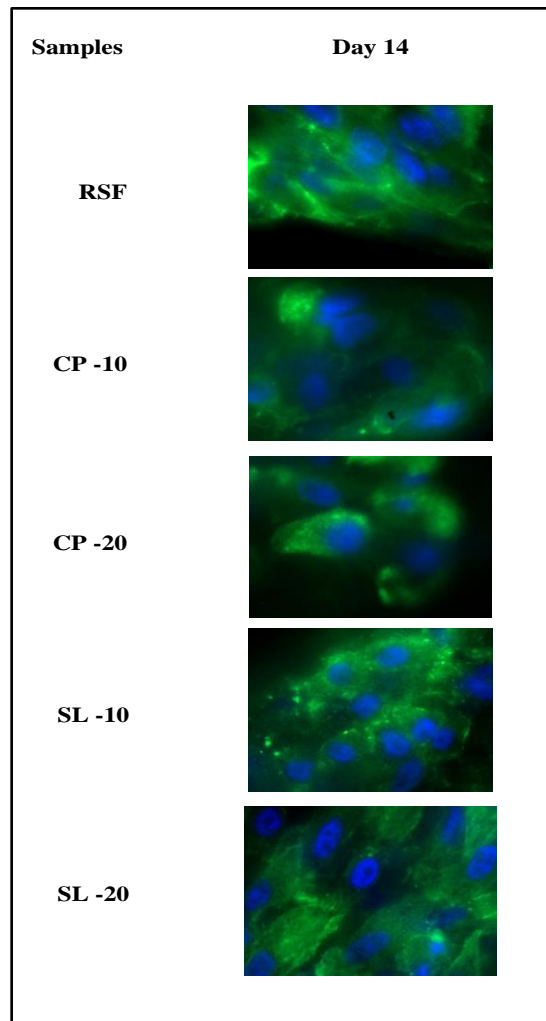


Figure 6.26 Actin staining highlighting the proliferating cells upon treatment with SL

### 6.3.5.2 Alkaline phosphatase assay:

The most calcified tissue in living organisms is bone. It exists in different sizes and shapes depending on its function and purpose. It is constantly being degraded and reformed. The formation of new bone requires differentiation of cells into osteogenic lineage. As the bone cells i.e osteoblast proliferate, they release the enzyme alkaline phosphatase. Apart from cell proliferation, cell differentiation is equally important for biomedical application<sup>202</sup>.

For this purpose, alkaline phosphatase assay was performed to determine the levels of osteogenic differentiation marker over the period of 14 days. For this assay, the samples used were same as that of proliferation assay.

From the graph in [Figure 6.27](#) it is observed that no significant difference in the ALP levels of control samples were observed. SL incorporated nanoparticles exhibited significantly higher levels of ALP on 14 day. The increase in ALP activity was directly proportional to the loading concentration. However, for control samples, opposite trend was observed, i.e ALP activity decreases with increasing loading of nanoparticles.

Thus, the *in vitro* studies prove that presence of SL in the calcium nanoparticles enhances their biological properties. Nanoparticles with SL exhibited better proliferation and ALP activity as compared to the control samples.

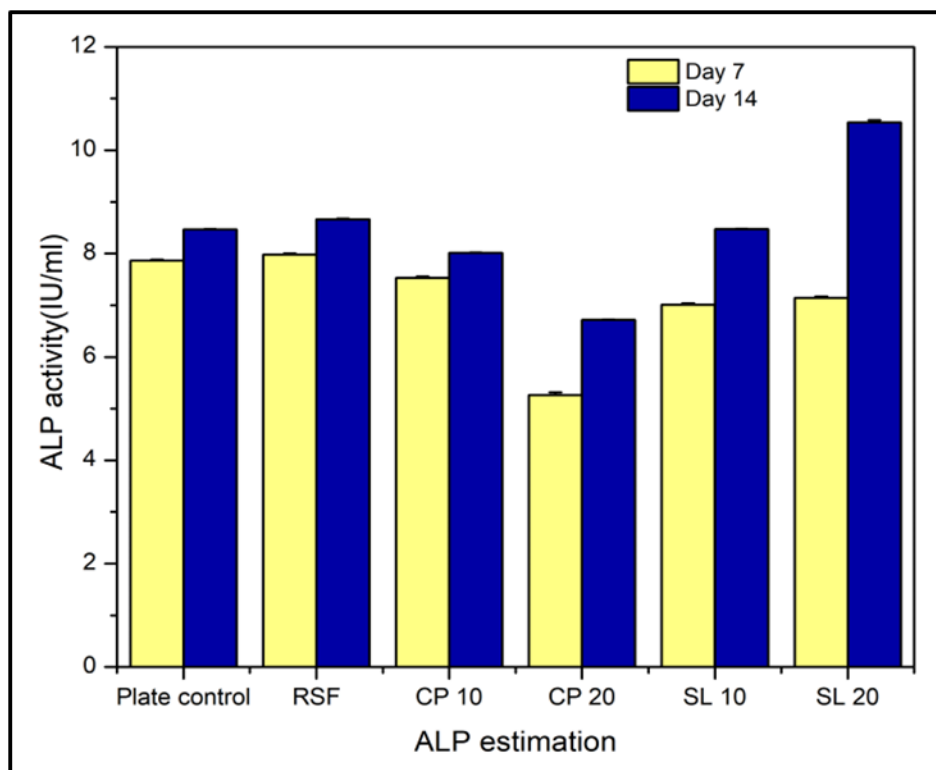


**Figure 6.27** Graph denotes the effect of synthesized nanoparticles with increasing loading on ALP activity of cells up to 14 days



## 6.4 Conclusion:

The biological properties of SL have been widely studied. It is well known that SL have good anti-bacterial, anti-cancer, anti-fungal and anti-viral properties. However, majority of the applications have been reported for oleic acid derived SL. Applications of newer synthesized SL are yet to be explored.

Earlier chapter discussed the benefits of short chain derived SL i.e MASL. To further assess its potential, we have synthesized calcium phosphate nanoparticles using MASL. This happens to be the first report on synthesis of inorganic nanoparticles using short chain derived SL. These nanoparticles were obtained by using biological and physical method of synthesis. The resulting nanoparticles were characterized using different techniques.

Interestingly, by this method of synthesis composite nanoparticles consisting of brushite and TCP are formed. Moreover, it was evident that presence of SL during the synthesis effectively changes the compositional and morphological properties of the nanoparticles.

The self-assembling ability of SL provides the necessary template for synthesizing calcium phosphate nanoparticles. These nanoparticles exhibit well defined flower shaped structure. Further, the presence of SL on nanoparticles has been lectin binding assay and thermogravimetric analysis. Furthermore, the biological properties of nanoparticles are also enhanced in presence of SL. SL nanoparticles resulted in better proliferation and better expression of ALP activity of bone cells.

Thus, to conclude, inorganic calcium phosphate nanoparticles are successfully synthesized using myristic acid derived SL. Moreover, the excellent properties of short chain derived SL render them beneficial for bone tissue application.

## **Chapter VII**

### **Conclusions and future work**

At the end, this chapter summarizes the work presented in the thesis. The highlights of the research work along with their scientific impact have been listed. Moreover, the scope for future potential of these synthesized biomolecules and their prospective path have been discussed.

### 7.1 Conclusions:

The aim of this work is to synthesize glycolipids using unconventional lipophilic substrates. The substrates were fed to the non-pathogenic yeast during biosynthesis process so as to impart structural diversity to the biomolecule. Substrate diversification and its correlation with the physiochemical properties of synthesized SL is not yet addressed. Our aim was to contribute to the knowledge in this particular area of SL. Moreover, the physical and biological properties of these synthesized molecules have been thoroughly studied.

Chapter II -III work focuses on understanding the effect of chain length of lipophilic substrate on the physical properties of the SL. Three different saturated fatty acids with increasing chain length were selected, these include; C14 myristic acid, C16 palmitic acid, C18 stearic acid. The unconventional substrates were incorporated by circumventing the fermentation process. Resting cell method along with wild strain of yeast results in successful production of short chain derived SL. Further the properties and performance of these SL was assessed using different techniques. It was observed that MASL, i.e short chain SL possesses better surfactant properties than longer chain derived SL (Palmitic and stearic). Physical properties of the synthesized SL are in accordance to the lipophilic substrate used.

Furthermore, Chapter IV aims to understand the effect of chain length on biological properties of SL. To address the global issue of anti-biotic resistance and targeted therapy for cancer, anti-bacterial and anti-cancer activities of all the synthesized SL were studied. For future therapeutic application of SL as anti-bacterial molecules, time and concentration dependent analysis was performed. It was observed that anti-bacterial activity was more pronounced in short chain derived SL which inhibited more than 80 % gram positive bacteria within 15 minutes and gram negative bacteria within 1h. A clear trend in the anti-bacterial activity was observed i.e as the chain length of substrate increases, the anti-bacterial activity decreases

An effective anti-cancer drug relies on targeted action and less harm to the normal cells. With this view, our aim was to explore the anti-cancer potential of short chain sophorolipids and to also assess its effect on the normal cell population. The anti-cancer activity of crude SL was assessed against cervical cancer and normal fibroblast cells. Results revealed that all synthesized SL possess anti cancer potential however, the ability to secure normal cells was observed only for short chain derived SL. Longer chain derived SL inhibited both cancerous and normal cells.

This chapter highlights the interesting finding of short chain derived SL; its potent ability to kill bacterial and cancer cells without affecting the normal cells is worth exploring. This chapter summarizes that, the nature of lipophilic substrate has a direct connection with its physical and biological properties. Shorter the chain length of lipophilic substrates, better are the physical and biological properties.

The promising results in the earlier chapter led to basic understanding of incorporation of short chain substrates into SL synthesis. This chapter work focuses on deducing the mechanism involved in incorporation of short chain substrates by yeast *S.bombicola*. Different media compositions and processes were evaluated to achieve higher yield. Further, the effect of unconventional substrate on yeast cell growth and product conversion was assessed. It was observed that myristic acid didn't hamper the yeast growth or product conversion. These findings led to understanding of the inherent need of myristic acid for yeast growth and metabolism. The fatty acid synthetase system of yeast is dependent on the exogenous supply of myristic acid.

Deciphering the mechanism involved in incorporation of short chain substrate, helped to broaden the basic knowledge regarding SL synthesis. To further broaden the applicability of this molecule, column purification was performed to separate individual congeners. Separation of individual congeners was beneficial in understanding the structural diversity of short chain derived SL.

To deduce the impact of acidic and lactonic components on the biological properties of molecules, anti cancer activity of purified congeners was performed. It was observed that lactonic components exhibit better biological properties and that acidic forms are more associated with physical attributes. Moreover, it was observed that the biological potential of crude SL was better as

compared to individual congener. The amalgamation of acidic and lactonic forms in crude SL prove more beneficial. These results are described in chapter V of the thesis.

Chapter VI focuses on synthesizing inorganic nanoparticles using MASL. The aim of this work was to broaden the applicability of short chain derived SL. The demand for biocompatible and bioresorbable bone filler is rapidly increasing. To address this issue, we aim to synthesize calcium phosphate nanoparticles using biosurfactant. Incorporation of SL leads to greener low-cost method of nanoparticle synthesis. Optimization of the process time and concentration was performed to decipher optimal conditions for synthesis. Use of SL into the process led to synthesis of nanoparticles consisting of brushite and tri calcium phosphates. These forms of calcium cements are most preferred due to their good biological and mechanical properties. Interestingly, the results revealed that presence of SL enhances the composition and morphology of the nanoparticles. The amphiphilic nature of SL stimulates the nucleation process thereby leading to formation of well-defined flower shaped particles. Deducing the role of SL into nanoparticle synthesis led to detection of presence of SL on the nanoparticles using different assays.

Lastly, the *in vitro* studies of the synthesized nanoparticles were performed. The results revealed that SL coated nanoparticles allowed proliferation and differentiation of bone cells over a time period of 14 days. The cell morphology remained good throughout the time period as observed in actin staining. These results highlight the excellent properties of MASL in synthesizing calcium phosphate nanoparticles and their future prospects in biomedical field.

## 7.2 Future prospects

During this thesis work we came across few potential leads with promising results that could be pursued further.

### 7.2.1 Upscaling of short chain derived sophorolipids

The toxicity of short chain substrates along with low product yield restricted the used of substrates for SL synthesis. Although the conventional substrates are more preferred by the yeast, their cost of production is exorbitantly high as compared to chemical surfactant. This limits the usage of SL in various sectors. Changing the lipophilic and hydrophilic substrates with cheaper alternatives might assist in reducing the production cost. Efforts have been made to utilize lignocellulosic, dairy wastes as substitutes for SL production. These efforts were successful in synthesizing SL however, the quality of the SL was compromised.

For SL synthesis a balance between the hydrophilic and the hydrophobic components is crucial. The nature of SL and product yield is highly dependent on the individual components. This thesis summarizes the use of short chain length fatty acid; myristic acid as promising substrate for SL synthesis. The synthesized SL exhibits excellent biological and physical properties. The chain length of fatty acid aids in improving the properties of SL thereby expanding the avenues for application of these biosurfactants.

Large scale production of these compounds is promising; however, the product quality and large quantity needs to be streamlined. Although number of developments have taken place in commercial market regarding longer chain derived SL, the usage is narrow and the production cost is still higher as compared to the chemical surfactants. Thus, in future, our research should be targeted on the economics of the fermentation process and quality of the synthesized SL.

This can be achieved by 2 generation substrate substitution i.e changing both the lipophilic and hydrophilic substrates with renewable alternatives and emphasizing on the properties of synthesized SL. Shorter chain derived SL exhibit CMC within the expected range for industrial purpose and therefore, commercial production using renewable substrates could be advantageous.

Moreover, short chain derived SL exhibited remarkable ability to synthesize calcium phosphate nanoparticles with preferred composition. Preliminary studies proved the ability of the nanoparticles to allow proliferation and differentiation of bone cells. In future, in vivo studies of the nanoparticles will assist in expanding the applicability of short chain derived SL for bone tissue application.

### **7.2.2 Self-assembling abilities of short chain derived sophorolipids**

SL have been shown to self-assemble into spherical micelles, rods, nano-fibers and sheets depending on the concentration, pH, type of SL (acidic/lactonic) and time. There are numerous reports on self-assemblies of longer chain derived SL. We studied the self-assembling properties of SLMA as a function of pH using FE-SEM. We report for the first time the self-assemblies of myristic acid derived SL. Subjecting the aqueous solution of SL to sonication results in formations of different structures. Initiation of assemblies begins within hours resulting in turbidity and with time the assemblies proliferate. Preliminary experiments suggest that the size of the assemblies is inversely proportional to the pH of the SLMA solution. As shown in [Figure 7.1](#), at pH 6, the assemblies form a dense network of nano-fibers while length of fibers is few hundred  $\mu\text{m}$ . At pH 8 the length of the fibers is drastically reduced and at pH 10 flat sheets assembly are observed. Such phenomenon are end results of various morphological parameters: Sugar moiety, degree of unsaturation and end group which need to be further explored for better understanding of the assembling behavior.

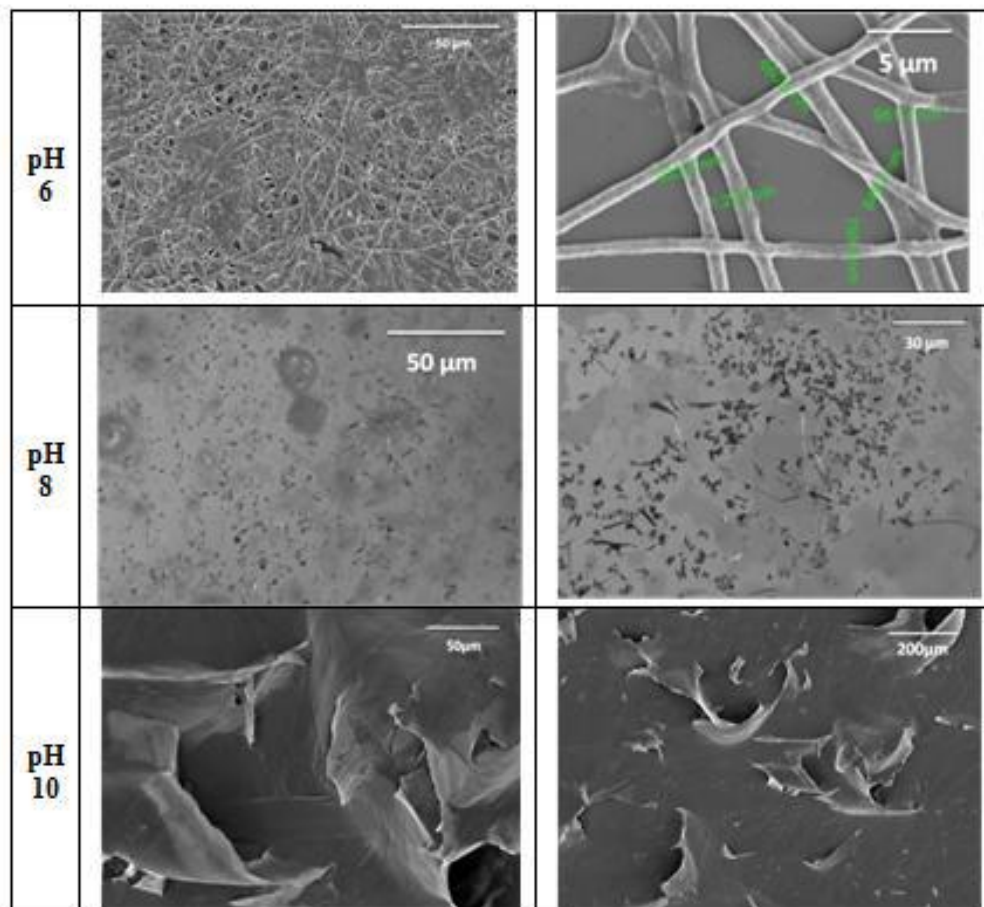


Figure 7.1 SEM images of pH dependent self assemblies of MASL

### 7.2.3 Effect of short chain sophorolipids on gelation of silk fibroin

Silk fibroin has been routinely used in biomedical sector due to its strength and biocompatibility. It can be fabricated into different forms like hydrogels, discs and films which can be used for tissue engineering application. Natural gelation of silk fibroins happens within 15-20 days, this hampers its clinical application.



Earlier reports suggest that use of OASL accelerates the gelation of silk fibroin. With this view, we explored the use of short chain derived SL as gelling agent of silk fibroin. Preliminary data suggests that MASL significantly reduces the gelation time of silk fibroin from days to minutes. Refer to [Figure 7.2](#). Further *in vitro* studies on these hydrogels will assist in fabricating 3D scaffolds for biomedical application.

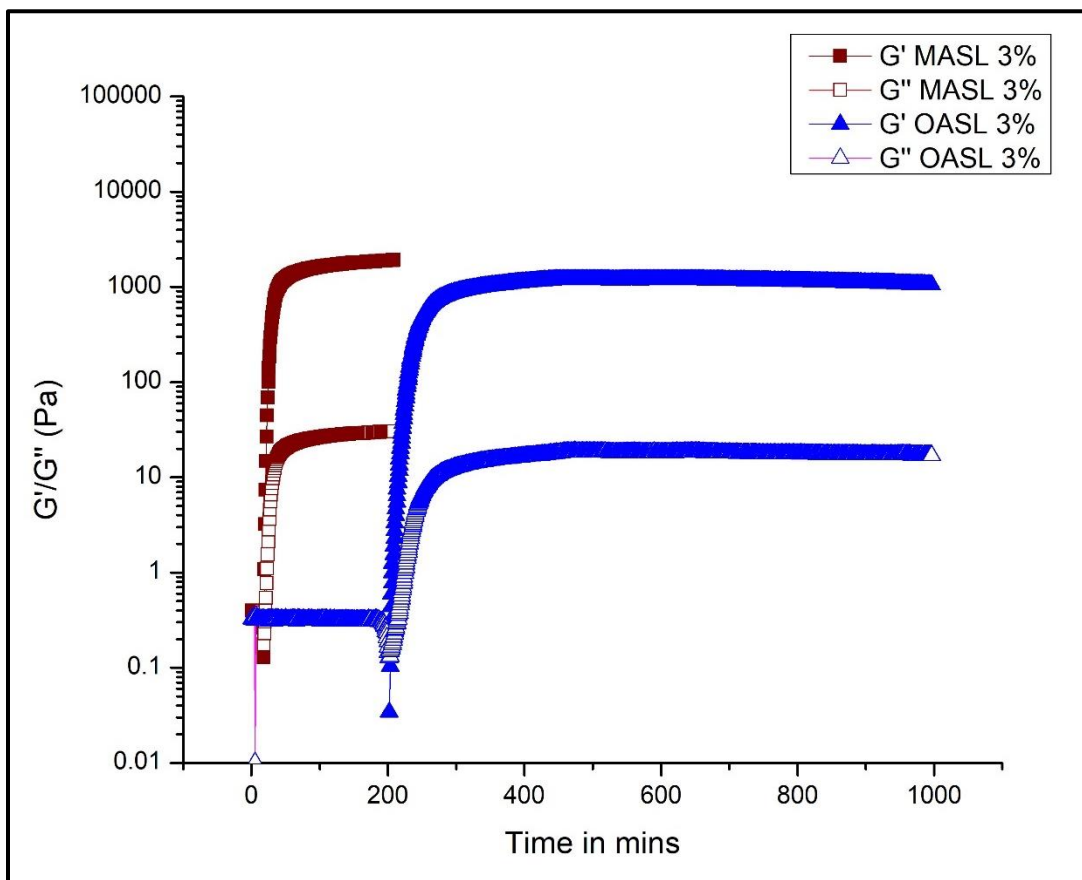


**Figure 7.2** Rheology experiments on MASL and OASL

## Appendix

Figure 8.1 reveals the mass spectrum of native MASL with molecular formula  $C_{26}H_{48}O_{13}$ . The spectrum shows presence of protonated molecular ion peak at  $m/z$  569.3170 (Figure A). The lactonic part (Figure 8.1B) ( $C_{26}H_{46}O_{12}$ ) is confirmed by the presence of sodium adduct at  $m/z$  573.2881.

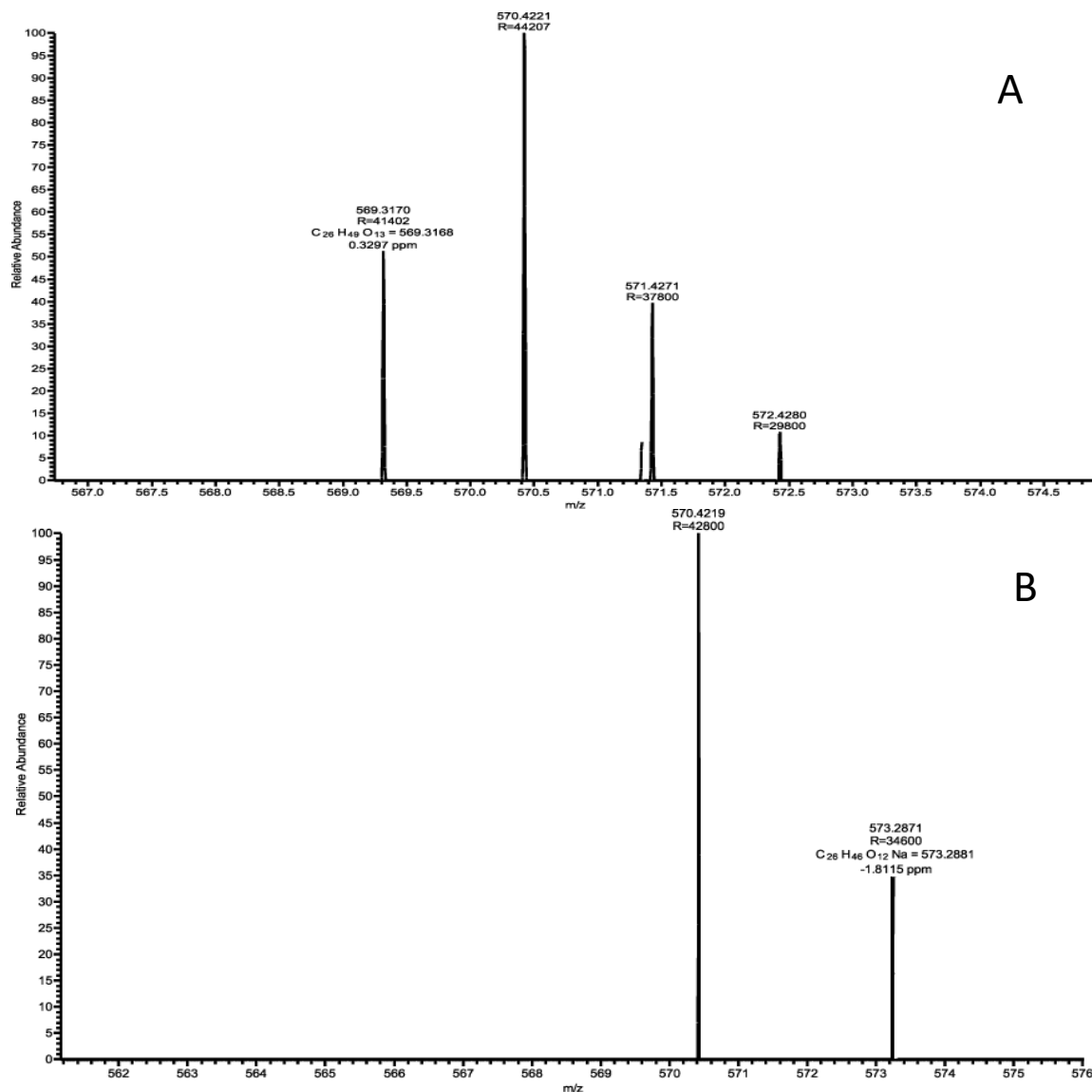
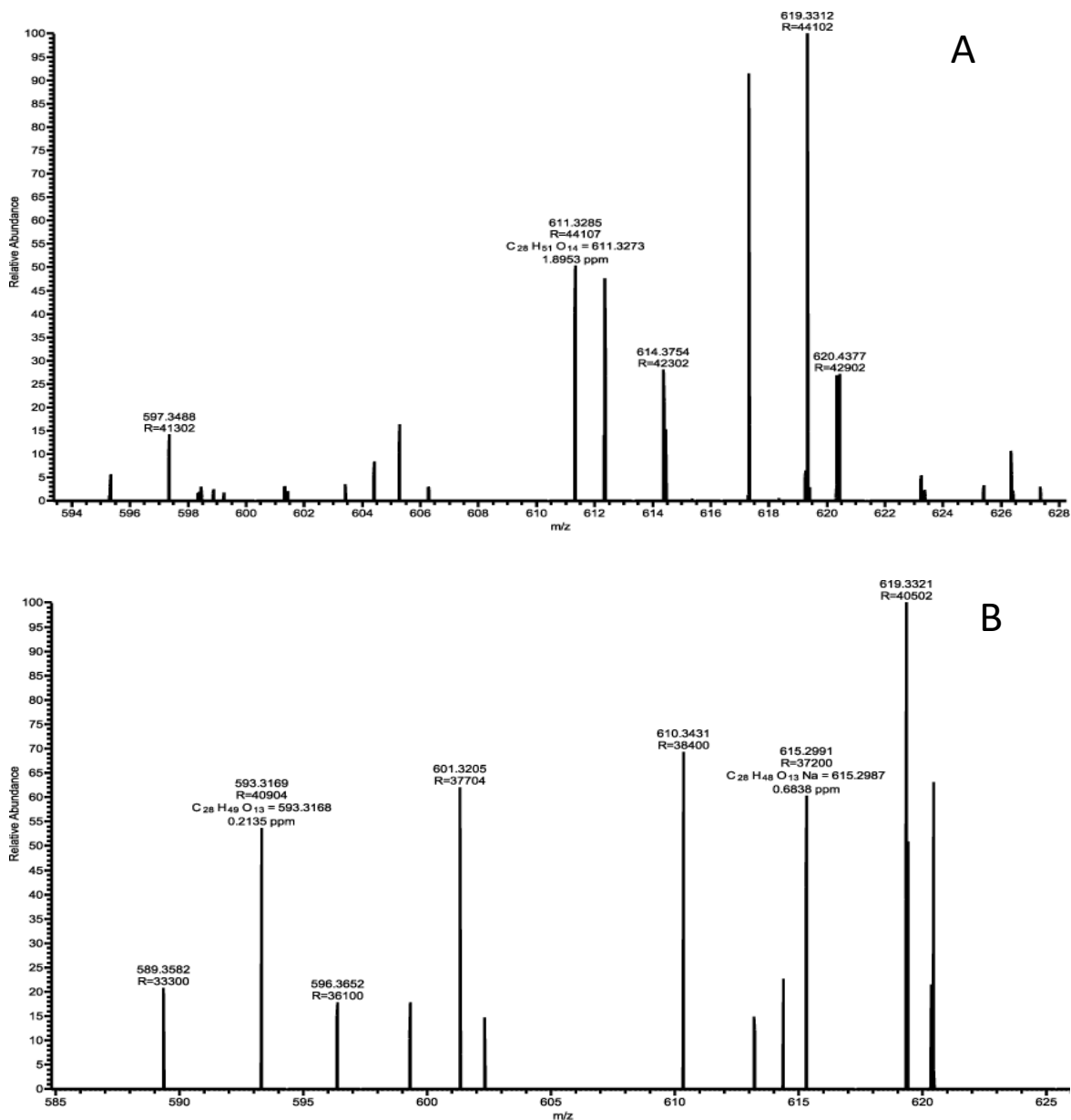


Figure 8.1 Mass spectra of native sophorolipid (MASL); A) acidic component; B) Lactonic component

**Figure 8.2** A reveals the mass spectrum of monoacetylated MASL with molecular formula  $C_{28}H_{50}O_{14}$ . The mass spectrum shows presence of protonated molecular ion peak at  $m/z$  611.3285. The lactonic part (**Figure 8.2B**) ( $C_{28}H_{48}O_{13}$ ) is also confirmed by presence of protonated molecular ion peak at  $m/z$  593.3169.



**Figure 8.2** Mass spectra of monoacetylated sophorolipid (MASL); A) acidic component; B) Lactonic component

The presence of diacetylated MASL form is revealed through [Figure 8.3A](#). The diacetylated form has molecular formula  $C_{30}H_{52}O_{15}$ , is depicted by its sodium adduct at  $m/z$  675.3203. The lactonic component ( $C_{30}H_{50}O_{14}$ ) is depicted by its sodium adduct at  $m/z$  657.3109. Refer [Figure 8.3B](#)

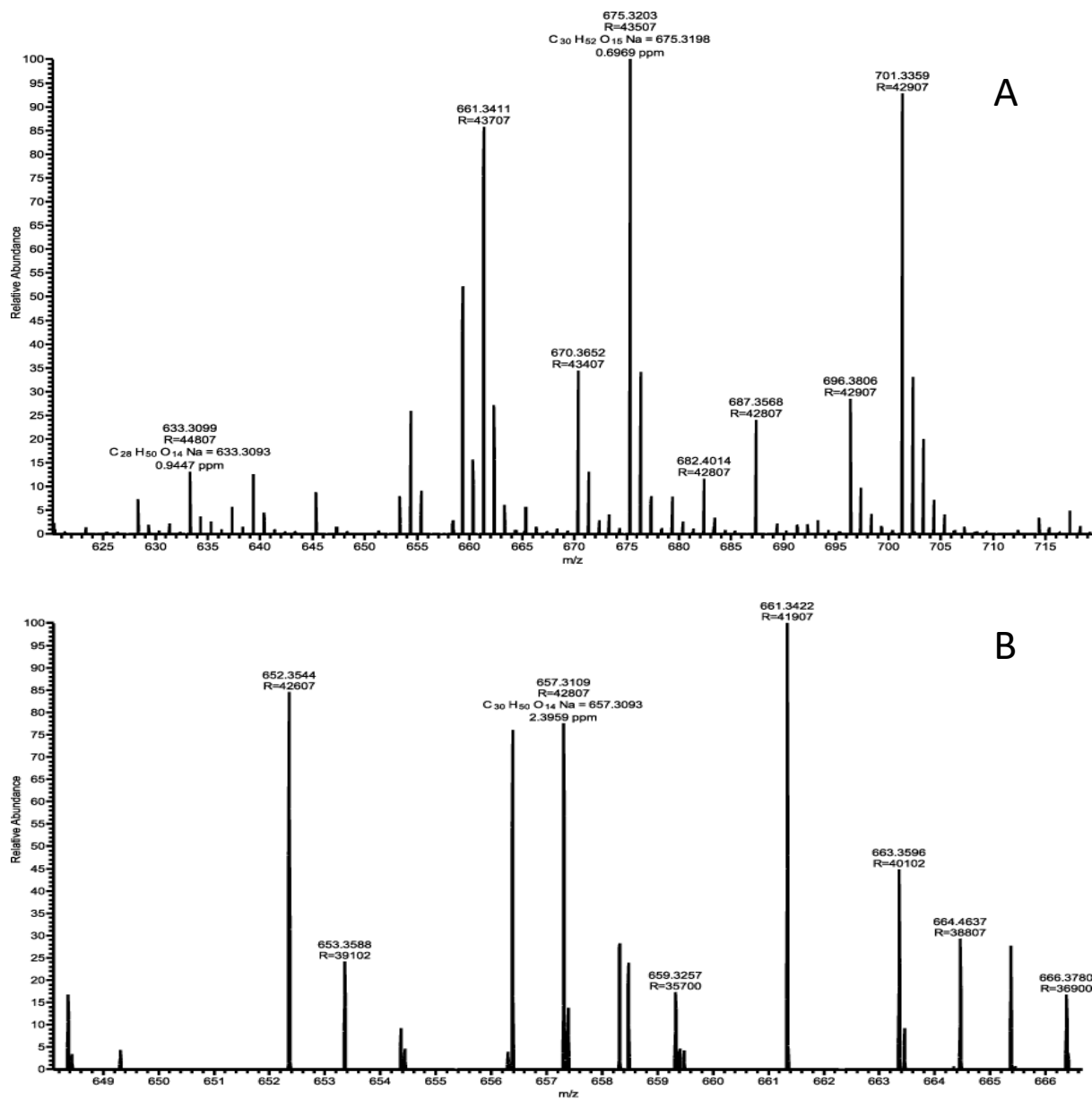


**Figure 8.3** Mass spectra of diacetylated sophorolipid (MASL); A) acidic component; B) Lactonic component

**Figure 8.4A**, depicts the mass spectra of native PASL with molecular formula  $C_{28}H_{52}O_{14}Na$ . The acidic form is confirmed by presence of sodium adduct at  $m/z$  619.3306. The lactonic component ( $C_{28}H_{51}O_{12}$ ) is depicted by its peak at  $m/z$  579.3376. Refer **Figure 8.4B**.

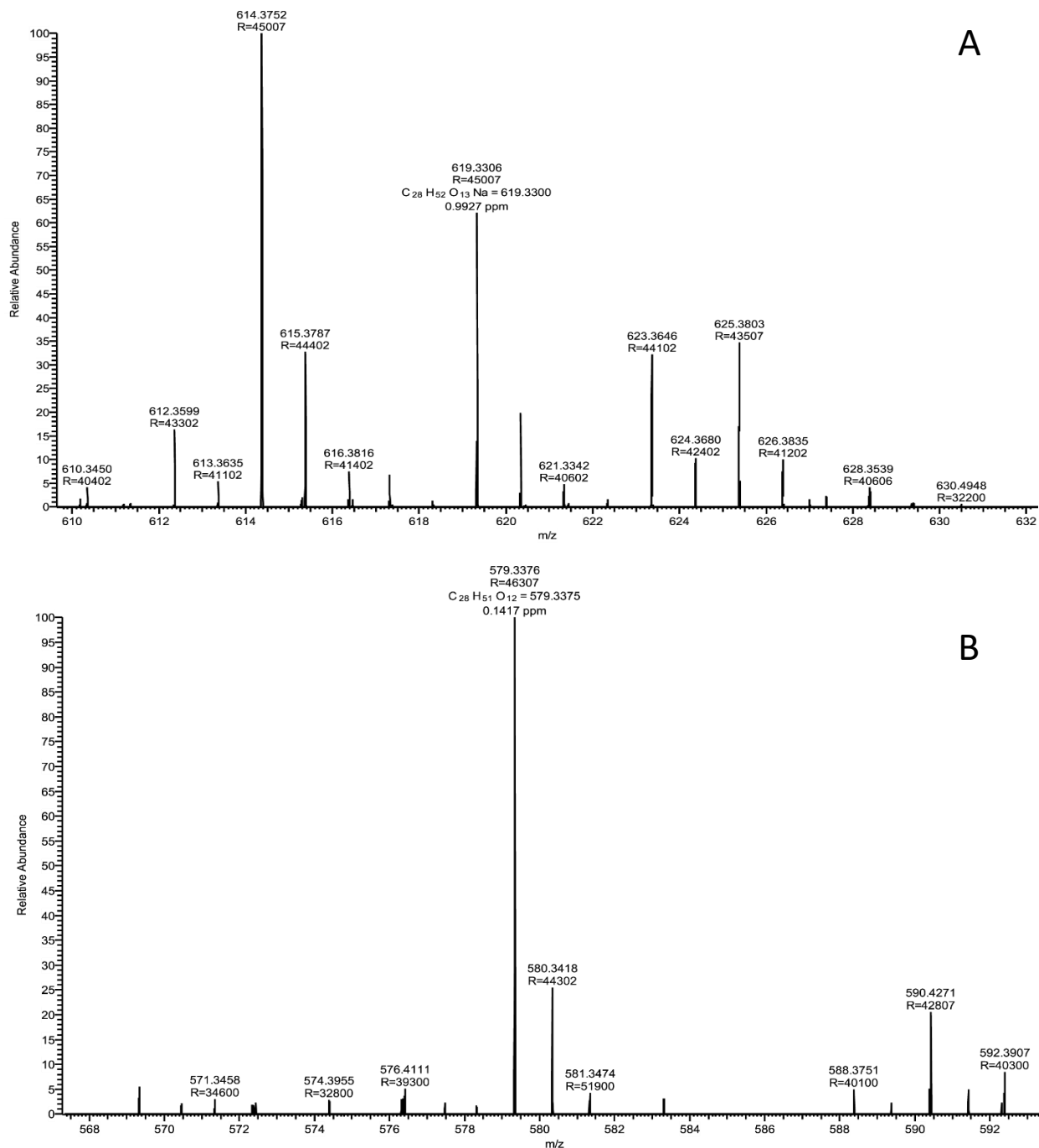


**Figure 8.4** Mass spectra of native sophorolipid (PASL); A) acidic component; B) Lactonic component

The acidic mono acetylation component is confirmed by presence of protonated molecular ion peak at  $m/z$  639.3589, with its sodium adduct at  $m/z$  661.3411 (Figure 8.5 A). The lactonic mono acetylation form is confirmed by presence of sodium adduct at  $m/z$  643.3469 with molecular formula  $C_{30}H_{52}O_{13}Na$ , Figure 8.5B.

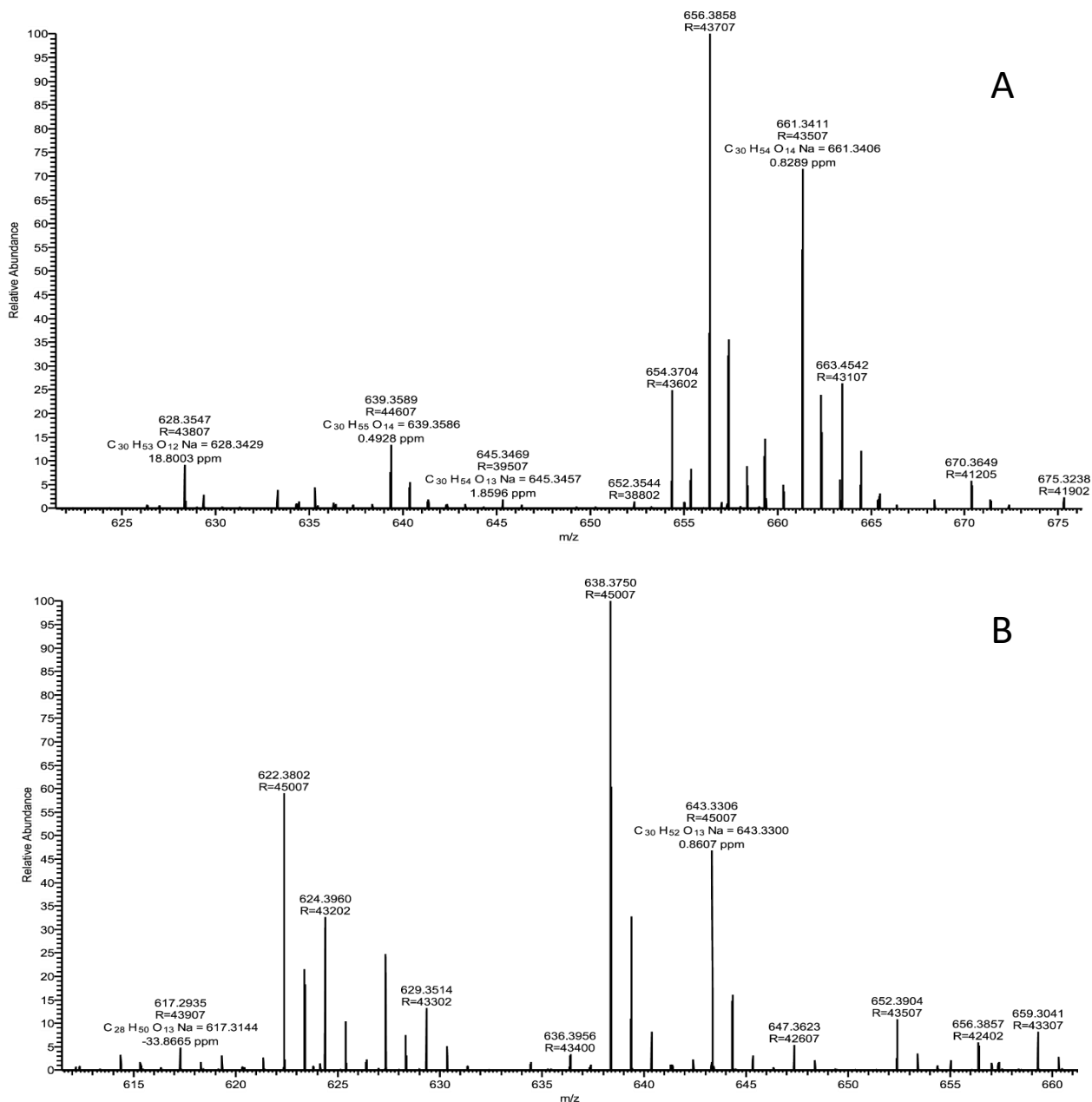


Figure 8.5 Mass spectra of monoacetylated sophorolipid (PASL); A) acidic component; B) Lactonic component

Figure 8.6A confirms the di acetylation acidic form by presence of sodium adduct at  $m/z$  703.36 with molecular formula  $C_{32}H_{56}O_{15}Na$ . The di acetylated lactonic form is confirmed by presence of sodium adduct at  $m/z$  685.3406, with molecular formula  $C_{32}H_{54}O_{14}Na$ . Refer to Figure 8.6B

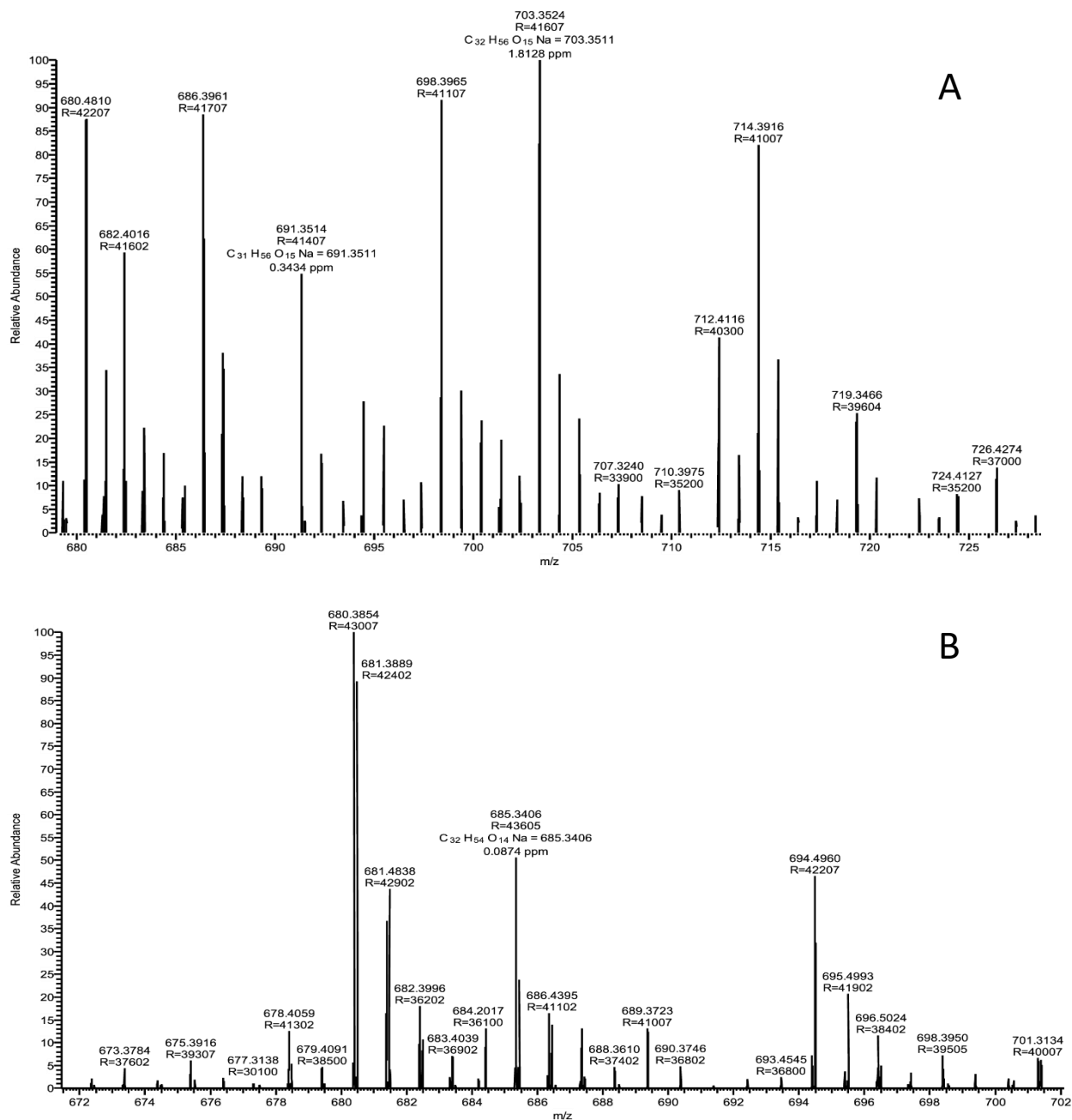


Figure 8.6 Mass spectra of diacetylated sophorolipid (PASL); A) acidic component; B) Lactonic component

Figure 8.7A confirms the presence of native sophorolipid, wherein the fatty acid is attached by the COOH. The acidic form is confirmed by the presence of peak at  $m/z$  603 with molecular formula  $C_{28}H_{52}O_{12}Na$  is depicted in Figure 8.7A.

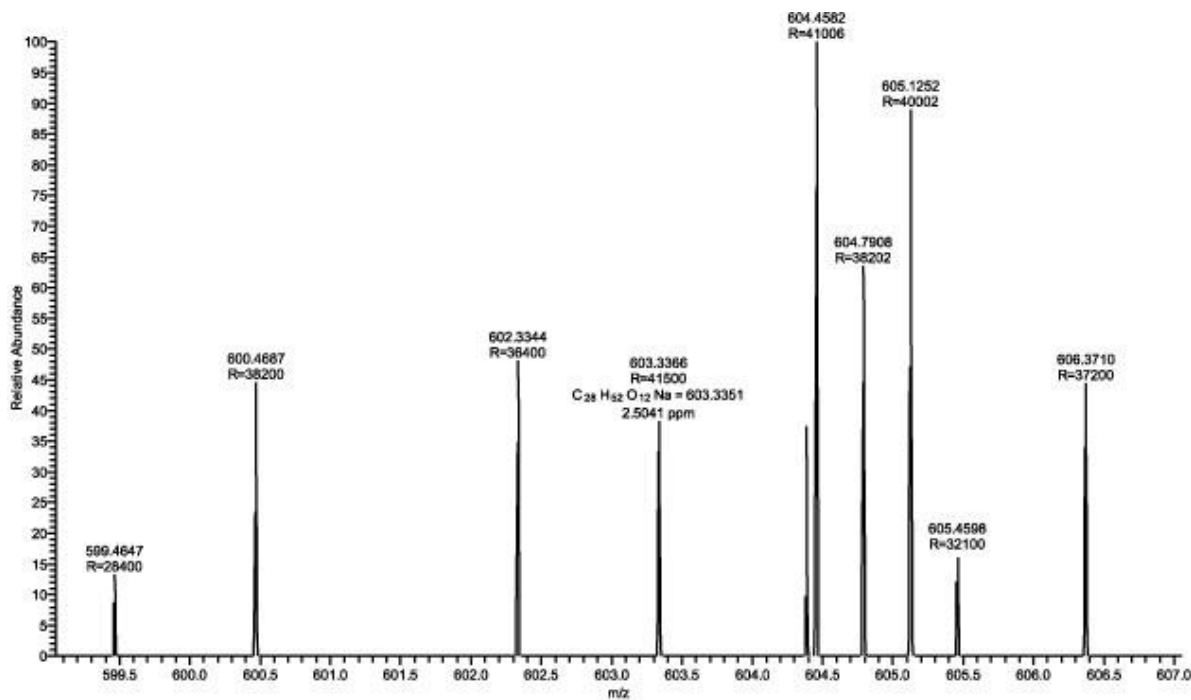
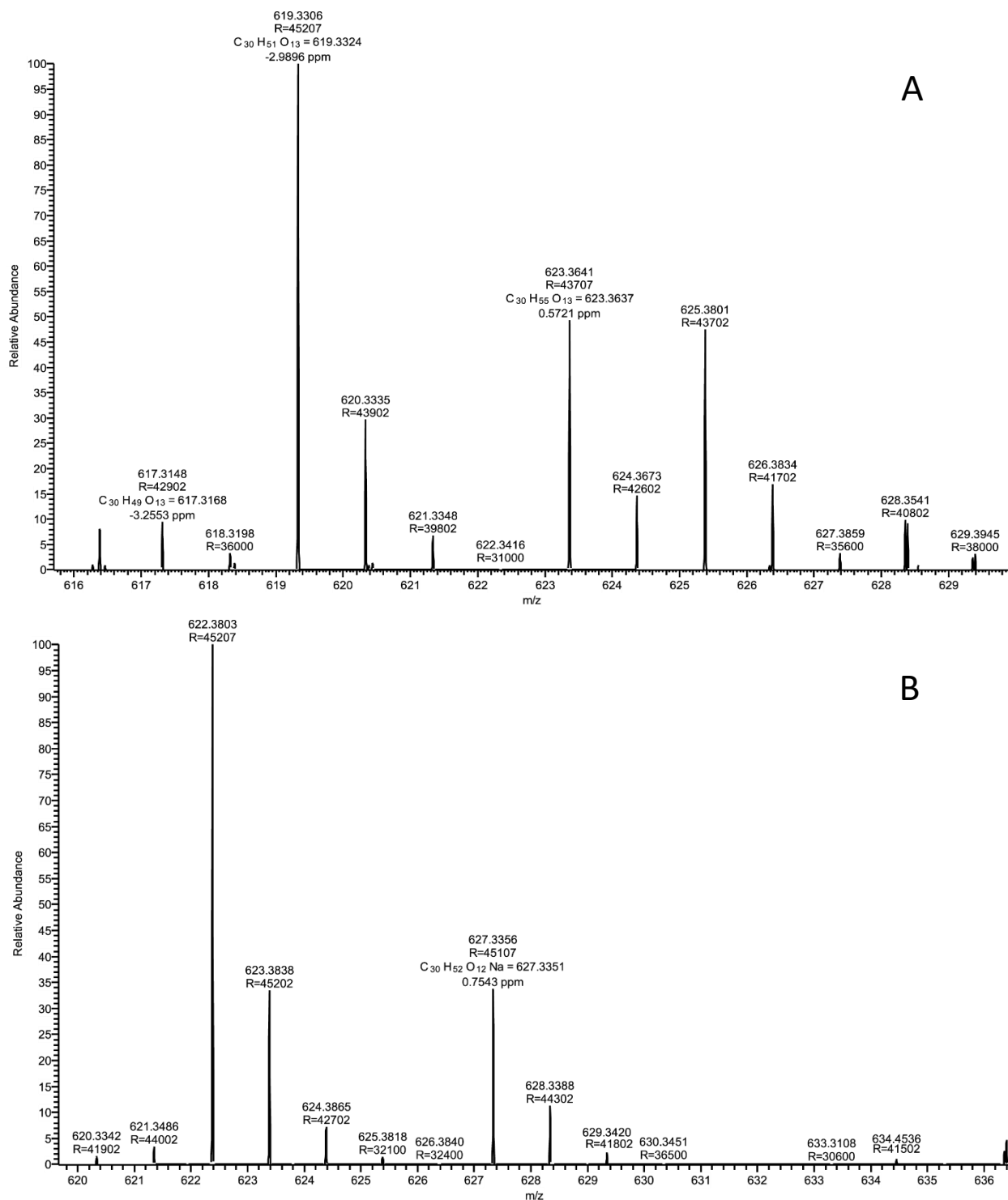


Figure 8.7 Mass spectra of native sophorolipid (PASL) with binding from COOH side A) acidic component

The acidic mono acetylation component is confirmed by presence of protonated molecular ion peak at  $m/z$  623.3641. The lactonic mono acetylation form is confirmed by presence of sodium adduct at  $m/z$  627.3356 with molecular formula  $C_{30}H_{52}O_{12}Na$ . Refer to Figure 8.8 A& B.





**Figure 8.8** Mass spectra of monoacetylated sophorolipid (PASL) with binding from COOH side A) acidic component; B) Lactonic component

**Figure 8.9A** confirms the di acetylation acidic form by presence of peak at  $m/z$  665.3744 with molecular formula  $C_{32}H_{56}O_{14}$ .

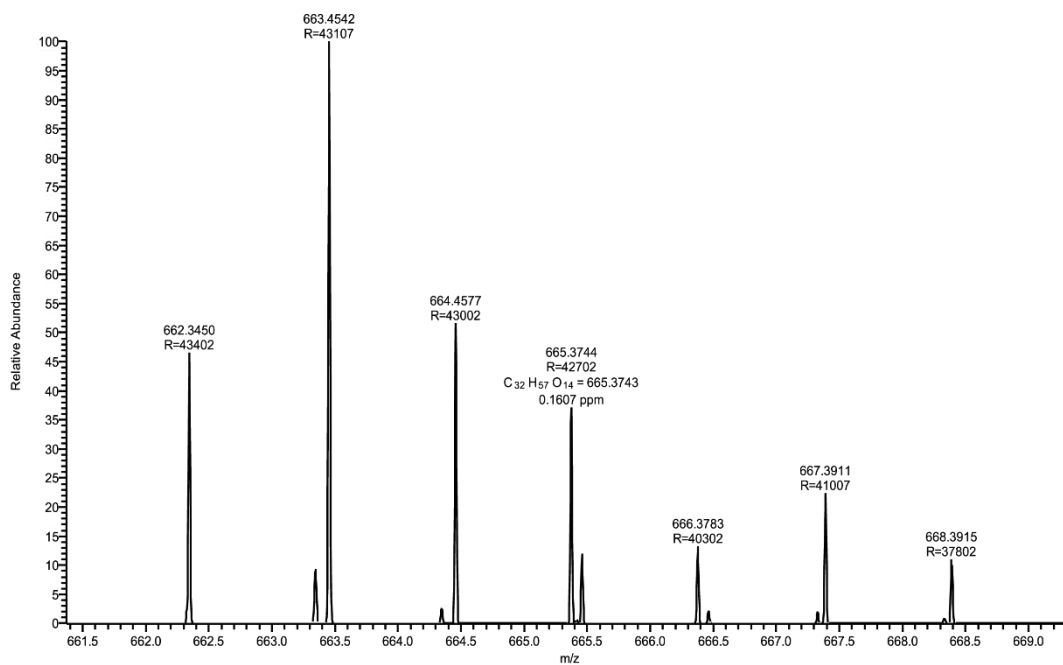


**Figure 8.9** Mass spectra of diacetylated sophorolipid (PASL) with binding from COOH side A) acidic component

Figure 8.10A confirms the native SASL by presence of protonated molecular ion peak at  $m/z$  625.3799, with molecular formula  $C_{30}H_{57}O_{13}$ . The lactonic component is confirmed by presence of sodium adduct at 629.3522 with molecular formula  $C_{30}H_{54}O_{12}Na$ , Figure 8.10 B

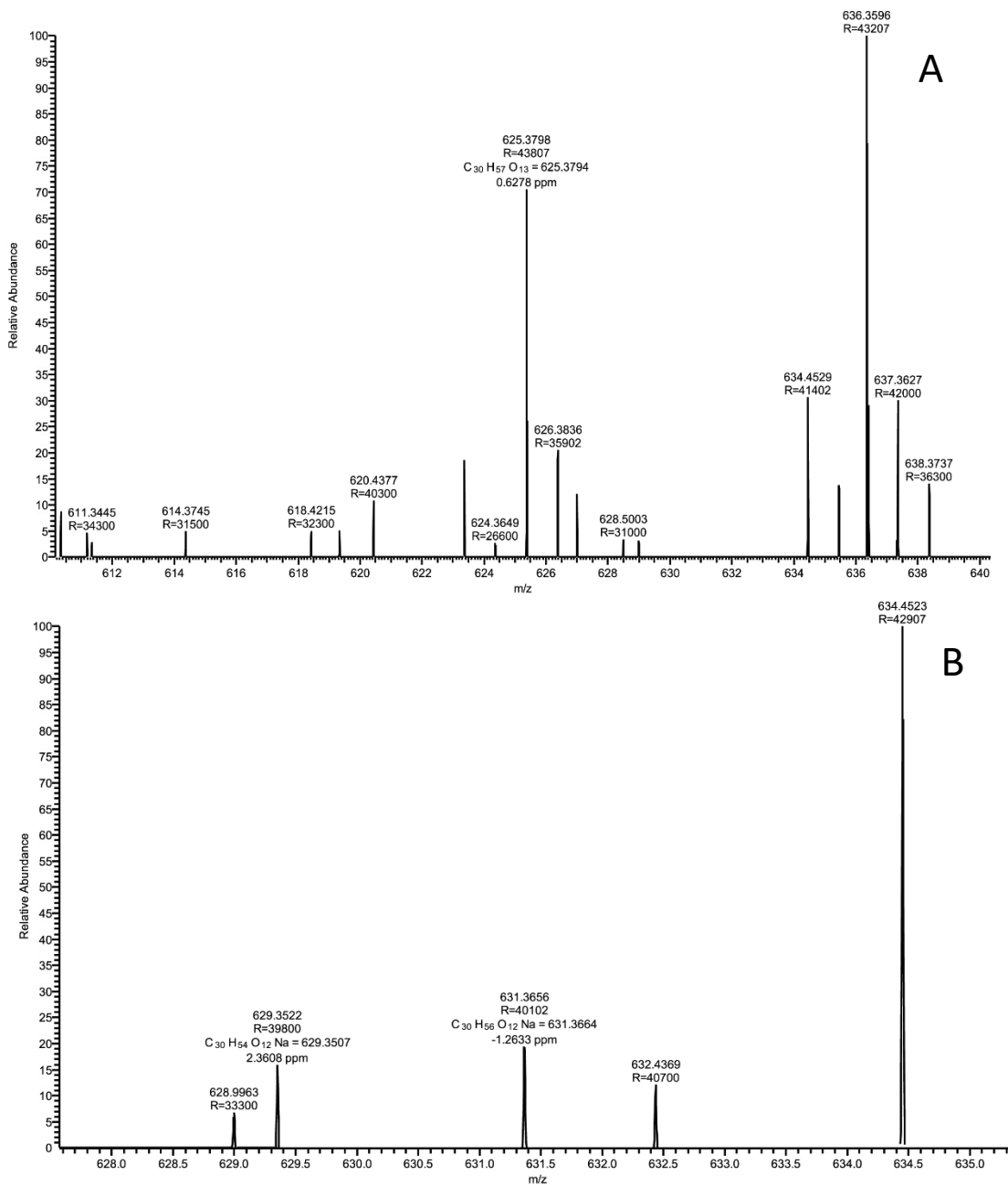
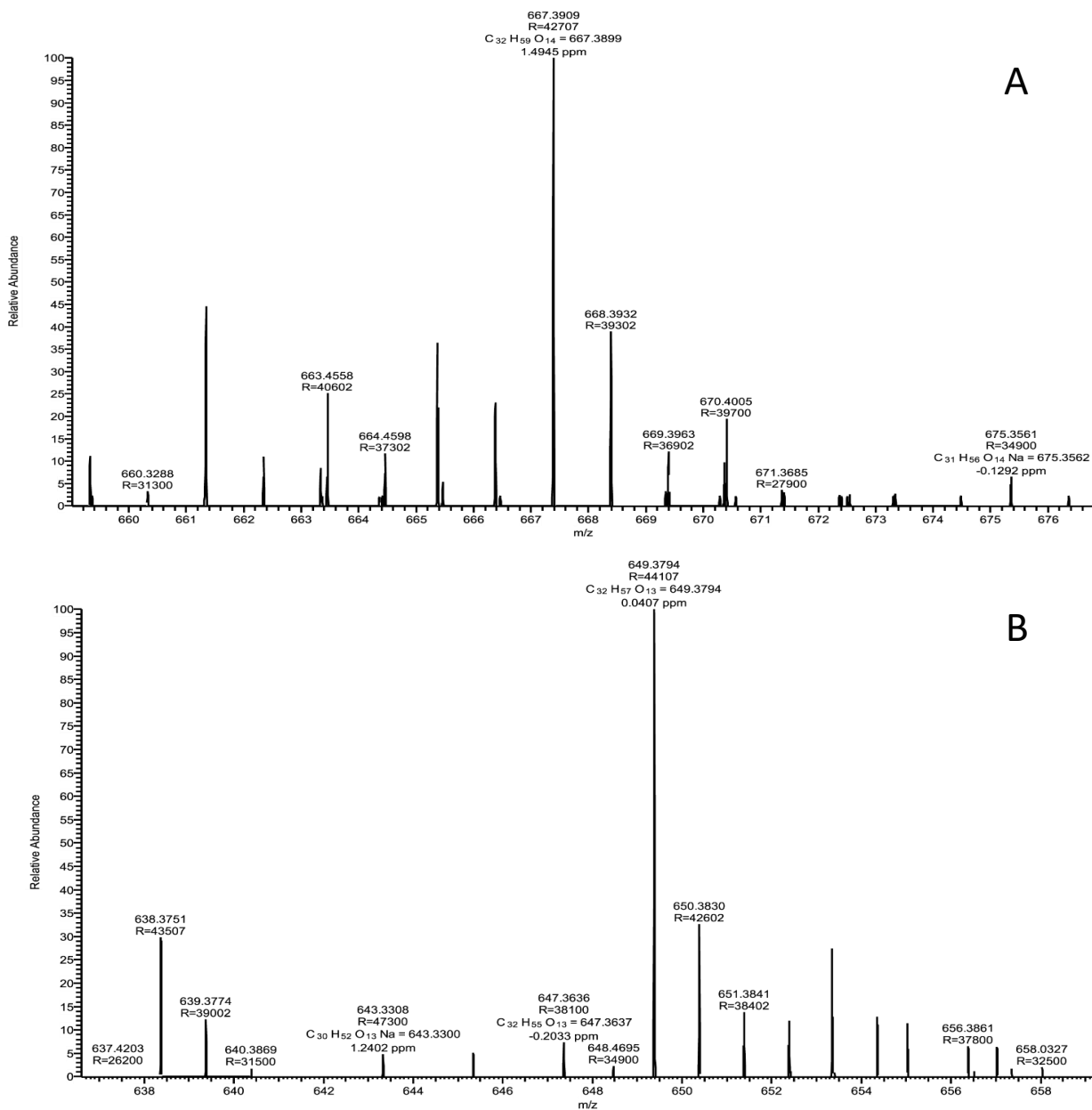


Figure 8.10 Mass spectra of native sophorolipid (SASL) A) acidic component; B) Lactonic component

**Figure 8.11A** confirms the acidic mono acetylated form by presence of protonated molecular ion peak at  $m/z$  667.3899, with molecular formula  $C_{32}H_{59}O_{14}$ . The presence of lactonic part is confirmed (**Figure 8.11 B**) by presence of protonated molecular ion peak at  $m/z$  649.3794 with molecular formula  $C_{32}H_{56}O_{13}Na$ .



**Figure 8.11** Mass spectra of monoacetylated sophorolipid (SASL) A) acidic component; B) Lactonic component

**Figure 8.12A** confirms the di acetylation acidic form by presence of sodium adduct at  $m/z$  713.3718 with molecular formula  $C_{34}H_{58}O_{14}Na$ .

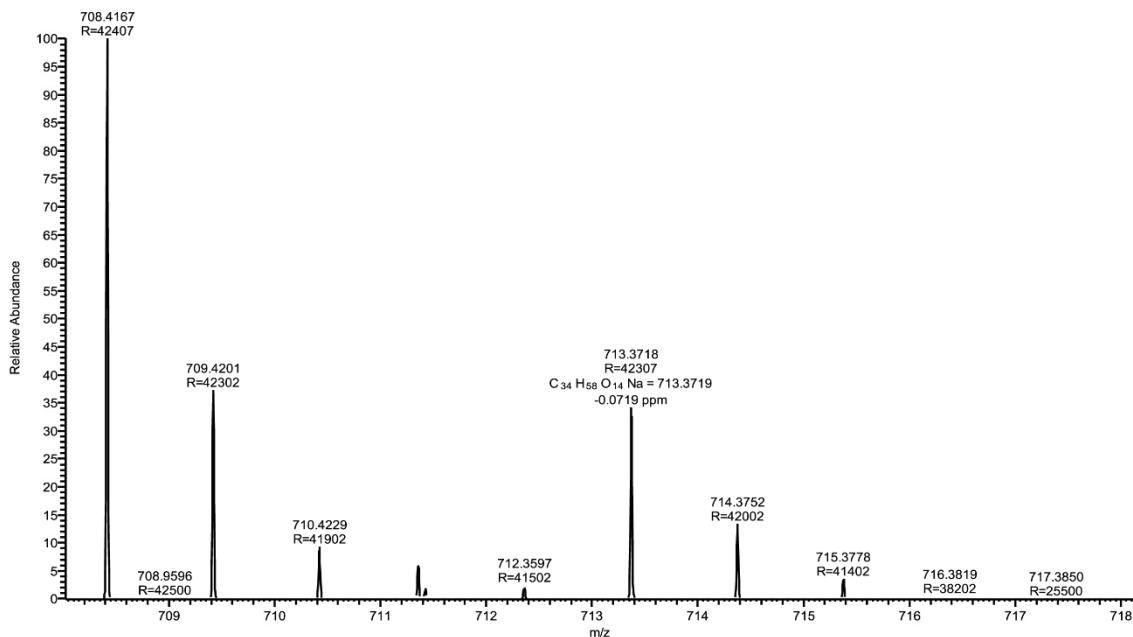


**Figure 8.12** Mass spectra of diacetylated sophorolipid (SASL) A) acidic component

**Figure 8.13A** confirms the presence of native sophorolipid, wherein the fatty acid is attached by the COOH side. The acidic form is confirmed by the presence of sodium adduct at  $m/z$  631.3656 with molecular formula  $C_{30}H_{56}O_{12}Na$ . The lactonic form is confirmed by presence of sodium adduct at  $m/z$  613.3560 with molecular formula  $C_{30}H_{54}O_{11}Na$ . Refer **Figure 8.13B**.

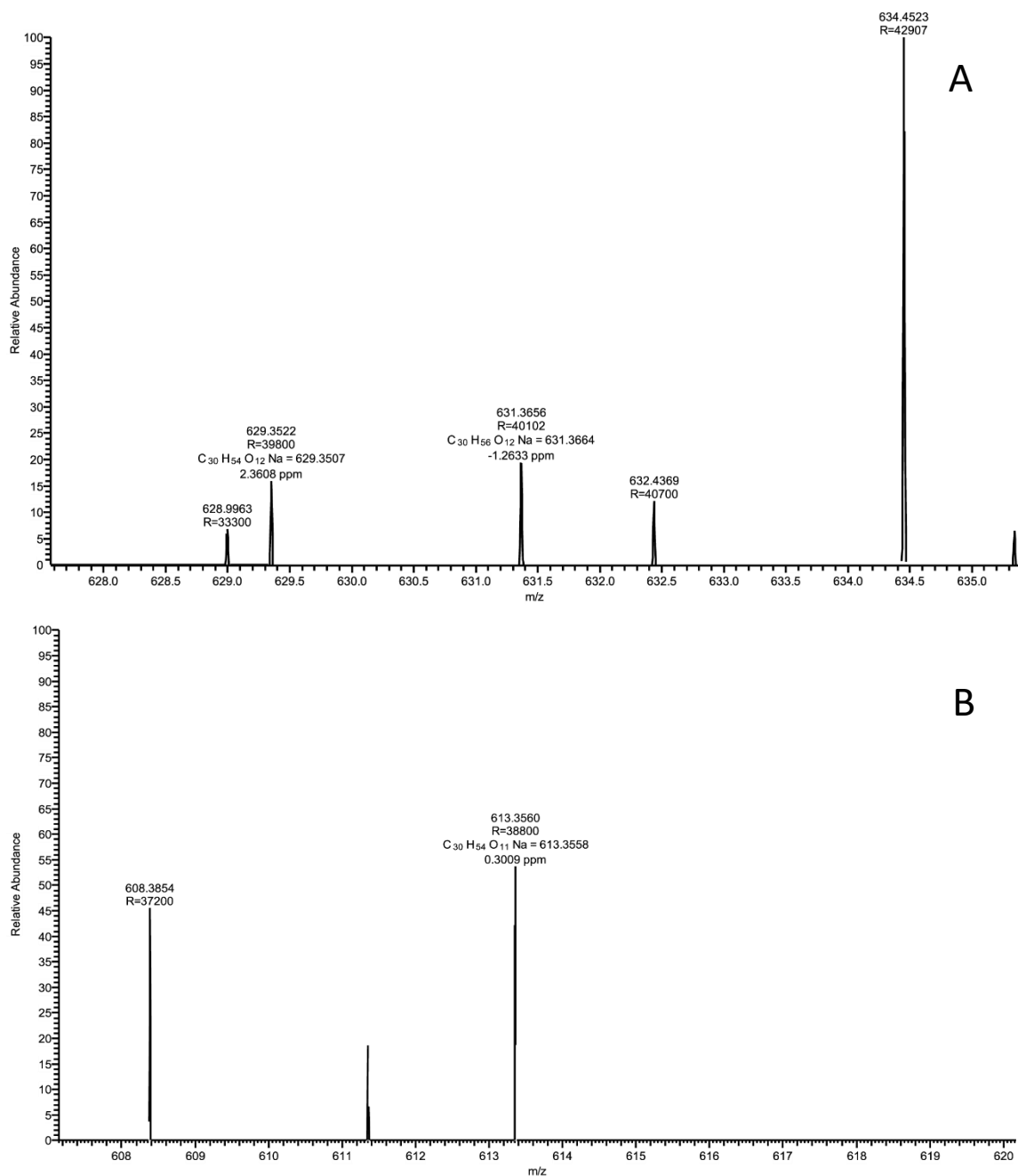


**Figure 8.13** Mass spectra of native sophorolipid (SASL) with binding from COOH side A) acidic component; B) Lactonic component

**Figure 8.14** A confirms the acidic mono acetylated form by presence of sodium adduct at m/z 673.3782, with molecular formula  $C_{32}H_{58}O_{13}Na$ . Chromatogram in **Figure 8.14** B confirms

presence of lactonic part by presence of sodium adduct at  $m/z$  655.3665 with molecular formula  $C_{32}H_{56}O_{12}Na$ .

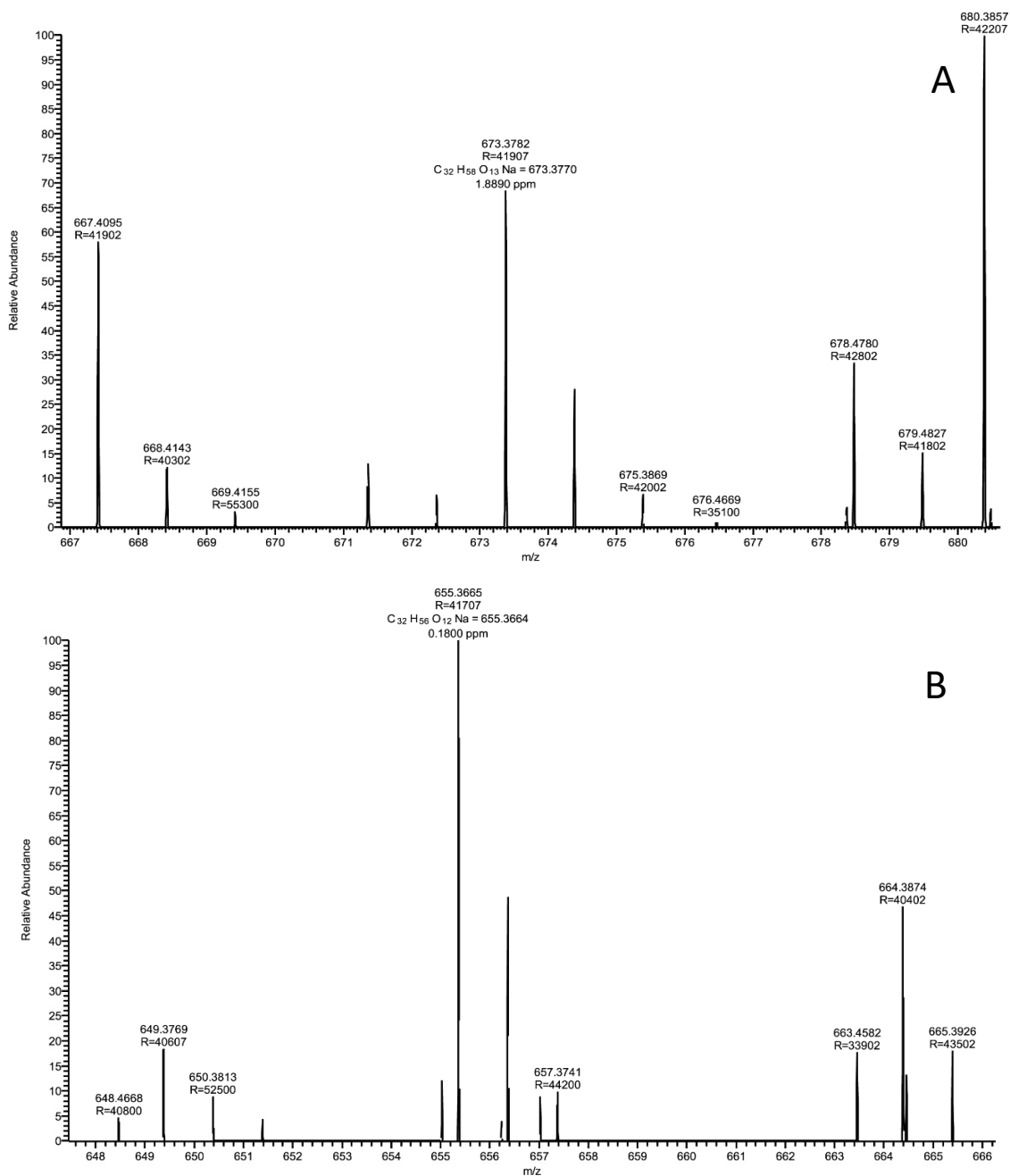


**Figure 8.14** Mass spectra of monoacetylated sophorolipid (SASL) with binding from COOH side  
A) acidic component; B) Lactonic component

## Bibliography

- (1) Van Renterghem, L.; Roelants, S. L. K. W.; Baccile, N.; Uyttensprot, K.; Taelman, M. C.; Everaert, B.; Mincke, S.; Ledegen, S.; Debrouwer, S.; Scholtens, K.; Stevens, C.; Soetaert, W. From Lab to Market: An Integrated Bioprocess Design Approach for New-to-Nature Biosurfactants Produced by *Starmerella Bombicola*. *Biotechnol. Bioeng.* **2018**, *115* (5), 1195–1206. <https://doi.org/10.1002/bit.26539>.
- (2) Gao, R.; Falkeborg, M.; Xu, X.; Guo, Z. Production of Sophorolipids with Enhanced Volumetric Productivity by Means of High Cell Density Fermentation. *Appl. Microbiol. Biotechnol.* **2013**, *97* (3), 1103–1111. <https://doi.org/10.1007/s00253-012-4399-z>.
- (3) Nitschke, M.; Costa, S. G. V. A. O. Biosurfactants in Food Industry. *Trends Food Sci. Technol.* **2007**, *18* (5), 252–259. <https://doi.org/10.1016/j.tifs.2007.01.002>.
- (4) Savarino, P.; Montoneri, E.; Bottigliengo, S.; Boffa, V.; Guizzetti, T.; Perrone, D. G.; Mendichi, R. Biosurfactants from Urban Wastes as Auxiliaries for Textile Dyeing. *Ind. Eng. Chem. Res.* **2009**, *48* (8), 3738–3748. <https://doi.org/10.1021/ie801853x>.
- (5) Sleiman, J. N.; Kohlhoff, S. A.; Roblin, P. M.; Wallner, S.; Gross, R.; Hammerschlag, M. R.; Zenilman, M. E.; Bluth, M. H. Sophorolipids as Antibacterial Agents. *Ann. Clin. Lab. Sci.* **2009**, *39* (1), 60–63.
- (6) Merrettig-Bruns, U.; Jelen, E. Anaerobic Biodegradation of Detergent Surfactants. *Materials (Basel)*. **2009**, *2* (1), 181–206. <https://doi.org/10.3390/ma2010181>.
- (7) Van Bogaert, I. N. A.; Zhang, J.; Soetaert, W. Microbial Synthesis of Sophorolipids. *Process Biochem.* **2011**, *46* (4), 821–833. <https://doi.org/10.1016/j.procbio.2011.01.010>.
- (8) Price, N. P. J.; Ray, K. J.; Vermillion, K. E.; Dunlap, C. A.; Kurtzman, C. P. Structural Characterization of Novel Sophorolipid Biosurfactants from a Newly Identified Species of *Candida* Yeast. *Carbohydr. Res.* **2012**, *348*, 33–41. <https://doi.org/10.1016/j.carres.2011.07.016>.
- (9) Sobrinho, H. B. .; Luna, J. M.; Rufino, R. D.; Porto, A. L.; Sarubbo, L. Biosurfactants:



- Classification, Properties and Environmental Applications. *Biotechnology* **2014**, *11* (January 2014), 1–29.
- (10) Dubey, P.; Selvaraj, K.; Prabhune, A. Physico-Chemical, Analytical and Antimicrobial Studies of Novel Sophorolipids Synthesized Using Cetyl Alcohol. *Prabhune al. World J. Pharm. Pharm. Sci.* **2014**, *3* (3).
- (11) Irorere, V. U.; Tripathi, L.; Marchant, R.; McClean, S.; Banat, I. M. Microbial Rhamnolipid Production: A Critical Re-Evaluation of Published Data and Suggested Future Publication Criteria. *Appl. Microbiol. Biotechnol.* **2017**, *101* (10), 3941–3951. <https://doi.org/10.1007/s00253-017-8262-0>.
- (12) Costa, S. G. V. A. O.; Déziel, E.; Lépine, F. Characterization of Rhamnolipid Production by *Burkholderia Glumae*. *Lett. Appl. Microbiol.* **2011**, *53* (6), 620–627. <https://doi.org/10.1111/j.1472-765X.2011.03154.x>.
- (13) Janek, T.; Krasowska, A.; Czyznikowska, Z.; Łukaszewicz, M. Trehalose Lipid Biosurfactant Reduces Adhesion of Microbial Pathogens to Polystyrene and Silicone Surfaces: An Experimental and Computational Approach. *Front. Microbiol.* **2018**, *9* (OCT), 1–14. <https://doi.org/10.3389/fmicb.2018.02441>.
- (14) Wang, Y.; Nie, M.; Diwu, Z.; Lei, Y.; Li, H.; Bai, X. Characterization of Trehalose Lipids Produced by a Unique Environmental Isolate Bacterium *Rhodococcus Qingshengii* Strain FF. *J. Appl. Microbiol.* **2019**, *127* (5), 1442–1453. <https://doi.org/10.1111/jam.14390>.
- (15) Spoeckner, S.; Wray, V.; Nimtz, M.; Lang, S. Glycolipids of the Smut Fungus *Ustilago Maydis* from Cultivation on Renewable Resources. *Appl. Microbiol. Biotechnol.* **1999**, *51* (1), 33–39. <https://doi.org/10.1007/s002530051359>.
- (16) Teichmann, B.; Linne, U.; Hewald, S.; Marahiel, M. A.; Bölker, M. A Biosynthetic Gene Cluster for a Secreted Cellobiose Lipid with Antifungal Activity from *Ustilago Maydis*. *Mol. Microbiol.* **2007**, *66* (2), 525–533. <https://doi.org/10.1111/j.1365-2958.2007.05941.x>.
- (17) Coelho, A. L. S.; Feuser, P. E.; Carciofi, B. A. M.; de Andrade, C. J.; de Oliveira, D. Mannosylerythritol Lipids: Antimicrobial and Biomedical Properties. *Appl. Microbiol. Biotechnol.* **2020**, *104* (6), 2297–2318. <https://doi.org/10.1007/s00253-020-10354-z>.
- (18) Niu, Y.; Wu, J.; Wang, W.; Chen, Q. Production and Characterization of a New Glycolipid, Mannosylerythritol Lipid, from Waste Cooking Oil Biotransformation by

- Pseudozyma Aphidis ZJUDM34. *Food Sci. Nutr.* **2019**, 7 (3), 937–948.  
<https://doi.org/10.1002/fsn3.880>.
- (19) Aparecida, C.; Queiroz, U.; Akemi, V.; Silveira, I.; Pedrine, M. A.; Celligoi, C. Antimicrobial Applications of Sophorolipid from *Candida Bombicola*: A Promising Alternative to Conventional Drugs. *J. Appl. Biol. Biotechnol.* **2018**, 6 (6), 87–90.  
<https://doi.org/10.7324/jabb.2018.60614>.
- (20) Joshi-Navare, K.; Shiras, A.; Prabhune, A. Differentiation-Inducing Ability of Sophorolipids of Oleic and Linoleic Acids Using a Glioma Cell Line. *Biotechnol. J.* **2011**, 6 (5), 509–512. <https://doi.org/10.1002/biot.201000345>.
- (21) Borsanyiova, M.; Patil, A.; Mukherji, R.; Prabhune, A.; Bopegamage, S. Biological Activity of Sophorolipids and Their Possible Use as Antiviral Agents. *Folia Microbiol. (Praha)*. **2016**, 61 (1), 85–89. <https://doi.org/10.1007/s12223-015-0413-z>.
- (22) Dengle-Pulate, V.; Chandorkar, P.; Bhagwat, S.; Prabhune, A. A. Antimicrobial and SEM Studies of Sophorolipids Synthesized Using Lauryl Alcohol. *J. Surfactants Deterg.* **2014**, 17 (3), 543–552. <https://doi.org/10.1007/s11743-013-1495-8>.
- (23) Jezierska, S.; Claus, S.; Van Bogaert, I. Yeast Glycolipid Biosurfactants. *FEBS Lett.* **2018**, 592 (8), 1312–1329. <https://doi.org/10.1002/1873-3468.12888>.
- (24) Coutte, F.; Lecouturier, D.; Dimitrov, K.; Guez, J. S.; Delvigne, F.; Dhulster, P.; Jacques, P. Microbial Lipopeptide Production and Purification Bioprocesses, Current Progress and Future Challenges. *Biotechnol. J.* **2017**, 12 (7), 1–10.  
<https://doi.org/10.1002/biot.201600566>.
- (25) Kanlayavattanakul, M.; Lourith, N. Lipopeptides in Cosmetics. *Int. J. Cosmet. Sci.* **2010**, 32 (1), 1–8. <https://doi.org/10.1111/j.1468-2494.2009.00543.x>.
- (26) Mandal, S. M.; Barbosa, A. E. A. D.; Franco, O. L. Lipopeptides in Microbial Infection Control: Scope and Reality for Industry. *Biotechnol. Adv.* **2013**, 31 (2), 338–345.  
<https://doi.org/10.1016/j.biotechadv.2013.01.004>.
- (27) Cooper, D. G.; Zajic, J. E.; Gracey, D. E. F. Analysis of Corynomycolic Acids and Other Fatty Acids Produced by *Corynebacterium Lepus* Grown on Kerosene. *J. Bacteriol.* **1979**, 137 (2), 795–801. <https://doi.org/10.1128/jb.137.2.795-801.1979>.
- (28) Toren, A.; Orr, E.; Paitan, Y.; Ron, E. Z.; Rosenberg, E. The Active Component of the

- Bioemulsifier Alasan from *Acinetobacter Radioresistens* KA53 Is an OmpA-like Protein. *J. Bacteriol.* **2002**, *184* (1), 165–170. <https://doi.org/10.1128/JB.184.1.165-170.2002>.
- (29) Shreve, G. S.; Makula, R. Characterization of a New Rhamnolipid Biosurfactant Complex from *Pseudomonas* Isolate DYNA270. *Biomolecules* **2019**, *9* (12), 1–11. <https://doi.org/10.3390/biom9120885>.
- (30) Zhao, F.; Han, S.; Zhang, Y. Comparative Studies on the Structural Composition, Surface/Interface Activity and Application Potential of Rhamnolipids Produced by *Pseudomonas Aeruginosa* Using Hydrophobic or Hydrophilic Substrates. *Bioresour. Technol.* **2020**, *295* (September 2019), 122269. <https://doi.org/10.1016/j.biortech.2019.122269>.
- (31) Franzetti, A.; Gandolfi, I.; Bestetti, G.; Smyth, T. J. P.; Banat, I. M. Production and Applications of Trehalose Lipid Biosurfactants. *Eur. J. Lipid Sci. Technol.* **2010**, *112* (6), 617–627. <https://doi.org/10.1002/ejlt.200900162>.
- (32) Oraby, A.; Werner, N.; Sungur, Z.; Zibek, S. Factors Affecting the Synthesis of Cellobiose Lipids by *Sporisorium Scitamineum*. *Front. Bioeng. Biotechnol.* **2020**, *8* (November), 1–15. <https://doi.org/10.3389/fbioe.2020.555647>.
- (33) Yu, M.; Liu, Z.; Zeng, G.; Zhong, H.; Liu, Y.; Jiang, Y.; Li, M.; He, X.; He, Y. Characteristics of Mannosylerythritol Lipids and Their Environmental Potential. *Carbohydr. Res.* **2015**, *407* (2015), 63–72. <https://doi.org/10.1016/j.carres.2014.12.012>.
- (34) Dolman, B. M.; Wang, F.; Winterburn, J. B. Integrated Production and Separation of Biosurfactants. *Process Biochem.* **2019**, *83* (April), 1–8. <https://doi.org/10.1016/j.procbio.2019.05.002>.
- (35) Dolman, B. M.; Kaisermann, C.; Martin, P. J.; Winterburn, J. B. Integrated Sophorolipid Production and Gravity Separation. *Process Biochem.* **2017**, *54*, 162–171. <https://doi.org/10.1016/j.procbio.2016.12.021>.
- (36) Zhao, H.; Shao, D.; Jiang, C.; Shi, J.; Li, Q.; Huang, Q.; Rajoka, M. S. R.; Yang, H.; Jin, M. Biological Activity of Lipopeptides from *Bacillus*. *Appl. Microbiol. Biotechnol.* **2017**, *101* (15), 5951–5960. <https://doi.org/10.1007/s00253-017-8396-0>.
- (37) Gutiérrez-Chávez, C.; Benaud, N.; Ferrari, B. C. The Ecological Roles of Microbial Lipopeptides: Where Are We Going? *Comput. Struct. Biotechnol. J.* **2021**, *19*, 1400–1413.
-

- <https://doi.org/10.1016/j.csbj.2021.02.017>.
- (38) Rosenberg, E.; Rubinovitz, C.; Legmann, R.; Ron, E. Z. Purification and Chemical Properties of *Acinetobacter Calcoaceticus* A2 Biodispersan . *Appl. Environ. Microbiol.* **1988**, *54* (2), 323–326. <https://doi.org/10.1128/aem.54.2.323-326.1988>.
- (39) Gorin, P. A. J.; Spencer, J. F. T.; Tulloch, A. P. Hydroxy Fatty Acid Glycosides of Sophorose From *Torulopsis Magnoliae*. *Can. J. Chem.* **1961**, *39* (4), 846–855. <https://doi.org/10.1139/v61-104>.
- (40) Kurtzman, C. P.; Price, N. P. J.; Ray, K. J.; Kuo, T. M. Production of Sophorolipid Biosurfactants by Multiple Species of the *Starmerella* (*Candida*) *Bombicola* Yeast Clade. *FEMS Microbiol. Lett.* **2010**, *311* (2), 140–146. <https://doi.org/10.1111/j.1574-6968.2010.02082.x>.
- (41) Konishi, M.; Yoshida, Y.; Horiuchi, J. ichi. Efficient Production of Sophorolipids by *Starmerella Bombicola* Using a Corncob Hydrolysate Medium. *J. Biosci. Bioeng.* **2015**, *119* (3), 317–322. <https://doi.org/10.1016/j.jbiosc.2014.08.007>.
- (42) Chen, J.; Song, X.; Zhang, H.; Qu, Y. B.; Miao, J. Y. Sophorolipid Produced from the New Yeast Strain *Wickerhamiella Domercqiae* Induces Apoptosis in H7402 Human Liver Cancer Cells. *Appl. Microbiol. Biotechnol.* **2006**, *72* (1), 52–59. <https://doi.org/10.1007/s00253-005-0243-z>.
- (43) Thaniyavarn, J.; Chianguthai, T.; Sangvanich, P.; Roongsawang, N.; Washio, K.; Morikawa, M.; Thaniyavarn, S. Production of Sophorolipid Biosurfactant by *Pichia Anomala*. *Biosci. Biotechnol. Biochem.* **2008**, *72* (8), 2061–2068. <https://doi.org/10.1271/bbb.80166>.
- (44) Poomtien, J.; Thaniyavarn, J.; Pinphanichakarn, P.; Jindamorakot, S.; Morikawa, M. Production and Characterization of a Biosurfactant from *Cyberlindnera Samutprakarnensis* JP52T. *Biosci. Biotechnol. Biochem.* **2013**, *77* (12), 2362–2370. <https://doi.org/10.1271/bbb.130434>.
- (45) Vit, P.; Pedro, S. R. M.; Roubik, D. W. Pot-Pollen in Stingless Bee Melittology. *Pot-Pollen Stingless Bee Melittology* **2018**, 1–481. <https://doi.org/10.1007/978-3-319-61839-5>.
- (46) Dierickx, S.; Castelein, M.; Remmery, J.; De Clercq, V.; Lodens, S.; Baccile, N.; De Maeseneire, S. L.; Roelants, S. L. K. W.; Soetaert, W. K. From Bumblebee to

- Bioeconomy: Recent Developments and Perspectives for Sophorolipid Biosynthesis. *Biotechnol. Adv.* **2022**, *54* (March), 107788.  
<https://doi.org/10.1016/j.biotechadv.2021.107788>.
- (47) Zhang, L.; Somasundaran, P.; Singh, S. K.; Felse, A. P.; Gross, R. Synthesis and Interfacial Properties of Sophorolipid Derivatives. *Colloids Surfaces A Physicochem. Eng. Asp.* **2004**, *240* (1–3), 75–82. <https://doi.org/10.1016/j.colsurfa.2004.02.016>.
- (48) Abhyankar, I.; Sevi, G.; Prabhune, A. A.; Nisal, A.; Bayatigeri, S. Myristic Acid Derived Sophorolipid: Efficient Synthesis and Enhanced Antibacterial Activity. *ACS Omega* **2021**, *6* (2), 1273–1279. <https://doi.org/10.1021/acsomega.0c04683>.
- (49) Van Bogaert, I. N. A.; Saerens, K.; De Muynck, C.; Develter, D.; Soetaert, W.; Vandamme, E. J. Microbial Production and Application of Sophorolipids. *Appl. Microbiol. Biotechnol.* **2007**, *76* (1), 23–34. <https://doi.org/10.1007/s00253-007-0988-7>.
- (50) Li, Y.; Chen, Y.; Tian, X.; Chu, J. Advances in Sophorolipid-Producing Strain Performance Improvement and Fermentation Optimization Technology. *Appl. Microbiol. Biotechnol.* **2020**, *104* (24), 10325–10337. <https://doi.org/10.1007/s00253-020-10964-7>.
- (51) Develter, D. W. G.; Laurysen, L. M. L. Properties and Industrial Applications of Sophorolipids. *Eur. J. Lipid Sci. Technol.* **2010**, *112* (6), 628–638.  
<https://doi.org/10.1002/ejlt.200900153>.
- (52) Daverey, A.; Pakshirajan, K. Production, Characterization, and Properties of Sophorolipids from the Yeast *Candida Bombicola* Using a Low-Cost Fermentative Medium. *Appl. Biochem. Biotechnol.* **2009**, *158* (3), 663–674.  
<https://doi.org/10.1007/s12010-008-8449-z>.
- (53) Daverey, A.; Pakshirajan, K. Sophorolipids from *Candida Bombicola* Using Mixed Hydrophilic Substrates: Production, Purification and Characterization. *Colloids Surfaces B Biointerfaces* **2010**, *79* (1), 246–253. <https://doi.org/10.1016/j.colsurfb.2010.04.002>.
- (54) Luong, N.; Hoa, H.; Loan, L. Q.; Eun-ki, K.; Ha, T. T.; Duy, N. D.; Khanh, H. Q.; Dung, N. H.; Chi, H.; City, M.; Chi, H.; City, M. Asia-Pacific Journal of Science and Technology Sugarcane Molasses and Coconut Oil. 1–8.
- (55) Takahashi, M.; Morita, T.; Wada, K.; Hirose, N.; Fukuoka, T.; Imura, T.; Kitamoto, D. Production of Sophorolipid Glycolipid Biosurfactants from Sugarcane Molasses Using

- Stammerella Bombicola NBRC 10243. *J. Oleo Sci.* **2011**, *60* (5), 267–273.  
<https://doi.org/10.5650/jos.60.267>.
- (56) Solaiman, D. K. Y.; Ashby, R. D.; Zerkowski, J. A.; Foglia, T. A. Simplified Soy Molasses-Based Medium for Reduced-Cost Production of Sophorolipids by *Candida Bombicola*. *Biotechnol. Lett.* **2007**, *29* (9), 1341–1347. <https://doi.org/10.1007/s10529-007-9407-5>.
- (57) Ashby, R. D.; Solaiman, D. K. Y.; Foglia, T. A. Property Control of Sophorolipids: Influence of Fatty Acid Substrate and Blending. *Biotechnol. Lett.* **2008**, *30* (6), 1093–1100. <https://doi.org/10.1007/s10529-008-9653-1>.
- (58) Imura, T.; Kawamura, D.; Morita, T.; Sato, S.; Fukuoka, T.; Yamagata, Y.; Takahashi, M.; Wada, K.; Kitamoto, D. Production of Sophorolipids from Non-Edible *Jatropha* Oil by *Stammerella Bombicola* NBRC 10243 and Evaluation of Their Interfacial Properties. *J. Oleo Sci.* **2013**, *62* (10), 857–864. <https://doi.org/10.5650/jos.62.857>.
- (59) Ahuekwe, E.; Okoli, B.; Stanley, O.; Kinigoma, B. Experimental Investigation of Sophorolipid Biosurfactants Produced by *Candida* and *Pleurotus* Species Using Waste Oils and Rice Bran and Their Oilfield Benefits. *J. Adv. Biol. Biotechnol.* **2016**, *7* (4), 1–15. <https://doi.org/10.9734/jabb/2016/27467>.
- (60) Samad, A.; Zhang, J.; Chen, D.; Liang, Y. Sophorolipid Production from Biomass Hydrolysates. *Appl. Biochem. Biotechnol.* **2014**, *175* (4), 2246–2257. <https://doi.org/10.1007/s12010-014-1425-x>.
- (61) Samad, A.; Zhang, J.; Chen, D.; Chen, X.; Tucker, M.; Liang, Y. Sweet Sorghum Bagasse and Corn Stover Serving as Substrates for Producing Sophorolipids. *J. Ind. Microbiol. Biotechnol.* **2017**, *44* (3), 353–362. <https://doi.org/10.1007/s10295-016-1891-y>.
- (62) Becerra, M.; Rodrigues, L. R.; Gualtar, C. De. Biosurfactants Production from Cheese Whey. **2008**, *661* (2), 81–104.
- (63) Daniel, H. J.; Reuss, M.; Syltatk, C. Production of Sophorolipids in High Concentration from Deproteinized Whey and Rapeseed Oil in a Two Stage Fed Batch Process Using *Candida Bombicola* ATCC 22214 and *Cryptococcus Curvatus* ATCC 20509. *Biotechnol. Lett.* **1998**, *20* (12), 1153–1156. <https://doi.org/10.1023/A:1005332605003>.
- (64) Daniel, H.; Otto, R. T.; Binder, M.; Syltatk, C. Production of Sophorolipids from Whey-

- Development of a Two-Stage Process with *Cryptococcus Curvatus* ATCC 20509 and *Candida Bombicola* ATCC 22214.Pdf. **1999**, 40–45.
- (65) Otto, R. T.; Daniel, H. J.; Pekin, G.; Müller-Decker, K.; Fürstenberger, G.; Reuss, M.; Sylđatk, C. Production of Sophorolipids from Whey: II. Product Composition, Surface Active Properties, Cytotoxicity and Stability against Hydrolases by Enzymatic Treatment. *Appl. Microbiol. Biotechnol.* **1999**, *52* (4), 495–501.  
<https://doi.org/10.1007/s002530051551>.
- (66) Daverey, A.; Pakshirajan, K.; Sumalatha, S. Sophorolipids Production by *Candida Bombicola* Using Dairy Industry Wastewater. *Clean Technol. Environ. Policy* **2011**, *13* (3), 481–488. <https://doi.org/10.1007/s10098-010-0330-4>.
- (67) Wang, H.; Tsang, C. W.; To, M. H.; Kaur, G.; Roelants, S. L. K. W.; Stevens, C. V.; Soetaert, W.; Lin, C. S. K. Techno-Economic Evaluation of a Biorefinery Applying Food Waste for Sophorolipid Production – A Case Study for Hong Kong. *Bioresour. Technol.* **2020**, *303* (November 2019), 122852. <https://doi.org/10.1016/j.biortech.2020.122852>.
- (68) Kaur, G.; Wang, H.; To, M. H.; Roelants, S. L. K. W.; Soetaert, W.; Lin, C. S. K. Efficient Sophorolipids Production Using Food Waste. *J. Clean. Prod.* **2019**, *232*, 1–11.  
<https://doi.org/10.1016/j.jclepro.2019.05.326>.
- (69) Bajaj, V. K.; Annapure, U. S. Castor Oil as Secondary Carbon Source for Production of Sophorolipids Using *Starmerella Bombicola* NRRLY-17069. *J. Oleo Sci.* **2015**, *64* (3), 315–323. <https://doi.org/10.5650/jos.ess14214>.
- (70) Hieu Hoa, N. L.; Loan, L. Q.; Eun-Ki, K.; Ha, T. T.; Duy, N. D.; Khanh, H. Q.; Dung, N. H. Production and Characterization of Sophorolipids Produced by *Candida Bombicola* Using Sugarcane Molasses and Coconut Oil. *Asia-Pacific J. Sci. Technol.* **2017**, *22* (2).
- (71) van Bogaert, I. N. A.; Roelants, S.; Develter, D.; Soetaert, W. Sophorolipid Production by *Candida Bombicola* on Oils with a Special Fatty Acid Composition and Their Consequences on Cell Viability. *Biotechnol. Lett.* **2010**, *32* (10), 1509–1514.  
<https://doi.org/10.1007/s10529-010-0323-8>.
- (72) Elshafie, A. E.; Joshi, S. J.; Al-Wahaibi, Y. M.; Al-Bemani, A. S.; Al-Bahry, S. N.; Al-Maqbali, D.; Banat, I. M. Sophorolipids Production by *Candida Bombicola* ATCC 22214 and Its Potential Application in Microbial Enhanced Oil Recovery. *Front. Microbiol.*

- 2015**, 6 (NOV), 1–11. <https://doi.org/10.3389/fmicb.2015.01324>.
- (73) Klekner, V.; Kosaric, N.; Zhou, Q. H. Sophorose Lipids Produced from Sucrose. *Biotechnol. Lett.* **1991**, 13 (5), 345–348. <https://doi.org/10.1007/BF01027680>.
- (74) Rashad, M. M.; Nooman, M. U.; Ali, M. M.; Al-Kashef, A. S.; Mahmoud, A. E. Production, Characterization and Anticancer Activity of *Candida Bombicola* Sophorolipids by Means of Solid State Fermentation of Sunflower Oil Cake and Soybean Oil. *Grasas y Aceites* **2014**, 65 (2). <https://doi.org/10.3989/gya.098413>.
- (75) Nooman, M. U.; Maha, H. M.; Al-Kashef, A. S.; Rashad, M. M. Hypocholesterolemic Impact of Newly Isolated Sophorolipids Produced by Microbial Conversion of Safflower Oil Cake in Rats Fed High-Fat and Cholesterol Diet. *Grasas y Aceites* **2017**, 68 (3). <https://doi.org/10.3989/gya.0219171>.
- (76) Shah, M. U. H.; Sivapragasam, M.; Moniruzzaman, M.; Talukder, M. M. R.; Yusup, S. B.; Goto, M. Production of Sophorolipids by *Starmerella Bombicola* Yeast Using New Hydrophobic Substrates. *Biochem. Eng. J.* **2017**, 127 (September 2018), 60–67. <https://doi.org/10.1016/j.bej.2017.08.005>.
- (77) Daniel, H. J.; Otto, R. T.; Reuss, M.; Sylдатк, C. Sophorolipid Production with High Yields on Whey Concentrate and Rapeseed Oil without Consumption of Lactose. *Biotechnology Letters*. 1998, pp 805–807. <https://doi.org/10.1023/B:BILE.0000015927.29348.1a>.
- (78) Jiménez-Peñalver, P.; Castillejos, M.; Koh, A.; Gross, R.; Sánchez, A.; Font, X.; Gea, T. Production and Characterization of Sophorolipids from Stearic Acid by Solid-State Fermentation, a Cleaner Alternative to Chemical Surfactants. *J. Clean. Prod.* **2018**, 172, 2735–2747. <https://doi.org/10.1016/j.jclepro.2017.11.138>.
- (79) Daverey, A.; Pakshirajan, K.; Sumalatha, S. Sophorolipids Production by *Candida Bombicola* Using Dairy Industry Wastewater. *Clean Technol. Environ. Policy* **2011**, 13 (3), 481–488. <https://doi.org/10.1007/s10098-010-0330-4>.
- (80) Deshpande, M.; Daniels, L. Evaluation of Sophorolipid Biosurfactant Production by *Candida Bombicola* Using Animal Fat. *Bioresour. Technol.* **1995**, 54 (2), 143–150. [https://doi.org/10.1016/0960-8524\(95\)00116-6](https://doi.org/10.1016/0960-8524(95)00116-6).
- (81) John, U. S.; John, M. C. Production and Application of Microbial Surfactant from Cassava



- Wastewater. *Am. J. Eng. Technol. Soc.* **2015**, 2 (4), 85–89.
- (82) Shah, V.; Jurjevic, M.; Badia, D. Utilization of Restaurant Waste Oil as a Precursor for Sophorolipid Production. *Biotechnol. Prog.* **2007**, 23 (2), 512–515.  
<https://doi.org/10.1021/bp0602909>.
- (83) Maddikeri, G. L.; Gogate, P. R.; Pandit, A. B. Improved Synthesis of Sophorolipids from Waste Cooking Oil Using Fed Batch Approach in the Presence of Ultrasound. *Chem. Eng. J.* **2015**, 263, 479–487. <https://doi.org/10.1016/j.cej.2014.11.010>.
- (84) Fleurackers, S. J. J. On the Use of Waste Frying Oil in the Synthesis of Sophorolipids. *Eur. J. Lipid Sci. Technol.* **2006**, 108 (1), 5–12. <https://doi.org/10.1002/ejlt.200500237>.
- (85) Jadhav, J. V.; Pratap, A. P.; Kale, S. B. Evaluation of Sunflower Oil Refinery Waste as Feedstock for Production of Sophorolipid. *Process Biochem.* **2019**, 78 (January), 15–24. <https://doi.org/10.1016/j.procbio.2019.01.015>.
- (86) Kim, H. S.; Kim, Y. B.; Lee, B. S.; Kim, E. K. Sophorolipid Production by *Candida Bombicola* ATCC 22214 from a Corn-Oil Processing Byproduct. *J. Microbiol. Biotechnol.* **2005**, 15 (1), 55–58.
- (87) Wadekar, S. D.; Kale, S. B.; Lali, A. M.; Bhowmick, D. N.; Pratap, A. P. Utilization of Sweetwater as a Cost-Effective Carbon Source for Sophorolipids Production by *Starmerella Bombicola* (ATCC 22214). *Prep. Biochem. Biotechnol.* **2012**, 42 (2), 125–142. <https://doi.org/10.1080/10826068.2011.577883>.
- (88) Jiménez-Peñalver, P.; Gea, T.; Sánchez, A.; Font, X. Production of Sophorolipids from Winterization Oil Cake by Solid-State Fermentation: Optimization, Monitoring and Effect of Mixing. *Biochem. Eng. J.* **2016**, 115, 93–100. <https://doi.org/10.1016/j.bej.2016.08.006>.
- (89) Lombardo, D.; Kiselev, M. A.; Magazù, S.; Calandra, P. Amphiphiles Self-Assembly : Basic Concepts and Future Perspectives of Supramolecular Approaches. **2015**, 2015.
- (90) Shaw, D.; Corocoran, T. Surface Activity and Micelle Formation. *Green Chem.* **2002**, 4.
- (91) Zhou, S.; Xu, C.; Wang, J.; Gao, W.; Akhverdiyeva, R.; Shah, V.; Gross, R. Supramolecular Assemblies of a Naturally Derived Sophorolipid. *Langmuir* **2004**, 20 (19), 7926–7932. <https://doi.org/10.1021/la048590s>.
- (92) Dhasaiyan, P.; Banerjee, A.; Visaveliya, N.; Prasad, B. L. V. Influence of the Sophorolipid Molecular Geometry on Their Self-Assembled Structures. *Chem. - An Asian*
-

- J.* **2013**, 8 (2), 369–372. <https://doi.org/10.1002/asia.201200935>.
- (93) Dhasaiyan, P.; Prevost, S.; Baccile, N.; Prasad, B. L. V. PH- and Time-Resolved in Situ SAXS Study of Self-Assembled Twisted Ribbons Formed by Elaidic Acid Sophorolipids. *Langmuir* **2018**, 34 (5), 2121–2131. <https://doi.org/10.1021/acs.langmuir.7b03164>.
- (94) Kim, K.; Yoo, D.; Kim, Y.; Lee, B.; Shin, D.; Kim, E. K. Characteristics of Sophorolipid as an Antimicrobial Agent. *J. Microbiol. Biotechnol.* **2002**, 12 (2), 235–241.
- (95) Díaz De Rienzo, M. A.; Stevenson, P.; Marchant, R.; Banat, I. M. Antibacterial Properties of Biosurfactants against Selected Gram-Positive and -Negative Bacteria. *FEMS Microbiol. Lett.* **2016**, 363 (2), fnv224. <https://doi.org/10.1093/femsle/fnv224>.
- (96) Hirlekar, S.; Abhyankar, I.; Kane, K.; Trimukhe, K.; Prabhune, A.; Nisal, A. Green Antibacterial Molecules: Sophorolipids with Varying Fatty Acid Chain. *Trends Biomater. Artif. Organs* **2021**, 35 (5), 431–437.
- (97) Patil, A.; Joshi-Navre, K.; Mukherji, R.; Prabhune, A. Biosynthesis of Glycomonoterpenes to Attenuate Quorum Sensing Associated Virulence in Bacteria. *Appl. Biochem. Biotechnol.* **2017**, 181 (4), 1533–1548. <https://doi.org/10.1007/s12010-016-2300-8>.
- (98) Hipólito, A.; Alves da Silva, R. A.; Caretta, T. de O.; Silveira, V. A. I.; Amador, I. R.; Panagio, L. A.; Borsato, D.; Celligoi, M. A. P. C. Evaluation of the Antifungal Activity of Sophorolipids from *Starmerella Bombicola* against Food Spoilage Fungi. *Biocatal. Agric. Biotechnol.* **2020**, 29 (June), 101797. <https://doi.org/10.1016/j.bcab.2020.101797>.
- (99) Chen, J.; Liu, X.; Fu, S.; An, Z.; Feng, Y.; Wang, R.; Ji, P. Effects of Sophorolipids on Fungal and Oomycete Pathogens in Relation to PH Solubility. *J. Appl. Microbiol.* **2020**, 128 (6), 1754–1763. <https://doi.org/10.1111/jam.14594>.
- (100) Sun, X. X.; Choi, J. K.; Kim, E. K. A Preliminary Study on the Mechanism of Harmful Algal Bloom Mitigation by Use of Sophorolipid Treatment. *J. Exp. Mar. Bio. Ecol.* **2004**, 304 (1), 35–49. <https://doi.org/10.1016/j.jembe.2003.11.020>.
- (101) Shah, V.; Doncel, G. F.; Seyoum, T.; Eaton, K. M.; Zalenskaya, I.; Hagver, R.; Azim, A.; Gross, R. Sophorolipids, Microbial Glycolipids with Anti-Human Immunodeficiency Virus and Sperm-Immobilizing Activities. *Antimicrob. Agents Chemother.* **2005**, 49 (10), 4093–4100. <https://doi.org/10.1128/AAC.49.10.4093-4100.2005>.
- (102) Daverey, A.; Dutta, K.; Joshi, S.; Daverey, A. Sophorolipid: A Glycolipid Biosurfactant as

- a Potential Therapeutic Agent against COVID-19. *Bioengineered* **2021**, *12* (2), 9550–9560. <https://doi.org/10.1080/21655979.2021.1997261>.
- (103) Fu, S. L.; Wallner, S. R.; Bowne, W. B.; Hagler, M. D.; Zenilman, M. E.; Gross, R.; Bluth, M. H. Sophorolipids and Their Derivatives Are Lethal Against Human Pancreatic Cancer Cells. *J. Surg. Res.* **2008**, *148* (1), 77–82. <https://doi.org/10.1016/j.jss.2008.03.005>.
- (104) Shao, L.; Song, X.; Ma, X.; Li, H.; Qu, Y. Bioactivities of Sophorolipid with Different Structures against Human Esophageal Cancer Cells. *J. Surg. Res.* **2012**, *173* (2), 286–291. <https://doi.org/10.1016/j.jss.2010.09.013>.
- (105) Ribeiro, I. A. C.; Faustino, C. M. C.; Guerreiro, P. S.; Frade, R. F. M.; Bronze, M. R.; Castro, M. F.; Ribeiro, M. H. L. Development of Novel Sophorolipids with Improved Cytotoxic Activity toward MDA-MB-231 Breast Cancer Cells. *J. Mol. Recognit.* **2015**, *28* (3), 155–165. <https://doi.org/10.1002/jmr.2403>.
- (106) Dubey, P.; Raina, P.; Prabhune, A.; Kaul-Ghanekar, R. Cetyl Alcohol and Oleic Acid Sophorolipids Exhibit Anticancer Activity. *Int. J. Pharm. Pharm. Sci.* **2016**, *8* (3), 399–402.
- (107) Bluth, M. H.; Kandil, E.; Mueller, C. M.; Shah, V.; Lin, Y. Y.; Zhang, H.; Dresner, L.; Lempert, L.; Nowakowski, M.; Gross, R.; Schulze, R.; Zenilman, M. E. Sophorolipids Block Lethal Effects of Septic Shock in Rats in a Cecal Ligation and Puncture Model of Experimental Sepsis. *Crit. Care Med.* **2006**, *34* (1), E188. <https://doi.org/10.1097/01.CCM.0000196212.56885.50>.
- (108) Hardin, R.; Pierre, J.; Schulze, R.; Mueller, C. M.; Fu, S. L.; Wallner, S. R.; Stanek, A.; Shah, V.; Gross, R. A.; Weedon, J.; Nowakowski, M.; Zenilman, M. E.; Bluth, M. H. Sophorolipids Improve Sepsis Survival: Effects of Dosing and Derivatives. *J. Surg. Res.* **2007**, *142* (2), 314–319. <https://doi.org/10.1016/j.jss.2007.04.025>.
- (109) Subramaniam, M. D.; Venkatesan, D.; Iyer, M.; Subbarayan, S.; Govindasami, V.; Roy, A.; Narayanasamy, A.; Kamalakannan, S.; Gopalakrishnan, A. V.; Thangarasu, R.; Kumar, N. S.; Vellingiri, B. Biosurfactants and Anti-Inflammatory Activity: A Potential New Approach towards COVID-19. *Curr. Opin. Environ. Sci. Heal.* **2020**, *17*, 72–81. <https://doi.org/10.1016/j.coesh.2020.09.002>.

- (110) Diaz-Rodriguez, P.; Chen, H.; Erndt-Marino, J. D.; Liu, F.; Totsingan, F.; Gross, R. A.; Hahn, M. S. Impact of Select Sophorolipid Derivatives on Macrophage Polarization and Viability. *ACS Appl. Bio Mater.* **2019**, *2* (1), 601–612.  
<https://doi.org/10.1021/acsabm.8b00799>.
- (111) Kasture, M.; Singh, S.; Patel, P.; Joy, P. A.; Prabhune, A. A.; Ramana, C. V.; Prasad, B. L. V. Multiutility Sophorolipids as Nanoparticle Capping Agents: Synthesis of Stable and Water Dispersible Co Nanoparticles. *Langmuir* **2007**, *23* (23), 11409–11412.  
<https://doi.org/10.1021/la702931j>.
- (112) Kasture, M. B.; Patel, P.; Prabhune, A. A.; Ramana, C. V.; Kulkarni, A. A.; Prasad, B. L. V. Synthesis of Silver Nanoparticles by Sophorolipids: Effect of Temperature and Sophorolipid Structure on the Size of Particles. *J. Chem. Sci.* **2008**, *120* (6), 515–520.  
<https://doi.org/10.1007/s12039-008-0080-6>.
- (113) Baccile, N.; Noiville, R.; Stievano, L.; Bogaert, I. Van. Sophorolipids-Functionalized Iron Oxide Nanoparticles. *Phys. Chem. Chem. Phys.* **2013**, *15* (5), 1606–1620.  
<https://doi.org/10.1039/c2cp41977g>.
- (114) Basak, G.; Das, D.; Das, N. Dual Role of Acidic Diacetate Sophorolipid as Biostabilizer for ZnO Nanoparticle Synthesis and Biofunctionalizing Agent against Salmonella Enterica and Candida Albicans. *J. Microbiol. Biotechnol.* **2014**, *24* (1), 87–96.  
<https://doi.org/10.4014/jmb.1307.07081>.
- (115) Kanwar, R.; Gradzielski, M.; Mehta, S. K. Biomimetic Solid Lipid Nanoparticles of Sophorolipids Designed for Antileprosy Drugs. *J. Phys. Chem. B* **2018**, *122* (26), 6837–6845. <https://doi.org/10.1021/acs.jpcc.8b03081>.
- (116) Hall, P. J.; Haverkamp, J.; Kralingen, C. G. Van; Schmidt, M. United States Patent ( 19 ). **1996**, No. 19.
- (117) Furuta, T.; Igarashi, K.; Hirata, Y. Low-Foaming Detergent Compositions. **2002**, *1* (19).
- (118) Joshi-Navare, K.; Khanvilkar, P.; Prabhune, A. Jatropha Oil Derived Sophorolipids: Production and Characterization as Laundry Detergent Additive. *Biochem. Res. Int.* **2013**, *2013*. <https://doi.org/10.1155/2013/169797>.
- (119) Chandran, P.; Das, N. Role of Sophorolipid Biosurfactant in Degradation of Diesel Oil by Candida Tropicalis. *Bioremediat. J.* **2012**, *16* (1), 19–30.

- <https://doi.org/10.1080/10889868.2011.628351>.
- (120) Feng, L.; Jiang, X.; Huang, Y.; Wen, D.; Fu, T.; Fu, R. Petroleum Hydrocarbon-Contaminated Soil Bioremediation Assisted by Isolated Bacterial Consortium and Sophorolipid. *Environ. Pollut.* **2021**, *273*, 116476. <https://doi.org/10.1016/j.envpol.2021.116476>.
- (121) Minucelli, T.; Ribeiro-Viana, R. M.; Borsato, D.; Andrade, G.; Cely, M. V. T.; de Oliveira, M. R.; Baldo, C.; Celligoi, M. A. P. C. Sophorolipids Production by *Candida Bombicola* ATCC 22214 and Its Potential Application in Soil Bioremediation. *Waste and Biomass Valorization* **2017**, *8* (3), 743–753. <https://doi.org/10.1007/s12649-016-9592-3>.
- (122) Qi, X.; Xu, X.; Zhong, C.; Jiang, T.; Wei, W.; Song, X. Removal of Cadmium and Lead from Contaminated Soils Using Sophorolipids from Fermentation Culture of *Starmerella Bombicola* CGMCC 1576 Fermentation. *Int. J. Environ. Res. Public Health* **2018**, *15* (11), 2334. <https://doi.org/10.3390/ijerph15112334>.
- (123) Cho, W. G.; Park, H. S.; Ahn, B. J. Sophorolipid의 항균효과와 화장품에의 응용 Antimicrobial Activities of Sophorolipids and Its Application for Cosmetics. **2008**, *34* (4), 317–323.
- (124) Lourith, N.; Kanlayavattanakul, M. Natural Surfactants Used in Cosmetics: Glycolipids. *Int. J. Cosmet. Sci.* **2009**, *31* (4), 255–261. <https://doi.org/10.1111/j.1468-2494.2009.00493.x>.
- (125) BROWN, M. J. Biosurfactants for Cosmetic Applications. *Int. J. Cosmet. Sci.* **1991**, *13* (2), 61–64. <https://doi.org/10.1111/j.1467-2494.1991.tb00549.x>.
- (126) Maeng, Y.; Kim, K. T.; Zhou, X.; Jin, L.; Kim, K. S.; Kim, Y. H.; Lee, S.; Park, J. H.; Chen, X.; Kong, M.; Cai, L.; Li, X. A Novel Microbial Technique for Producing High-Quality Sophorolipids from Horse Oil Suitable for Cosmetic Applications. *Microb. Biotechnol.* **2018**, *11* (5), 917–929. <https://doi.org/10.1111/1751-7915.13297>.
- (127) Gaur, V. K.; Regar, R. K.; Dhiman, N.; Gautam, K.; Srivastava, J. K.; Patnaik, S.; Kamthan, M.; Manickam, N. Biosynthesis and Characterization of Sophorolipid Biosurfactant by *Candida* Spp.: Application as Food Emulsifier and Antibacterial Agent. *Bioresour. Technol.* **2019**, *285* (March), 121314.

- <https://doi.org/10.1016/j.biortech.2019.121314>.
- (128) Hipólito, A.; Caretta, T. de O.; Silveira, V. A. I.; Bersaneti, G. T.; Mali, S.; Celligoi, M. A. P. C. Active Biodegradable Cassava Starch Films Containing Sophorolipids Produced by *Starmerella Bombicola* ATCC® 22214<sup>TM</sup>. *J. Polym. Environ.* **2021**, *29* (10), 3199–3209. <https://doi.org/10.1007/s10924-021-02103-8>.
- (129) Silveira, V. A. I.; Marim, B. M.; Hipólito, A.; Gonçalves, M. C.; Mali, S.; Kobayashi, R. K. T.; Celligoi, M. A. P. C. Characterization and Antimicrobial Properties of Bioactive Packaging Films Based on Polylactic Acid-Sophorolipid for the Control of Foodborne Pathogens. *Food Packag. Shelf Life* **2020**, *26* (May), 1–7. <https://doi.org/10.1016/j.fpsl.2020.100591>.
- (130) Ma, X.; Meng, L.; Zhang, H.; Zhou, L.; Yue, J.; Zhu, H.; Yao, R. Sophorolipid Biosynthesis and Production from Diverse Hydrophilic and Hydrophobic Carbon Substrates. *Appl. Microbiol. Biotechnol.* **2020**, *104* (1), 77–100. <https://doi.org/10.1007/s00253-019-10247-w>.
- (131) Denge-Pulate, V.; Dubey, P.; Bhagwat, S.; Prabhune, A. Hplc-Ms, Hrms Analysis of Microbial Acid Free, Short Chain Alkyl Sophorosides. *World J. Pharm. Pharm. Sci.* **2014**, *3* (10), 264–270.
- (132) Kumar, M.; Sarma, D. K.; Shubham, S.; Kumawat, M.; Verma, V.; Nina, P. B.; JP, D.; Kumar, S.; Singh, B.; Tiwari, R. R. Futuristic Non-Antibiotic Therapies to Combat Antibiotic Resistance: A Review. *Front. Microbiol.* **2021**, *12* (January), 1–15. <https://doi.org/10.3389/fmicb.2021.609459>.
- (133) Tong, S. Y. C.; Davis, J. S.; Eichenberger, E.; Holland, T. L.; Fowler, V. G. Staphylococcus Aureus Infections: Epidemiology, Pathophysiology, Clinical Manifestations, and Management. *Clin. Microbiol. Rev.* **2015**, *28* (3), 603–661. <https://doi.org/10.1128/CMR.00134-14>.
- (134) Sousa, A. M.; Pereira, M. O. Pseudomonas Aeruginosa Diversification during Infection Development in Cystic Fibrosis Lungs-A Review. *Pathogens* **2014**, *3* (3), 680–703. <https://doi.org/10.3390/pathogens3030680>.
- (135) Ge, X. Antimicrobial Biomaterials with Non-Antibiotic Strategy. *Biosurface and Biotribology* **2019**, *5* (3), 71–82. <https://doi.org/10.1049/bsbt.2019.0010>.

- (136) Jiao, Y.; Tay, F. R.; Niu, L. na; Chen, J. hua. Advancing Antimicrobial Strategies for Managing Oral Biofilm Infections. *Int. J. Oral Sci.* **2019**, *11* (3), 1–11. <https://doi.org/10.1038/s41368-019-0062-1>.
- (137) Li, D.; Zhou, B.; Lv, B. Antibacterial Therapeutic Agents Composed of Functional Biological Molecules. *J. Chem.* **2020**, *2020*. <https://doi.org/10.1155/2020/6578579>.
- (138) Khameneh, B.; Iranshahy, M.; Soheili, V.; Sedigheh, B.; Bazzaz, F. Khameneh2019.Pdf. *Antimicrob. Resist. Infect. Control* **2019**, *8*, 1–28.
- (139) Wang, H.; Roelants, S. L. K. W.; To, M. H.; Patria, R. D.; Kaur, G.; Lau, N. S.; Lau, C. Y.; Van Bogaert, I. N. A.; Soetaert, W.; Lin, C. S. K. Starmerella Bombicola: Recent Advances on Sophorolipid Production and Prospects of Waste Stream Utilization. *J. Chem. Technol. Biotechnol.* **2019**, *94* (4), 999–1007. <https://doi.org/10.1002/jctb.5847>.
- (140) Murfin, J.; Irvine, F.; Meechan-Rogers, R.; Swift, A. Education, Income and Occupation and Their Influence on the Uptake of Cervical Cancer Prevention Strategies: A Systematic Review. *J. Clin. Nurs.* **2020**, *29* (3–4), 393–415. <https://doi.org/10.1111/jocn.15094>.
- (141) Joseph, E.; Patil, A.; Hirlekar, S.; Shete, A.; Parekh, N.; Prabhune, A.; Nisal, A. Glycomonoterpene-Functionalized Crack-Resistant Biocompatible Silk Fibroin Coatings for Biomedical Implants. *ACS Appl. Bio Mater.* **2019**, *2* (2), 675–684. <https://doi.org/10.1021/acsabm.8b00515>.
- (142) Parekh, N.; Hushye, C.; Warunkar, S.; Sen Gupta, S.; Nisal, A. In Vitro Study of Novel Microparticle Based Silk Fibroin Scaffold with Osteoblast-like Cells for Load-Bearing Osteo-Regenerative Applications. *RSC Adv.* **2017**, *7* (43), 26551–26558. <https://doi.org/10.1039/c7ra03288a>.
- (143) Zhang, X.; Ashby, R. D.; Solaiman, D. K. Y.; Liu, Y.; Fan, X. Antimicrobial Activity and Inactivation Mechanism of Lactonic and Free Acid Sophorolipids against Escherichia Coli O157:H7. *Biocatal. Agric. Biotechnol.* **2017**, *11*, 176–182. <https://doi.org/10.1016/j.bcab.2017.07.002>.
- (144) Amerikova, M.; Pencheva El-Tibi, I.; Maslarska, V.; Bozhanov, S.; Tachkov, K. Antimicrobial Activity, Mechanism of Action, and Methods for Stabilisation of Defensins as New Therapeutic Agents. *Biotechnol. Biotechnol. Equip.* **2019**, *33* (1), 671–682. <https://doi.org/10.1080/13102818.2019.1611385>.

- (145) Tsuchido, T.; Hiraoka, T.; Takano, M.; Shibasaki, I. Involvement of Autolysin in Cellular Lysis of *Bacillus Subtilis* Induced by Short- and Medium-Chain Fatty Acids. *J. Bacteriol.* **1985**, *162* (1), 42–46. <https://doi.org/10.1128/jb.162.1.42-46.1985>.
- (146) Rossi F, Noren H, Jove R, Beljanski V, G. K. Differences and Similarities between Post-Keynesian,. **2020**, 1–16.
- (147) Cordoní, A.; Prades, J.; Frau, J.; Vögler, O.; Funari, S. S.; Perez, J. J.; Escribá, P. V.; Barceló, F. Interactions of Fatty Acids with Phosphatidylethanolamine Membranes: X-Ray Diffraction and Molecular Dynamics Studies. *J. Lipid Res.* **2010**, *51* (5), 1113–1124. <https://doi.org/10.1194/jlr.M003012>.
- (148) Erin Currie<sup>1</sup>, Almut Schulze<sup>2</sup>, Rudolf Zechner<sup>3</sup>, Tobias C. Walther<sup>4</sup>, and R. V. F.; Jr.<sup>1</sup>, 5, 6. Fatty Acid Metabolism and Cancer. *Adv. Exp. Med. Biol.* **2021**, *1280* (2), 231–241. [https://doi.org/10.1007/978-3-030-51652-9\\_16](https://doi.org/10.1007/978-3-030-51652-9_16).
- (149) Brinkmann, C. R.; Thiel, S.; Otzen, D. E. Protein-Fatty Acid Complexes: Biochemistry, Biophysics and Function. *FEBS J.* **2013**, *280* (8), 1733–1749. <https://doi.org/10.1111/febs.12204>.
- (150) Oliveira, M. R. De; Camilios-neto, D.; Baldo, C.; Magri, A.; Antonia, M.; Colabone, P. Biosynthesis And Production Of Sophorolipids. *Int. J. Sci. Technol. Res.* **2014**, *3* (11), 133–146.
- (151) Claus, S.; Van Bogaert, I. N. A. Sophorolipid Production by Yeasts: A Critical Review of the Literature and Suggestions for Future Research. *Appl. Microbiol. Biotechnol.* **2017**, *101* (21), 7811–7821. <https://doi.org/10.1007/s00253-017-8519-7>.
- (152) Van Bogaert, I.; Fleurackers, S.; Van Kerrebroeck, S.; Develter, D.; Soetaert, W. Production of New-to-Nature Sophorolipids by Cultivating the Yeast *Candida Bombicola* on Unconventional Hydrophobic Substrates. *Biotechnol. Bioeng.* **2011**, *108* (4), 734–741. <https://doi.org/10.1002/bit.23004>.
- (153) Shah, S.; Prabhune, A. Purification by Silica Gel Chromatography Using Dialysis Tubing and Characterization of Sophorolipids Produced from *Candida Bombicola* Grown on Glucose and Arachidonic Acid. *Biotechnol. Lett.* **2007**, *29* (2), 267–272. <https://doi.org/10.1007/s10529-006-9221-5>.
- (154) Adan, A.; Alizada, G.; Kiraz, Y.; Baran, Y.; Nalbant, A. Flow Cytometry: Basic



- Principles and Applications. *Crit. Rev. Biotechnol.* **2017**, *37* (2), 163–176.  
<https://doi.org/10.3109/07388551.2015.1128876>.
- (155) Li, H.; Guo, W.; Ma, X. jing; Li, J. shan; Song, X. In Vitro and in Vivo Anticancer Activity of Sophorolipids to Human Cervical Cancer. *Appl. Biochem. Biotechnol.* **2017**, *181* (4), 1372–1387. <https://doi.org/10.1007/s12010-016-2290-6>.
- (156) Duronio, R. J.; Rudnick, D. A.; Johnson, R. L.; Johnson, D. R.; Gordon, J. I. Myristic Acid Auxotrophy Caused by Mutation of *S. Cerevisiae* Myristoyl-CoA:Protein N-Myristoyltransferase. *J. Cell Biol.* **1991**, *113* (6), 1313–1330.  
<https://doi.org/10.1083/jcb.113.6.1313>.
- (157) Schimke, R. T.; Dahms, N. M.; Breitmeyer, J.; Kornfeld, S. Figs. 3. **1987**, No. 14.
- (158) Van Bogaert, I. N. A.; Develter, D.; Soetaert, W.; Vandamme, E. J. Cerulenin Inhibits de Novo Sophorolipid Synthesis of *Candida Bombicola*. *Biotechnol. Lett.* **2008**, *30* (10), 1829–1832. <https://doi.org/10.1007/s10529-008-9764-8>.
- (159) Nguyen, L. N.; Trofa, D.; Nosanchuk, J. D. Fatty Acid Synthase Impacts the Pathobiology of *Candida Parapsilosis* in Vitro and during Mammalian Infection. *PLoS One* **2009**, *4* (12).  
<https://doi.org/10.1371/journal.pone.0008421>.
- (160) Wang, X.; Xu, N.; Li, Q.; Chen, S.; Cheng, H.; Yang, M.; Jiang, T.; Chu, J.; Ma, X.; Yin, D. Lactonic Sophorolipid–Induced Apoptosis in Human HepG2 Cells through the Caspase-3 Pathway. *Appl. Microbiol. Biotechnol.* **2021**, *105* (5), 2033–2042.  
<https://doi.org/10.1007/s00253-020-11045-5>.
- (161) Banfalvi, G. Methods to Detect Apoptotic Cell Death. *Apoptosis* **2017**, *22* (2), 306–323.  
<https://doi.org/10.1007/s10495-016-1333-3>.
- (162) Murad, H.; Hawat, M.; Ekhtiar, A.; AlJapawe, A.; Abbas, A.; Darwish, H.; Sbenati, O.; Ghannam, A. Induction of G1-Phase Cell Cycle Arrest and Apoptosis Pathway in MDA-MB-231 Human Breast Cancer Cells by Sulfated Polysaccharide Extracted from *Laurencia Papillosa*. *Cancer Cell Int.* **2016**, *16* (1), 1–11. <https://doi.org/10.1186/s12935-016-0315-4>.
- (163) Kumar, N.; Afjei, R.; Massoud, T. F.; Paulmurugan, R. Comparison of Cell-Based Assays to Quantify Treatment Effects of Anticancer Drugs Identifies a New Application for Bodipy-L-Cystine to Measure Apoptosis. *Sci. Rep.* **2018**, *8* (1), 1–11.
-

- <https://doi.org/10.1038/s41598-018-34696-x>.
- (164) Cai, Y.; Tang, R. Calcium Phosphate Nanoparticles in Biomineralization and Biomaterials †. **2008**, 3775–3787. <https://doi.org/10.1039/b805407j>.
- (165) Płaza, G. A.; Chojniak, J.; Banat, I. M. Biosurfactant Mediated Biosynthesis of Selected Metallic Nanoparticles. *Int. J. Mol. Sci.* **2014**, 15 (8), 13720–13737. <https://doi.org/10.3390/ijms150813720>.
- (166) Singh, S.; Bhardwaj, P.; Singh, V.; Aggarwal, S.; Mandal, U. K. Synthesis of Nanocrystalline Calcium Phosphate in Microemulsion — Effect of Nature of Surfactants. **2008**, 319, 322–329. <https://doi.org/10.1016/j.jcis.2007.09.059>.
- (167) Ijaz, I.; Gilani, E.; Nazir, A.; Bukhari, A. Green Chemistry Letters and Reviews Detail Review on Chemical , Physical and Green Synthesis , Classification , Characterizations and Applications of Nanoparticles. **2020**. <https://doi.org/10.1080/17518253.2020.1802517>.
- (168) Chandran, S. P.; Chaudhary, M.; Pasricha, R.; Ahmad, A.; Sastry, M. Synthesis of Gold Nanotriangles and Silver Nanoparticles Using Aloe Vera Plant Extract. **2006**, 577–583.
- (169) Elumalai, K.; Velmurugan, S. Ac Ce p Te d Cr T. *Appl. Surf. Sci.* **2015**. <https://doi.org/10.1016/j.apsusc.2015.03.176>.
- (170) Optimization of Biological Synthesis of Silver Nanoparticles Using Lactobacillus Casei Subsp . Casei Hassan Korbekandi , a \* Siavash Iravani b and Sajjad Abbasi C. **2012**, No. September 2011. <https://doi.org/10.1002/jctb.3702>.
- (171) Du, L.; Wang, E. Biosynthesis of Gold Nanoparticles Assisted by Escherichia Coli DH5 a and Its Application on Direct Electrochemistry of Hemoglobin. **2007**, 9, 1165–1170. <https://doi.org/10.1016/j.elecom.2007.01.007>.
- (172) ' G. S. . and T. J. B. The in Vitro Formation of Placer Gold by Bacteria. **1994**, 58 (20), 4527–4530.
- (173) Pavani, K. V; Kumar, N. S.; Sangameswaran, B. B. Synthesis of Lead Nanoparticles by Aspergillus Species. **2012**, 61 (1), 61–63.
- (174) Yageshni Govender Æ Tamsyn RiddinGericke, M.; Whiteley, Æ. C. G. Bioreduction of Platinum Salts into Nanoparticles : A Mechanistic Perspective. **2009**, 95–100. <https://doi.org/10.1007/s10529-008-9825-z>.

- (175) Fayaz, A. M.; Balaji, K.; Kalaichelvan, P. T.; Venkatesan, R. Colloids and Surfaces B : Biointerfaces Fungal Based Synthesis of Silver Nanoparticles — An Effect of Temperature on the Size of Particles. **2009**, *74*, 123–126. <https://doi.org/10.1016/j.colsurfb.2009.07.002>.
- (176) Annamalai, J.; Nallamuthu, T. Characterization of Biosynthesized Gold Nanoparticles from Aqueous Extract of *Chlorella Vulgaris* and Their Anti-Pathogenic Properties. **2015**, 603–607. <https://doi.org/10.1007/s13204-014-0353-y>.
- (177) Caliskan, G.; Mutaf, T.; Agba, H. C.; Elibol, M. Green Synthesis and Characterization of Titanium Nanoparticles Using Microalga , *Phaeodactylum Tricornutum* Green Synthesis and Characterization of Titanium Nanoparticles Using. *Geomicrobiol. J.* **2022**, *39* (1), 83–96. <https://doi.org/10.1080/01490451.2021.2008549>.
- (178) Singh, S.; Patel, P.; Jaiswal, S.; Prabhune, A. A. A Direct Method for the Preparation of Glycolipid – Metal Nanoparticle Conjugates : Sophorolipids as Reducing and Capping Agents for the Synthesis of Water Re-Dispersible Silver Nanoparticles and Their Antibacterial Activity W. **2009**, 646–652. <https://doi.org/10.1039/b811829a>.
- (179) Kasture, M.; Singh, S.; Patel, P.; Joy, P. A.; Prabhune, A. A.; Ramana, C. V; Prasad, B. L. V; Chemistry, M.; Di, V.; Chemistry, O.; Di, V.; V, B. Di; Chemical, N.; June, R. V. Multiutility Sophorolipids as Nanoparticle Capping Agents : Synthesis of Stable and Water Dispersible Co Nanoparticles. **2007**, No. 9, 11409–11412.
- (180) Shikha, S.; Chaudhuri, S. R.; Bhattacharyya, M. S. Facile One Pot Greener Synthesis of Sophorolipid Capped Gold Nanoparticles and Its Antimicrobial Activity Having Special Efficacy Against Gram Negative *Vibrio Cholerae*. **2020**, 1–13. <https://doi.org/10.1038/s41598-019-57399-3>.
- (181) Abd-elwahab, S. F. M. S. I. E. M. A. A. S. M. Effect of Preparation Conditions on the Nanostructure of Hydroxyapatite and Brushite Phases. *Appl. Nanosci.* **2016**, *6* (7), 991–1000. <https://doi.org/10.1007/s13204-015-0509-4>.
- (182) Bunaciu, A. A.; Aboul-enein, H. Y. X-Ray Diffraction : Instrumentation and Applications Critical Reviews in Analytical Chemistry X-Ray Diffraction : Instrumentation and Applications. **2015**, No. April. <https://doi.org/10.1080/10408347.2014.949616>.
- (183) Dey, K.; Pal, M.; Rout, K. C.; Das, A.; Mukherjee, R.; Kharul, U. K.; Banerjee, R.

- Selective Molecular Separation by Interfacially Crystallized Covalent Organic Framework Thin Films. **2017**. <https://doi.org/10.1021/jacs.7b06640>.
- (184) Dubey, P.; Kumar, S.; Ravindranathan, S.; Vasudevan, S.; Aswal, V. K.; Rajamohan, P. R.; Nisal, A.; Prabhune, A. PH Dependent Sophorolipid Assemblies and Their Influence on Gelation of Silk Fibroin Protein. *Mater. Chem. Phys.* **2018**, *203*, 9–16. <https://doi.org/10.1016/j.matchemphys.2017.09.045>.
- (185) Dhaware, V.; Shaikh, A. Y.; Kar, M.; Hotha, S.; Sen Gupta, S. Synthesis and Self-Assembly of Amphiphilic Homoglycopolyptide. *Langmuir* **2013**, *29* (19), 5659–5667. <https://doi.org/10.1021/la400144t>.
- (186) Dubey, P.; Kumar, S.; Aswal, V. K.; Ravindranathan, S.; Rajamohan, P. R.; Prabhune, A.; Nisal, A. Silk Fibroin-Sophorolipid Gelation: Deciphering the Underlying Mechanism. *Biomacromolecules* **2016**, *17* (10), 3318–3327. <https://doi.org/10.1021/acs.biomac.6b01069>.
- (187) Peppas, B. N. A.; Hilt, J. Z.; Khademhosseini, A.; Langer, R. Hydrogels in Biology and Medicine : From Molecular Principles to Bionanotechnology \*\*. **2006**, 1345–1360. <https://doi.org/10.1002/adma.200501612>.
- (188) Hirlekar, S.; Ray, D.; Aswal, V. K.; Prabhune, A. A.; Nisal, A. Lauric Acid Sophorolipid: Accelerating the Gelation of Silk Fibroin. *ACS Omega* **2020**, *5* (44), 28571–28578. <https://doi.org/10.1021/acsomega.0c03411>.
- (189) Parekh, N. A.; Deshpande, R. V.; Shukla, S. G.; Nisal, A. A. Silk Fibroin 3D Microparticle Scaffolds with Bioactive Ceramics : Chemical , Mechanical , and Osteoregenerative Characteristics. **2020**, *2000458*, 1–11. <https://doi.org/10.1002/adem.202000458>.
- (190) Cama, G.; Barberis, F.; Capurro, M.; Di Silvio, L.; Deb, S. Tailoring Brushite for in Situ Setting Bone Cements. *Mater. Chem. Phys.* **2011**, *130* (3), 1139–1145. <https://doi.org/10.1016/j.matchemphys.2011.08.047>.
- (191) PD1, B. L.; Deng-xing Lun MSC. Composites in Orthopaedics. **2012**, No. February, 139–144. <https://doi.org/10.1111/j.1757-7861.2012.00189.x>.
- (192) Cama, G.; Barberis, F.; Botter, R.; Cirillo, P.; Capurro, M.; Quarto, R.; Scaglione, S. Preparation and Properties of Macroporous Brushite Bone Cements. *Acta Biomater.* **2009**, *5* (6), 2161–2168. <https://doi.org/10.1016/j.actbio.2009.02.012>.

- (193) Liu, L.; Wu, Y.; Xu, C.; Yu, S.; Wu, X.; Dai, H. Synthesis , Characterization of Nano-  $\beta$  - Tricalcium Phosphate and the Inhibition on Hepatocellular Carcinoma Cells. **2018**, *2018*.
- (194) Theiss, F.; Apelt, D.; Brand, B.; Kutter, A.; Zlinszky, K.; Bohner, M.; Matter, S.; Frei, C.; Auer, J. A.; Rechenberg, B. Von. Biocompatibility and Resorption of a Brushite Calcium Phosphate Cement. **2005**, *26*, 4383–4394.  
<https://doi.org/10.1016/j.biomaterials.2004.11.056>.
- (195) Gilardi, M. A 3D Vascularized Bone Remodeling Model Combining Osteoblasts and Osteoclasts in a CaP Nanoparticle-Enriched Matrix. **2016**.
- (196) Heinz, H.; Pramanik, C.; Heinz, O.; Ding, Y.; Mishra, R. K.; Marchon, D.; Flatt, R. J.; Estrela-lopis, I.; Llop, J.; Moya, S.; Ziolo, R. F. Surface Science Reports Nanoparticle Decoration with Surfactants : Molecular Interactions , Assembly , and Applications. *Surf. Sci. Rep.* **2017**, *72* (1), 1–58. <https://doi.org/10.1016/j.surfrep.2017.02.001>.
- (197) Thanh, N. T. K.; Maclean, N.; Mahiddine, S. Mechanisms of Nucleation and Growth of Nanoparticles in Solution. **2014**, *3* (1).
- (198) Tojo, C.; Dios, M. De; Barroso, F. Surfactant Effects on Microemulsion-Based Nanoparticle Synthesis. **2011**, 55–72. <https://doi.org/10.3390/ma4010055>.
- (199) Nosrati, H.; Quang, D.; Le, S.; Zolfaghari, R.; Canillas, M.; Eric, C. Nucleation and Growth of Brushite Crystals on the Graphene Sheets Applicable in Bone Cement. *Boletín la Soc. Española Cerámica y Vidr.* **2020**, 1–8.  
<https://doi.org/10.1016/j.bsecv.2020.05.001>.
- (200) Karageorgiou, V.; Tomkins, M.; Fajardo, R.; Meinel, L.; Snyder, B.; Wade, K.; Chen, J.; Vunjak-novakovic, G.; Kaplan, D. L. Porous Silk Fibroin 3-D Scaffolds for Delivery of Bone Morphogenetic Protein-2 in Vitro and in Vivo. <https://doi.org/10.1002/jbm.a>.
- (201) Matsumoto, A.; Chen, J.; Collette, A. L.; Kim, U. J.; Altman, G. H.; Cebe, P.; Kaplan, D. L. Mechanisms of Silk Fibroin Sol-Gel Transitions. *J. Phys. Chem. B* **2006**, *110* (43), 21630–21638. <https://doi.org/10.1021/jp056350v>.
- (202) Deshpande, R.; Shukla, S. Silk Fibroin and Ceramic Scaffolds : Comparative in Vitro Studies for Bone Regeneration. **2021**, No. February, 1–12.  
<https://doi.org/10.1002/btm2.10221>.

## ABSTRACT

---

**Name of the Student: Isha Abhyankar**  
**Faculty of Study: Biological Sciences**  
**AcSIR academic centre/CSIR Lab: CSIR-NCL**

**Registration No. :10BB19J26011**  
**Year of Submission: 2022**  
**Name of the Supervisor (s): Dr. Anuya Nisal**

**Title of the thesis: Biotransformation of short chain fatty acids into sophorolipids for biomedical applications**

---

Sophorolipids (SL) are extracellularly synthesized biosurfactants obtained from yeast *S. bombicola*. The fermentation process requires supplementation of hydrophilic and lipophilic substrates. The viscous product obtained at the end of fermentation cycle is a mixture of molecules. The structural variations are dependent on the nature of substrates and fermentation conditions.

SLs are important biosurfactants exhibiting varied biological properties. These properties along with their amphiphilic nature renders these biomolecules worthy for commercial market. Despite their discovery decades ago, the commercial applicability is still restrictive. The main reason for this is the chain length of lipophilic substrate and production cost. The biotransformation process is catalyzed via enzymatic machinery of the yeast. Traditionally, SL are synthesized using oleic acid (unsaturated fatty acid- C18:1) as primary lipophilic source owing to its involvement in the fatty acid synthetase system of the yeast. However, this chain length specificity restricts the usage. Lowering the chain length of substrate might enhance the physical and biological properties of the biosurfactants.

With this view, the thesis focuses on synthesizing SL using unconventional substrates and thereby understanding the effect of short chain fatty acids on physical and biological attributes. This understanding will assist in exploring the substrate range for synthesis of SL along with their plausible use for commercial application.

The following objectives are covered in the thesis:

1. Deciphering the effect of chain length of substrate on chemical, physical and biological properties of sophorolipid
2. Deducing the underlying mechanism of short chain substrates in sophorolipid; production and application
3. Synthesizing calcium phosphate nanoparticle using short chain derived sophorolipid

## List of publications:

1. **Isha Abhyankar**, Asmita Prabhune, Anuya Nisal,' Myristic acid derived sophorolipid: efficient synthesis and enhanced anti-bacterial activity, ACS Omega, 2021 (DOI: 10.1021/acsomega.0c04683)
2. **Isha Abhyankar** <sup>#</sup>, S Hirlekar <sup>#</sup>, K Kane, K Trimukhe, A Prabhune, A Nisal,'Green anti-bacterial molecules: Sophorolipids with varying fatty acid chain\_ Trends in Biomaterials & Artificial Organs 35 (5) 2021 (# Contributed equally)
3. **Isha Abhyankar**, Asmita Prabhune, Anuya Nisal, Synthesis of SL-coated calcium nanoparticles for bone tissue application (Manuscript under preparation)
4. **Isha Abhyankar**, Asmita Prabhune, Anuya Nisal, Anti-cancer activity of short chain derived sophorolipids (Manuscript under preparation)

## Book Chapter:

- Philem Pushparani Devi, **Isha Abhyankar**, Pradeep Kumar Singh; Endophytes as Nanofactories, Nanotechnology in sustainable agriculture, CRC Press (2021)

## Provisional patent filing

- “Composition of calcium phosphate nano-particles with sophorolipids and process of synthesis thereof. No- 202211035664.





